APPLICATIONS OF CHIRAL SELECTORS AND REPLACEABLE SUPPORTS FOR CAPILLARY ELECTROPHORETIC SEPARATIONS

A thesis presented for the degree of

Doctor of Philosophy

By

Priyanga Wickramanayake

Bachelor of Science (Monash University)

Department of Applied Chemistry

Faculty of Applied Science

Royal Melbourne Institute of Technology

Melbourne, Victoria, Australia

March 2007

STATEMENT OF AUTHENTICITY

I, Priyanga Wickramanayake, hereby declare the work presented in this thesis, unless otherwise acknowledge, is my own original work towards the degree of Doctor of Philosophy, and has not been previously submitted for any academic awards.

The work described in this research project was conducted in the Department of Applied Chemistry, RMIT University, between March 2002 and March 2007.

Priyanga Wickramanayake

March 2007

PUBLICATIONS

During the course of the work, the following articles were accepted:

1. Wickramanayake, P.U., Tran, T.C., Hughes, J.F., Macka, M., Simpson, N., Marriott, P. (2006), "Simultaneous separation of nitrofuran and their metabolites by using micellar electrokinetic capillary chromatography" *Electrophoresis*, **27** (20), 4069-4077.

2. Wickramanayake, P.U., Hughes, J. F., Macka, M., Marriott, P. (2006), Proceeding of the 29th International Symposium on capillary chromatography, Riva Del Garda - Italy

3. Wickramanayake, P.U., Hughes, J. F., Macka, M., Marriott, P. (2005), Proceeding of the 13th Annual RACI Research & Development Topics in Analytical Chemistry, Monash University - Mt. Elisa

4. Wickramanayake, P.U., Hughes, J. F., Macka, M., Marriott, P. (2004), Proceeding of the 12th Annual RACI Research & Development Topics in Analytical Chemistry, Melbourne University - Melbourne

5. Wickramanayake, P.U., Hughes, J. F., Macka, M., Marriott, P. (2003), Proceeding of the 11th Annual RACI Research & Development Topics in Analytical Chemistry, University of Technology - Sydney

6. Wickramanayake, P.U., Hughes, J. F., Macka, M., Marriott, P. (2002), Proceeding of the 10th Annual RACI Research & Development Topics in Analytical Chemistry, Deakin University - Warrnabool

A further paper is in preparation:

Wickramanayake, P.U., Hughes, J. F., Macka, M., Marriott, P. "Replaceable stationary phases for capillary electro chromatography"

ACKNOWLEDGMENTS

My father is my inspiration to come this far.

I would like to express my sincere gratitude to my senior supervisor, Prof. Philip Marriott. I would, especially, like to thank him for his expertise in chromatography, for his guidance and sincere encouragement throughout the course of the work.

I am grateful to my co-supervisor, Dr. Jeff Hughes for his assistance in the optimisation study. I am also greatful to Dr. Mirek Macka and Dr. Craig Trenerry for their valuable assistance and suggestions in the study. Grateful acknowledgement is made to Mr. Paul Morrison for his technical assistance in the instrumentation and to Mrs. Anne Hughes for her assistance in proof reading of the thesis.

To my manager Allan Spencer, section leader Julie Liu for their flexibility and support during the last two years.

To my postgraduate fellows Tin, Michael, Con and Weeraya, thank you for your friendship and for making it an enjoyable time.

To my friends Shashika, Sandun, Suba, Natalie, Nalini, Myya and Olivia for their support and taking care of my daughter.

I am indebted to my family (sister, brother and bil Manjula) for their tremendous support and encouragement during my studies. To my little daughter Gimaya, who grew up with very little attention from me.

To my mum for her sacrifice to make my dreams come true. Finally, especial thanks to my husband for his sacrifice and support during my studies. Without my mum's and husband's tremendous support I could not have completed this project.

TABLE OF CONTENTS

CHAPTER 4: OPTIMISATION PARAMETERS AND STRATEGIES FOR CE SEPARATION

CHAPTER 5: SEPARATION OF NIROFURANS THEIR METABOLITES USING MICELLAR ELECTROKINETIC CAPILLARY CHROMATOGRAPHY

LIST OF FIGURES

LIST OF TABLES

LIST OF ABBREVIATIONS

BGE	Background electrolyte
CE	Capillary Electrophoresis
CE-MS	Capillary Electrophoresis-Mass Spectrometry
CGE	Capillary Gel Electrophoresis
CZE	Capillary Zone Electrophoresis
EOF	Electroosmotic Flow
FSE	Free Solution Electrophoresis
HPCE	High Performance Capillary Electrophoresis
ITP	Isotachophoresis
LLE	Liquid-Liquid Extraction
LVSS	Large Volume Sample Stacking
MECC	Micellar Electrokinetic Capillary Chromatography
MEKC	Micellar Electrokinetic Chromatography
NSM	Normal Stacking Mode
SPE	Solid Phase Extraction
SPME	Solid Phase Micro Extraction
ACN	Acetonitrile
CD	Cyclodextrin
α-CD	α-Cyclodextrin
β-CD	β-Cyclodextrin
γ-CD	γ-Cyclodextrin
HP-β-CD	Hydroxypropyl-β-Cyclodextrin
TM-β-CD	Trimethyl-β-Cyclodextrin
[CD]	Cyclodextrin concentration
H_3PO_4	Phosphoric acid

MeOH	Methanol
SDS	Sodium dodecyl sulfate
SDC	Sodium deoxy cholate
CCD	Central Composite Design
CEF	Chromatographic Exponential Function
CRF	Chromatographic Resolution Function
CMC	Critical Micelle Concentration
Ropt	Optimum Resolution
Tmax	Maximum acceptable time
t_f	Final time
LOD	Limit of Detection
N	Efficiency
R_s	Resolution
t_{mg}	Migration time
t_r	Retention time of the solute
t_0	Retention time of the unretained peak
t_{mc}	Retention time of the micelle
μ_{ep}	Electrophoretic mobility
ε	Dielectric constant
η	Viscosity
NFAs	Nitrofuran antibiotics
NFMs	Nitrofuran metabolites
NFs	Nitrofurans
CEF	Chromatographic Exponential Function
EU	European Union
MRL	Maximum residue limit
MRPL	Minimum required performance limit
AOZ	3-amino-2-oxazolidone
AMOZ	5-morpholinomethyl-3-amino-oxozolidone

SEM	Semicarbazide
AHD	1-aminohydantoin
2-NBA	2-nitrobenzaldehyde
%(w/w)	Percentage weight by weight
SE_{height}	Stacking Enhancement Factors
HCl	Hydrochloric acid
NaOH	Sodium hydroxide

ABSTRACT

The popularity of capillary electrophoresis (CE) as a separation technique has been established over the years. CE offers the advantages of high resolution, high separation efficiency, fast approaches of method development, a range of operational modes and low consumption of reagents.

The strategy employed here for the development of chromatographic separations involved the utilization of experimental designs, multi-linear regression and response surface methodology to build empirical models that related the chromatographic quality to the factors influencing the separation.

Separation of Nitrofuran antibiotics (NFAs) and their metabolites (NFMs) by using micellar electrokinetic capillary chromatography was successfully completed. The best conditions found to give optimum resolution from the optimization study was pH 9.0, 80 mM SDC concentration, 16 kV with running buffer consisting of 20 mM borate and 20 mM phosphate concentration using a 73 cm x 75 μm column, resulting in completely resolved NFAs and NFMs within 16 min. It is interesting that all the compounds can be reliably separated with the one mixture, and single CE condition. Whilst all antibiotics have shorter migration time than their respective derivatised metabolites, as a group apart from nitrofurantoin the antibiotics elute before the metabolites. The analytical figures of merit for CE analysis exhibited excellent reproducibility of absolute and relative migration times, and acceptable reproducibility of relative response areas. Successful separation of metabolite derivatives was achieved when the developed method was applied to a spiked prawn sample.

The chiral separation of Triadimenol was successfully completed using micellar electrokinetic capillary chromatography. The best conditions found to give optimum resolution from the optimisation study were pH 6.0, 20% methanol, 50 mM SDS concentration, 18 kV with running buffer consisting of 20 mM borate and 20 mM phosphate concentration using a 64.5 cm x 50 μm column, resulted in baseline resolution of all Triadimenol isomers within 18 min. The optimised separation conditions were applied to a blank grape

sample and to a spiked grape sample. No peaks were observed in the blank grape sample whereas the spiked grape sample had two diastereoismer peaks with poor detection sensitivity. Increase in detection sensitivity is necessary to determine the possibility of resolution of all the isomers of Triadimenol, in the spiked grape sample and the blank.

Online preconcentration techniques were attempted to for Triadimenol isomer separation. When using online preconcentration technique of sweeping, a 30-fold increase in detection sensitivity of Triadimenol was observed compared to MEKC mode. However enantiomer separation was not possible with sulfated-β-CD chiral selector. The best conditions were found to be pH 2.5, 50 mM SDS concentration, -20 kV with running buffer consisting of 20 mM phosphate concentration, using a 64.5 cm x 50 μm column, resulting in diastereoisomer separation within 8 min.

Final stage of the project was to create stationary phase beds in capillaries and micro-channels that could be removed and re-created, thus providing a fresh stationary phase. The replaceable stationary phase (RSP) can be used as an operating mode of CE/CEC. Preparation of reversible stationary phase (RSP) inside the capillary column was successfully performed using low methoxy pectin (LMP). LMP renders a capability of reversible thermogelation. Electroosmotic flow (EOF) and sufficient hydrophobicity of LMP gel allow separation of analytes. The porosity of LMP RSP was adequate to support EOF. Successful separation with good reproducibility of areas and migration times was obtained for Caffeine, Aspartame, Benzoic acid, Saccharine (CABS) mixture and NFAs. After performing continuous analyses, the aging of RSP was observed. Temperature was the ‘switch’, which applied to remove aged RSP. RSP was recreated for further analysis of analytes. RSP was UV transparent, capable of handling various analytes and different buffer electrolytes including aqueous-organic solvents.

CHAPTER 1

LITERATURE REVIEW

1.1 Background

The study of modern pharmaceuticals and their analysis in almost all variety of matrices depend on entirely upon advanced instrumental separation, measurement and identification tools. The development of chromatographic methods closely parallels their application and exploitation in the pharmaceutical area, however not all chromatographic methods are universally applicable to all pharmaceuticals. As a benchmark we can emphasize the key tools of high performance liquid chromatography (HPLC) and gas chromatography (GC), hyphenated with a broad range of detection methods as the basis for pharmaceutical analysis. Among these two, HPLC is the most relevant due to its suitability for polar/ thermally labile compound analysis, which increasingly characterise pharmaceutical compounds, although GC is applicable to compounds that are thermally stable. Both have dedicated mass spectrometric detection methods specifically catering for the analysis of compounds within the respective mobile phases, however main study detection methods of UV-vis and flame ionisation (FID) or other common detectors are still common for LC and GC respectively.

While many pharmaceutical researchers have how adopted very sophisticated methods based on HPLC and ancillary classes of separation tools (gel permeation chromatography and ion chromatography, etc), over the past 15-20 years a concentrated effort in developing capillary electrophoresis (CE) based methods is apparent. While CE is not likely to challenge HPLC as the operating tool for pharmaceutical analysis, it does offer specific advantages for high resolution and micro-scale analysis.

Chromatography is a major analytical technique used for the identification, separation and determination of chemical components in complex mixtures. Chromatography has already been employed to study trace organic compounds and illicit drug use [1].

Electrophoresis is defined as the differential movement of charged species (ions) by attraction or repulsion in an electric field. Tiselius first introduced it as a separation technique in 1930. He discovered that when a protein mixture was placed in a buffer solution, to which was applied an electric field, the sample components migrated in a direction and at a rate determined by their charge and mobility. This work of

Tiselius on electrophoresis led him to win a Nobel Prize in 1948, recognising the nature of separation of chemical species in the discovery process, and knowledge generation.

Hjerten described open tube electrophoresis in 1967 [2]. In 1981, Jorgenson and Lukacs discovered Capillary Zone Electrophoresis (CZE) in the fused silica capillary, which is one of the most widely accepted CE techniques today [3]. CZE was initially applied to the analysis of biological macromolecules such as proteins, peptides, nucleotides, aminoacids, oligonucleotides, and DNA etc. It is apparent that the early work of Jorgenson and Lukacs produced results that exhibited a “theoretical achievable efficiency”. Terabe and co-workers developed the technique known as Micellar Electro Kinetic Capillary chromatography (MEKC), which has further diversified the applications of CE by including separation of neutral substances [4]. Due to the diversity of application, the number of publications of CE has dramatically risen.

CE is recognized as a powerful analytical and separation technique. It was evaluated in the past as a method for analysis in the pharmaceutical industry as an alternative technique to High Performance Liquid Chromatography (HPLC), although it seems to have become a complementary technique [5]. The separation capacity of CE was very well established in such research fields as DNA fingerprinting, proteomics and the Human Genome Project. Brumley examined some applications of CE in environmental analysis, analysing semi volatiles such as phenols and aliphatic amines, non-volatiles such as herbicides, dyes, surfactants and explosives [6]. Brumley concluded that CE separations can not only be used for important analyses for drugs, DNA sequencing and proteins, but can be used more broadly for environmental analysis. Industrial sample analysis will presumably also be a future important application area for CE as more applications are explored.

CE separates species in an applied electric field based on the different velocities of the species in an electrolyte inside a separation capillary. The technique of CE has become popular, due to the fact that it offers some promising features such as short analysis time, high resolution efficiency, ready optimisation, widely variable operation conditions, use of small volumes of analytes, reduced consumption of reagents and little waste solution.

Fig 1.1: Method development scheme for the CE separations

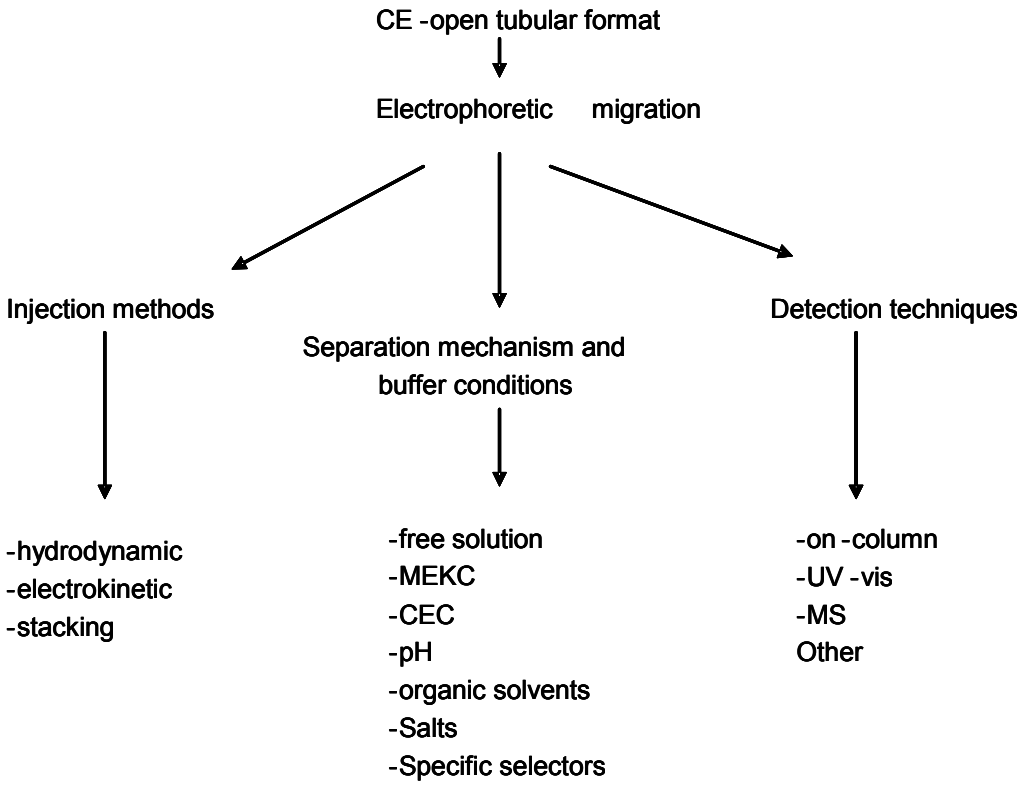

1.2 Nitrofuran antibiotics and metabolites

1.2.1 Chromatographic Determination

Evaluations of bound residues of veterinary drugs such as furazolidone, furaltadone, nitrofurazone and nitrofurantoin, which belong to the class of nitrofurans (NFAs) and their metabolites 3-amino-2-oxolidone (AOZ), 5-morpholinomethyl-3-amino-oxolidone (AMOZ), semicarbazide (SEM), 1-aminohydantoin (AHD) respectively have been recognised as an important aspect of food safety. The structures of NFAs and NFMs are shown in Fig 5.1 (Chapter 5). Due to the suspected carcinogenic nature of nitrofuran metabolites (NFMs), the European Union (EU) prohibited their use in food animal production by their listing in Annex 1V of the Council Regulation 2377/90 [7]. Due to the absence of a maximum residue limit

(MRL) of nitrofurans (NFs), the presence at any concentration in animal feed can violate the law [8, 9]. The use of NFAs in food-producing animals has been banned and should be completely absent from food products within the European Union from 1995 and in the United States from 2002 because of their potentially harmful carcinogenicity and mutagenicity effects on human health [9-11]. However with the improvement of analytical methods the EU Commission Decision of 13 March 2003 has set up a minimum required performance limit (MRPL) set at 1µg/ kg for each NFM for any method combined with the analysis of NFs in poultry meat and aquaculture products [12]. A growing interest in analysis and information on the subject still persists today because the problems related to NFMs have not yet been eradicated.

In 2002, it was discovered that NFA residues occurred in fish products, such as shrimp and catfish originating from southeastern Asian countries. The research on the antibacterial action of NFs commenced when it was observed in 1946 that nitrofurazone increased the lag phase of bacterial growth [13]. In those days nitroheterocyclic molecules were very popular for the management of infectious diseases, especially the 5-nitrofurans as well as the 5-nitroimidazole compounds, which are widely used as antiprotozoal, antibacterial and anticancer agents [14, 15].

The presence of the 5-nitro group [16] is the main characteristic of NFAs, which contributes to the wide range of antimicrobial activities. Therefore NFAs have been widely used as veterinary drugs and are often added to feeds to prevent and control several bacterial and protozoan infections such as E.coli and Salmonella, especially in cattle, prawns and poultry [9, 17, 18].

Pires et al. discovered that the nitroheterocyclics cytotoxicity depends on the chemical nitro group reduction, which afterwards results in damage to DNA; although the actual mechanism is not yet fully understood [19].

Merino et al. suggested a mechanism of biological action for these drugs in which the nitro group reduction formed intermediate species that react with DNA by oxidising it and liberating thymidine phosphate, which causes harmful effects to DNA by destabilising the double helix [20].

A growing interest in analysis and information on the subject still persists today because the problems related to NFMs have not yet been eradicated. The use of NFAs in food-producing animals has been banned and should be completely absent from food products within the European Union from 1995 and in the United States from 2002 because of their potentially harmful carcinogenicity and mutagenicity effects on human health [9-11]. The NFAs consist of bi-polar molecules having antibiotic moiety and a neutral chemical deposit, which differ from one molecule to another. When the drug is administered to an animal, the antibiotic moiety reacts quickly and the inactive counter part is rapidly excreted in the urine. The neutral chemical residue (metabolite) covalently binds to circulating tissue proteins, leaving traces within the animal after months of administration. When the NFMs bind to the protein, they produce a very stable adduct due to the amide bond, which is most probably inactive. This adduct can act as a probe for determination of nitrofuran residues in food.

McCracken et al. [21] have developed a method for determination of the NFM, AOZ in porcine tissue. The porcine tissue was analysed using thermospray mass spectrometry-liquid chromatography, monitoring the positive ion *m /z* 253 with filament-assisted ionization, and 2-nitrobenzaldehyde was used as a derivatising reagent.

Draisci et al. [22] have determined nitrofuran residues, furazolidone, furaltatode and nitrofurazone in avian eggs using HPLC-UV photodiode-array (HPLC-DAD). HPLC-ionspray mass spectrometry (HPLC-MS) with an atmospheric pressure ionization source was used for conformation of identity of nitrofuran residues.

Conneely et al. [18] have extracted the protein-bound nitrofuran residue, AOZ, using solid phase extraction (SPE) followed by chromatographic determination with tandem mass spectrometry. The comparison of AOZ detection by liquid chromatography with UV or tandem mass spectrometry showed an agreement within 10% for incurred porcine liver samples.

Pereira et al. [23] have demonstrated the detection of nitrofuran residues in salt samples by liquid chromatography coupled to tandem mass spectrometry (LC-MS-MS). This method includes a hexane

extraction of the SEM followed by derivatisation with 2-NBA. All four compounds were simultaneously analysed by this method.

Leiner et al. [8] have developed a method, which enable simultaneous detection of all nitrofuran residues by LC-MS-MS. The sample clean-up and analyte enrichment was performed by SPE with a sorbent following combined hydrolysis of the protein bound drug metabolites derivatisation of the homogenized tissue with 2-NBA. Limit of detection (LOD) of 0.5- 5 ng g^{-1} tissue and limit of quatification (LOQ) of 2.5- 10 ng g^{-1} were obtained using electrospray ionisation in positive mode.

O'Keeffe et al. [11] have developed methods for determining furazolidone and furaltadone using HPLC-MS. High recovery of bound residues were observed and good reproducibility of assays were shown. The developed methods were then applied to a study on the perseverance of the bound residues of furazolidone in pig liver after administration of the drug. It was discovered at least 6 weeks after the administration that biological active metabolites of the active metabolite of the drug persist as bound residues in liver. The outcome of this project has enhanced the knowledge on bound residues including the analytical methods and toxicity in edible tissues.

Moittier et al. [24] have suggested a method based on isotope dilution liquid chromatography-tandem mass spectrometry (LC-MS/MS) for the low level identification of NFMs in meat. Prior to analysis of LC-MS/MS by positive electrospray ionisation, liquid-liquid extraction (LLE) and clean-up on a polymeric SPE were conducted. This method demonstrates the capability to quantify the presence of these NFMs at levels under the MRPL.

Effkemann et al. [10] proposed a method for quantitative determination of NFMs detection by using triple-quadrupole LC-MS-MS in complex food matrixes. After derivatisation with 2-nitrobenzaldehyde (2-NBA), samples were prepared with several LLE steps using ethyl acetate and hexane. Due to the hydrophobicity of the derivatising reagent and stronger retention of analytes on the reversed-phase columns, there was better separation of the derivatised analyte molecules from complex matrix compounds.

Hormazabal et al. have developed a LC-MS method for simultaneous determination of NFMs. Analytes were extracted with tricholoro acetic acid and clean up was performed with SPE after derivatisation with 2-NBA. Acetonitrile-water were used to elute derivatised NFMs and were extracted with chloroform. The limit of detection varied from 0.2 ng g^{-1} – 0.5 ng g^{-1} [25] .

Hoenicke et al. [26] published a case study of NFs. This paper includes how to control the zero tolerance of NFs in food animal products.

Hruska et al. have demonstrated a monoclonal-based ELISA, coupled with an assay buffer method for the monitoring of AOZ in egg samples. The analytes were extracted as nitrophenyl derivatives using SPE after acid hydrolysis. The detection capability of ELISA's for AOZ in eggs was 0.6 µg kg^{-1}, 0.3 µg kg^{-1}, 0.3 µg kg^{-1} for buffer, solvent and solid phase extraction respectively. Those values were below the MRPL for tissue bound residues of NFAs set in the Commission's decision [27].

Cooper et al. proposed the first enzyme-linked immunoabsorbant assay for detection of AOZ residues in prawns. Prawn samples were derivatised using o-NBA, extracted into ethyl acetate, washed with hexane and applied to a competitive enzyme immunoassay based on a rabbit polyclonal antiserum. The LOD of the assay was 0.1-µgkg^{-1} [28]. Table 1.1 summarises selected publications of detection techniques used in NF analysis.

Table 1.1 Summary of selected publications of NF analysis of detection techniques

Analyte(s)	Technique	References
AOZ	LC- thermospray MS	McCracken 1997 [21]
AOZ, AMOZ, SEM	LC-UV-Vis photodiode-array	Drasci 1997 [22]
AOZ, AMOZ, SEM, AHD	LC-tandem MS	Leiner 2001[8]
AOZ	LC-tandem MS and UV	Conneely 2003 [18]
AOZ, AMOZ, SEM, AHD	Triple-quadrupole LC-MS-MS	Effkemann 2004 [10]
AOZ, AMOZ	LC-MS	O'Keeffe 2004 [11]
AOZ	Enzyme immunoassay	Cooper 2004 [28]
AOZ, AMOZ, SEM, AHD	LC-MS	Hormazabal 2004 [25]
AOZ, AMOZ, SEM, AHD	LC-MS-MS	Pereira 2004 [23]
AOZ, AMOZ, SEM, AHD	LC-electrospray ionization-tandem MS	Mottier 2005 [24]
AOZ, AMOZ, SEM, AHD	LC-tandem MS	Pak-sin 2005 [29]
AOZ, AMOZ, SEM, AHD	LC-MS-MS	Hartig 2005 [30]
AOZ, AMOZ, SEM, AHD	LC-tandem MS	Finzi 2005 [31]
AOZ	Monoclonal based ELISA	Hruska 2006 [27]

Capillary electrophoresis can be regarded as an attractive separation technique with respect to analysis of NFM; apparently no literature has been published for analysis of NFAs or NFMs by using CE. Hence the goal of the present study was to develop a simple, fast analysis that enables simultaneous separation, detection of four NFAs and their metabolites (Chapter 5).

1.2.2 Sample Cleanup and Preconcentration

Relatively poor detectability in terms of concentration sensitivity when using spectrophotomeric detection is one of the problems in CE. To enhance the detectability, several concentration techniques can be employed in CE systems including electro kinetic chromatogrphy (EKC). These concentration techniques include LLE, SPE, and Solid-Phase Micro Extraction (SPME) and are frequently utilised to increase the concentration of analytes present in trace amounts, prior to analysis. Recently LLE is being replaced by SPE and SPME because the latter methods do not require large volumes of high purity, toxic, inflammable solvents and the concentration step is faster and more economical. In some instances, before the analytes are separated, the sample must be cleaned up to avoid interferences. SPE has been used as a cleanup and preconcentration technique so that the limit of detection and the selectivity are improved [32]. SPE has been the most popular cleanup method prior to CE analysis, using a wide variety of adsorbents ranging from nonpolar, e.g. C_8, C_{18} to polar (i.e. silica gel, florisil and alumina). It is also named column or adsorption chromatography since the extraction substrate is prepared by filling normal glass chromatographic columns with solid adsorbents. However it is commercially available as disposable cartridges and disks. The SPE columns have been widely used to clean up extracts obtained from other extraction methods and for diverse matrices.

Veraart et al. [33] have described an on-line SPE apparatus for CE. A programmed SPE unit is connected to the CE instrument by means of a laboratory-made interface. The polyetheretherketone (PPEK) tubing interface permits a continuous flow of the CE buffer through the interface and at the end of the SPE step, the analytes are desorbed using a solvent that is flushed through the interface via a loop. The system was used to analyse about 900 complex biological samples for a year.

1.3 Chiral Separation

The technique of chiral analysis is becoming increasingly important in both the pharmaceutical and food industries. In the last five years, of the 10 most down loaded papers in the Journal of Chromatography, 6 were in the area of chiral separation. The fact that the Nobel Prize for Chemistry in 2001 was awarded to Dr. Knowles, Dr. Noyori and Dr. Sharpless for their contributions in the study on the improvement of asymmetric catalysis and the synthesis of chiral compounds indicate that scientists have paid great attention to the importance of chirality. Thus asymmetric synthesis and chiral separation, and will play an even more crucial roles in life sciences, the pharmaceutical industry and other fields in the future.

Electromigration techniques have attracted increasing interest for enantiomer separation in recent years. The U.S. Food and Drug Administration have firm regulations for the purity of compounds in the drug industry. Hence, the preparation of pure enantiomeric standards should involve further research to establish the individual metabolism of each enantiomer [34].

CE has been established as one of the major techniques in the field for chiral analysis. In general, a chiral environment is required for enantioselective separations, and therefore the most common approach in CE is the addition of a chiral selector to the buffer solution in order to form a dynamic association complex. Cyclodextrins (CDs) are the most widely used chiral selectors. Enantioselective inclusion of chiral analytes in the cavity of CDs is a very well established separation principle, and has been applied to the resolution of a broad range of compounds by CE [35]. The combination of CDs with borate and phosphate buffer has recently demonstrated to be a valuable tool for the chiral resolution compounds containing the diol functional group, such as nucleotides, carbohydrates and other compounds of biological interest [36, 37].

CDs are non-ionic cyclic oligosaccharides consisting of six, seven and eight glucose units, and are called α, β and γ-CDs respectively. Native CD can be derivatised; these CDs include dimethyl (DM- β-CD), trimethyl (TM-β-CD) and hydroxy propyl (HP- β-CD). At the present stage, several ionic derivatised ionic CDs i.e. sulfated and carboxymethylated CDs are available.

Chiral selectivity results from inclusion of a hydrophobic portion of the solute in the cavity and also from the hydrogen bonding to the chiral hydroxyl moieties. The Dalgleish “3-point” principle is widely accepted as the basis upon which chiral resolution is achieved with the presence of a chiral selector. The first publications on drug analysis in CE emerged in 1986 [38, 39]. Fig 1.2 shows a schematic representation of interaction between the chiral selector and enantiomers.

Fig 1.2: Schematic representation of interaction between the chiral selector and enantiomers

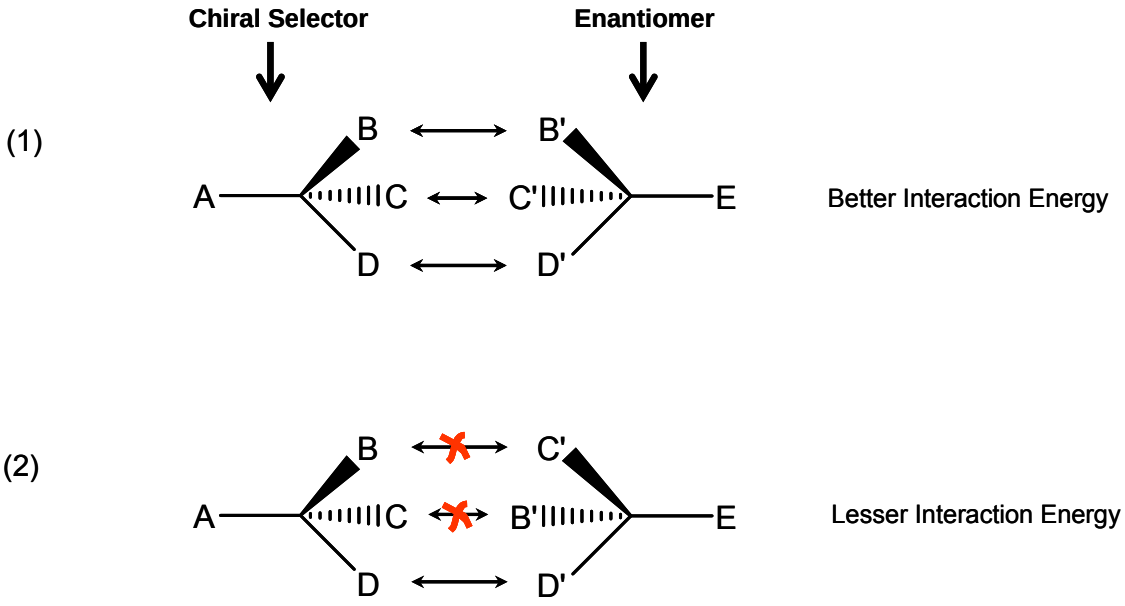

First interaction of Fig 1.2 shows good interaction energy between stereochemically oriented groups and one enantiomer, with specific groups on a chiral selector that provide some measure of ‘weak dissociation’. The second interaction in this case is for the other enantiomer, which exhibits less interaction. The extent/energy of interaction determines the extent to which migration (or dissociation constant) of the enantiomers is modified by the selector, which is then translated into a separation difference. The energy difference can be minimal.

Recently, several derivatised ionic CDs are used as pseudostationary phases in EKC or CDEKC, where enantiomer separation is also performed [40]. In MEKC, the addition of CD to electrolyte solution as a

chiral selector has also been utilised for chiral separation [41], this technique is known as cyclodextrin-modified micellar electrokinetic chromatography (CD-MEKC).

A modified charged β-CD, i.e. sulfobutyl ether-β-CD, has been investigated as a chiral selector for the separation of underivatised anionic and cationic compounds of pharmaceutical interest, uncharged phenyl alcohol, and dansyl amino acids in CE by Desiderio and Fanali [42].

Chiral separation of some β-blocker drugs was carried out based on the work of Pak et al. [43-45] in order to understand the chiral separation mechanism by using β-CD as a chiral selector and to measure enantiomeric excess. Enantiomeric separation of propranolol and its metabolites by CE using chiral selectors was achieved. Enantiomeric resolution and separation were achieved to some degree for propranolol and most of its metabolites by using HP-β-CD as the chiral selector. With charged carboxymethyl- β-CD (CM-β-CD), enhancement of the enantiomeric resolution was achieved, apart from the glycol metabolite. Moreover, chiral resolution of the compounds studied was achieved in a single analysis using a buffer system of borate with charged CM-β-CD and uncharged β-CD, where near baseline resolution was found for propranolol glycol (Pr-glycol) enantiomers. It was found that native β-CD was required for the latter metabolites chiral resolution.

Quang et al. [46] have employed β-CD in the chiral separation of basic compounds in CE using short chain tetraalkylammonium cations to reverse electro-osmotic flow (EOF), thus improving resolution. To further improve chiral resolution they used various modified β-CDs, such as DM-β-CD and HP-β-CD to separate a range of basic drugs. They have found some drugs were resolved well with some modified β-CD whereas other drugs were poorly resolved [47, 48]. This points to the widely held belief that proper choice of chiral selector is still largely by trial-and-error, and it is difficult to predict the degree of resolution achievable.

Pierre and Sentell [49] have used different β-CDs, i.e. β-CD, Me- β-CD, HP- β-CD, in the chiral separation of basic pharmaceuticals, i.e. propranolol, metroprolol, terbutaline, atropine and chloropheniramine. The effect of pH, CD types and the concentration on resolution was studied. They have found that optimisation

of chiral separation not only depends on pH, CD types and concentration but also on the degree of binding between the CD and solute.

Borate has been employed as a buffer component for the separation of carbohydrates and biologically active compounds [50, 51]. It has been suggested that the role of borate in complexation for cis-diol molecules is to impart a modified charge to the product through a complexation mechanism. A significant change in the charge-to-mass ratio of the cis-diol compound is the result due to the complexation of these compounds to the freely ionised hydroxyl group of borate. Borate complexation with the compounds that contain cis-diol groups results in differences in mobility. Therefore, cis-diol compounds can be separated from non cis-diol-containing molecules that only differ slightly in structure but have identical net charge [52]. This highlights the relative ease with which migration in CE may be modified simply by adjusting or altering the buffer composition.

1.3.1 Chiral separation of Triadimenol fungicides

Triadimenol belongs to class of triazole alcohols. Triadimenol is a vital systemic fungicide used in Australian viticulture for the control of powdery mildew. The triadimenol chiral analysis was initially conducted using chiral GC [53] by Clark et al., where the retention time was more than 39 min. Burden et al. [54] have reported derivatising triadimenol with chiral acid chlorides followed by resolution of diastereoisomeric esters by achiral GC.

Otsuka et al. [55] have successfully separated all the enantiomers of Triadimenol by EKC using CDs as chiral selectors. They have employed both the neutral CD derivative HP-β-CD and an ionic hepatakis-6-sulfato- β-CD as an additive in CD-MEKC and as a chiral pseudostationary phase in CDEKC respectively. To improve the method's concentration sensitivity, on-line preconcentration techniques were conducted for both CDEKC and CD-MEKC systems. Stacking with a reverse migrating pseudostationary phase (SEMP) was the preconcentration technique performed in the CDEKC system whereas sweeping was used in the CD-MEKC system under acidic conditions.

Wu et al. [56] have reported simultaneous chiral separation of triadimefon and triadimenol by sulfated-β-CD-mediated CE. They have observed that, at pH 2-4, sulfated-β-CD demonstrated strong chiral recognition towards both triadimefon and triadimenol through multiple interactions between sulfated-β-CD and the analytes that included electrostatic interaction, hydrogen bonding and inclusion effects using phosphate buffer. When using phosphate buffer with 2% sulfated -β-CD at pH 2.5 (optimal conditions), chiral separation of the isomers of triadimenol and triadimefon was obtained within half an hour. The developed method was then applied in the study of stereoselectivity associated with the biotransformation of triadimefon to triadimenol by soil microorganisms.

Nozal et al. [57] have developed a method for separation of triadimefon and triadimenol enantiomers and diastereoisomers by supercritical fluid chromatography. They have employed a chiralpak AD column with different modifiers such as methanol, ethanol and 2-propranolol. Methanol and ethanol gave the best results for the enantiomeric separation of the two compounds. The chiral separation of a mixture of triadimefon and triadimenol was obtained within 15 min using an ethanol gradient. When separating triadimenol diastereoisomers using achiral columns, it was found that the effect of organic modifiers used were dependent on the stationary phase and the best resolution was achieved with Spherex Diol columns.

Williams et al. [58] have reported separation of enantiomers of triadimenol using MECC mode with CD as chiral selector and organic modifiers. They discovered that the factors affecting chiral resolution include capillary operating temperature, applied voltage, column diameter, type of CD and the concentration of CD. The best chiral resolution was demonstrated when using hepatakis-2, 6-di-O-methyl- β-CD (di-Ome-β-CD). The chiral resolution was further improved upon addition of organic modifiers. The resolution of enantiomers was further enhanced when operating the capillary at low temperature and low applied voltage. The authors obtained the baseline resolution of Triadimenol A and partial resolution of Triadimenol B within 35 min.

The goal of the present study on Triadimenol was to develop a simple, fast analysis for complete resolution of all the isomers of Triadimenol and then to apply the developed method to Triadimenol spiked grape samples to determine the isomer ratios after the application (Chapter 6).

1.4 On-line Sample Concentration

Many reports have been published regarding sample analysis by MEKC and CZE with a UV detector, although the detection sensitivity remains a limitation. The detection sensitivity of CE can be improved by applying sample concentration either prior to analysis or at the injection step. The concentration sensitivity of analytes can be improved for CE analysis by on-line concentration techniques such as sample stacking, sweeping and isotachophoresis. Due to the simplicity of on-line concentration techniques, they can easily be implemented. Previously mentioned on-line concentration techniques can be applied to charged and neutral molecules, with the exception of isotachophoresis, which cannot be applied to neutral analytes [59].

Sweeping is a comparatively new on-line sample concentration technique in MEKC. It is known as the sorption and accumulating of analyte molecules by the pseudostationary phase (PS) that enters and fills the sample zone upon application of voltage. This concept was initially proposed by Gilges [60], however, it was not well established until more recently.

Albert et al. have reported the quantitative analysis of anions with polarity switching [61]. A further technique was illustrated by them regarding increasing sample concentration involving hydrodynamic injection of a large sample volume, followed by the removal of the large plug of low conductivity sample matrix out of the column using polarity switching. They also mentioned a method for large volume stacking without polarity switching, however at present the removal of a large plug of low conductivity matrix is performed using an EOF modifier, the dissolution of which will act as a pump without the need for polarity switching [62]. Using an EOF modifier or adjusting the pH, separate analysis of anions [61, 63, 64] and

cations [65] can surpass the performance of the polarity-switching procedure, which can lead to irreproducibility and cannot be implemented in every commercial instrument.

Chien and Burgi [66] explored the case of field-amplified sample injection, where samples were prepared using a low-conductivity buffer and injected into the column using electrokinetic injection. At the injection point, the number of positive ions injected was proportional to the field enhancement factor. The negative ions pushed away from the column by the high field strength and hence negative ions were not enhanced. The EOF velocity of the bulk solution is much slower than the electrophoretic velocity of the sample; hence one can inject and enhance both the cations and anions into the column by polarity switching of electrodes at the appropriate time.

Quirino et al. [67] have investigated the sample concentration in MEKC by sample stacking and sweeping using microemulsion and a single isomer sulfated β-CD as the psuedostationary phase. Quirino et al. have described the concentration mechanism when the sample matrix is a high resistivity non-micellar aqueous solution in MEKC. After an extensive experimental study, it was established that the total focusing effect is brought about by the cumulative effect of sweeping and sample stacking. To obtain maximum concentration outcome, compounds of low to moderate retention factor (k) and compounds showing high k values must be dissolved in low and high conductivity matrices, respectively.

Quirino and Terabe [68] have devised a combined mode for the stacking of analytes in which the sample is concentrated first by the field-amplified injection under non-micellar conditions. Once the buffers are changed and the polarity is reversed to induce sweeping of the analytes into a micellar solutioin, it was observed to achieve around a million-fold enhancement in sensitivity for some cations.

Quirino et al. [69] have presented the idea of sweeping neutral analytes in MEKC applying a high salt containing a matrix or under a reduced electric field using anionic micelles with the presence of electroosmotic flow. Three vital processes were discovered. First, stacking of micelles at the cathodic interface between the sample solution and background solution zone was identified, followed by the sweeping of the analyte molecules by the stacked micelles that enter the sample zone. Finally, the

destacking of the stacked micelle at the anodic interface between the sample and background electrolyte zones occurred.

Lately, Breadmore et al. [70] reported a novel ion-exchange preconcentration procedure using an immobilised resin phase within a section of the CE column. This was useful for ion analysis at trace levels.

Igarashi et al. [71] have developed a method for determining ppb levels of tryptophan derivatives by MEKC with a sweeping effect. In this study, perfluoro surfactant was used as a separation medium. Under acidic conditions, with a negligible EOF, neutral substances were efficiently concentrated and separated by micelles with 10-fold improvement of detection sensitivity.

Markuszewski et al. [72] have proposed a mechanism for determining pyridine and adenine nucleotide metabolites in *Bacillus subtilis* cell extract by sweeping borate complexation CE. The authors have claimed nanomolar detectability of analytes by CE with UV photometric detection through effective focusing of a large sample plug (~10% of capillary length) using sweeping by borate complexation method.

Britz- McKibbin et al. [73] have discussed three on-line preconcentration techniques: Dynamic pH junction, sweeping and dynamic pH junction-sweeping which can be used for trace analysis of metabolites in the human genome project. The authors have claimed increase in concentration sensitivity over three orders of magnitude while generating extremely sharp detector bandwidths for high resolution separations. Sweeping using charged micelles is optimal for hydrophobic (neutral) metabolites that possess a high retention factor ($k' > 2$) under suppressed EOF conditions.

Chiang et al. [74] have developed two preconcentration methods for detection of trace amounts of ephedra-alkaloids including ephedrine, norephidrine, norpseudoephedrine, psuedoephedrine, methylephedrine, methylpsuedoephedrine. The authors reported ~10^4 amplification effect of analytes using cation-selective exhaustive injection and sweeping MEKC (CSEI-Sweep-MEKC).

Yu et al. [75] have developed a method for the detection of four toxic pyrrolizidine alkaloids in Chinese herbal medicine. In this study, direct electrokinetical focusing of a large sample volume injection (up to 20% of capillary length) on the capillary was performed using the dynamic pH junction-sweeping method. Table 1.2 summarises selected publications of preconcentration techniques used.

Table 1.2 Summary of selected publications of different preconcentration techniques

Technique(s)	Reference:
Stacking with polarity switching mode	Albert et al.[61]
Stacking without polarity switching mode	Albert et al.[61]
Field-amplified polarity switching	Chien and Burgi [66]
Stacking and Sweeping using microemulsion	Quirino et al. [67]
Stacking with field-amplified injection under non-micellar conditions	Quirino and Terabe [68]
Sweeping of neutral analytes in electrokinetic chromatography with high-salt-containing matrixes.	Quirino et al. [69]
Ion-exchange preconcentration	Breadmore et al. [70]
Sweeping	Igarashi et al. [71]
sweeping by borate complexation	Markuszewski et al. [72]
Dynamic pH junction, sweeping and dynamic pH junction-sweeping	Britz- McKibbin et al. [73]
Cation-selective exhaustive injection and sweeping MEKC	Chiang et al. [74]
Dynamic pH junction-sweeping	Yu et al. [75]

1.4.1 On-line Sample Concentration of Triadimenol

Wu et al. [76] have reported separation of triadimefon and triadimenol by a preconcentration technique known as sulfated-β-CD-mediated CE. The authors claimed simultaneous resolution of all chiral isomers of triadimefon and triadimenol within 30 min when using phosphate buffer with 2% sulfated -β-CD at pH 2.5. When developing the proposed technique, chiral recognition was believed to be due to the inclusion effect between the analytes and the cavity of sulfated-β-CD, in which electrostatic interaction and hydrogen bonding and spatial configuration were believed to have a role in defining the inclusion strength.

Otsuka et al [55] have reported enantioseparation of triadimenol by EKC using both neutral and ionic CDs as chiral selectors. HP-γ-CD, neutral CD derivative was used in CD modified MEKC (CD-MEKC) and hepatakis-6-sulfato-β-CD (HS-β-CD) as an ionic chiral pseudostationary phase in CDEKC. On-line preconcentration techniques of sweeping and stacking were applied to CD-MEKC and CDEKC systems respectively. Around 10-fold increase in the detection sensitivity was obtained, however baseline resolution was not obtained for any of the on-line concentration techniques.

The goal of our study of on-line preconcentration technique on Triadimenol was to develop a simple, fast analysis for complete resolution of all the isomers of Triadimenol and then to apply the developed method to Triadimenol spiked grape samples to determine the isomer ratios after the application (Chapter 7).

1.5 Non-particulate beds in capillary electrophoresis

Capillary electrochromatography (CEC) is a reasonably novel electrokinetic separation technique representing a hybrid of HPLC and CE. In CEC, the mobile phase is driven through the capillary by EOF, using typical HPLC mobile and stationary phases that provide necessary chromatographic interactions. In CEC, the column serves not only as the separation chamber but also as the pumping machine to drive the mobile phase through the system (there is no supplementary mechanical pump). Open tubular columns

and packed columns are the two major types of columns used in CEC. Packed columns comprise the main class of CEC columns, which comprises of nonpolar, octadecylated or ion exchange particles. The main advantage of CEC is the possibility of using small micrometer and nanometer size particles. High separation efficiency is achieved in packed-CEC without needing ultra high pressure as in HPLC, in order to drive the mobile phase through the columns packed with such small particles. Compared to CE, CEC is not limited to charged solutes as both neutral and charged species may interact with the stationary phase. Therefore, the potential for CEC is much wider [77].

In 1974, Pretorius [78] was one of the early dominant pioneers of CEC who demonstrated the advantages of electroosmosis as a pumping mechanism for chromatographic separations.

In 1981, Jorgenson and Lucas published CEC analyses of 9-methylanthracene and perylene on an octadecylated (ODS) packed capillary column [3].

Tsuda revealed the possibility of obtaining CEC separations by the simultaneous use of both electroosmotic and pressure driven flows in the separation column in 1987[79].

Non-particulate bed techniques, which are also known as monolith or continuous bed, has become an established class of chromatographic separation media. Hjerten et al. first proposed it in 1989 [80] and it is regarded as an alternative for the classical packed columns in chromatography. Authors prepared monolithic capillaries compressed with polyacrylamide gels for separation of proteins using HPLC and low molecular mass compounds [80, 81]. The enormous potential of monolith-based phases was recognised and demonstrated during the preliminary studies conducted in various research fields [80, 82].

The advantages of monoliths include ease of preparation, low back pressure compared to packed-bed columns, the sorbent being formed in situ, and since the monolith is chemically bonded to the inner wall of the capillary, no retaining frits are required. The sorbents in general are chemically inert to analytes [83].

A number of non-particulate products have been released by companies such as Chromolith (Merck, Darmstadt, Germany), CIM (Bia Separations, Ljubljana, Slovenia) and Uno (Bio-Rad Laboratories, Richmond, CA, USA). The continuous bed based products are recognised as the fourth generation of biochromatographic stationary phases after the polysaccharide-based, crosslinked, coated and monodisperse materials [84].

The flexibility of the continuous bed lies in the unlimited choice of potential comonomers containing the functionalities of interest, which can be incorporated into the stationary phase and used for long periods with the required selectivity. Due to the advantages of the monolith it has recently become the competitor of chip-based microanalysis.

The biggest challenge for CEC/ packed beds is the creation of uniform packing bed out of small particles in narrow capillaries. Currently, a variety of packing procedures are available, ranging from slurry [85-87], electrokinetic [88, 89], centripetal [90], and supercritical fluid [91], packing methods. A great difficulty still remains with the ability to pack, long, narrow-bore capillaries. Packed capillaries need end frits to retain packing particles within the packed capillary bed. To allow a uniform mobile phase through the column, frits must possess high porous structure.

Two major directions can be identified, based on the nature of monolithic material: (1) organic polymer-based monoliths and (2) bonded silica-based monoliths. In the first direction, fabrication of monoliths is accomplished through a single-step polymerisation reaction of an organic monomeric precursor [77]. Polymer based monoliths possess exceptional pH stability and they are much simpler than packed capillaries. The limitations of polymerised monoliths include the tendency to swell during exposure to various solvents in the running mobile phases [92, 93].These structural changes may lead to changes in the column during the course of its use.

The formation of monolithic columns with bonded silica stationary phase through the use of sol-gel chemistry is an alternative approach. A majority of chromatographic applications is performed in reversed

phase (RP) conditions. Until now most experimental work has been directed towards designing RP continuous beds [94].

A one step preparation of a continuous bed for RP CE was described by J.-L. Liao [95]. The authors conducted the above task by employing an aqueous micellar polymerisation medium to dissolve the nonpolar comonomers with polar counterparts. To dissolve the nonpolar comonomers, Triton X-100 was used as a neutral surfactant above its critical micelle concentration. The continuous beds formed by this technique were of moderate hydrophobicity.

An additional method was developed in order to increase the hydrophobic ligand density for CEC and capillary liquid chromatography (cLC) [96]. In this method, a continuous bed was formed in a methacrylaxypropyl trimethoxysilane pretreated capillary using 2-hydroxyethyl methacrylate (HEMA) and piperazine diacrylamide (PDA) as comonomers. In the next step polymerisation of allyl glycidyl ether, HEMA, PDA was conducted in the presence of dextraneas hydroxyl-rich and electroosmosis-creating substances to immobilize dextrane polymer. The final step was to attach octadecyl ligands covalently via in situ reaction with the 1,2-epoxyoctadecane in the organic medium.

Fréchet and co-workers recounted in a series of applications on the use of methacrylate monomers for the preparation of HPLC [97] and CEC [98, 99] monolithic capillaries through copolymerisation.

Palm and Novotny [100] proposed a further step in continuous bed formation of RP CEC. Formaldehyde as the polar organic solvent, was used to dissolve comonomers and to conduct polymerisation. Formaldehyde is compatible with the water-based radical polymerisation and capable of dissolving the organic/inorganic salts present. The authors claimed the efficiency of these beds is up to almost 400,000 plates m^{-1} for alkyl phenones in reversed phase. These continuous beds suffered from hydrodynamic impermeability; therefore electroosmotic conditioning had to be used. These continuous beds can be dried during chromatographic use but cannot be reconditioned by means of electroosmosis nor by pressure. This was a significant disadvantage.

Hoegger and Freitag [101] demonstrated a one-step approach in preparation and evaluation of the acrylamide-based monolithic columns. In this method, PDA, *N, N*-dimethylacrylamide, butyl acrylate and hexyl acrylate were dissolved either in aqueous buffer or its mixture with formamide to form the RP continuous beds. It was revealed that the size of flow-through channels could be reproducibly adjusted by selection of the ionic strength of the monomer solution by porosymetric evaluation.

Fujimoto et al. [93, 102] reported the usage of cross-linked polyacrylamides for the separation of dansylated amino acids and neutral steroids on monolithic CEC capillaries.

Tanaka and co-workers [103] have the first reported first uniform porous silica monolithic columns for HPLC in 1996. The sol-gel method was adapted to create silica monoliths in the capillary format and these were derivatised for reversed phase CEC applications in 2000 [104]. In the sol-gel process, chlorosilanes and methoxysilanes undergo hydrolytic polymerisation in the presence of aqueous acid and poly ethylene glycol. To prevent shrinkage of the monolithic structure, the silica network must bond to the silanol groups on the capillary wall. The macroporous morphology is created when transition structures during spinodal decomposition are fixed permanently by the sol-gel transition. Silica monolithic structures differ from those formed from organic polymers because of their bimodal pore distribution and the presence of mesopores within the silica structure.

Haynes et al. [77] have reported a sol-gel chemistry-based approach to the preparation of monolithic columns using a single solution without needing the use of particles. In this approach, a commercially available sol-gel precursor, N-octadecyldimethyl [3-trimethoxysilyl) propyl] ammonium chloride is used to form a monolithic bed. A single step process is used in situ to create a monolithic bed of stationary phase, which is chemically bonded to the inner walls of the fused-silica capillary.

Anion-exchange CEC using monolithic silica columns have received very little attention. Breadmore et al. fabricated monolithic silica columns with soluble cationic polymer poly diallyldimethylammonium chloride (PDDAC). These columns were used to separate inorganic anions [105].

Hutchinson et al. demonstrated preparation and characterisation of anion-exchange latex-coated silica monoliths for the separation of inorganic ions in CEC [106]. These columns were prepared using 70 nm quaternary ammonium, anion-exchange latex particles, which were bound electrostatically to monolithic silica skeleton synthesised in a fused silica capillary. The authors claimed the capacity of a 50-μm-diameter 25 cm latex-coated silica monolith with 0.342 nanoequivalents and 80,000 theoretical plates per column. The EOF was reversed after application of latex-coating and resulted in anions being separated in the co-EOF mode.

Hjertén et al. synthesised an enantiomer-selective gel using human serum albumin derivatised with acrylate groups via protein reaction with glycidylacrylate [107]. The derivatised protein solution was mixed with ammonium peroxodisulfate and tetramethylethylenediamine and drawn into the linear acrylamide polymer-pre-coated fused silica capillary for in situ polymerization. Using the prepared column, chiral separation of D, L- kynurenine in the protein based homogeneous gel was demonstrated.

Messina et al. [108] have demonstrated enantioseparation of 2-aryloxypropionic acids on chiral porous monolithic columns by CEC. In this method, the stationary phase was prepared from silanised fused-silica capillaries by in situ copolymerisation. The chiral stationary phases were prepared by reaction of the epoxy-groups at the surface of the monolith with (+)-1-(4-aminobutyl)-*(5R, 8S, 10R)*-terguride. The authors claimed successful diastereomeric complex formation due to hydrogen bonds between basic nitrogen (proton acceptor), and nitrogen of urea chain (proton donor) of the chiral selector and the carboxylic group.

Shi et al. [83] proposed urea-formaldehyde resin as a hard template for the synthesis of inorganic monoliths. The authors claimed successful preparation of three kinds of inorganics: silica, zirconia and titania, by using this new template. The use of organic free precursors for preparation of inorganic monoliths was allowed due to hydrophilic characteristics of urea-formaldehyde resin.

The problems of CEC using packed capillary columns were caused by column preparation, especially particle packing, fabrication of frits, bubble formation due to frits and non-uniformed field strengths, limited

stability and fragility of packed columns [109]. Tendency towards miniaturisation in a capillary and chip format is evident to overcome the problems of packed capillary columns in CEC.

Previously discussed chromatographic stationary phases incorporated in miniaturised separation systems lead to the conclusion that the technologies are lacking that allow one to easily and quickly create stationary phase beds in capillaries and micro-channels that could be removed and re-created, thus providing a new or regenerated stationary phase.

1.5.1 Replaceable Stationary Phases in CEC

The aim of present study was to synthesise a polymer capable of forming homogeneous thermo reversible gel compatible material with aqueous-organic buffer electrolytes that provides sufficient zeta potentials for EOF. The replaceable stationary phase (RSP) can be used as an operating mode of CEC, (Chapter 8)

Hjerten et al. have demonstrated applications of thermoreversible gels for CEC. The authors prepared charged or charged-polymer-entrapped homogenous gels as electroosmosis-generating stationary phases for CEC. Low melting point agarose was used in preparation of homogeneous gel. Due to high UV absorbance, the protein solution was filled up to the detection window and “on-capillary” detection in the segment without the gel was performed [110].

Maruška et al. [110] have demonstrated formation of homogeneous RP for electrochromatography. In this method agarose was derivatised by covalent attachment of hydrophobic alkyl ligands containing ionic groups in the capillaries. The authors claimed high separation efficiencies up to 300, 000 plates per meter. However derivatisation and preparation procedure appeared to be lengthy.

1.6 References

1. Harris, D.C., *Quantitatie Chemical Analysis.* 5th ed. 1999, New York: W. H.Freeman and Company.

2. Heiger, D.N., *High performance capillary electrophoresis*. 2nd ed. 1992: Hewlett-Packard, Germany.

3. Jorgenson, J.W. and K.D. Lukacs, *Zone electrophoresis in open tubular glass capillaries.* J. High Resol. Chromatogr., 1981. **4**: p. 230-231.

4. Terabe, S., et al., *Electrokinetic Separations with Micellar Solutions and Open-Tubular Capillaries. Anal. Chem.*, 1984. **56**(1): p. 111-113.

5. Altria, K.D., *Optimization and improvement of sensitivity in capillary electrophoresis for quantitation of selected pharmaceuticals.* LC-GC, 1993. **11**(6): p. 438-442.

6. Brumley, W.C., *Environmental applications of capillary electrophoresis for organic pollutant determination.* LC-GC, 1995. **13**: p. 556-568.

7. 1442/95, E.U.C.R., *amending Annexes I, II, III and Iv of Regulation (ECC) No 2377/90 laying down a Community procedure for the establishment of maximum residue limits of veterinary medicinal products in foodstuffs of animal origin.* Off.J.Eur.Communities., 1995. **L143**: p. 26-30.

8. Leitner, A., P. Zollner, and W. Linder, *Determination of the metabolites of nitrofuran antibiotics in animal tissue by high-performance liquid chromatography-tandem mass spectrometry. J. Chromatogr. A*, 2001. ***939***: p. 49-58.

9. Takino, M., *Determination of the Metabolites of Nitrofuran Antibacterial Drugs in Chicken Tissue by Liquid Chromatograph-Electrospray Ionization-Mass Spectrometry (LC-ESI-MS).* Agilent Technologies in house technical paper (www.getech.com): p. 1-9.

10. Effkemann, S. and F. Feldhusen, *Triple-quadrupole LC-MS-MS for determination of nitrofuran metabolites in complex food matrixes.* Anal Bioanal Chem, 2004. **378**: p. 842-844.

11. O'Keeffe, M., et al., *Nitrofuran antibiotic residues in pork The FoodBRAND retail survey. Anal. Chim. Acta*, 2004. ***520***: p. 125-131.

12. 2003/181/EC, E.U.C.R., *Amending decision 2002/657/EC as regards the setting of minimum performance limits (MRPLs) for certain residues in food animal origin.* Off.J.Eur.Communities., 2003. **L71**: p. 17-18.

13. Cramer, D.L. and M.C. Dodd, *The mode of action of nitrofuran compounds.* J Bacteriol, 1946. **51**(3): p. 293-303.

14. Wolff, M.E., *Burger's Medicinal Chemistry*. Part II, 4th ed. 1979, New York: John Wiley & Sons.

15. Boll, S., et al., *Trypanosoma cruzi:effect and mode of action of nitroimidazole and nitrofuran derivatives.* Electroanalysis, 2003. **15**: p. 19.

16. Weston, A. and P.R. Brown, *HPLC and CE- principles and practice*. 1997, Califonia: Academic Press Limited.

17. Robert, D.G.K. and J.R. McCracken, *Determination of furazolidone in animal feeds using liquid chromatography with UV and thermospray mass spectrometric detection.* J. Chromatogr. B., 1997. **691**: p. 87.

18. Conneely, A., et al., *Isolation of bound residues of nitrofuran drugs from tissue by solid-phase extraction with determination by liquid chromatography with UV and tandem mass spectrometric detection. Anal. Chim. Acta*, 2003. ***483***: p. 91-98.

19. Pires, J.R., et al., *Investigation of 5-nitrofuran derivatives: synthesis, antibacterial activity, and quantitative structure-activity relationships.* J Med Chem, 2001. **44**: p. 3673.

20. Edwards, D.I., *Nitroimidazole drugs-action and resistance mechanisms I. Mechanism of action.* Antimicrob Chemother, 1993. **9**: p. 31.

21. McCracken, J.R. and G.K. Kennedy, *Determination of the furazolidone metabolite, 3-amino-2-oxalidone, in porcine tissue using liquid chromatography-thermospray mass spectrometry and the occurrence of residues in pigs produced in Northern Ireland. J. Chromatogr. B*, 1996. ***691***: p. 87-94.

22. Draisci, R., et al., *Determination of nitrofuran residues in avian eggs by liquid chromatography-UV photodiode array detection and confirmation by liquid chromatography-ionspray mass spectrometry. J. Chromatogr. A*, 1997. ***777***: p. 201-211.

23. Pereira, A.S., et al., *Analysis of nitrofuran metabolic residues in salt by liquid chromatography-tandem mass spectrometry.* Analytica Chimica acta, 2004. **514**: p. 9-13.

24. Mottier, P., et al., *Quantitative determination of four nitrofuran metabolites in meat by isotope dilution liquid chromatography-electrospray ionisation-tandem mass spectrometry. J. Chromatogr. A*, 2005. **1067**(1-2): p. 85- 91.

25. Hormazabal, V., *Analysis of nitrofuran residues in animal feed using liquid chromatography and photodiode-array detection.* J Liq. Chromatogr Relat Technol, 2004. **27**: p. 2759-2770.

26. Hoenicke, K. and R. Gatermann, *How can zero toleranxes be controlled? The case study of Nitrofurans.* Accred Qual Assur, 2006. **11**: p. 29-32.

27. Franek, M., et al., *Validation of monoclonal antibody-based ELISA for the quantification of the furazolidone metabolite (AOZ) in eggs using various sample preparation.* Veterinarni Medicina, 2006. **51**(5): p. 248-257.

28. Cooper, K.M., et al., *Production and characterisation of polyclonal antibodies to a derivative of 3-amino-2-oxalidinone, a metabolite of the nitrofuran furazolidone, in prawn tissue by enzyme immunoassay.* Food Additives and Contaminants, 2004a. **21**: p. 841-848.

29. Chu, P.-S. and M.I. Lopez, *Liquid chromatography- tandem mass spectrometry for the determination of protein bound residues in shrimp dosed with nitrofurans.* J. Agric. Food Chem., 2005. **53**(23): p. 8934- 8939.

30. Hartig, L. and K.V. Czapiewski, *Detecting nitrofuran metabolites in animal products using LC/MS/MS.* www.spectroscopyeurope.com, 2005. **17**(3): p. 21-23.

31. Finzi, J.K., et al., *Determination of nitrofuran metabolites in poultry muscle and eggs by liquid chromatography-tandem mass spectrometry.* J. Chromatogr. B., 2005. **824**: p. 30-35.

32. Redondo, M.J., et al., *Optimization of a solid-phase extraction technique for the extraction of pesticides from soil samples.* J. Chromatogr.A, 1996. **719**: p. 69-76.

33. Veraart, J.R., et al., *At-line solid phase extraction for capillary electrophoresis: application to negatively charged solutes.* J. Chromatogr. B, 1998. **719**: p. 199-208.

34. Kintz, P., et al., *Doping control for â-adrenergic compounds through hair analysis.* J. Forensic Sci., 2000. **45**: p. 170-174.

35. Schmid, M.G., et al., *Capillary electrophoresis chiral resolution of vicinal diols by complexation with borate and cyclodextrin: Comparative studies on different cyclodextrin derivatives. Chirality.* 1997. **9**: p. 153-156.

36. Hulst, A.D. and N. Verbeke, *Chiral separation by capillary electrophoresis with oligosaccharides.* J. Chromatogr., 1992. **608**: p. 275-287.

37. Busch, S., J.C. Kraak, and H. Poppe, *Chiral separation by complexation with proteins in capillary zone electrophoresis.* J. Chromatogr., 1993. **635**: p. 119-126.

38. Fujirawa, S. and S. Honda, *Determination of cinnamic acid and its analogues by electrophoresis in fused silica capillary tube.* Anal. Chem, 1996. **58**: p. 1811-1814.

39. Altria, K.D. and C.F. Simpson, *Measurement of electroendosmotic flows in high voltage capillary zone electrophoresis.* Anal. Proc., 1986. **23**: p. 453-454.

40. Fillet, M., P. Hubert, and J. Crommen, *Enantiomeric separation of drugs using mixtures of neutral and charged cyclodextrins.* J. Chromatogr. A, 2000. **875**: p. 123-134.

41. Koppenhoefer, B., et al., *Separation of drug enantiomers by capillary electrophoresis in the presence of neutral cyclodextrins.* J. Chromatogr. A, 2000. **875**: p. 135-161.

42. Desiderio, C. and S. Fanali, *Use of negative charged sulfobutyl ether-â-cyclodextrin for enantiomeric separation by capillary electrophoresis.* J. Chromatogr. A., 1995. **716**: p. 183-196.

43. Pak, C., *Enantiomeric Separation of Propranolol and its Metabolites by Capillary Electrophoresis using Chiral Selectors*, D.o.A.C. Doctor of Philosophy Thesis, RMIT University, Melbourne, Victoria, 2001, Editor. 2001.

44. Pak, C., et al., *Enantiomeric separation of propranolol and selected metabolites by using capillary electrophoresis with hydroxypropyl-â-cyclodextrin as chiral selector.* J. Chromatogr. A, 1998. **793**: p. 357-364.

45. Pak, C., et al., *Borate complexation and mixed cyclodextrin additives for chiral separation of propranolol and its metabolites by using capillary electrophoresis.* J. High Resol. Chromatogr., 1998. **21**(12): p. 640-644.

46. Lin, C.-E., et al., *Migration behavior and selectivity of b-blockers in micellar electrokinetic chromatography: Influence of micelle concentration of cationic surfactants.* J. Chromatogr. A, 1997. **775**: p. 349-357.

47. Quang, C. and M.G. Khaledi, *Direct separation of the enantiomers of â-blockers by cyclodextrin-mediated capillary zone electrophoresis.* J. High Resol. Chromatogr., 1994. **17**: p. 99-101.

48. Quang, C. and M.G. Khaledi, *Extending the scope of chiral separation of basic compounds by cyclodextrin-mediated capillary zone electrophoresis.* J. Chromatogr., 1995. **692**: p. 253-265.

49. St Pierre, L. and K.B. Sentell, *Cyclodextrins as enantioselective mobile phase modifiers for chiral capillary electrophoresis: Effect of pH and cyclodextrin concentration.* J. Chromatogr. B, 1994. **657**: p. 291-300.

50. Brown, P.R. and E. Grushka, *Advances in Chromatography*. Vol. 34. 1994, New York: Marcel Dekker Inc.

51. EI Rassi, Z.i.B., P.R. and E. Grushka, *Advances in Chromatography*. Vol. 34. 1994, New York, USA: Marcel Dekker. 177-250.

52. Landers, J.P., *Handbook of Capillary Electrophoresis*. 1994, USA: CRC Press Inc.

53. Clark, T. and A. Deas, *Separation of enantiomers of fungicides and some analogues by capillary gas chromatography using Chirasil Val.* J. Chromatogr., 1985. **329**: p. 181-185.

54. Buren, R.S., A.H.D. Deas, and T. Clark, *Separation of enantiomers of fungicidal and plant growth regulatory triazone alcohols using chiral derivatisation and capillary gas chromatography.* J. Chromatogr., 1987. **391**: p. 273-279.

55. Otuska, K., et al., *On-line preconcentration and enantioselective separation of triadimenol by electrokinetic chromatography using cyclodextrins as chiral selectors.* Journal of Pharmaceutical and Biomedical Analysis, 2003. **30**: p. 1861-1867.

56. Wu, Y.S., H.K. Lee, and S.F.Y. Li, *High-performance chiral separation of fourteen triazole fungicides by sulfated a-cyclodextrin-mediated capillary electrophoresis.* J. Chromatogr. A, 2001. **912**: p. 171-179.

57. del Nozal, M.J., et al., *Separation of triadimefon and triadimenol enantiomers and diastereoisomers by supercritical fluid chromatography.* Journal of Chromatography A, 2003. **986**: p. 135-141.

58. Williams, B.D. and V.C. Trenerry, *The direct separation of the diastereoisomers and enantiomers of the fungicide triadimenol by micellar electrokinetic capillary chromatography.* J. CAP. ELEC., 1996. **003**(4): p. 223- 228.

59. Chen, S. and M.L. Lee, *isotachophoresis-capillary zone electrophoresis on directly couple different diameters.* Anal. Chem, 1998. **70**: p. 3777- 3780.

60. Gilges, M., *Determination of impurities in an acidic drug substance by micellar electrokinetic chromatography.* Chromatographia, 1997. **44**: p. 191- 196.

61. Albert, M., et al., *Large-volume stacking for quantitative analysis of anions in capillary electrophoresis 1. Large volume stacking with polarity switching.* J. Chromatogr. A, 1997. **757**: p. 291- 296.

62. Albert, M., et al., *Large-volume stacking for quantitative analysis of anions in capillary electrophoresis 11. Large volume stacking without polarity switching.* J. Chromatogr. A, 1997. **757**: p. 291- 296.

63. Quirino, J.P. and S. Terabe, *Sample stacking of fast-moving anions in capillary zone electrophoresis with pH-suppressed electroosmotic flow.* J. Chromatogr. A, 1999. **850**(1- 2): p. 339- 344.

64. Burgi, D.S., *Large volume stacking of anions in capillary electrophoresis using an electroosmotic flow modifier as a pump.* Anal. Chem, 1993. **65**: p. 3726- 3729.

65. Quirino, J.P. and S. Terabe, *Large volume sample stacking of positively chargeable analytes in capillary zone electrophoresis without polarity switching: Use of low reversed electroosmotic flow induced by a cation surfactant at acidic pH.* Electrophoresis, 2000. **21**(2): p. 355- 359.

66. Chien, R.L. and D.S. Burgi, *Field-amplified polarity-switching injection in high performance capillary electrophoresis.* J. Chromatogr.A, 1991. **559**: p. 153- 161.

67. Quirino, J.P., et al., *Sample concentration by sample stacking and sweeping using a microemulsion and a single-isomer sulfated [beta]-cyclodextrin as psuedostationary phases in electrokinetic chromatography.* J. Chromatogr.A, 1999. **838**(1-2): p. 3- 10.

68. Quirino, J.P. and S. Terabe, *Approaching a million-fold sensitivity increase in capillary electrophoresis with direct ultraviolet detection: Cation- selective exhaustive injection and sweeping.* Anal. Chem, 2000. **72**(5): p. 1023- 1030.

69. Quirino, J.P., S. Terabe, and P. Bocek, *Sweeping of neutral analytes in electrokinetic chromatography with high-salt-containing matrixes.* Anal. Chem., 2000. **72**: p. 1934-1940.

70. Breadmore, M.C., et al., *On-capillary ion-exchange preconcentration of inorganic anions in open-tubular capillary electrochromatography with elution using transient-isotachophoretic gradients. 2. Characterization of the isotachophoretic gradient.* Anal. Chem, 2001. **73**: p. 820-828.

71. Takagai, Y. and S. Igarashi, *Determination of ppb Levels of Tryptophan Derivatives by Capillary Electrophoresis with Homogeneous Liquid-Liquid Extraction and Sweeping Method.* Chem. Pharm. Bull., 2003. **51**(4): p. 373-377.

72. Markuszewski, M.J., et al., *Determination of pyridine and adenine nucleotide metabolites in Bacillus subtilis cell extract by sweeping borate complexation capillary electrophoresis.* J. Chromatogr. A., 2003. **989**(2): p. 293-301.

73. Britz-McKibbin, P. and S. Terabe, *On-line preconcentration strategies for trace analysis of metabolites by capillary electrophoresis.* J. Chromatogr. A., 2003. **1000**(1-2): p. 1903-2003.

74. Chiang, H.-Y. and S.-J. Sheu, *Analysis of ephedra-alkaloids using sweeping and cation-selective exhaustive injection and sweeping micellar electrokinetic chromatography methods.* Electrophoresis, 2004. **25**: p. 370-676.

75. Yu, L. and S.F.Y. Li, *Dynamic pH junction-sweeping capillary electrophoresis for online preconcentration of toxic pyrrolizidine alkaloids in Chinese herbal medicine.* Electrophoresis, 2005. **26**: p. 4360-4367.

76. Wu, Y.S., H.K. Lee, and S.F.Y. Li, *Simultaneous chiral separation of triadimefon and triadimenol by sulfated β-cyclodextrin-mediated capillary electrophoresis.* Electrophoresis. 2000. 21(8) 1611-1619.

77. Hayes, J.D. and A. Malik, *Sol-gel monolithic columns with reversed electroosmotic flow for capillary electrochromatography.* Anal. Chem, 2000. **72**: p. 4090-4099.

78. Pretorius, V., B.J. Hopkins, and J.D. Schieke, *Electroosmosis. New concept of high speed liquid chromatography.* J. Chromatogr., 1974. **99**: p. 23-30.

79. Tsuda, T., *Electrochromatography using high applied voltage.* Anal. Chem, 1987. **59**: p. 521-523.

80. Hjerten, S., J.-L. Liao, and R. Zhang, *High-performance liquid chromatography on continuous polymer beds.* J. Chromatogr., 1989. **473**: p. 273- 275.

81. Li, Y.M., et al., *Continuous beds for microchromatography:cation exchange chromatography.* Anal. Biochem., 1994. **223**(153-158).

82. Svec, F. and J.M.J. Fréchet, *Continuous rods of macroporous polymer as high-performance liquid chromatography separation media.* Anal. Chem, 1992. **64**: p. 820- 822.

83. Zhi-Guo, S., X. Lan-Ying, and F. Yu-Qi, *A new template for the synthesis of porous inorganic oxide monoliths.* Journal of Non-Crystalline Solids, 2006. **352**: p. 4003-4007.

84. Iberer, G., et al., *Column watch: monoliths as stationary phases for separating biopolymers-fourth generation chromatography sorbents.* LC-GC Europe, 1999. **17**(11): p. 998-1005.

85. Van den Bosch, S.E., et al., *Experiences with packed capillary electrochromatography at ambient pressure.* J. Chromatogr. A., 1996. **755**: p. 165-177.

86. Seifer, R.M., et al., *Capillary electrochromatography with 1.8 μm ODS-modified porous silica particles.* J. Chromatogr. A., 1998. **808**: p. 71-77.

87. Dittmann, M.M. and G.P. Rozing, *Capillary electrochromatography-A high-efficiency micro-separation techniques.* J. Chromatogr. A., 1996. **744**: p. 63-74.

88. Dulay, M.T., et al., *Automated capillary electrochromatography:reliability and reproducibility results.* J. Chromatogr. A., 1996. **725**: p. 361-366.

89. Yan, C., et al., *Capillary electrochromatography:Analysis of polycyclic aromatic hydrocarbons.* Anal. Chem, 1995. **67**: p. 2026-2029.

90. Colon, L.A., et al. *Advances in capillary electrochromatography*. in *Ninth International Symposium on High Performance Capillary Electrophoresis (HPCE'97)*. 1997. Anahem, CA.

91. Xin, B. and M.L. Lee, *Design and evaluation of a new capillary electrochromatography.* Electrophoresis, 1999. **20**: p. 67-73.

92. Pietrzyk, D.J., *In packing and stationary phases in Chromatographic techniques*, K.K. Unger, Editor. 1990, Marcel Dekker: New York.

93. Fujimoto, C., Y. Fujise, and E. Matsuzawe, *Fritless packed columns for capillary electrochromatography: Separation of uncharged compounds on hydrophobic hydrogels.* Anal. Chem, 1996. **68**: p. 2753-2757.

94. Kornyšova, O., et al., *Non-particulate (continuous bed or monolithic) acrylate-based capillary columns for reversed-phase liquid chromatography and electrochromatography.* J. Chromatogr. A., 2005. **1071**: p. 171-178.

95. Liao, J.L., et al., *Preparatioin of continous beds derivatized with alkyl and sulfonate groups for capillary electrochromatography.* Anal. Chem, 1996. **68**: p. 3468-3474.

96. Ericson, C., et al., *Preparation of continuous beds for electrochromatography and reversed-phase liquid chromatography of low molecular mass compounds.* J. Chromatogr. A., 1997. **767**: p. 33-41.

97. Svec, F. and J.M.J. Frechet, *Modified poly(glycidal methacrylate-co-ethylene-dimethacrylate) continuous rod columns for preparative-scale ion-exchange chromatography proteins.* J. Chromatogr. A., 1995. **702**: p. 89-95.

98. Svec, F., et al., *Design of the monolithic polymers used in capillary electrochromatography columns.* J. Chromatogr. A., 2000. **887**((1+2)): p. 3-29.

99. Peters, E.C., et al., *Molded rigid polymer monoliths as separation media for capillary electrochromatography.1.Fine control of porous properties and surface chemistry.* Anal. Chem, 1997. **70**: p. 2288-2295.

100. Palm, A. and M.V. Novotny, *Macroporous polyacrylamide/Poly(ethylene glycol) matrixes as stationary phases in capillary electrochromatography.* Anal. Chem, 1997. **69**: p. 4499-4507.

101. Hoegger, D. and R. Freitag, *Acrylamide-based monolithis as robust stationary phases for capillary electrochromatography.* J. Chromatogr. A., 2001. **914**: p. 211-222.

102. Fujimoto, C., *Charged polyacrylamide gels for capillary electrochromatographic separations of uncharged, low molecular weight compounds.* Anal. Chem, 1995. **67**: p. 2050-2053.

103. Minakuchi, H., et al., *Octadecylsilylated porous silica rods as separation media for reversed-phase liquid chromatography.* Anal. Chem, 1996. **68**: p. 3498-3501.

104. Ishizuka, N., et al., *Performance of a monolithica silica column in a capillary under pressure-driven and electrodriven conditions.* Anal. Chem, 2000. **72**: p. 1275-1280.

105. Breadmore, M.C., et al., *Towards a micro-chip based chromatographic platform. Part I: Evaluation of sol-gel phases for capillary electrochromatography.* Electrophoresis, 2003. **23**: p. 3487-3495.

106. Hutchinson, J.P., et al., *Preparation and characterisation of anion-exchange latex-coated silica monoliths for capillary electrochromatography.* J. Chromatogr. A, 2006. **1109**(1): p. 10-18.

107. Hjerten, S., et al., *An approach to ideal separation media for electrochromatography.* Journal of Capillary Electrophoresis, 1998. **5**((1+2)): p. 13-26.

108. Messina, A., et al., *Enantioseparation of 2-aryloxypropionic acids on chiral porous monolithic columns by capillary electrochromatography. Evaluation of column performance and enantioselectivity.* J. Chromatogr. A., 2006. **1120**: p. 69-74.

109. Augustin, V., et al., *In situ synthesis of monolithic stationary phases for electrochromatographic separations: Study of polymerization conditions.* J. Chromatogr. A., 2006. **1119**((1-2)): p. 80-87.

110. Maruška, A. and O. Kornyšova, *Homogeneous reversed-phase agarose thermogels for electrochromatography.* J. Chromatogr. A., 2004. **1044**: p. 223-227.

CHAPTER 2

TECHNIQUE DESCRIPTION and SEPARATION MECHANISMS in CAPILLARY ELECTROPHORESIS

2.1 Capillary Electrophoresis

Electrophoresis has been acknowledged as one of the most extensively used techniques for the separation of analytes by the use of an electric field. Electrophoresis separation technique was developed in 1937 by Tiselius [1] in his doctoral thesis for which he won the Nobel Prize in 1948. He found that when a mixture of proteins was placed in a buffer in the presence of an electric field, the sample components traveled in a direction and at a rate determined by their charge and mobility [1].

Electrophoresis is the term used to describe the movement of charged species (ions) by the attraction or repulsion to and from an electrode in an electric field. It employs narrow bore (20 – 200 μm) buffer-filled capillaries to perform high efficiency separations for both large and small molecules. Electro-Osmotic Flow (EOF) is a unique feature of CE, which provides flow of electrolyte in an electric field. The separation takes place in an open capillary tube commonly made of fused silica. Under the influence of an electric field, electrophoretic and electro-osmotic flows of buffer solutions and ionic species are generated within the capillary. Under normal EOF, in an aqueous solution at pH closer to 3, the silanol groups in the fused silica capillary will dissociate to generate a negative surface. The counter cations from the buffer will correlate and accrue at the surface to form an electric double layer with a zeta potential drop at the capillary surface. The electric double layer consists of a fixed and a mobile layer. The mobile layer contains solvated ions, and as the voltage is applied, the anions move toward the cathode (negative electrode) hence creating EOF in the same direction. Cations move before the EOF marker (net electrophoretic mobility of cations will be greater than electroosmotic mobility) due to their attraction towards the cathode and anions move after EOF due to attraction towards the anode, but still carried towards the cathode since EOF is stronger than the attraction of anions toward the anode. The neutral molecules move with the same mobility as EOF since they have zero electrophoretic mobility. Therefore neutral molecules cannot be separated by normal CE mode; hence Micellar Electrokinetic Capillary Chromatography (MEKC) mode is required.

Figure 2.1: A Schematic representation of EOF in CE

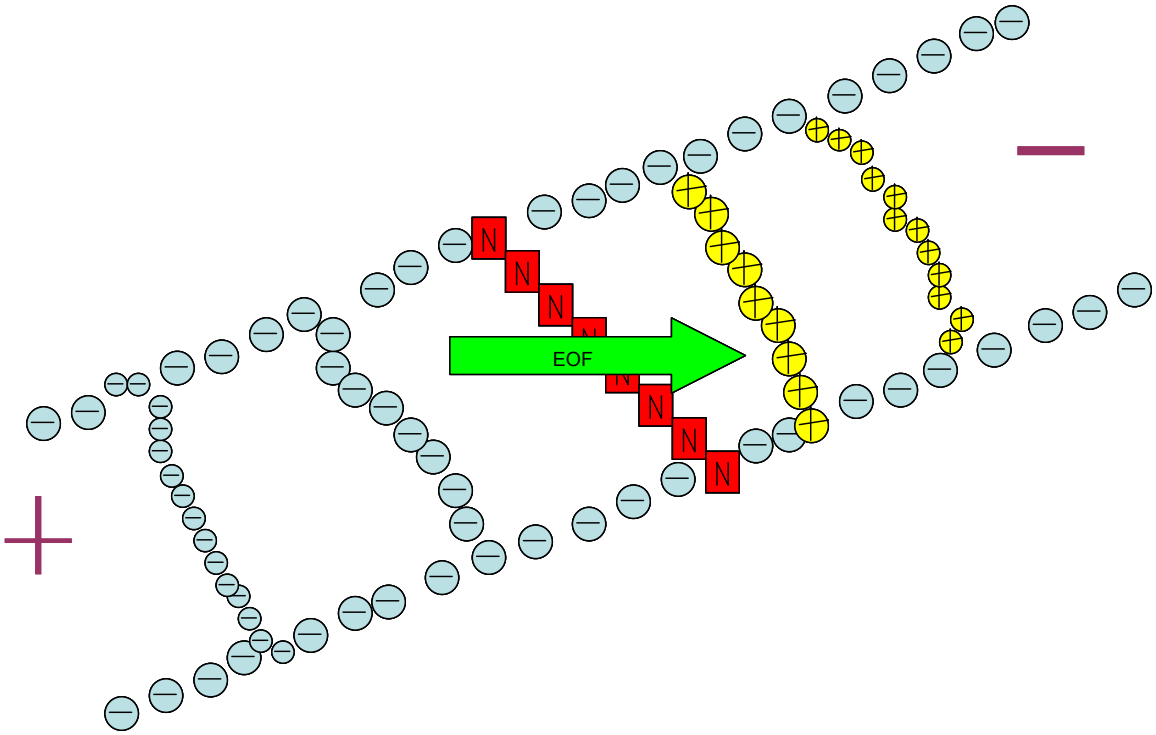

In 1967 Hjerten illustrated zone electrophoresis in free solution. He used tubes of quartz glass with inner diameter of 1-3 mm and coated with methylcellulose (to prevent electro-osmosis) to conduct electrophoresis. The technique of free solution electrophoresis was employed in the separation of a wide variety of molecules including proteins, nucleic acids and viruses [1]. Capillary Zone Electrophoresis (CZE), a widely recognized CE separation technique, was originally developed using fused silica capillaries by Jorgenson and Lukacs in the early 1980s. CZE initially employed a fused silica capillary of 75 µm to analyse biological macromolecules such as proteins, amino acids, peptides, nucleotides, oligonucleotides and DNA [2]. The applicability of CE widened with the introduction of the MEKC technique by Terabe in 1984, which enabled neutral molecules to be separated. Many improvements in CE were developed in the next few years after the introduction of MEKC.

Capillary electrophoresis has developed rapidly over the last fifteen years. It has become popular due to its ease of adjustment of buffer systems and conditions to tune the separation to achieve resolution of target compounds, speed, simplicity, resolving power, minimal amounts of buffer and sample

requirements (less than 50 nL) and adaptability towards a selection of applications using different analytical conditions compared to HPLC. CE has been applied widely to many analytes from a variety of different areas. Due to low volume consumption, CE has become a microscale analytical technique for exploring microbiological and microenvironmental, as well as neutral, molecules and macromolecules. CE has been applied to the analysis of a wide variety of analytes including vitamins [3], environmental [4], biomedical [5] and pharmacological samples [6] and food additives [7, 8]. The number of CE installations in laboratories is increasing globally. There have been more than 7000 publications on CE applications and they are still increasing sharply [9].

***Figure 2.2*:** A schematic representation of CE instrument

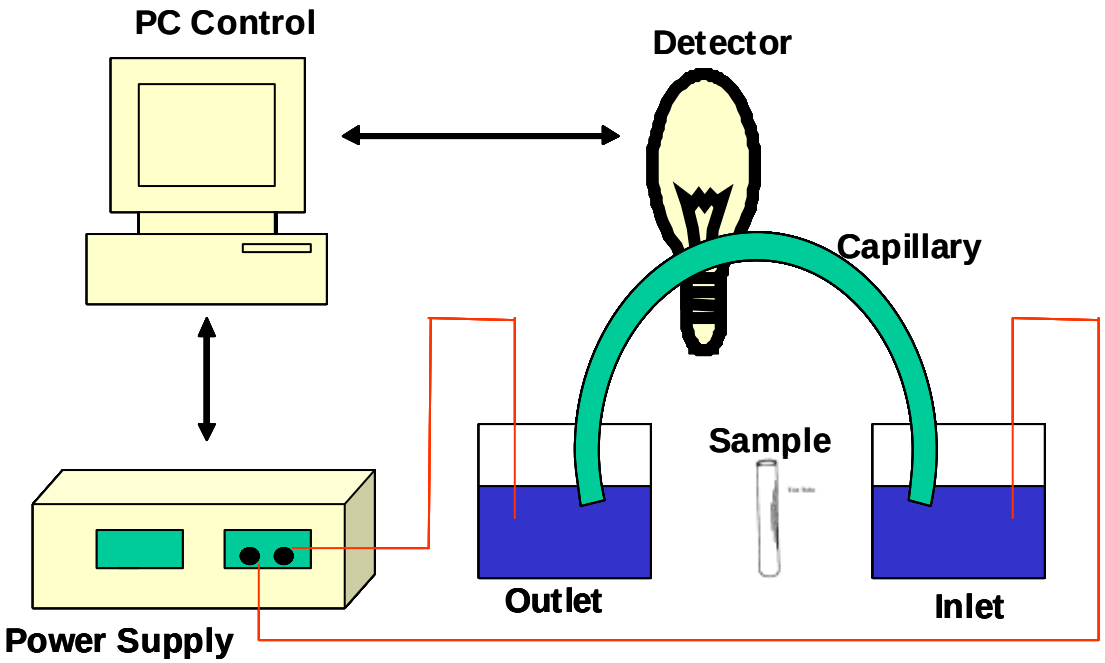

Fig 2.2 is a schematic diagram of the essential components of CE. The two ends of a fused-silica capillary are placed in buffer reservoirs filled with the buffer electrolyte. The CE is connected to a high-voltage power supply and the two electrodes are submerged in the buffer reservoirs to make electrical contact between the high voltage power supply and the capillary. The sample is filled into the capillary by swapping the inlet reservoir with a sample reservoir and applying either pressure (hydrodynamic injection) or an electric field (electrokinetic injection). Once the injection is completed, the electric field is applied in

order for separation to occur. The detection is completed at the opposite end directly through the capillary wall for optical detection or by combining with the other detection techniques, such as mass spectroscopy or electrochemical detection through specially designed interfaces that are required to minimise post-capillary dispersion during the detection step.

CEC is an amalgam technique between high performance liquid chromatography (HPLC) and the traditional polyacrylamide gel electrophoresis, using the resolving technique of electrophoresis combined with the instrumentation and automation concept of chromatography [1]. It derived from a family of techniques that utilise narrow bore columns to conduct high efficiency resolutions for both small and large molecules.

2.1.1 Electrophoretic Mobility

The mobility (movement) of a charged analyte under the power of an applied electric field is determined by its electrophoretic mobility (μ_e). Electrophoretic mobility is dependent on viscosity of the background electrolyte, charge density of solute and ionic characteristics of the capillary surface and electric double layer. Electrophoretic mobility is temperature dependent. The apparent electrophoretic mobility (μ_a) is the sum of EOF (μ_{eof} with the presence of EOF) and the electrophoretic mobility of the analyte (μ_e).

$$\mu_a = \mu_e + \mu_{eof} \quad \text{.....Equation 01}$$

The apparent mobility can also be determined using equation 02

$$\mu_a = \frac{l}{tE} = \frac{lL}{tV} \quad \text{.....Equation 02}$$

Where:

l = effective capillary length (cm)

L= total capillary length (cm)

t= migration time (s)

E= electric field (V/cm)

V= applied voltage (V)

The apparent mobility is measured in the presence of EOF and expressed as cm^2/ Vs. Neutral markers such as methanol, acetone, dimethyl sulfoxide, benzene can be used to measure the mobility of EOF [1]. The analytes migrate through the separation system according to their electrophoretic velocity. If a solute is positively charged, it gets attracted towards the cathode, whereas negatively charged solutes get attracted towards the anode.

2.1.2 Electroosmotic Flow (EOF)

Electroosmotic flow (EOF) is established in the separation capillary after the application of an electric field and describes the movement of the liquid phase through the separation system. The movement of the mobile phase is based on electroosmosis. EOF arises in fused silica capillaries due to dissociation of acidic silanol (Si-OH) groups at the surface of the capillary when in contact with a background electrolyte solution, according to:

$$\equiv SiOH \rightleftharpoons \equiv SiO^-(s) + H^+(aq)$$

Counterions (cations, in most cases) in the buffer are attracted to the surface of the negatively charged silanol groups to maintain charge balance. A double layer is then created resulting a potential difference (known as zeta potential).

Figure 2.3: Representation of double layers at the capillary wall

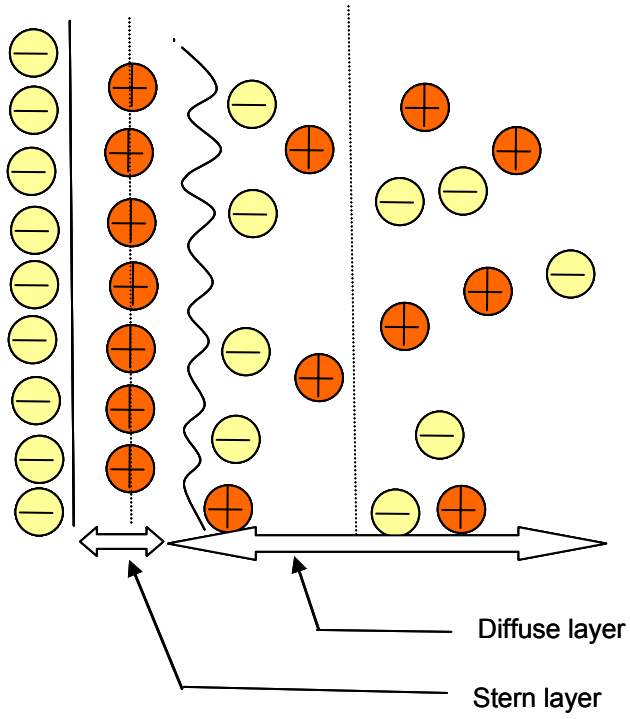

Hydrated cations in the background electrolyte solution are attracted to the negatively charged silanol groups and become arranged into double layers. As illustrated in Fig 2.3, one layer is firmly bound by electrostatic forces (compact layer), and the other is more loosely bound (diffuse layer). EOF arises when an electric field is applied. Anions are attracted to the anode and cations are attracted to the cathode. The accumulation of 'mobile' charge at the capillary wall can now migrate under the effect of the applied voltage. Hence cations will migrate towards the cathode and cause the bulk solution to move along with this diffuse chromatographic layer. The bulk solution moves towards the cathode, leading to electroosmotic solution flow.

The degree of the EOF can be expressed with respect to velocity by:

$$V_{EOF} = \mu_{eof} .E = (\varepsilon\zeta/\eta)E \quad \text{.....Equation 03}$$

Where:

$V_{EOF=}$ Velocity

ζ = Zeta potential

η = viscosity

ε = dielectric constant

E= electric field

μ_{eof}=mobility of electroosmotic flow

pH is the controlling factor of EOF due to its role in dissociation of the silanol groups. EOF is the major driving force, which causes the movement of nearly all species, irrespective of their charge, in the same direction. Usually the capillary surface is negatively charged and the EOF flow is from anode to cathode. Cations move faster since electrophoretic attraction is toward the cathode, and the EOF is in the same direction. Neutral molecules are carried at the same velocity as the EOF and anions migrate slowest since they are attracted to the anode, but are still carried by the EOF toward the cathode. EOF is not considerable at low pH due to protonation of the silanol group at the capillary wall whereas high pH results in deprotonation of the silanol group creating a quite considerable EOF. EOF can vary by more than an

order of magnitude between pH 2 and 12 depending on the specific conditions such as ionic strength of back ground electrolyte, which also have a significant impact on the EOF. The zeta potential is dependent on the ionic strength of the buffer electrolyte. Increased ionic strength results in double-layer compression, reduced zeta potential and decreased EOF [1]. The flat profile of flow within the capillary is a unique feature of EOF, as illustrated in Fig 2.4.

Figure 2.4: Flow profile and corresponding solute zone: A) EOF B) laminar flow

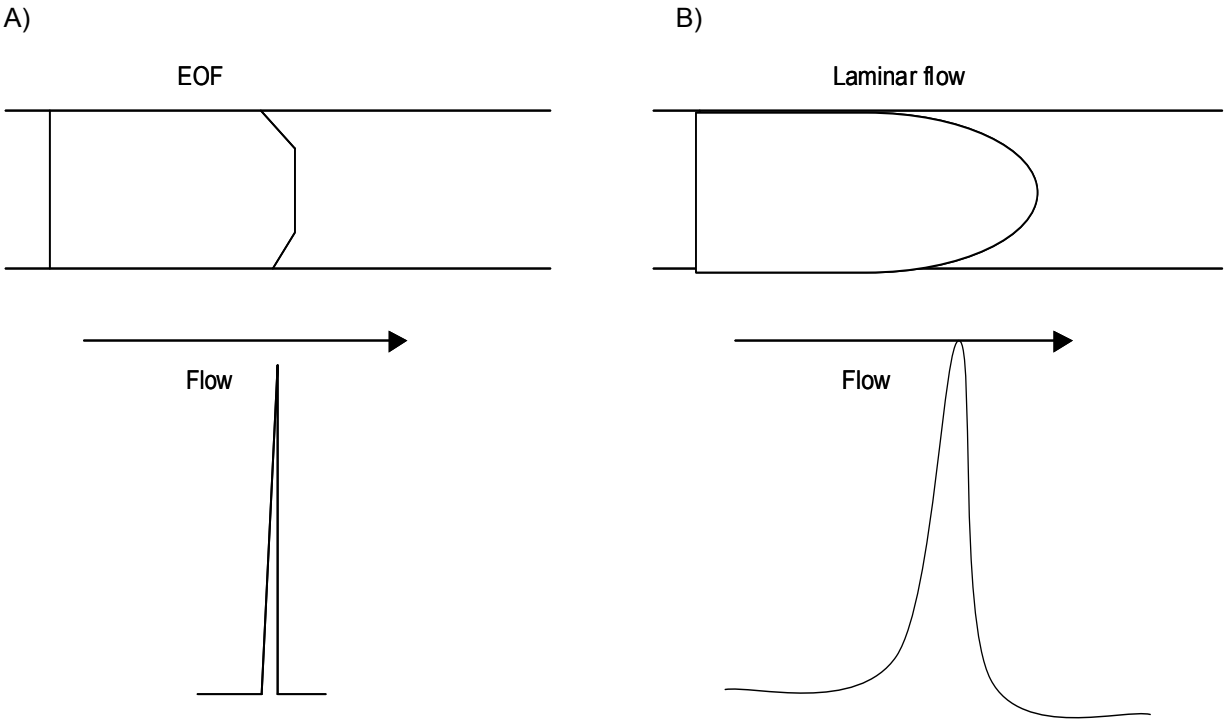

The flow within the capillary is nearly uniform laterally across the capillary due to their being no pressure drop within the capillary, and the driving force of the flow is uniformly distributed. The flat profile illustrated in Fig 2.4a is valuable since it does not directly contribute to the dispersion of solute zones. Note that the zone dispersion at the limit arises from molecular diffusion; contributes to band spreading are further discussed below. This is in comparison with that produced by an external pump, which yields a laminar flow (Fig 2.4b), due to the sheer force at the wall. Multi-flow effects supplement molecular diffusion, which

results in a broadened zone. Thus, in theory CE should be able to achieve much greater efficiency (defined by band spreading as a function of separation time) than pressure driven separation systems.

2.1.3 Factors affecting Efficiency

Different solutes have different mobilities; hence they migrate through the capillary at different speeds. This is the basic principle of CE separation; different migration speeds provide the basis for separation. Dispersion in CE can have a number of contributors on top of longitudinal diffusion. Dispersion can cause the zone length to change, and therefore affect solute separation. The factors that affect efficiency include joule heating, injection plug length, longitudinal diffusion, electromigration dispersion and sample adsorption, unleveled buffer reservoirs, detector cell size and mismatched conductivities.

2.1.3.1 Joule heating

Joule heating leads to temperature gradients and laminar flow. The transmission of electric current through an electrical solution results in the generation of heat arising from frictional collisions between mobile ions and buffer molecules. The capillary dimensions determine the degree of heating, i.e. a narrow bore capillary avoids joule heating due to alleviation of heat dissipation, conductivity of buffer, and the applied voltage [1]. Excessive heating may lead to a thermal gradient across the column, which can affect analyte movements through effects on μ_e for each solute and cause zone broadening [10].

2.1.3.2 Injection Plug length

It is vital to use as small as possible a sample plug length during injection for CE analysis. Injection lengths should be less than the diffusion-controlled zone length. The efficiency of analysis will be sacrificed and poor injections will be reflected in poor peak effieciency, if the sample plug length is longer than the dispersion caused by diffusion. Usually the sample plug length is required to be less than 1- 2% of the total capillary length unless sample preconcentration techniques such as stacking and sweeping cause injection zone compression to take place.

2.1.3.3 Sample adsorption

Irreversible or slowly reversible interaction of solute with the capillary walls usually leads to severe peak tailing for CE analysis. Ionic interactions are the primary cause of adsorption to the fused silica walls (i.e. between negatively charged walls and cationic solutes). Consequently, using coated capillaries can minimize deleterious interactions. Note that usually sorptive partitioning will not be desirable at the coated surface.

2.1.3.4 Electrodispersion

Differences in solute mobility cause the separation in electrophoresis. Dispersion, the spreading of the solute zone, is an outcome of differences in solute velocity within that zone. Dispersion should be controlled because it increases the length of the zone and the mobility difference necessary to obtain separation. Differences in running buffer conductivity and that of the solute zone can have major consequences result in skewed peak shapes, along with such effects as solute concentration or focusing (low conductivity solute) and solute defocusing (high conductivity solute) [10]. When the running buffer has a higher mobility than the solute zone, the leading edge of the solute zone will be sharp and the tailing edge will be diffuse. An opposite effect can be seen when the solute zone has higher mobility than the running buffer: the leading edge of the solute will be diffused and the tailing edge will be sharp. Symmetrical peaks are produced when the conductivities are equivalent.

2.1.4 Sample Injection methods

In order to maintain high efficiency, CE only requires minute volumes of samples. The injection volume should be kept as a small proportion to the volume of the capillary [11]. The sample plug length should be less than 1-2% of the total capillary length. The injection volume varies between 1- 50 nL depending on the capillary diameter. 10 µL of sample volume is sufficient to perform a large number of injections leading CE to be a regarded as a microscale technique; however small volumes increase sensitivity problems for low concentration samples. Hydrodynamic and electrokinetic injection methods are the most frequently used injection techniques.

2.1.4.1 Hydrodynamic injection

The most widely accepted sample injection method is hydrodynamic injection. The sample is loaded into the capillary by application of pressure at the injection end of the capillary, by siphoning action achieved by elevating the injection reservoir relative to the exit reservoir or by a vacuum at the exit end of the capillary. The quantity of sample loaded into the capillary is almost independent of the sample matrix. The volume, and hence quantity of sample injected is a function of the pressure difference across the capillary, the capillary internal dimensions, the injection time, solute solution and buffer viscosities [12]. The typical injection times and pressure vary from 0.5-5 s and 25-100 mbar respectively.

2.1.4.2 Electrokinetic injection

Due to simplicity and ease of control, electrokinetic or electromigration techniques may often be the chosen method. It is accomplished by replacing the injection-end reservoir with the sample vial and applying voltage. In electrokinetic injection, the sample enters the capillary by electrophoretic mobility and the pumping action of the EOF. A key feature of electrokinetic injection is that the amount loaded is dependent on the electrophoretic mobility of the individual solutes [1, 13, 14]. This leads to discrimination of ionic species since the high mobility ions are loaded to a level superior to those with less mobility; hence the injected amount is not representative of each analyte present in the original sample.

2.1.5 Online Sample Concentration- Stacking and Sweeping

The detection sensitivity of CE is relatively low due to the use of a low sample volume and narrow optical path length for on-capillary photometric detection compared to other chromatographic techniques. Quite a few techniques have been introduced to enhance the detection sensitivity by on-capillary sample concentration during or just after sample injection. The “Stacking” technique is one of the simplest on-capillary concentration methods and can take place as ions cross or stack at a boundary that separates regions of the high electric field sample zone and low electric field background solution zone. The difference in migration velocity of the pseudostationary phase (discussed below in section 2.2.5) within the two zones is the basis of the focusing effect. Stacking effectively means that the sample is introduced as a broad sample plug, and then the analytes are condensed in space into a narrow zone. Therefore, their

localised concentration is improved by the extent of zone compression. Stacking of target analytes can be obtained by dissolving the sample in a low conductivity buffer or water, for example 100 to 1000 times lower conductivity than that of background electrolyte, and performing hydrodynamic or electrokinetic sample injection. More than 10-fold sample enrichment can be accomplished by using this stacking technique. If the conductivity of the sample and background electrolyte is similar, stacking can be obtained by injecting a short water plug before sample introduction[15, 16].

"Sweeping" is known as the 'sorption' and accumulating of analytes by the pseudostationary phase that penetrates or passes into the sample zone devoid of pseudostationary phase, upon application of voltage. It is independent of the EOF and can be used for both charged and uncharged analytes [17]. Theoretically unlimited sample enrichment can be obtained for analytes that have high affinities toward the pseudostationary phase. The sample is dissolved in a matrix that is free of pseudostationary phase and has conductivity similar to background electrolyte. The sample is introduced by hydrodynamic injection at the cathodic end. Negative polarity voltage is then applied with the presence of a background electrolyte in the inlet vial; anionic pseudostationary phase will flow through the capillary and sweep the analytes. By using this sweeping technique, the detection sensitivity of both neutral and charged species can be improved, whereas the stacking technique is only successful for ionisable analytes. Sensitivity improvement of 100-5000 fold can be achieved by sweeping, as has been demonstrated by Quirino and Terabe [18, 19]. Theory and principles of online preconcentration techniques are discussed in Chapter 7.

2.1.6 Resolution

The purpose of all chromatographic methods is to separate the individual components in the sample. The resolution, R_s, is used to express the level of separation between two adjacent components, 1 and 2. [13].

$$Rs = \frac{2(t_{mig,2} - t_{mig,1})}{(W_1+W_2)} = \frac{t_{mig,2}-t_{mig,1}}{4\sigma} \qquad \text{.....Equation 04}$$

Where:

W= peak width (in time) at baseline

t = migration time (s)

σ = temporal standard deviation of peak width

R_s value corresponds to 2.0 in this thesis

2.2 Separation modes of CE

The flexibility of CE originates partially from its various modes of operation. The fundamental electrophoretic separation modes in CE include Capillary Zone Electrophoresis (CZE), Capillary Gel Electrophoresis (CGE), Capillary Isoelectric Focusing (CEIF), Capillary Isotachophoresis (CITP), Capillary Electro Chromatography (CEC), and Micellar Electrokinetic Chromatography (MEKC). A few fundamental modes of CE will be discussed below.

2.2.1 Capillary zone electrophoresis (CZE)

CZE is the most basic and widely used mode of CE and it can be used for the analysis of both cations and anions in a single analysis. In CZE the composition of the background electrolyte is constant both in the capillary and the buffer reservoirs around the two electrodes. Upon introduction of a sample, each species of analytes migrate in the buffer electrolyte in a discrete zone and at a different velocity compared with other species. In CZE the cations and anions migrate in opposite directions; however the number of analytes swept towards the cathode due to electroosmotic flow is relatively high compared with the electrophoretic velocity of analytes. In a typical study conducted at a pH above 4, electroosmosis is relatively high, and the EOF ensures that both migration of cations and anions are towards the cathode. When applying “positive” potential electrolytes, analytes elute from the capillary in order of decreasing positive charge. Cations elute first due to the direction of migration being the same as the direction of EOF (co-migration). Neutral analytes elute next however they remain unresolved as they lack electrophoretic mobility. Anions elute last because they have a tendency to migrate in the opposite direction to the EOF (i.e. back towards injection end). Different migration magnitudes of analytes are due mainly to different charge densities of the ionic species, which can be affected by the pH of the buffer electrolyte. Usually, optimisation of separation can be achieved by altering buffer pH. When changes to

buffer pH do not support successful separation, selectivity can be obtained by the addition of additives into the buffer electrolyte (additives such as: ion-pairing reagents, complexing agents, chelating agents, organic solvents and various shape-selective additives). For example, cyclodextrins (CDs) are used as chiral selectors and can contribute to shape selectivity even for achiral analytes for improving separation under certain conditions [20, 21].

The use of CDs as chiral selectors in CZE is one of the most popular techniques. To achieve chiral recognition, various types of CDs are used in CD-CZE, including natural non-ionic CDs such as α, β, γ CDs, derivatised neutral CDS such as dimethyl, trimethyl and hydroxy propyl CDs, or derivatised ionic CDs such as carboxymethylated and sulfated CDs. The mechanism by which separation occurs with CD additives is via the selective inclusion of solute into the cavity of the CD molecule. The derivatised forms of CDs offer quite different molecular association behaviour. The derivatised CDs can improve the properties of the native form of CDs, such as enantioselectivity and solubility, thus permitting a wider range of compounds to be separated. The separation mechanism occurs via stereospecific inclusion of solute molecules into the cavity of the CD molecule, thus generating a host-guest complex. In the separation of isomers, one form of isomer favors inclusion into the cavity of the CD compared to the other isomer. Hence the isomer, which was included into the CD cavity, will have a reduced mobility, assuming the CD to be the slower moving species in the buffer electrolyte. This association is a dynamic process and is known as host-guest complexation. The differences in mobility between the complexed and uncomplexed form lead to the resolution of enantiomeric compounds. The resolution of isomers depends on the stability of the complex formed.

Figure 2.5: A schematic diagram showing the CZE separation of analyte zones

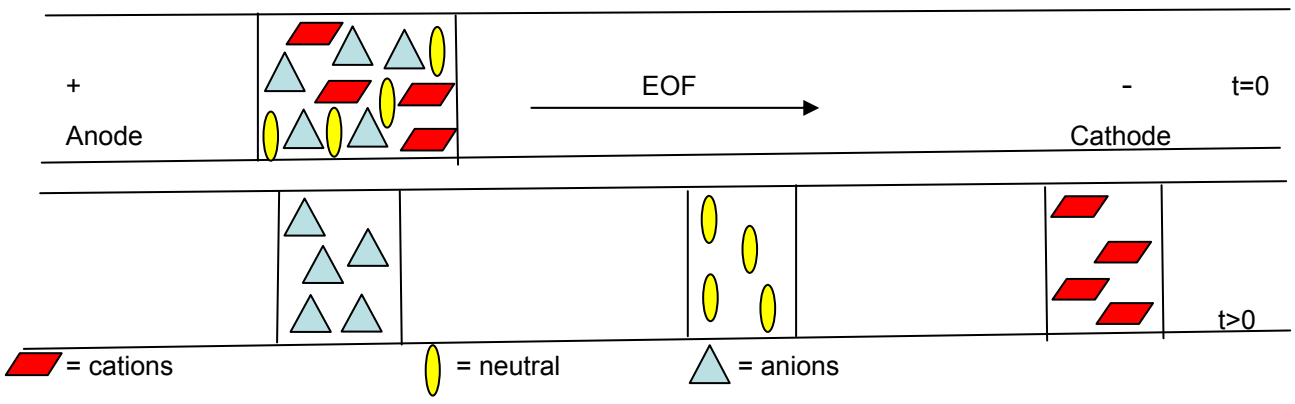

2.2.2 Capillary Gel electrophoresis (CGE)

CGE is the CE-analog of the long-established slab-gel electrophoresis. The separation is conducted by filling the capillary with a sieve-like matrix such as agarose or cross-linked polyacrylamide [22]. This mode can be used to analyse oligonucleotides, proteins and DNA, where the mechanism is a combination of electrophoretic mobility and size of solute (or size of solute to pore size of gel).

2.2.3 Capillary Electro Chromatography (CEC)

CEC is an emerging technique however apparently not without its technical difficulties. CEC is a hybrid of liquid chromatography (LC) and CE [23]. CEC is effectively HPLC in packed microbore columns, performed using a CE instrument thus providing an electrodriven migration force. In CEC the capillary is filled with a stationary phase similar to those used in LC. The transport through the column is performed by electroosmosis and electrophoretic mobility. Upon application of an electric field the EOF moves the mobile phase through the packed column. The separation selectivity is dependent on partition of analytes between the stationary phase and the mobile phase. Peak dispersion is minimised by a uniform velocity profile. Neutral solutes can be analysed efficiently using this mode. The molecules that obtain separation by CEC vary from small inorganic and organic moieties to peptides and proteins [24].

2.2.4 Capillary Isotachophoresis (CITP)

CITP consist of two buffer reservoirs comprising different solutions. The analytes are sandwiched in between leading and trailing electrolytes (the solutions in each reservoir), which leads to a steady state in which the solute zones migrate in the order of decreasing mobility [25]. Migration of all solute zones at the same velocity and all having the concentration of the leading electrolyte are the unique concepts of CITP. Samples can be concentrated by many orders of magnitude.

2.2.5 Micellar Electrokinetic Capillary Chromatography (MEKC)

MEKC was introduced in 1984 by Terabe [26]. It is now recognised as a powerful separation technique for electrically neutral analytes. This separation technique might be constrained as having principles of both electrophoresis (ion separation) and chromatography (partition). The key feature of MEKC is the addition of surfactant into the buffer solution. Upon addition of surfactant above its critical micelle concentration (CMC), aggregation of the surfactant molecules develops the micellar phase, which then acts as the pseudostationary phase. The formation of a micellar phase is a prerequisite for the separation in MEKC and this now provides a partitioning mechanism to be introduced into the electrophoretic experiment.

Micelles are amphiphilic (10-50 C units) and consist of a hydrophilic head group and a hydrophobic tail [27]. Surfactants that can be used in MEKC include anionic (sodium dodecyl sulfate), cationic (cetyltrimethylammonium bromide), zwitterionic and nonionic surfactants (surfactants should be miscible, compatible with aqueous and other buffers). Separation of neutral analytes occurs via interaction of the analyte with the micelle. Association of the analyte with the micelle results in the retardation of analyte velocity [27]. The neutral analytes are separated based on their hydrophobicity. Separation of neutral analytes in MEKC depends on the partitioning of neutral analytes between the electrokinetically migrated micellar phase and the electroosmotically pumped aqueous phase. Analytes partitioned fully into the micelle would reach the detector at the same time t_m (migration time of micelle), which is longer than t_0 (a fully excluded neutral analyte time) as the anionic micelles migrate upstream. When a neutral analyte equlibriates or partitions between the micelle interior and free solution, its migration time is decreased because it has a net migration faster than the micelle. In this circumstance, the neutral analyte reaches the detector between the migration times t_0 and t_m. The more time the neutral analyte spends within the micelle, the longer the migration time becomes. The higher the hydrophobicity of a neutral molecule, the more time it spends within the micelle, resulting in a longer migration time.

Fig: 2.6: Schematic representation of the separation principle of MEKC

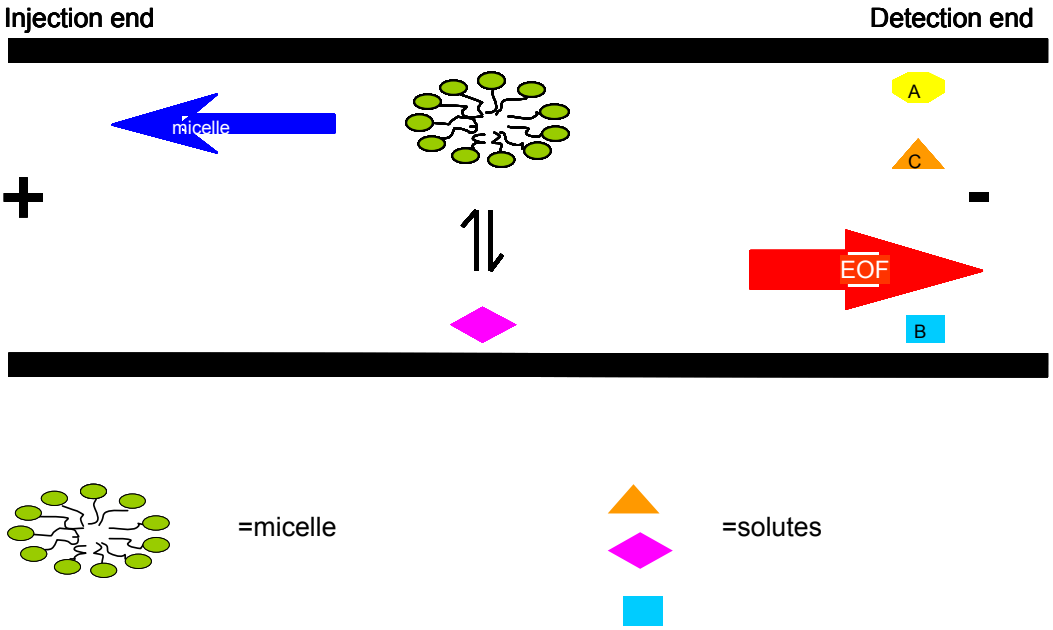

Anionic micelles migrate toward the cathode due to the EOF mobility being larger than the electrophoretic mobility of the micelles attraction. Cationic micelles behave in the opposite way to anionic micelles; hence polarity reversal is required to enable analyte migration toward the detector. Without the presence of the micelles, neutral solutes would reach the detector at the same time, t_0. Unretained molecules migrate at the same rate as EOF. Cation and anion migration times are also affected by the micelle, due to analyte partitioning between the solutes and the micelle and electrostatic interaction with the micelle. The partition coefficient (K) of analytes can be altered by using different types of surfactants such as anionic, cationic and neutral. Cationic surfactants also change the charge on the wall, which leads to change in EOF direction. Analytes that are hard to separate with the CZE mode such as amino acids, carbohydrates, nucleic acids, peptides, phenols, organonucleic acids can be analysed using MEKC. MEKC is most suited for low-to-medium hydrophobicity compounds.

Figure 2.7: A schematic representation of an ionic micelle

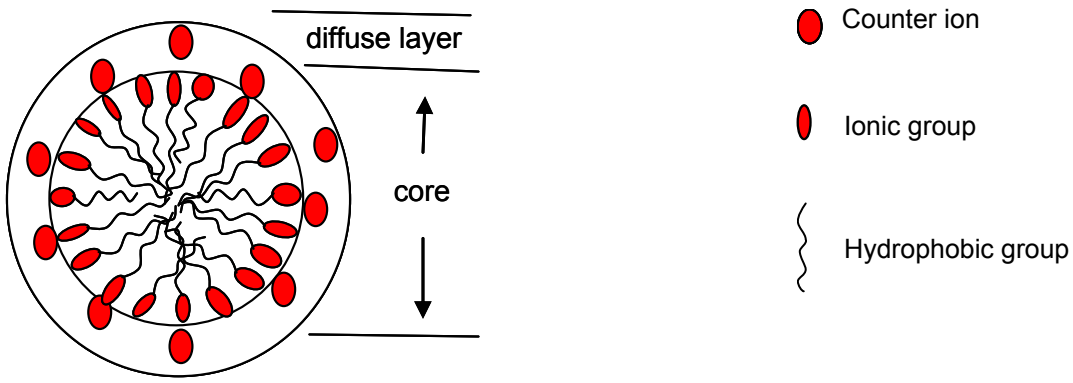

The capacity factor (k) is a measure of the ratio of total mole of solutes in the micellar phase to those in the aqueous phase. The capacity factor can be determined by equation 5 [13, 21].

$$k = \frac{t_R - t_0}{t_0 \left[1 - \frac{t_R}{t_m} \right]} \quad \text{.....Equation 05}$$

t_R = migration time of the solute

t_0 = migration time of unretained solute moving at the same rate as EOF “dead time”

t_m= micelle migration time

k = capacity factor

Migration time of neutral analytes occurs within a time window as shown in Fig 2.8. Hydrophobic neutral solutes do not interact with the micelle; hence they elute with the EOF. Electrically neutral solutes elute between t_0 and t_m. In an analysis, it is ideal to have slow EOF and high mobility micelles [27], which lead to increase in capacity of the MEKC method. Note that charged solutes may also be analysed by using MEKC, but will migrate outside or within the ‘window’ according to their specific electrophoretic and k properties.

Figure 2.8: Typical elution window solutes in MEKC

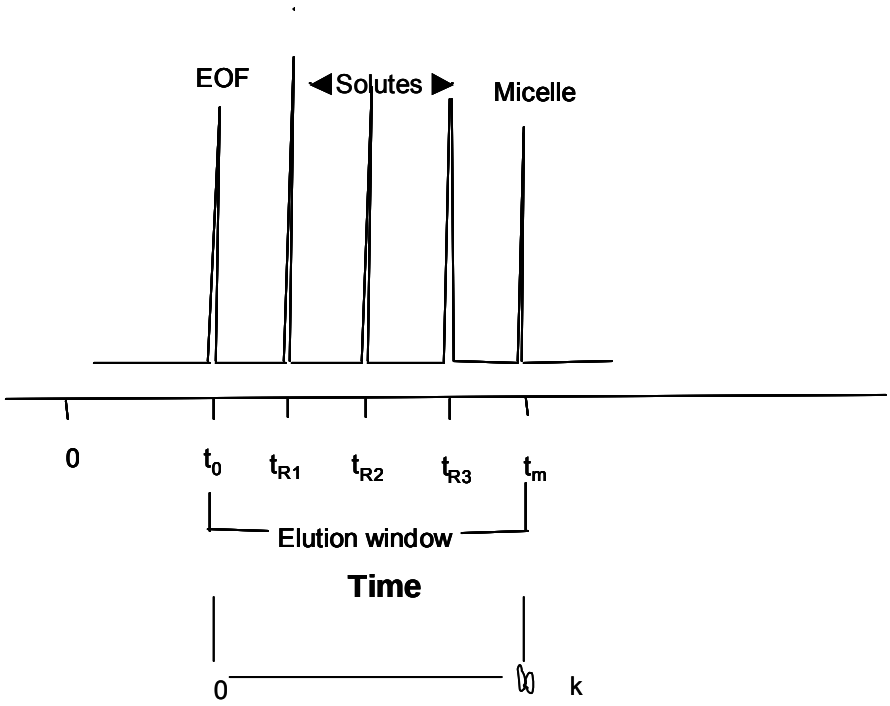

2.3 Optimisation of CE

Usually the optimisation procedure is one of the most complicated phases of method development, as so many parameters need to consider (i.e. mode of CE, choice of detection, buffer property choices that maximize the separation of solutes). To achieve successful optimisation, its early stages depend on a laborious experimental schedule that determines the effects of significant factors on the chosen analytical response (separation). Optimisation of a separation technique is traditionally performed by systematically varying one factor whilst holding remaining factors at a constant level (one-variable-at-a-time optimisation). The drawback to this approach is the large number of experiments that may need to be performed, leading to lengthy time requirements and cost, which often makes this strategy impracticable to be done thoroughly. In addition, if interactive effects of two or more variables were crucial to compute

the overall best result, the “one-variable-at-a-time” approach would not reveal this. The alternative approach to “one-variable-at-a-time” is to employ an experimental design approach.

2.3.1 Experimental Design approach

Experimental designs are statistical approaches, which can be applied to any experiment with “outcome” (response) determined by experimental variables. Multi-variate optimisation events involve a simultaneous alteration of all experimental parameters examined according to an experimental design. Experimental designs are setup in such a way that maximum information is obtained from a minimum number of experiments [28]. The main advantages of using a multi-variate setup in optimising a separation technique include reduction in the number of experiments and improved statistical interpretations, which lead to reduction in time and cost requirements. Also, interaction effects between significant factors can be investigated with multi-variate experiments, which would be impossible to do with a uni-variate setup.

A common approach for optimisation is to first screen for significant factors using a full or fractional factorial design [29]. A multi-level response surface design such as the Central Composite Design can then be used to optimise the factors [29]. Response models from experimental designs, such as Central Composite Designs, can offer a primary indication of robustness of the method [29, 30]. A validation and robustness check can then be carried out using a reduced factorial design applied in the domain around the optimal region. Chapter 4 discusses the theory of experimental design in detail.

2.4 Derivatisation

Just as the chromatographic separation technique must be carefully selected and adjusted to give suitable separation of target compounds, so the detector used as a chemical transducer to record the elution of compounds must be appropriate for the compounds. Sometimes available detectors are not suitable and modification of the compound is required.

Chemical derivatisation is a process where a compound or analyte with poor sensitivity or detectability, due to its transparency in the detector, is chemically modified to produce a new compound, which has suitable spectroscopic properties for analysis using a chromatographic instrument [13]. The derivatisation can be performed as pre-column derivatisation or as post-column derivatisation. Pre-column derivatisation is conducted before analytes are separated with either manual or by an automate derivatisation system. Pre-column derivatisation can be performed for small molecules such as amino acids. Post-column derivatisation is usually performed after analytes are separated but before the analytes reach the detector. Post-column derivatisation is usually performed for large molecules such as peptides [31]. Post-column derivatisation needs to be done carefully to minimise band broadening (i.e. post column fluorescence detection). The pre-column derivatisation has major advantages. These advantages include no restrictions on the reaction kinetics, provided that the reaction goes to completion within a reasonable time, yielding one derivatisation product of the compound without the formation of side products and the degradation products or the excess reagent formed during derivatisation will usually be separable from the derivative. However pre-column derivatisation alters chemistry of the compound; so alters the migration time. The disadvantages of post-column derivatisation include time-consuming procedures, due to each sample needing individual handling, and occurrence of potentially interfering peaks in the electropherogram, due to degradation products or impurities of reagents and solvents, in CE also the design limitations.

Derivatisation reactions can be either labelling or non-labelling reactions. In labelling reactions, the analyte reacts with another organic molecule, such as a chromophore, a flurophore, a radiophore or electrophore to enhance detectability and chromatographic properties. In non-labelling reactions, the analyte is converted to a suitable derivative by means of several manipulation mechanisms that are not based; in general, on the attachment of another molecule to the analyte (this enhances separation property, i.e. better GC or HPLC peak shape).

UV-vis and fluorescence detection is often hindered by the poor spectral properties at the applied analytical wavelengths of the native compound (i.e. amino acids). After derivatisation, UV-vis and fluorescence detection offers the advantage of a relatively free choice of the label enabling the introduction of a derivative with a high absorptivity.

2-nitrobenzaldehyde is the derivatising reagent used in the nitrofuran study in this thesis. 2-nitrobenzaldehyde in combination with a primary amine group yields a nitrophenyl derivative with intense UV absorptivity and also increased molecular weight. The derivatisation step helps to prevent the metabolites of the nitrofuran antibiotics from rebinding to protein and also to produces derivatives which possess a chromophore suitable for UV detection. Heating and evaporation are important steps of the derivatisation procedure. According to a previous study [32], longer reaction time of the derivatisation process was reported. There was no increase in analyte signal observed after this time. The heating block used in nitrofuran study is shown Fig 3.1 of Chaper 3.

2.5 Sample Extraction Techniques

The purification of analytes from the matrix and the concentration enhancement can be done using sample extraction techniques such as Liquid- Liquid Extraction (LLE) and Solid Phase Extraction (SPE).

2.5.1 Liquid-Liquid Extraction (LLE)

Liquid-Liquid Extraction is known as a solvent extraction technique. The separation of analytes using LLE is based on their preference for two different immiscible liquids, normally organic solvent and water-based solvent. It is an extraction of an analyte from one liquid phase to another liquid phase. Solvents vary in their extraction capacity depending on their own solute structure. The organic solvents generally used for extraction are toluene, diethyl ether, di-isopropyl ether, di-choromethane and light petroleum. The solvent selected will depend upon the solubility of the analyte to be extracted in that solvent and upon the ease with which the solvent can be separated from the solute. Diethyl ether's dominant solvent properties and low boiling point renders its removal extremely simple [33]. A distribution ratio in a solvent extraction is estimated by how well extracted a species is. The distribution ratio (D) is equal to the concentration of a species in the organic phase divided by its concentration in the aqueous phase.

All the compounds of interest will migrate into the extracting phase for samples of high partition coefficient; a low coefficient means very little of the compound of interest has migrated into the extracting

phase. Most of the sample ends up in the extracting solvent when the partition coefficient has been maximised and it results in a better interaction of analyte-extracting solvent than the analyte-sample matrix [34].

2.5.2 Solid Phase Extraction (SPE)

Solid Phase Extraction (SPE) is one of the various techniques offered to bridge the gap that exists between the sample collection and the analysis step [32]. The devices used in SPE are small cartridges or disks that contain a small quantity of sorbent either held in place by two frits, in the case of the cartridges, or enmeshed in a network of inert fibres, in the case of the disks. The major advantage of the disks is that faster flow rates during sample loading (20-80 mL/min) may be compared with the cartridges (1-10 mL/min), owing to the large cross-sectional area and adsorption surface of the disks [13]. SPE is a successful technique for the extraction of nitrofuran derivative due to its sample clean up ability. The sorbent material of the SPE cartridges enables a strong and quite selective retention of the nitro-aromatic derivatives (π-π interaction) while most of the matrix compounds are weakly retained. The three major steps of SPE are:

- Concentration
- Sample Clean up
- Matrix removal/Solvent exchange

Concentration of analytes is important to achieve higher response especially for analytes in trace amounts in order to quantify the solutes accurately. The concentration step is performed by passing a large volume of sample through the smallest bed of sorbent which will retain all of the analytes. The elution volume is the lowest possible to ensure the maximum concentration of the analytes. Sample clean up steps ensure the purity of the analytes during the matrix removal step. The sample is converted into a form that is compatible with the instrument to be employed. A schematic representation of principles of SPE is shown in Fig 2.9. Fig 3.2 and 3.3 of Chapter 3 show the SPE apparatus used in nitrofuran study and schematic representation of preparation steps of SPE and the respectively.

Figure 2.9: A schematic representation of the major steps of Solid Phase Extraction

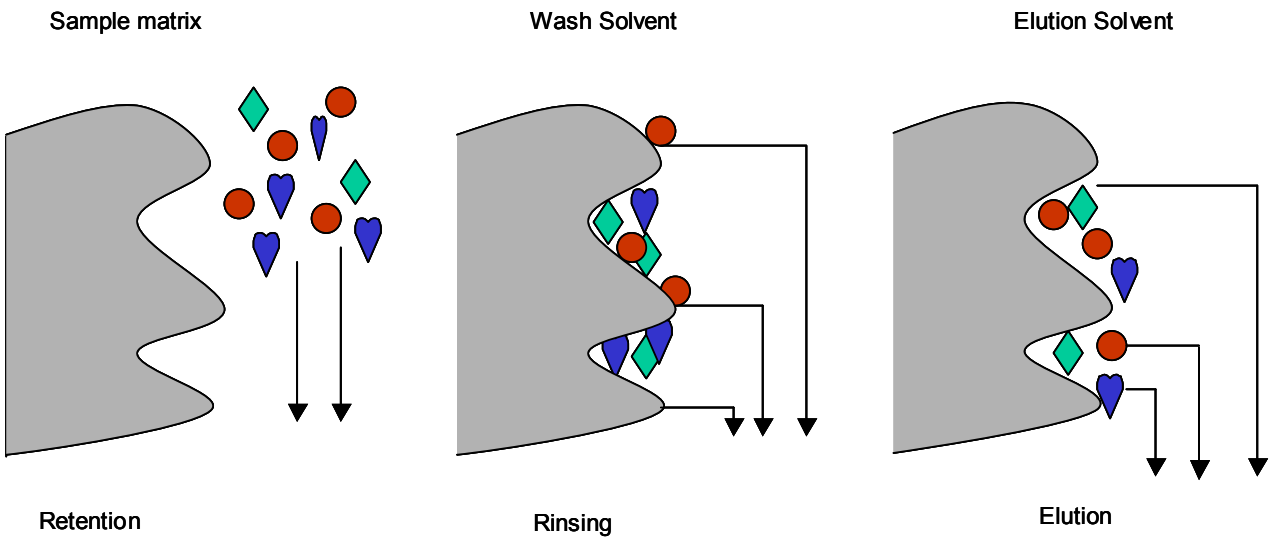

2.6 References

1. Heiger, D.N., *High performance capillary electrophoresis*. 2nd ed. 1992: Hewlett-Packard, Germany.

2. Jorgenson, J.W. and K.D. Lukacs, *Zone electrophoresis in open tubular glass capillaries.* J. High Resol. Chromatogr., 1981. **4**: p. 230-231.

3. Chiari, M., et al., *Determination of total vitamin C in fruits by capillary zone electrophoresis.* J. Chromatogr. A, 1993. **761**: p. 297- 305.

4. Paterson, B., C.E. Cowie, and P.E. Jackson, *Determination of phenolic compounds in surface water using liquid chromatography with electrochemical detection.* J. Chromatogr. A, 1996. **731**: p. 95-102.

5. Lehmann, R., W. Voelter, and H.M. Liebich, *Capillary electrophoresis in clinical chemistry.* J. Chromatogr. B., 1997. **697**: p. 3-35.

6. Steuer, W., I. Grant, and F. Erni, *Comparison of high-performance liquid chromatography, supercritical fluid chromatography and capillary zone electrophoresis in drug analysis.* J. Chromatogr., 1990. **507**: p. 125-140.

7. Ng, C.L., H.K. Lee, and S.F.Y. Li, *Analaysis of food additives by ion-pairing electrokinetic chromatography.* J. Chromatogr. Sci., 1992. **30**: p. 167-170.

8. Jimidar, M., et al., *Comparison of capillary zone electrophoresis with high-performance liquid chromatography for the determination of additives on food stuffs.* J. Chromatogr., 1993. **636**: p. 179-186.

9. Altria, K.D., *Overview of capillary electrophoresis and capillary electrochromatography.* J. Chromatogr. A, 1999. **856**: p. 443-463.

10. Foret, A., *Electrophoresis library.* by Ed Radola, B. J., 1993: p. 375.

11. Sepaniak, M.J. and R.O. Cole, *Column efficiency in micellar electrokinetic capillary chromatography.* Anal. Chem., 1987. **59**: p. 472-476.

12. Yang, Q., K. Hidajat, and S.F.Y. Li, *Trends in capillary electrophoresis.* J. Chromatographic Science, 1997. **35**: p. 358- 373.

13. Weston, A. and P.R. Brown, *HPLC and CE- principles and practice*. 1997, Califonia: Academic Press Limited.

14. Taylor, P.N., M.D. Scrimshaw, and J.N. Lester, *Supercritical fluid extraction ofacidic herbicides from sediment.* Intern. J. Environ. Anal. Chem., 1998. **69**(2): p. 141-155.

15. Quirino, J.P., et al., *Sample concentration by sample stacking and sweeping using a microemulsion and a single-isomer sulfated [beta]-cyclodextrin as pseudostationary phases in electrokinetic chromatography.* J. Chromatogr. A, 1999. **838**(1-2): p. 3-10.

16. Shihabi, Z.K., *Stacking in capillary zone electrophoresis.* J. Chromatogr. A, 2000. **902**: p. 107-117.

17. Quirino, J.P., J.-B. Kim, and S. Terabe, *Sweeping: concentration mechanism and applications to high sensitivity analysis in capillary electrophoresis.* J. Chromatogr. A., 2002. **965**: p. 357- 373.

18. Quirino, J.P., S. Terabe, and P. Bocek, *Sweeping of neutral analytes in electrokinetic chromatography with high-salt-containing matrixes.* Anal. Chem., 2000. **72**: p. 1934-1940.

19. Quirino, J.P. and S. Terabe, *Sweeping of Analyte Zones in Electrokinetic Chromatography. Anal. Chem.,* 1999. **71**(8): p. 1638-1644.

20. Harris, D.C., *Quantitative chemical analysis.* 5 th ed. W. H. Freeman, New York, 1999: p. 899.

21. Weinberger, R., *Practical capillary electrophoresis.* San Diego, USA, Academic Press Inc, 1993: p. 312.

22. Yin, H.F., J.A. Lu, and G. Schomburg, *Production of polyacrylamide gel filled capillaries for capillary gel electrophoresis (CGE).* J. High Resol. Chromatogr., 1990. **13**(9): p. 624-627.

23. Pretorius, V., B.J. Hopkins, and J.D. Schieke, *Electroosmosis. New concept of high speed liquid chromatography.* J. Chromatogr., 1974. **99**: p. 23-30.

24. Colon, L.A., Y. Guo, and A. Fremier, *Capillary Electrochromatography.* Anal. Chem, 1997. **69**(15): p. 461A-467A.

25. Kenndler, E., *Capillary zone electrophoresis and isotachophoresis: a comparison by information theory.* Chromatographia, 1990. **30**(11-12): p. 713-718.

26. Terabe, S., et al., *Electrokinetic Separations with Micellar Solutions and Open-Tubular Capillaries. Anal. Chem.*, 1984. **56**(1): p. 111-113.

27. Terabe, S., *Micellar Electrokinetic Chromatography.* Califonia, USA, Beckman Instruments Inc, 1992.

28. Safa, F. and M.R. Hadjmohammadi, *Chemometric approach in optimization of micellar liquid chromatographic separation of some halogenated phenols. Anal. Chim. Acta,* 2005. ***540***: p. 121-126.

29. Altria, K.D., et al., *Application of chemometis experimental designs in capillary electrophoresis.* Electrophoresis, 1995. **16**: p. 2143-2148.

30. Nguyen, A.M., *Development of a Supercritical Fluid Extraction- Gas Chromatography Method for Analysis of Synthetic Pyrethroids on Wool, in Applied Chemistry.* 1997.

31. Henk, L. and W.J.M. Underberg, *Detection- Orientated Derivatization Techniques in Liquid Chromatography*. 1990, New York: Marcel Dekker, Inc.

32. Leitner, A., P. Zollner, and W. Linder, *Determination of the metabolites of nitrofuran antibiotics in animal tissue by high-performance liquid chromatography-tandem mass spectrometry. J. Chromatogr. A*, 2001. ***939***: p. 49-58.

33. Jeffery, G.H., et al., *Vogel's Text book of quantitative chemical analysis*. 5th ed. 1989, New York: John Wiley & Sons, Inc.

34. Simpson, N.J.K., *Solid-Phase Extraction: Principles, Techniques, and Applications*. 2000, New York: Marcel Dekker.

CHAPTER 3

EXPERIMENTAL PROCEDURES AND METHODS

3.1 Instrumentation

3.1.1 Capillary Electrophoresis

Most experiments were carried out on the Applied Biosystem Inc. (model ABI 270 HT, San Jose, CA, USA) and Agilent -3D (model HP-3D, Wald Bronn, Germany) instruments. The ABI instrument is an enclosed CE unit with a UV-VIS detector and temperature control (which was maintained at 25°C throughout). Electrokinetic or hydrodynamic / (vacuum) injections can be performed using this CE instrument. The hydrodynamic injection is limited to only 5" or 20" Hg with time interval in units of 0.1 min can be performed.

The sweeping technique, replaceable stationary phase creation were carried out using an Agilent-3D system equipped with a diode array detector, which can be used to detect a signal wavelength versus a reference wavelength, and record absorbance spectra. Both hydrodynamic and electrokinetic injections can be performed using the Hewett Packard -3D instrument controlled by Chemstation. The electropherograms were recorded at 25°C.

The experimental settings used for both ABI and HP-3D systems for the two application areas are described below.

a) Analysis of nitrofuran antibiotics (NFAs) and metabolites (NFMs).

The wavelength was set at 275 nm with direct UV detection for the ABI instrument. The voltage used was varied between 10 kV to 20 kV. Electrokinetic injection of samples was carried out at 5 kV for 0.1 min.

b) Analysis of triadimenol isomer A and B

The separations were carried out using the ABI instrument with wavelength set at 220 nm. Samples were injected using electrokinetic injection at 5 kV for 0.1 min. The analysis was performed between 10 kV and 20 kV.

c) Stacking and Sweeping of triadimenol A and B

Stacking and Sweeping was carried out using an Agilent-3D instrument. The wavelength was set at 220 nm (4 nm band width) with the reference at 280 nm (20 nm) for the Agilent-3D instrument. In large volume stacking with polarity switching mode, the attempted sample plug length was 240 s at 50 mbar and 20 kV of negative polarity allowed for 50 s. The duration of the negative polarity was then reduced subsequently to 40 s, 30 s and 20 s to observe any peaks. Hydrodynamic injection of 50 millibar for 25 s injection was performed for the sweeping technique. The analysis was performed between 16 kV and 20 kV.

d) Analysis of mixture of Caffeine, Aspartame, Benzoic acid and Saccharine by RSP

The analysis was carried out using an Agilent-3D instrument. The wavelength was set at 211 nm. The voltage was varied between 16 kV to 20 kV. Hydrodynamic injection was performed using 50 millibar for 5 s duration. The separation temperature was maintained at 15ºC.

e) Analysis of NFA mixture by RSP

The analysis was carried out using an Agilent-3D instrument. The wavelength was set at 362 nm. The voltage varied between 16 kV to 20 kV. Hydrodynamic injection was performed using 50 millibar for 5s duration. The separation temperature was maintained at 15ºC.

3.1.2 Analytical balance

Weighing was performed using an analytical balance, which is accurate to 1 μg, (Denver Instrument Company, AA-200DS).

3.1.3 pH meter

A Metrohm 620 pH meter (Herisau, Switzerland) with an anode refillable double junction combination pH electrode was used for pH readings. The pH meter was calibrated with pH 7 followed by pH 4 or pH 10

accordingly. The glass electrode was stored in potassium chloride solution, rinsed with distilled water and dried between sample measurements.

3.1.4 Conductivity Meter

Conductivity measurements were made using the Activon model 301 conductivity meter. Calibration of the conductivity meter was performed with either 0.1 N or 0.01 N potassium chloride.

3.1.5 Microscope

Nikon labophoto 2 model was used in viewing the capillary column interior, in the replaceable stationary phase study with 40x magnification.

3.2 Computer Software

3.2.1 Capillary Electrophoresis Data Acquisition and Result Presentation

For the ABI CE, data were obtained by Shimadzu Class LC-10 (Shimadzu Oceania, Sydney, Australia) data acquisition software version 1.41. Data were converted from the Class LC-10 software into Microsoft Excel for Windows as text files and then imported to Origin 4.1 Graphics Program (Version 4.0, Microcal Software Inc., North Hampton, MA, USA) for electropherogram presentation. The response scale of the data system throughout the thesis is represented in a scale of mAU or μV.

For the Agilent-3D instrument, data were acquired by the Chemstation software and then exported from Chemstation software into .csv text files. The csv files were opened in Origin 6.0, or in Microsoft Excel and then imported into Origin 6.0, to create stacked or single layered chromatograms. The response scale of the data was expressed in mAU. CE expert software (Beckman Instruments, Inc., Fulleton, CA) was employed to calculate the length of sample injection.

3.2.2 Experimental Design

Minitab for Windows version 14 (Minitab Inc., State College, PA, USA) and Statistica version 05 (StatSoft, Inc, Tulsa, OK, USA) were used for experimental design and statistical data analysis. Minitab enables a

broad range of applications such as Fractional Factorial and Central Composite designs as well as Multivariate Regression data analysis. Statistica version 5 was used for surface plots.

3.3 Capillary column

Capillary columns were prepared from 50 µm and 75 µm uncoated fused silica capillaries (Phenomenex, Torrence, CA).

3.3.1 Preparation of Capillary Column

Capillary columns were prepared by cutting the appropriate length of uncoated fused silica capillary followed by removal of the polyamide coating at the window position. This was done by burning off a part of the capillary using a gas flame at an appropriate distance from the outlet end of the capillary coating in order to create a detection window. A capillary window of 0.5 cm was created to produce a transparent light path to match the slit on the detector of the CE. The outside of the capillary was then wiped with ethanol to clean it and to remove residual burnt polyamide coating. Once polyimide coating was removed, care was taken with handling due to the brittleness of the capillary column**.** Analysis of nitrofuran was performed using a 75 µm x 73 cm capillary column whereas separation of triadimenol fungicides was performed using a 50 µm x 64.5 cm capillary column. Sweeping of triadimenol was performed by using a 50 µm x 64.5 cm capillary column. The reversible stationary phase created using a 75 µm x 64.5 cm capillary column.

3.3.2 Conditioning of Capillary Columns

In order to activate the silica on the capillary wall, as a routine conditioning regime, the capillaries were washed daily with 1N NaOH for 10 min followed by purified water for 15 min. To ensure repeatability the capillary was flushed between runs with 0.1 N NaOH for 3 min followed by purified water for 5 min and electrophoretic buffer for 3 min. The new capillary columns were pressure rinsed with 1.0 N sodium hydroxide for 30 min followed by 40 min with water. To ensure reproducibility during the sweeping technique with triadimenol fungicides capillaries were flushed with 0.1N NaOH for 3 min followed by methanol for 3 min and purified water for 5 min between runs.

3.4 Chemicals

Four parent drugs, furazolidone, furaltadone, nitrofurazone, nitrofurantoin and their metabolites (AOZ, SEM, AHD, AMOZ), 2-NBA, sodium dodecyl sulfate, sodium dodeoxy cholate (SDC), β cyclodextrin, Hydroxy propyl β cyclodextrin, cobalt (11) chloride 6-hydrate, sulfated cyclodextrin sodium salt, Tartaric acid (L), tartaric acid (D), antimonyl tartrate were purchased from Sigma Aldrich (Sydney, Australia). The Bond ELUT C_{18} SPE cartridges were obtained from Varian P/L (Mulgrave, Australia). Acetonitrile (HPLC grade), hydrochloric acid and sodium hydroxide, dichoromethane, diethyl ether, glycine, sodium sulfate, potassium hydrogencarbonate, calcium chloride hydrate were obtained from Ajax (Sydney, Australia). HPLC grade methanol, acetic acid, ethanol, acetone, hexane were from BDH (Poole, England) and sodium borate and potassium dihydrogen orthophosphate were from Merck (Kilsyth, Australia). Low methoxy pectin was purchased from Hercules (Copenhagen, Denmark). Triadimenol isomer A and B were provided from the Department of Natural Resources and Environment (Australia). Deionised water was further purified using an Ultrapure Milli-Q system for all experiments. Electrophoresis and preconcentration techniques were performed in fused silica capillaries of 50 μm inner diameter and 375 μm outer diameter obtained from (Phenomenex, Torrence, CA).

3.5 Methods

3.5.1 Nitrofuran antibiotics and metabolite analysis methods

3.5.1.1 Buffer and Sample Preparation for Nitrofuran antibiotics and metabolite analysis

Stock solutions (1000 μg mL^{-1}) of NFA were prepared by dissolving the approximate mass of solid in 30:70 acetonitrile: water, stored at 4ºC in the dark and then diluted to the desired concentration prior to use. 1000 μg mL^{-1} stock solutions of NFM were prepared in Milli-Q water. The running electrolyte contained sodium borate, potassium dihydrogen orthophosphate and the appropriate concentration of surfactant, adjusted to the desired pH value with either 0.1 N hydrochloric acid or 0.1 N sodium hydroxide. The borate to phosphate buffer ratio in the electrolyte was varied in order to determine the best ratio. It

was observed that SDC did not readily dissolve in the phosphate buffer in the absence of borate in the electrolyte, and pH adjustments were most appropriately performed when phosphate was present in the electrolyte with borate. Organic solvents were added to buffer on a *v/v%* basis. The pH values of the electrolyte solutions were adjusted after addition of the organic solvents. All solutions were filtered with 0.45 µm syringe filters (Advatec MFS Inc., Dublin, CA, USA).

3.5.1.2 Derivatisation procedure for NFMs

To 600 µL of a solution comprising all NFMs in a glass vial, 10 mL of 125 mM HCl and 150 µL of 2-NBA were added. According to previous studies the mixture was vortexed for 2 min and kept in an aluminium-heating block at 37° C for 16 h [1]. It was found during the course of this study that effective derivatisation could be achieved by heating for 1 h in the heating block at a temperature of 70° C. Fig 3.1 shows a picture of heating block used in the NF study. The mixture was then removed and allowed to cool to room temperature, and pH was adjusted to 7.4 with 2 N aqueous NaOH. Other derivatising reagents such as pyridine-3-carboxaldehyde, 2,4-dinitrobenzaldehyde and s-hydroxyl-5-nitrobenzaldehyde were used to reduce the analysis time. Unfortunately none of these derivatising reagents gave shorter analysis time or better sensitivity [1].

Figure 3.1: Photograph of the heating block used in the derivatising procedure of nitrofuran metabolites

3.5.1.3 Solid- Phase Extraction (SPE)

The sample clean up and analyte enrichment was perfomed by SPE. SPE provides effective analyte clean up, and the sorbent material of SPE cartridges enables a strong and quite selective retention of the nitro-amide derivative (π- π interaction) while most of the matrix compounds are weakly retained. The derivatised solution was applied to a Varian Bond ELUT C_{18} SPE cartridge, which was preconditioned under vacuum with 3 mL of acetonitrile followed by 3 mL of water [2]. After the sample was loaded, the cartridge was dried by passing air through for 1 min and then washed with 2 mL of water. 3 mL of hexane was then applied to the cartridge to elute excess reagent (2-NBA). Without the hexane step, 2-NBA appears as a large interfering peak in the CE analysis; >90% of 2-NBA is removed in this step. Little analyte loss occurs during this hexane wash, as there were negligible analyte peaks in the hexane eluate. Initially 2 mL of ethyl acetate followed by evaporation under nitrogen was attempted for recovery of analytes. The choice of ethyl acetate was changed to acetonitrile due to observation of analyte loss during evaporation. Elution of analytes was obtained with 600 μL of acetonitrile followed by 1.4 mL of water. The eluates were filtered through a 0.45 μm filter prior to CE analysis. The total recovery of analytes from SPE was ~80%. Recoveries of NFMs from aqueous solution were therefore found to be adequate. Fig 3.2 and 3.3 represent the SPE apparatus used in NF study and the schematic of SPE respectively.

Figure 3.2: Photograph of Solid Phase Extraction setup

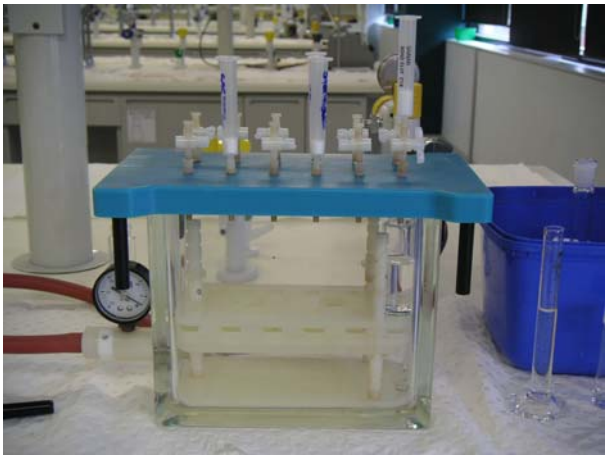

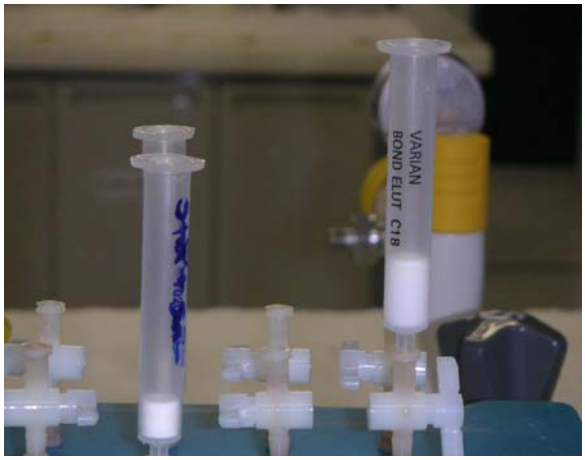

Figure 3.3: A schematic representation of Solid Phase Extraction process

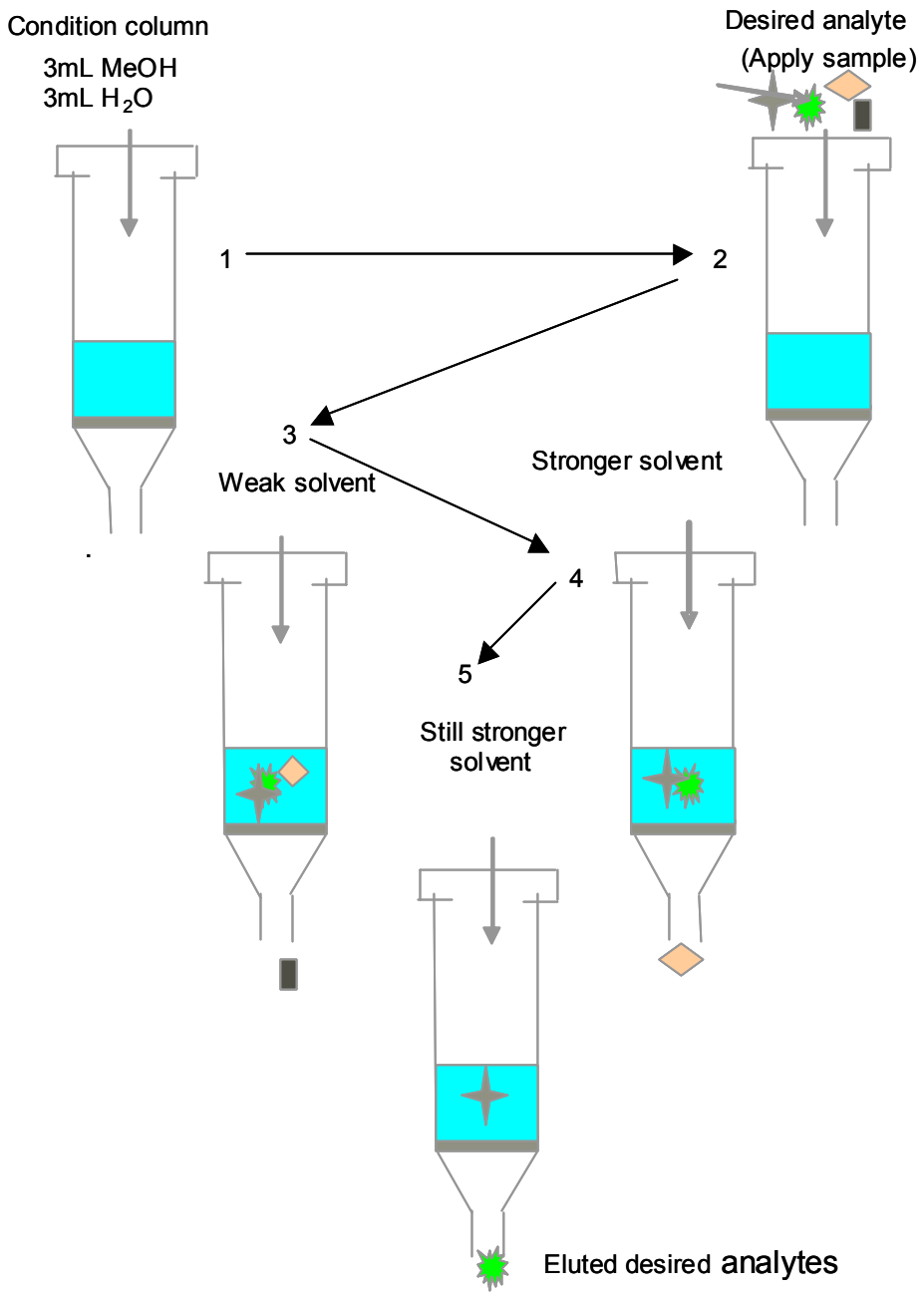

Steps 3-5 are solvent elimination steps which successively elute off undesired matrix material, then finally the target analyte.

3.5.1.4 Preparation of prawn samples for analysis

1 g of frozen prawns was ground and transferred to a 25 mL glass vial, 10 mL of 0.125 M hydrochloric acid was added and centrifuged at 2000 rpm for 15 min. The sample was filtered and then spiked with 375 µL of 100 $\mu g\ mL^{-1}$ of the metabolite mix followed by derivatisation and SPE procedure as above.

3.5.2 Triadimenol fungicides analysis methods

3.5.2.1 Buffer and Sample Preparation for Triadimenol Analysis

Stock solutions (1000 $\mu g\ mL^{-1}$) of Triadimenol isomer A and isomer B were prepared by dissolving the approximate mass of solid in HPLC grade methanol, stored at 4°C in the dark and then diluted to desired concentration prior to use. The running electrolyte contained 20 mM disodium hydrogen phosphate, 20 mM sodium borate, 50 mM sodium dodecyl sulphate and concentration of hydroxyl propyl cyclodextrin varying between 10-30 mM and percentage of methanol between 10-20% adjusted to desired pH value with either hydrochloric acid or sodium hydroxide. Initially beta cyclodextrin was attempted as a chiral selector. Finally hydroxy propyl cyclodextrin was the chosen chiral selector. All solutions were filtered with 0.45 µm syringe filters.

3.5.2.2 Preparation of grape samples for analysis

50 g of the frozen grape sample was spiked with (5 $\mu g\ mL^{-1}$ and 20 $\mu g\ mL^{-1}$) appropriate amounts of Triadimenol stock solutions. 200 mL of acetone was then added to the grape sample and blended for 5 min. A further 50 mL of acetone was used for washing up blending rods and filtering apparatus. The spiked grape sample was then filtered and filtrate was collected to use in liquid-liquid extraction.

3.5.2.3 Liquid- liquid Extraction (LLE)

To the filtrate of the grape sample, 650 mL of 4% sodium sulfate and 100 mL of dichloromethane was added. The mixture was shaken for about 1 min and allowed to settle inside the glass funnel. The filtrate

was then collected, a further 50 mL of dichloromethane was added and the above procedure was repeated twice. The final filtrate was added to a round bottom flask with boiling chips and keeper solution. The mixture was then heated in the water bath. Once the solution volume reached about 10 mL, 20 mL of hexane was added. The hexane step was repeated twice further and the final solution was retained for testing.

3.5.3 Preconcentration methods

3.5.3.1 Sweeping of Triadimenol fungicides

The background electrolyte containing 20 mM phosphate and 50 mM SDS was prepared each day by dilution of stock solutions, with pH adjustment using hydrochloric acid or sodium hydroxide as required. Cyclodextrin was dissolved in a phosphate buffer at the concentration required for the sulfated beta cyclodextrin sodium salt. Stock solutions (1000 $\mu g\ mL^{-1}$) of Triadimenol isomer A and isomer B were prepared by dissolving the approximate mass of solid in HPLC grade methanol, stored at 4°C in the dark and then diluted to desired concentration with a matrix that was free of SDS (pseudostationary phase). All solutions were filtered using 0.45 µm syringe filters.

3.5.4 Optimisation Study for Nitrofuran and Triadimenol analysis

Optimisation studies were conducted using a fractional factorial design (FFD), Central Composite Design (CCD) and full factorial design as part of a strategy to determine how factors, such as pH, buffer concentrations, voltage, and surfactant concentration affect the experimental goals; analysis time and resolution. To determine the optimum conditions for the compounds analysed, the experimental data obtained were treated using multi-linear regression. The Chromatographic Exponential Function (CEF) [3] was used as the objective function, to calculate the overall chromatogram quality.

The effects of pH, borate and phosphate concentration, surfactant concentration and voltage on the separation of nitrofuran antibiotics and metabolites were studied. Optimisation with 5 factors required 24 separate experimental conditions, and so experiments were performed in two orthogonal blocks, with

experiments carried out over two days. The order was randomised with each block. The individual experiment conditions used for screening of Nitrofuran analysis are listed in Table 3.1.

Table 3.1 Parameters setting used for optimisation study (FFD)

Run Number	Block	pH	[SDC] (mM)	Voltage (kV)	[Borate] (mM)	[Phosphate] (mM)
1	2	9.5	100	10	40	0
2	2*	8.5	60	15	20	20
3	2*	8.5	60	15	20	20
4	2*	8.5	60	15	20	20
5	2	9.5	100	10	0	40
6	2	7.5	20	10	0	40
7	2	9.5	100	20	0	0
8	2*	8.5	60	15	20	20
9	2	9.5	100	20	40	40
10	2	7.5	20	20	40	40
11	2	7.5	20	10	40	0
12	2	7.5	20	20	0	0
13	1*	8.5	60	15	20	20
14	1	9.5	20	10	40	40
15	1	9.5	20	20	0	40
16	1*	8.5	60	15	20	20
17	1*	8.5	60	15	20	20
18	1	7.5	100	10	40	40
19	1	7.5	100	20	40	0
20	1	7.5	100	10	0	0
21	1	9.5	20	20	40	0
22	1	9.5	20	10	0	0
23	1*	8.5	60	15	20	20
24	1	7.5	100	20	0	40

The centre points are shown asterisked (*).

3.5.5 Preparation of Reversible Stationary Phase (RSP)

3.5.5.1 Preparation of low methoxy pectin gel

Low methoxy pectin was chosen as the pore forming agent to create RSP. Smith [4] has proposed the following characteristics regarding low methoxy pectin. Low methoxy pectin at pH range of 2.5- 5.5, with soluble solids range of 30- 80%, with the presence of Ca^{2+} 10- 70 mg g^{-1} of pectin becomes cohesive to brittle in nature. Hence 0.2 g of low methoxy pectin was mixed with 10 mg of calcium chloride and dissolved with 20 mL of water. It was observed that the low methoxy pectin needed to dissolve fully before addition of $Ca^{2+.}$ The pH of the mixture was observed to be pH 4.0 and no pH adjustment was necessary. The mixture was then filtered through a 0.45 µm syringe filter.

3.5.5.2 Filling of RSP into the capillary column

The low methoxy pectin mixture was then filled into two electrolyte vials. The vials were then placed at the injection end and the detection end. The system was then flushed with 1000 milibar for 10 min with the low methoxy pectin and allowed for gelation over two days. Sample runs were conducted until observation of peak splitting in analysis.

3.5.5.3 Removing of RSP from the capillary column

The aged stationary phase was removed as required using hot water. The capillary column was flushed with hot water for two hours. The inlet containing hot water was replaced every 15 min to maintain high temperature of the inlet. The outlet vial contained material similar in consistency to glue, and this could most probably be the dissolved stationary phase flushed out of the capillary column. After complete removal of stationary phase, the capillary column was flushed with air to ensure a dry environment inside the capillary column.

3.5.5.4 Recreating RSP inside the capillary column

Low methoxy pectin gel was prepared and presse flushed into the capillary column as discussed in 3.5.7.1 and 3.5.7.2 respectively. The sample runs were performed and compared with previous runs before removing stationary phase for reproducibility, conductivity and a repeat analysis to check if the open-column result would be generated.

3.5.5.5 Buffer and Sample Preparation for analysis of mixture of Caffeine, Aspartame, Benzoic acid and Saccharine (CABS mixture) by RSP

Stock solutions (500 μg mL^{-1}) of CABS mixture were prepared by dissolving the approximate mass of solid in water and then diluted to the desired concentration prior to use. The running electrolyte contained 20 mM sodium borate, 20 mM potassium dihydrogen orthophosphate and 50 mM SDS. The pH values of the electrolyte solutions were adjusted with either 0.1 N hydrochloride acid or 0.1 N sodium hydroxide. All solutions were filtered with 0.45 μm syringe filters.

3.5.5.6 Buffer and Sample Preparation for analysis of Nitrofuran antibiotics (NFA) by RSP

Stock solutions (1000 μg mL^{-1}) of NFA were prepared by dissolving the approximate mass of solid in 30:70 acetonitrile: water, stored at 4ºC in the dark and then diluted to the desired concentration prior to use.The running electrolyte contained 20 mM sodium borate, 20 mM potassium dihydrogen orthophosphate and 80 mM SDS. The pH values of the electrolyte solutions were adjusted to 9.0 with 0.1 N sodium hydroxide. All solutions were filtered with 0.45 μm syringe filters. 20% methanol was added to the running electrolyte on a *v/v* basis.

3.6 References

1. Leitner, A., P. Zollner, and W. Linder, *Determination of the metabolites of nitrofuran antibiotics in animal tissue by high-performance liquid chromatography-tandem mass spectrometry. J. Chromatogr. A*, 2001. ***939***: p. 49-58.

2. Conneely, A., et al., *Isolation of bound residues of nitrofuran drugs from tissue by solid-phase extraction with determination by lidquid chromatography with UV and tandem mass spectrometric detection. Anal. Chim. Acta*, 2003. ***483***: p. 91-98.

3. Morris, V.M., et al., *Optimization of the capillary electrophoresis separation of ranitidine and related compounds.* J. Chromatogr. A, 1997. ***766***: p. 245-254.

4. Owen, R.F., *Food Chemistry*. 3rd ed. 1996, New York: Marcel Dekker.

CHAPTER 4

OPTIMISATION PARAMETERS and STRATEGIES for CE

4.1 Introduction

Optimisation of a separation method can be complicated due to the broad variety of parameters and significant factors, which need controlling to obtain resolution and to meet other experimental goals. For example, conditions that increase the resolution of one peak pair may decrease the resolution of another peak pair. In order to obtain the best compromise between contradictory criteria the optimal conditions chosen needs a multi-criteria decision making approach. The dual goals of optimisation are to obtain the maximum resolution with in the minimum total run time.

Usually the optimisation procedure is one of the most complicated phases of method development. To achieve successful optimisation, its early stages depend on a laborious schedule that determines the effects of significant factors on the chosen analytical response. Optimisation of a separation technique is traditionally performed by systematically varying one factor whilst holding remaining factors at a constant level (one-variable-at-a-time optimisation). The drawback for this approach is the large number of experiments that may need to be performed, leading to lengthy time requirements and cost, which often makes this strategy impracticable to be done thoroughly. In addition, if synergistic effects of two or more variables are crucial to compute the overall best result, the “one-variable-at-a-time” approach would not reveal this. The alternative approach to “one variable-at-a-time” is to employ an experimental design approach. Experimental designs are statistical approaches, which can be applied to any experiment with “outcome” (response) determined by experimental variables. Multi-variate optimisation events involve a simultaneous alteration of all experimental parameters examined according to an experimental design. Experimental designs are setup in such a way that maximum information is obtained from a minimum number of experiments [1]. The main advantages of using a multi-variate setup in optimising a separation technique include reduction in the number of experiments and improved statistical interpretations, which lead to reduction in time and cost requirements. Also, interaction effects between significant factors can be investigated with multi-variate experiments, which would be impossible to do with a uni-variate setup.

A variety of chemometric experimental designs have been used for the optimisation of CE separation techniques, for example: fractional factorial designs (FFD) [2, 3], factorial design [4], central composite design [5], Plackett-Burman design [6], overlapping resolution mapping [7, 8] and a simplex design [9].

Popular experimental designs in screening are FFD and Plackett-Burman designs whereas the CCD, which is a full factorial design with centre points and axial points, can subsequently be used to optimise most significant factors.

Plackett- Burman designs are useful for checking the robustness of an analytical method. In experimental design a robust analytical method is one where the response remains the same with slight modification in factor levels. For a robustness check, a few centre points are added to a reduced factorial design to evaluate the method repeatability and to establish that the response surface has no curvature. If such a curvature is identified, the initial design can be enhanced with axial points and new centre points to build a composite design [10].

Mikali et al. [6] described a MEKC method for the separation of phenols and the chiral separation of (+)-1-(9-anthryl)-2-propyl chloroformate-derivatised amino acids using a Plackett-Burman design for initial screening and then using a factorial design for optimisation of significant factors. The parameters optimised in this study were pH of background electrolyte, concentration of the primary surfactant, concentration of the secondary surfactant, buffer concentration, temperature in the capillary compartment, the amount of organic modifier (acetonitrile), the concentration of urea as an organic modifier and the separation voltage. The initial screening demonstrated that four of the eight factors could be fixed, as the level of these factors did not alter the final result. The second step was to conduct a full factorial design using the remaining four significant factors in order to reveal if any interaction effects were present. The significant factors used in the full factorial design were pH, the percentage of acetonitrile, concentration of primary surfactant and concentration of secondary surfactant. Response surfaces were also used to evaluate the robustness of the proposed method around the optimal region.

Miyawa et al. [11] developed a CEC method to separate the antibacterial 3-[4-(methylsulfinyl) phenyl]-5s-acet-amidomethyl-2-oxazolidinone from its related S-oxidation products. A CCD was applied to optimise the method and three factors were selected for the study: applied potential, volume fraction of acetonitrile and buffer concentration. Average selectivity, optimisation criterion Cr and chromatographic optimisation function were three optimisation criteria used in this study.

Optimal conditions were achieved for the separation of ranitidine hydrochloride and related compounds using CE by applying experimental designs. A two level FFD was employed to screen for the significant factors. A second FFD was also used for screening due to observation of significant curvature of the initial FFD. CCD was applied to determine the optimal conditions for the significant factors. [2].

Nine porphyrins were analysed using an overlapping resolution mapping scheme by CE. It was established that the method was speedy and uncomplicated, and required a small number of experiments to be conducted to determine the optimum conditions [12].

Safa developed a separation method for nine chlorophenols by micellar liquid chromatography using a face-centered cube CCD [13]. From the experiments it was evident that the retention time of the chlorophenol isomers vary as a function of pH, SDS and propanol concentration. The polynomial model obtained for robustness was established using a cross-validation strategy. The polynomial model disclosed that all three significant factors have negative impact on the retention time values.

Kincl et al [16] employed experimental design in the development and optimisation of Diclofenac sodium and Naclofen release method. In this design, a three-level factorial Box-Benken design was used in order to illustrate and optimise six parameters that influence the release of dichofenac from the tablets (rotation speeds of the stirring elements, pH, ionic strengths of the dissolution medium, applied salt, type of dissolution apparatus and producer of the on-line connected dissolution apparatus). After initial optimisation it was found that rotation speeds of the stirring elements, pH and ionic strengths of the dissolution medium affect the release of dichofenac from the tablets.

4.2 Experimental Design

In experimental designs, variables are coded with values of “+1” and “-1” given to “high” and “low” levels respectively in the variable range. The centre points in experimental design are represented by “0”. This gives equal weight to all variables in the regression equation and removes bias, which may arise due to different magnitude of variables. Centre point replicates are used to estimate reproducibility of the method

and are also included to check whether the response surface has curvature [10]. The “level” in an experimental design is a specific value at which an experiment is run.

In experimental design when high numbers of experiments need to be performed within a single day, experiments can be divided into blocks according to different specifications [1]. The blocks need to retain the essential feature of the original design that the factors are orthogonal (uncorrelated). Cube points and axial points are usually positioned in different blocks. An adequate number of experiments in each block can be obtained by further splitting of cube points. The center points are evenly distributed in each block, which allows the estimation of the blocking effect [14].

4.2.1 Factorial Design

The first step of the general strategy for optimisation is frequently a screening design, using a two level full or half factorial design with one or several centre points (to evaluate the experimental error and to detect for a possible curvature), then to optimise the significant factors using a CCD. If curvature is detected in the initial design, it can be expanded with axial points and new centre points to construct a composite design [10].

4.2.2 Central Composite Design

A CCD consists of a two-level factorial design with centre points and a star design forming a five level design where levels are set at $-\alpha$, -1, 0, +1, $+\alpha$. The points forming a star are the axial points. (Diagram 5.1) Each point on the corner of the cube and the axial points represent one experiment run. The distance of the axial points, α, varies depending on the number of factors to be optimised [15]. CCD has two significant features: rotatability and orthogonality. A rotatable design predicts responses of all points except centre points, and has the same variances regardless of direction. Orthogonality allows direct and independent estimation of parameters [1]. The main feature of a rotatable design is uniform distribution of

information[2]. To guarantee rotatability, α should be $\sqrt[4]{2^k}$ where k is the number of factors. This equals 1.414 and 1.682 for two and three factor designs respectively.

After establishing the significant factors that influence the performance of a method by using a screening design it may then be appropriate to optimise the method by acquiring response surfaces. The relationship between one or more response variables and a set of quantitative parameters can be examined by using multi-level response surface methods, for instance Box-Benkhen or Central Composite Designs [16]. The aim of the optimisation stage is to locate the conditions for an optimum separation. A simultaneous design such as CCD can create an experimental model that gives information on the relationship between the factors and the response. Response surface designs are the best experimental designs for the purpose of modelling and optimisation [1]. A three-dimensional response surface can be created from the experimental model, giving a visual representation of the effects of two factors on the response. These plots can supply a graphical illustration of the data over the ranges observed and can be used to forecast areas of most favorable performance. From the experimental models the conditions for an optimum separation can be found. The response surface design is a polynormial model where the "surface" is represented mathematically.

Response surface diagrams can be produced for each response. The response surfaces are then evaluated to obtain an initial indication of the robustness of the method. Robustness of a method is valuable information relating to method performance and can be demonstrated by the influence of small changes away from a set value. Given the model has three factors, one factor was held steady for each plot. Response surface plots help to find the optimal levels of the chosen factors. These plots can be used to analyse the relationship between dependent and independent variables.

The equation below can be used to calculate the α, in order to obtain the rotatability and orthogonality of the axial spacing of the design [2].

$$\alpha = \sqrt[4]{2^k}$$ (for rotatability) ..... Equation (4.1)

$$\alpha^2 = \frac{\sqrt{(Nc + Na + No)Nc + Na}}{2}$$ (for orthogonality)..... Equation (4.2)

k = the number of factors

Nc = number of factorial or cube points (=2^k)

Na = number of star or axial points (=2k)

No = number of centre points

The simplest way to design axial spacing is to fulfill rotatability first and then to add centre points as required until orthogonality is obtained, as rotatability does not depend on number of centre points. The value α varies according to the type of design and according to the number of variables to sustain orthogonality of a design [17]. Table 4.1 shows the orthogonality and rotatability settings of *k* factors. A common variation of the CCD used is the face-centered CCD. In this design α is set as 1. This means the design is no longer rotatable but it has the advantage that the high and low levels for axial and cube point are the same.

The CCD, along with multi-linear regression, can estimate the main effects, b_i, two way interactions, b_ib_j, and the second order effects, b_i^2. Coefficients of the polynomial equation can be determined by regression analysis. The polynomial equation communicates the response to the factors, forming the Empirical Model [18]. The polynomial equation can be used to assess the linear, quadratic and interactive effects of independent variables on the selected responses.

$$Y= b_o + b_1X_1+\ldots + b_nX_n+ b_{12}X_1X_2+ \ldots b_{n-1,\ n}X_{n-1}X_n+ b_{11}X_1^2+ \ldots +b_{nn}X_n^2$$ .....Eqn (4.3)

Where:

b_0 : the intercept

b_1 to b_n : the main effect coefficient

b_{12} to $b_{n-1,\ n}$: the two way interaction coefficient

b_{11} to b_{nn} : the second order coefficient

Figure 4.1: CCD for a three factor design

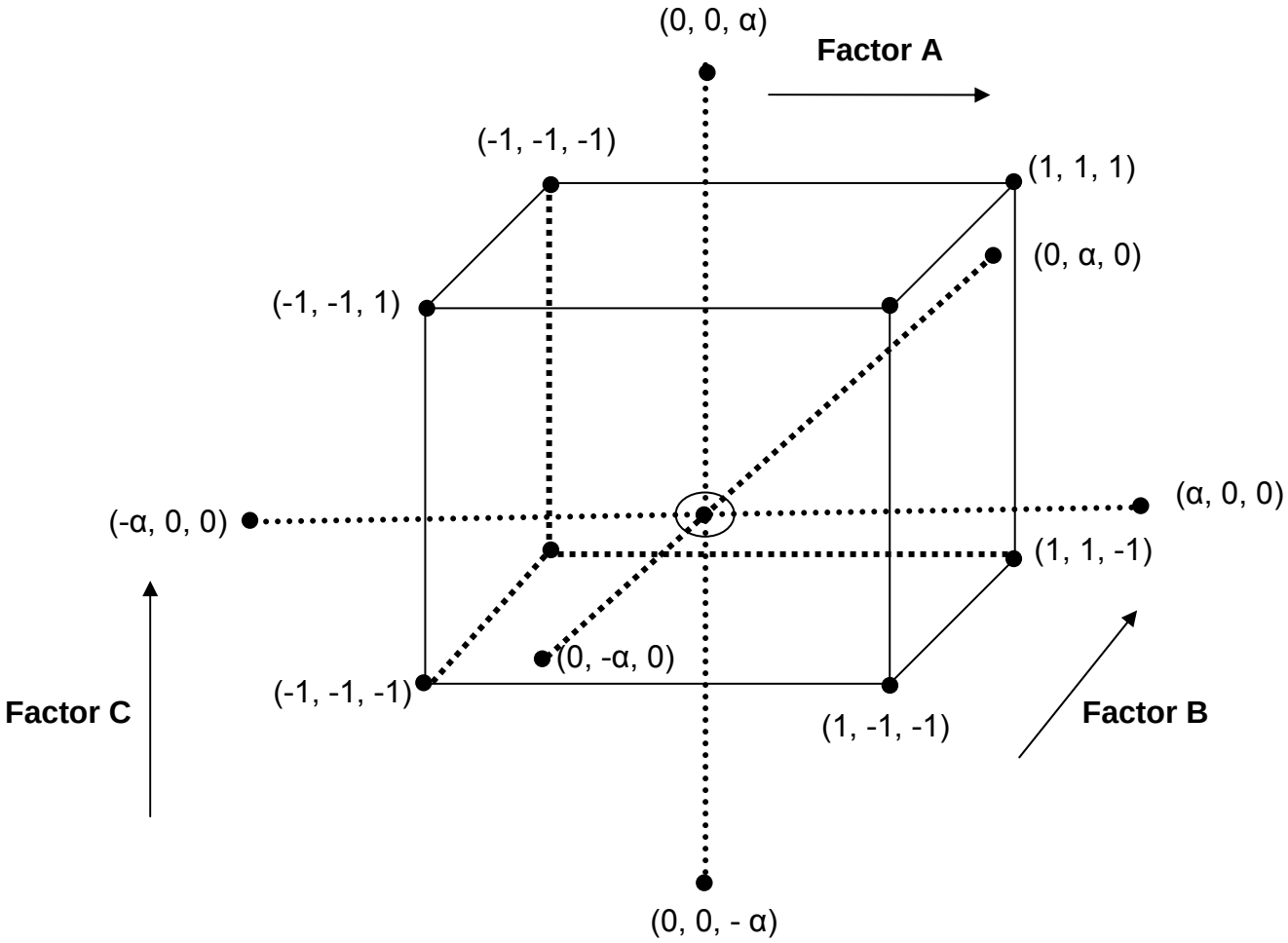

Table 4.1: The number of cube points, axial points and centre points for rotatable and orthogonal CCD with 2-6 significant factors

k	*Nc*	*Na*	*No*	α
2	4	4	8	1.414
3	8	6	9	1.682
4	16	8	12	2.000
5	32	10	17	2.378
6	64	12	24	2.828

4.3 Chromatographic Exponential Function (CEF)

In many experiments, there is a clearly identifiable response value. The response value may be the solute recovery in an extraction or it may be the single measure of yield in a chemical reaction. In a chromatographic separation, defining the quality of the chromatogram can be subjective. To overcome this problem, Objective Functions (OF) are designed to provide a single response value revealing the quality of the chromatogram [19]. Chromatographic Response Function (CRF) is one of the objective functions, which was proposed by Berridge [11]. CRF was criticised because poorly resolved peaks do not have a high influence on the CRF value, and the quality of an electropherogram is then determined mainly by the well-resolved peaks.

The Chromatographic Resolution Statistic (CRS), introduced by Schbach and Excoffier [11], has been employed by Arnoldsson and Kaufmann in order to optimise the separation of lipids by liquid chromatography as the response for a full factorial design [17].

The CRF and CRS functions were improved on by Morris et al. [2] who introduced the Chromatographic Exponential Function (CEF) and applied it to the GC separations of phenols. The CEF, defined in equation (5.4), was used to determine the quality of each test run, which is based on separation between peaks, and elution time of the final component. For this function an optimum resolution and desired total analysis time is also chosen. This function gives a single number to describe the quality of the chromatogram. CEF is used as the response variable in an optimisation strategy involving a CCD, multi regression and response surface modelling [20]. One of the advantages of CEF is not having undefined points and the relative influence of elution time and resolution can be adjusted. It is not required to identify peaks when using CEF, and the response value is not affected by peak cross overs [19]. The CEF was employed in this research study.

$$CEF=\left[\left[\sum_{i=1}^{n-1}\left(1-e^{a\left(R_{opt}-R_i\right)}\right)^2\right]+1\right]\left(1+\frac{t_f}{t_{max}}\right) \quad \text{....Equation (4.4)}$$

Resolution Factor Time Factor

where:

R_{opt} is the optimum resolution (at least 1.5 for adequately resolved peaks)

a adjusts the weighing of the resolution term relative to the time term

t_{max} is the maximum acceptable time

t_f is the final peak elution time

R_i is the resolution of *i* th peak pair for each experiment result, and

n is the number of expected peaks.

A minimum in the CEF value corresponds to the best separation result. Using the CEF function as the response variable in this study, the optimum resolution was set to 2.0 and maximum acceptable time was set at 15 minutes.

The absence of a prominent peak is treated as the peak having a resolution of zero, resulting in a high exponential value. An optimum electropherogram with all peaks resolved to minimum R_{opt} and with a total elution time of less than t_{max} would result in a CEF value between 1 and 2 [21]. The target is to minimise the CEF value.

4.4 Results and Discussion

The application of statistical experimental design to the optimisation of nitrofurans and triadimenol fungicides was performed to determine optimal operating conditions. In nitrofuran separation method, the experiments were conducted using FFD and CCD as a part of a strategy to determine how the significant factors such as pH, buffer concentrations, voltage, and surfactant concentration affect experimental goals, analysis time and resolution.

4.4.1 Optimisation of the Buffer Composition of Nitrofuran analysis

A typical electropherogram of the Nitrofuran antibiotics (NFAs) and metabolites (NFMs) mixture prior to optimisation of the separation conditions is shown in Fig 4.2.

Figure 4.2: Electropherogram showing the separation of NFAs and NFMs prior to optimisation

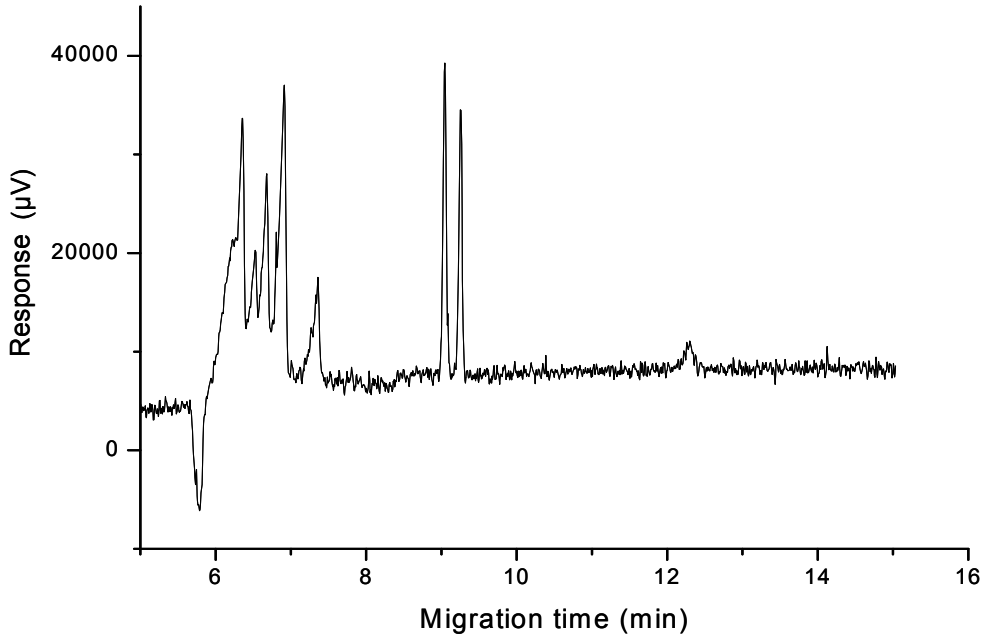

Minitab for Windows version 14 (Minitab Inc., State College, PA, USA) was used to generate experimental designs. The first step was to define the experimental domain by finding the extremes for parameters such as borate and phosphate concentrations in the buffer, concentration of sodium deoxy cholate (SDC/SDQ), applied voltage and the pH of the running buffer as shown in Table 4.2.

Table 4.2: Experimental Domain for parameters

Parameters	SDC concentration	Voltage	Borate concentration	Phosphate concentration	pH
Range	0-100 mM	8-20 kV	0-40 mM	0-40 mM	7.0-10.0

After finding the workable ranges for each CE parameter, a FFD was then employed to screen for the significant factors. In this design, a five-factor system was used at two experiment levels ('high' and 'low') plus centre points. Two level factorial designs evaluate each factor simultaneously at varying combinations of high and low values. These two level designs can determine the main effects and the interactions between factors but they cannot determine the second order effect, that is curvature in the model. This system required 24 runs for the experimental design as shown in Tables 4.3 and 4.4.

In the FFD, there are 8 centre points; the experimental runs were separated into two blocks that ran over two days due to the high number of runs to be performed over one day. This means that each block contains a group of 12 experiments. The order of runs within the blocks was randomised. The centre points were run on each day to ensure that running the system in blocks did not introduce bias. Table 4.4 gives the experimental results and CEF values of these runs. The design was analysed using a regression approach. The regression coefficient obtained from the data of the experimental design is R^2 of 100.0%. R^2 is a statistical estimate (taking the number of terms in the model and number of experimental runs into account) used to evaluate the adequacy of the model.

Shown in Fig 4.3 are the main effect plots generated with Minitab of the data from the initial optimisation study. Main effects plots show the averages of all runs at the high and low settings for that variable and the centre point average. They indicate how a variable affects the response. The most significant variables have the steepest slopes. The plots indicate that a low concentration of borate results in a very high response, which was not suitable to use. pH, voltage, SDC concentration and phosphate concentration were also significant. The fact that the centre points are not on a straight line between low and high also indicates that there is curvature in at least one of the variables, which needs to be examined further.

Table 4.3: Levels of the significant factors used in the FFD of NFAs and NFMs separation method

Coded value	Actual value				
	[Borate] (mM)	[Phosphate] (mM)	pH	Voltage (kV)	[Surfactant] (mM)
-1	0	0	7.5	10	20
0	20	20	8.5	15	60
+1	40	40	9.5	20	100

Note: The center points are shown asterisked (*).

Table 4.4: FFD used in the initial optimisation of NFAs and NFMs separation method

Run Number	Block	pH	[SDC] (mM)	Voltage (kV)	[Borate] (mM)	[Phosphate] (mM)	CEF
1	2	9.5	100	10	40	0	18
2	2*	8.5	60	15	20	20	11
3	2*	8.5	60	15	20	20	12
4	2*	8.5	60	15	20	20	294376
5	2	9.5	100	10	0	40	1000000
6	2	7.5	20	10	0	40	1000000
7	2	9.5	100	20	0	0	1000000
8	2*	8.5	60	15	20	20	12
9	2	9.5	100	20	40	40	12
10	2	7.5	20	20	40	40	2618
11	2	7.5	20	10	40	0	578
12	2	7.5	20	20	0	0	1000000
13	1*	8.5	60	15	20	20	12
14	1	9.5	20	10	40	40	414463
15	1	9.5	20	20	0	40	1000000
16	1*	8.5	60	15	20	20	12
17	1*	8.5	60	15	20	20	12
18	1	7.5	100	10	40	40	1000000
19	1	7.5	100	20	40	0	183
20	1	7.5	100	10	0	0	1000000
21	1	9.5	20	20	40	0	3007
22	1	9.5	20	10	0	0	1000000
23	1*	8.5	60	15	20	20	12
24	1	7.5	100	20	0	40	1000000

Figure 4.3: The main effect plots of significant factors of FFD of initial optimisation

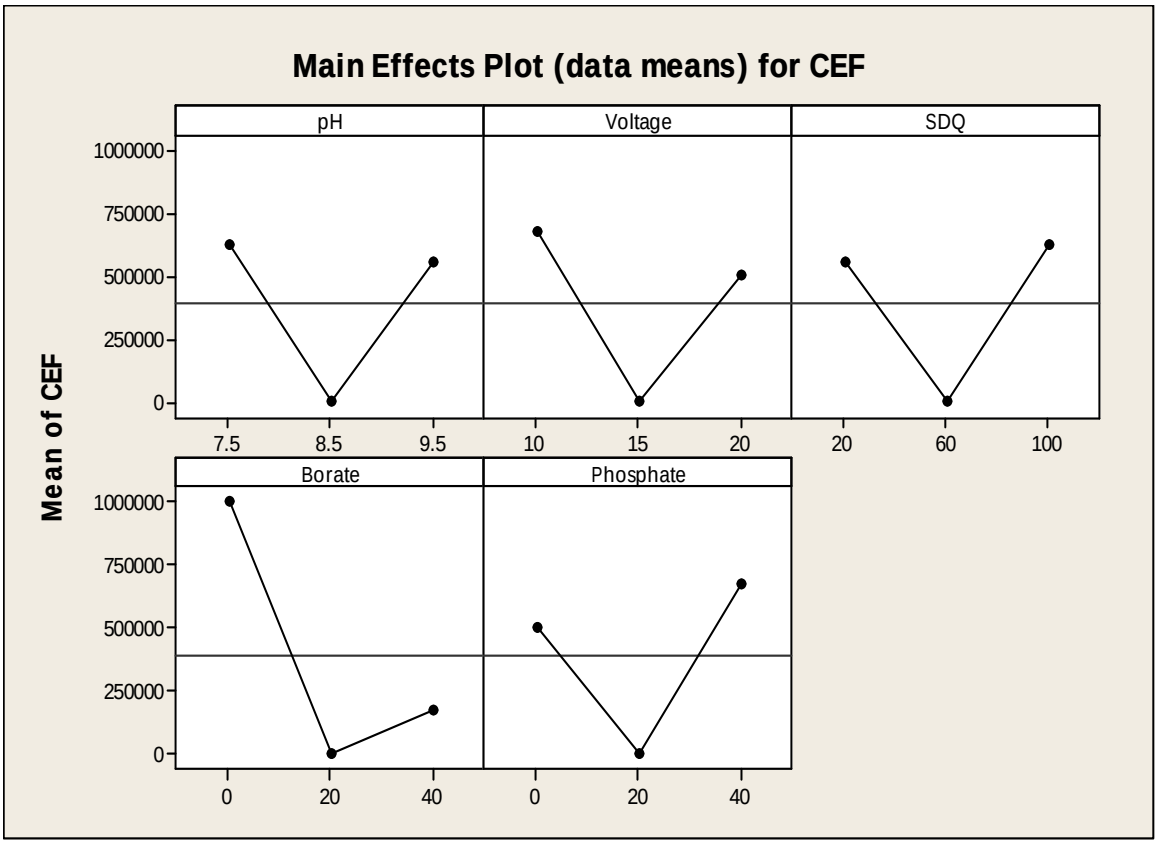

It was observed that SDC did not readily dissolve in the phosphate buffer in the absence of borate in the electrolyte, and pH adjustments were aided when phosphate was present in the electrolyte with borate. The highest CEF values were detected when borate was absent in the buffer and the lowest CEF values of FFD were from centre points.

For the next step of optimisation, CCD was chosen to evaluate the effects of selected variables on the responses and to optimise the procedure. The CCD design employed was a two level factorial with centre points and star design, forming a five level design, where levels are set at -α, -1, 0, +1, +α. The design shown in Table 5.5 is for 3 factors (pH, voltage and SDC concentration). Borate to phosphate buffer ratio in the electrolyte was fixed to 20 mM borate: 20 mM phosphate. pH and SDC concentration were narrowed down in the CCD design. The pH, SDC and Voltage levels are shown in Tables 4.5 and 4.6. The centre point was pH 9.0, 80 mM of SDC concentration and voltage of 16 kV.

This system involves 20 runs for the design with 6 centre points 8 cube points and 6 axial points. The alpha value of this design set to 1.68.The regression coefficient obtained from the data of the experimental design is R^2 of 89.1%.

The highest CEF values of CCD were detected when surfactant concentration was below 70 mM and the lowest values resulted with centre points and also with pH higher than 8.8 and voltage higher than 16 kV. However with pH above 9.2 and voltage above 18 kV the CE traces had a high signal to noise ratio. Some sample CE traces of CCD are shown in Fig 4.4a and 4.4b. The peak numbering of Fig 4.4, 4.5 a and b as specified in Fig 5.1 of Chapter 5.

Table 4.5: Levels of the significant factors used in the CCD for NFAs and NFMs separation

Coded value	Actual value		
	pH	[Surfactant] (mM)	Voltage (kV)
-α	8.5	60	10
-1	8.8	70	12
0	9.0	80	16
+1	9.2	90	18
+α	9.5	100	20

Table 4.6: CCD used in the final optimisation of NFAs and NFMs separation

Run Number	Block	pH	[Surfactant] (mM)	Voltage (kV)	CEF
1	1	8.8	70	18	9094
2	1	8.5	80	16	4304
3	1	9.2	70	18	277222
4	1	9.2	70	12	372250
5	1	9.5	80	16	16
6	1*	9.0	80	16	18
7	1*	9.0	80	16	15
8	1	8.8	70	12	82
9	1	9.2	90	18	15
10	1	8.8	90	12	21
11	1	9.0	100	16	15
12	1	9.2	90	12	21
13	1*	9.0	80	16	21
14	1	9.0	80	20	19
15	1	9.0	60	16	902
16	1*	9.0	80	16	15
17	1	8.8	90	18	14
18	1*	9.0	80	16	15
19	1*	9.0	80	16	16
20	1	9.0	80	10	20

Figure 4.4a: Electropherogram of a selected condition of CCD used in the optimisation process (condition used: 20 mM borate, 20 mM phosphate, pH=9.0, 60 mM SDC, voltage 16 kV).

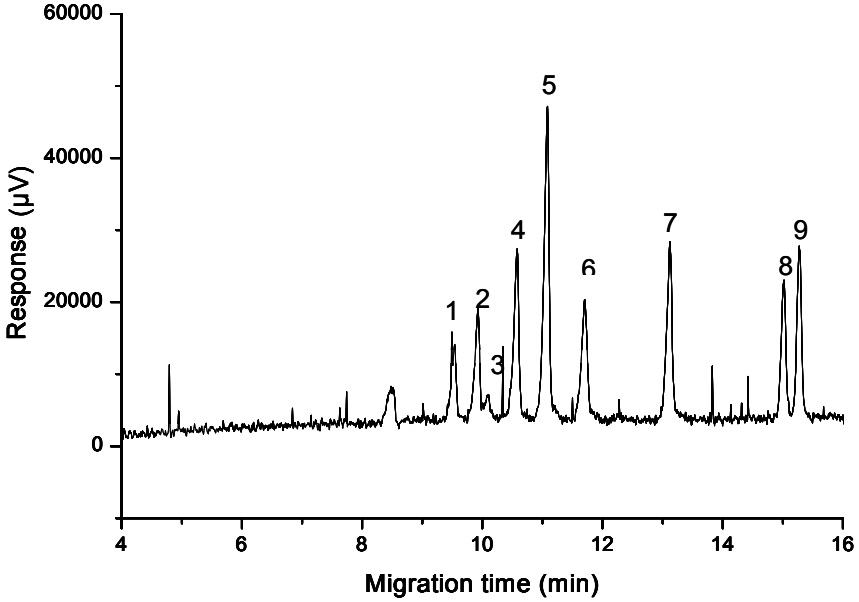

Figure 4.4b: Electropherogram showing the centre point of CCD used in optimisation process (conditions used: 20 mM borate, 20 mM phosphate, pH=9.0, 80 mM SDC, voltage 16 kV).

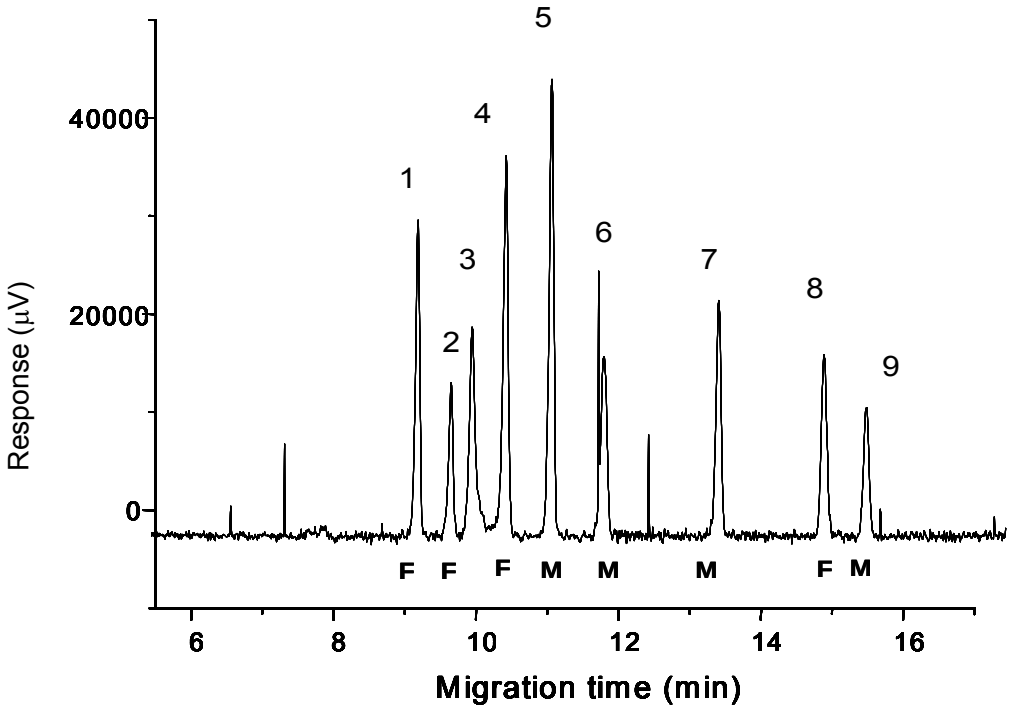

NFAs are indicated using **F** and NFMs are indicated using **M**.

The output from the Minitab analysis is in appendix 1.To improve the overall fit of the model the three runs with the highest CEF were omitted. This gave an overall R^2 of 91%, indicating a reasonable fit. As the aim is to find the optimal conditions these points were well removed from the optimal region. The most significant factor was pH, with curvature in the pH effect. SDQ was the next most significant factor. Examination of the results from the 3 experiments with very high CEF does not show a clear trend but high voltage coupled with lower SDQ and pH seems to lead to poor results.

The response surfaces of CCD of optimisation are shown in Figs 4.5 a-c. Although the response surfaces are complex they do indicate a minimum response for CEF near the centre point (pH 9.0, 80 mM SDQ, 16 kV). This is also the value predicted by the response optimizer in Minitab. The full output for the analysis is shown in appendix 1.

Figure 4.5a: The response surface models for the optimisation of NFA and NFM: pH vs SDQ

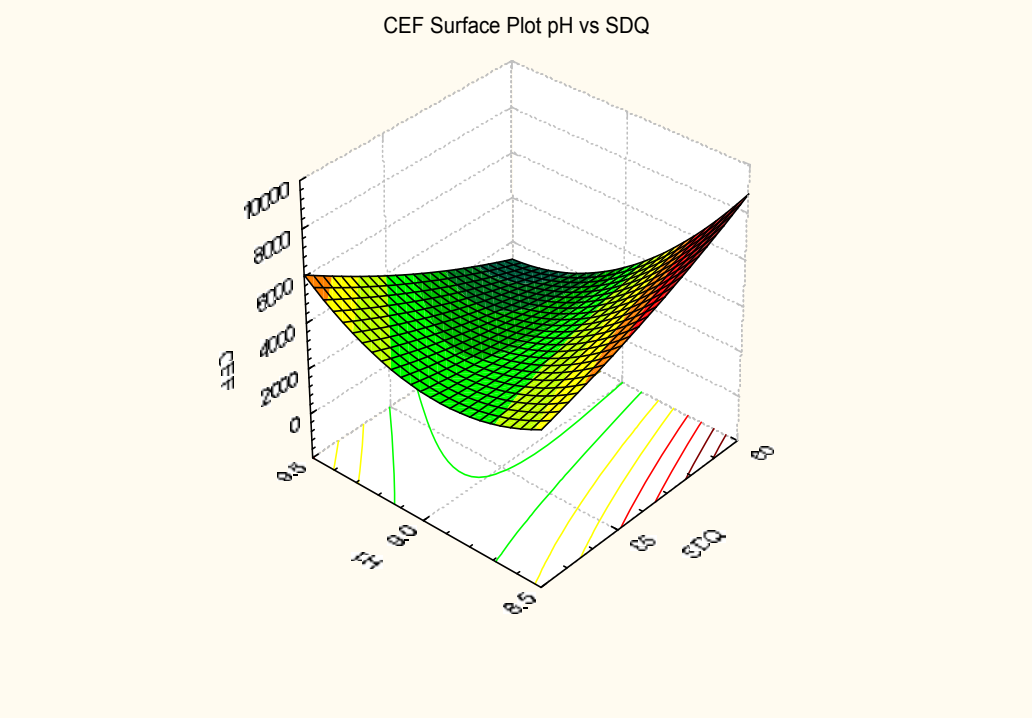

Figure 4.5b: The response surface models for the optimisation of NFA and NFM: pH vs voltage

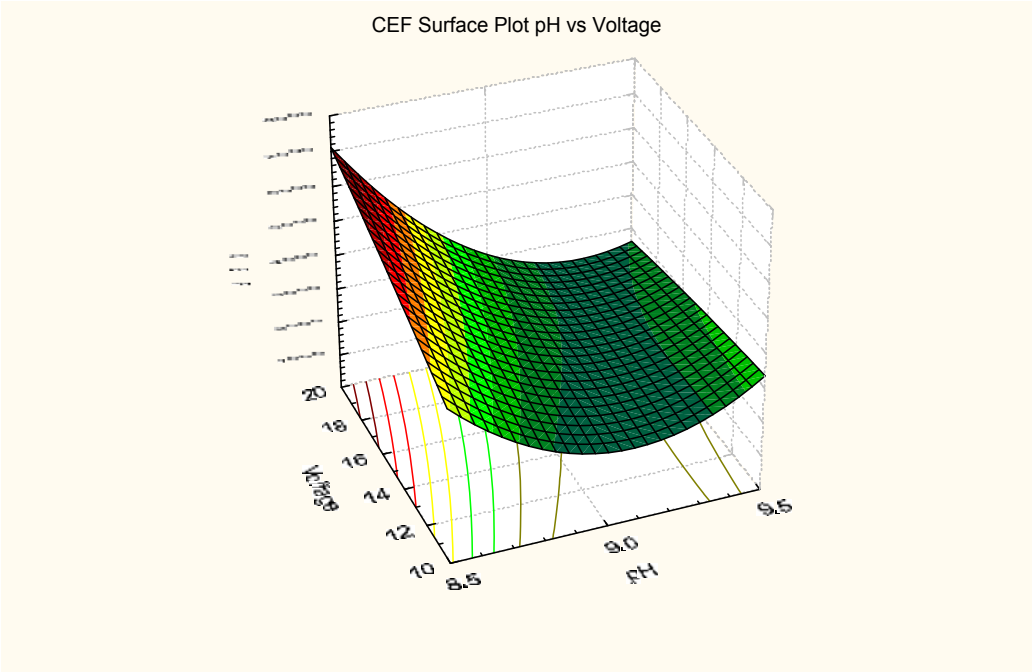

Figure 4.5c: The response surface models for the optimisation of NFA and NFM: SDQ vs voltage

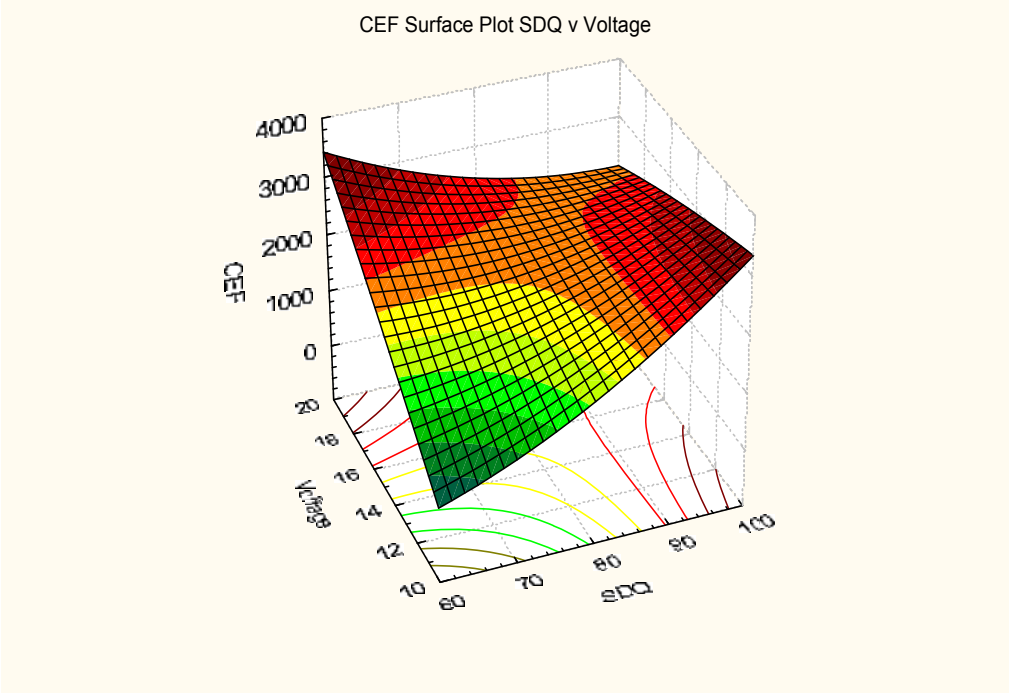

4.4.2 Validation and ruggedness of Nitrofuran separation method

The validation and ruggedness study is performed to examine whether the centre point is the true optimum, to see whether the centre point is reproducible and rugged. Response surface plots and main effect plots were used to examine the criteria of validation and ruggedness study.

The validation and the ruggedness test were conducted using a full factorial design with 12 runs (4 centre points were included), after obtaining the optimum conditions for NFAs and NFMs analysis. In this design a three factor system was used at three different experimental levels: -1, 0, + 1. Three significant factors were varied (pH, voltage and surfactant concentration) at three different levels as shown in Tables 5.7 and 5.8. Borate to phosphate buffer ratio in the electrolyte was fixed to 20 mM borate: 20 mM phosphate. The centre point was at a pH 9.0, 80 mM of SDC concentration and voltage of 16 kV.

The main effects plots show the method is reasonable rugged with only small changes in CEF across the domain – changes of the order of 5 in the CEF function do not indicate significant differences in electropherogram quality. Also the lowest response was obtained at the centre point and this result was reproducible.

Table 4.7: Levels of the significant factors used in full factorial design of NFAs and NFMs separation method

Coded value	Actual value		
	pH	Voltage (kV)	[Surfactant] (mM)
-1	8.8	14	70
0	9.0	16	80
+1	9.2	18	90

Table 4.8: full factorial design used in validation and ruggedness of NFAs and NFMs separation method

Run Number	Block	pH	[Surfactant] (mM)	Voltage (kV)	CEF
1	1	9.2	90	18	16
2	1	8.8	90	14	19
3	1	8.8	90	18	17
4	1	9.2	90	14	22
5	1	8.8	70	14	34
6	1	9.2	70	14	20
7	1	8.8	70	18	17
8	1*	9.0	80	16	16
9	1*	9.0	80	16	16
10	1	9.2	70	18	17
11	1*	9.0	80	16	17
12	1*	9.0	80	16	17

4.4.3 Optimisation of the Buffer Composition of Triadimenol analysis

In the Triadimenol separation method, the optimisation experiments were conducted using CCD as a part of a strategy to determine how the significant factors such as pH, buffer concentrations, voltage, and surfactant concentration affect experimental goals, analysis time and resolution. A typical electropherogram of the Triadimenol mixture prior to optimisation of the separation conditions is shown in Fig 4.6.

Figure 4.6: Electropherogram showing the resolution of Triadimenol diastereoisomers by MEKC mode

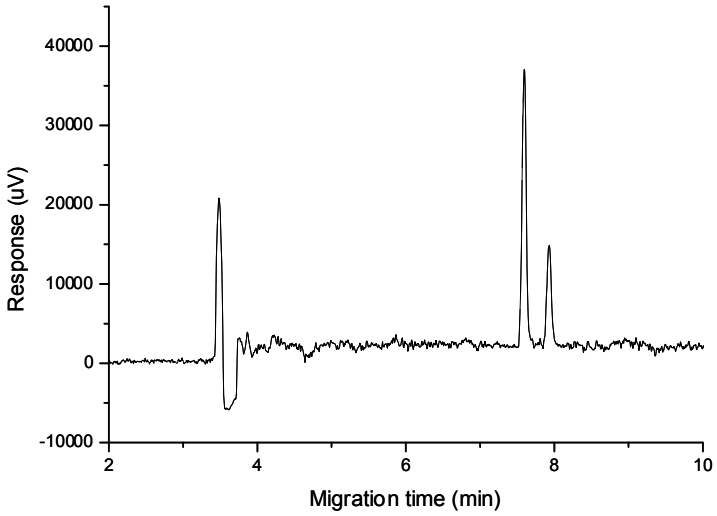

The first step of Triadimenol analysis was to define the experimental domain by finding the extremes for parameters such as borate and phosphate concentrations in the buffer, SDS concentration, % methanol, applied voltage and the pH of the buffer electrolyte. Previously used phosphate and borate concentrations in buffer electrolyte (20 mM phosphate and 20 mM borate) from Chapter 5, together with 50 mM SDS were tried. Table 4.9 shows the experimental parameters used at the early stages.

Table 4.9: Experimental Domain for parameters

Parameter	Chiral selector	pH	% Methanol	Voltage
Range	10- 30 mM	5.5- 9.5	10- 25%	14- 20 kV

The optimisation of triadimenol fungicides was performed using a CCD with 18 runs (8 cube points, 2 centre points in cube, 6 axial points, and 2 centre points in axial). In this design a three factor system was used at three different experimental levels: -1, 0, + 1 with the α value set to 1 (i.e a face-centred CCD). Three significant factors were varied (pH, voltage and % methanol) at three different levels as shown in Tables 4.10 and 4.11. Borate to phosphate buffer ratio in the electrolyte was fixed to 20 mM with 50 mM concentration of SDS. The centre point was at a pH 6.0, voltage of 18 kV and 20% methanol. Table 4.11 gives the experimental results and CEF responses of these runs.

Table 4.10: CCD used in optimisation of Triadimenol separation method

Run Number	Block	pH	% Methanol	Voltage (kV)	CEF
1	1	6.0	20	20	11
2	1*	6.0	20	18	11
3	1	6.0	25	18	109
4	1	6.0	15	18	13
5	1*	6.0	20	18	8
6	1	5.5	20	18	49
7	1	6.5	20	18	15
8	1	6.0	20	16	30
9	1	5.5	25	20	49
10	2	6.5	15	20	27
11	2	6.5	25	20	174
12	2*	6.0	20	18	10
13	2	6.5	25	16	646
14	2*	6.0	20	18	9
15	2	5.5	15	20	643
16	2	5.5	25	16	309
17	2	5.5	15	16	90
18	2	6.5	15	16	47

Table 4.11: Levels of the significant factors used in CCD of Triadimenol separation method

Coded value	Actual value		
	pH	Voltage (kV)	% Methanol (mM)
-1	5.5	16	15
0	6.0	18	20
+1	6.5	20	25

The output from the Minitab analysis is in appendix 1.

Response surface diagrams are shown in Figure 4.7.The optimum conditions are located where the surface is at a minimum. In Figure 4.7 (a, b and C), it is clearly demonstrated that the % methanol, buffer pH and voltage have a significant effect. As the CEF achieves an optimum at the lower end of the range, this means that the region around the optimum is expanded. The lowest CEF value is obtained from the centre point of the design. Hence centre point indicates the optimal conditions of the Triadimenol separation.

Figure 4.7 a: The response surface model for the optimisation of Triadimenol separation method: voltage and % methanol

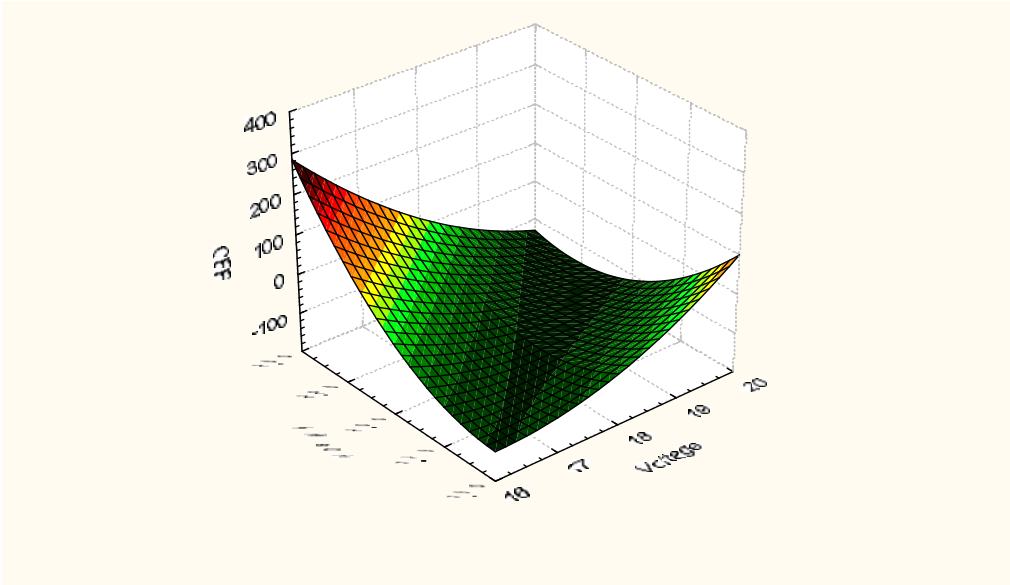

Figure 4.7 b: The response surface model for the optimisation of Triadimenol separation method: voltage and pH

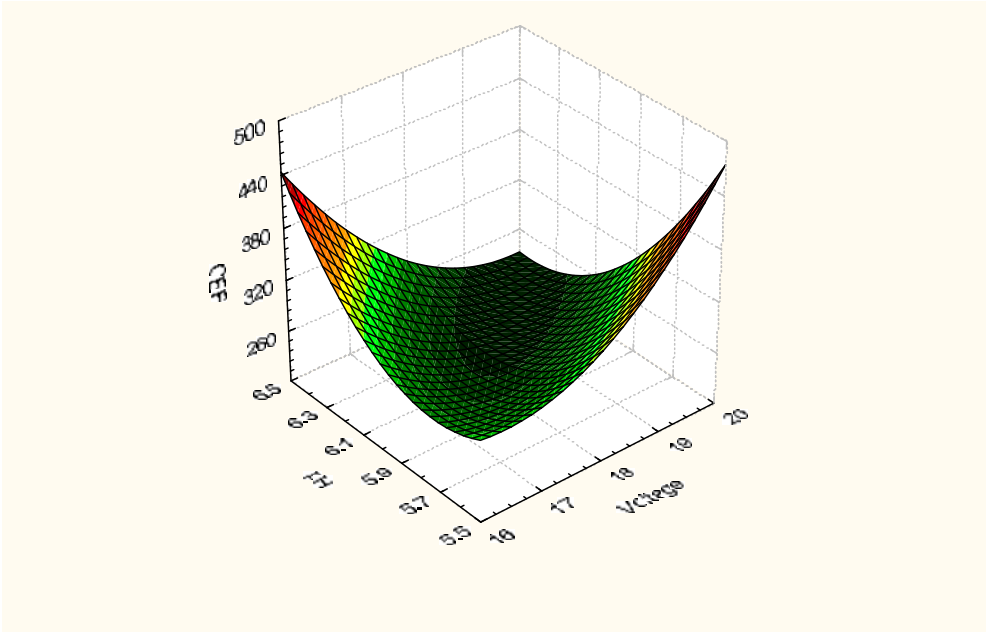

Figure 4.7 c: The response surface model for the optimisation of Triadimenol separation method: pH and % methanol

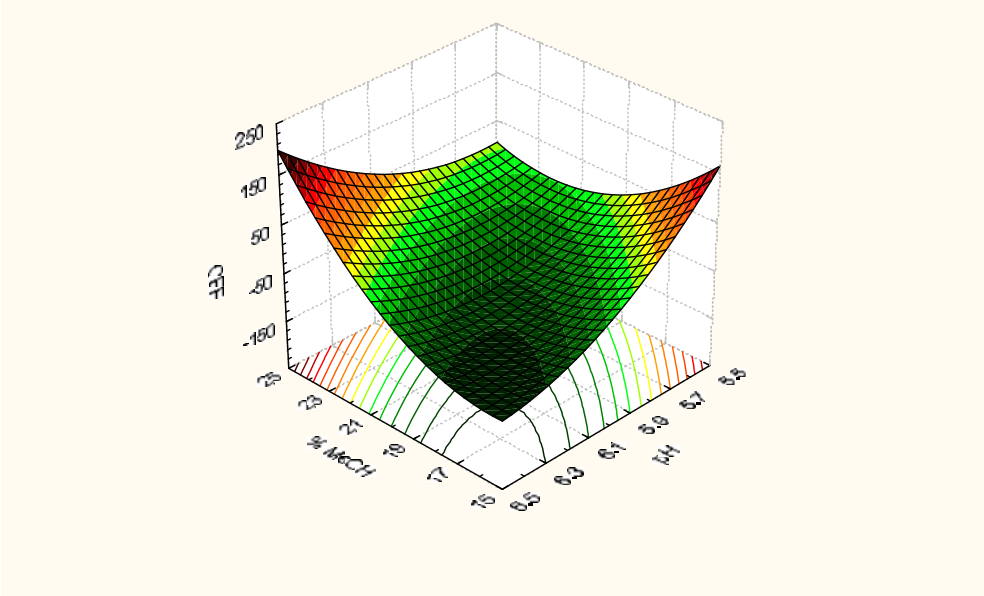

Figure 4.8: Electropherogram showing the centre point of CCD in optimisation of Triadimenol

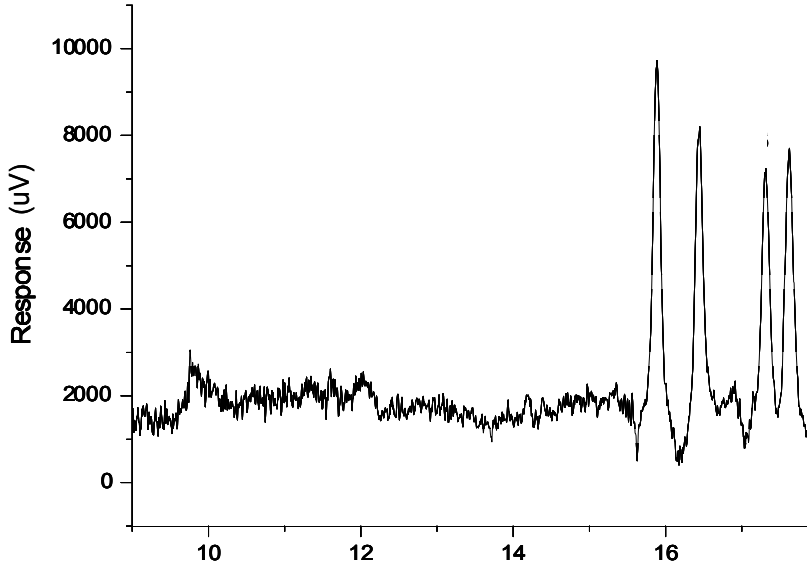

As shown in Fig 5.8 chiral resolution of Triadimenol isomers were achieved within 18 min. The lowest CEF value obtained was the centre point of the design.

4.5 Conclusion

Statistically supported experimental designs have been established as an important tool in optimisation study of nitrofurans and triadimenol fungicide separation. The duration of optimisation study using experimental design was much shorter compared to a one-at-a-time optimisation technique. The optimisation study took few days to complete instead of months when individual parameters were optimised, with the latter approach arguably not as rigorous. It is a cost-effective way of obtaining maximum amount of information in a short period of time with the least number of experiments.

During initial screening of nitrofuran study, a FFD with five significant factors at three levels was used to investigate the influence of significant variables on the resolution of nitrofuran. After the initial screening the concentration of borate and phosphate was fixed and the other three variables were evaluated at five levels using a CCD. Ruggedness of nitrofuran separation method was achieved using a full factorial design. The best conditions found to give optimum resolution from the optimisation study was pH 9.0, 80 mM SDC concentration, 16 kV with running buffer consisting of 20 mM borate and 20 mM phosphate concentration.

Optimisation of Triadimenol was performed using a CCD with three significant factors at the different levels. The best conditions found to give optimum resolution from the optimisation study was pH 6.0, 20% methanol, 50 mM SDS concentration, 18 kV with running buffer consisting of 20 mM borate and 20 mM phosphate concentration.

Response surface designs and main effect plots were also employed as a part of the strategy to confirm the effects of significant variables on the resolution.

4.6 References

1. Morgan, E., *Chemometrices: Experimental Design*. 1991, London: Joh, Wiley and Sons Ltd.

2. Morris, V.M., et al., *Optimization of the capillary electrophoresis separation of ranitidine and related compounds.* J. Chromatogr. A, 1997. ***766***: p. 245-254.

3. Nielsen, M.S., P.V. Nielsen, and J.C. Frisvad, *Micellar electrokinetic capillary chromatography of fungal metabolites resolution optimized by experimental design.* J. Chromatogr. A, 1996. **721**(2): p. 337-344.

4. de Oliveira, M.A.L., et al., *Factorial design of electrolyte system for separation of fatty acids by capillary electrophoresis.* J. Chromatogr.A, 2001: p. 533-539.

5. Beijersten, I. and D. Westerlund, *Derivatisation of dipeptides with 4-fluoro-7-nitro-2,1,3-benzoxadiazole for laser-induced fluorescence and separation by micellar electrokinetic chromatography.* J. Chromatogr. A, 1995. **761**(1-2): p. 389-399.

6. Mikaeli, S., G. Thorsen, and B. Karlberg, *Optimisation of resolution in micellar electrokinetic chromatography by multivariate evaluation of electrolytes.* J. Chromatogr. A, 2001. **907**: p. 267-277.

7. Vindevogel, J. and P. Sandra, *Resolution optimization in micellar electrokinetic chromatography: use of Placke statistical design for the analysis of testosterone esters.* Anal. Chem, 1991. **63**: p. 1530-1536.

8. Rogan, M., K.D. Altria, and D.M. Goodall, *Plackett-Burmann Experimental Design in chiral analysis using capillary electrophoresis.* Chromatographia, 1994. **38**: p. 723.

9. Castagnola, M., et al., *Optimization of phenylthiohydantoinamino acid separation by micellar electrokinetic capillary chromatography.* J. Chromatogr., 1992. **638**: p. 327-334.

10. Groupy, J., *What kind of experimental design for finding and checking robustness of analytical methods? Anal. Chim. Acta*, 2005. ***544***: p. 184-190.

11. Miyawa, J.H., M.S. Alasamdrp, and C.M. Riley, *Application of a modified central composite design to optimize the capillary electrochromatographic separation of related S-oxidation compounds.* J. Chromatogr.A, 1997. **769**: p. 145-153.

12. Yao, Y.J., H.K. Lee, and S.F.Y. Li, *Optimization of separation of porphyrins by micellar electrokinetic chromatography using overlapping resolution mapping scheme.* J. Chromatogr., 1993. **637**: p. 195-200.

13. Safa, F. and M.R. Hadjmohammadi, *Chemometric approach in optimization of micellar liquid chromatographic separation of some halogenated phenols. Anal. Chim. Acta,* 2005. ***540***: p. 121-126.

14. Palasota, J.A. and S.N. Deming, *Central composite experimental designs.* J. Chem., 1992. **69**: p. 560-563.

15. Ryswyk, H.V. and G.R.V. Hecke, *Attaining optimal conditions. J. Chem.*, 1991. ***68***: p. 878-882.

16. Kincl, M., S. Turk, and F. Vrecer, *Application of experimental design methodology in development and optimization of drug release method.* International Journal of Pharmaceutics, 2005. **291**: p. 39-49.

17. Gabrielsson, J., N.-O. Lindberg, and T. Lundstedt, *Multivariate methods in pharmaceutical applications.* J. Chemometrices, 2002. **16**: p. 141-160.

18. Daali, Y., et al., *Experimental design for enantioselective separation of celiprolol by capillary electrophoresis using sulfated-β-cyclodextrin.* Electrophoresis, 1999. **20**: p. 3224-3431.

19. Vanbel, P.F., J.A. Gilliard, and B. Tilquin, *Chemometric optimization in drug analysis by HPLC: a critical evaluation of the quality criteria used in the analysis of drug purity.* Chromatographia, 1993. **36**: p. 120-124.

20. Morris, V.M., et al., *Optimization of the capillary electrophoresis separation of ranitidine and related compounds.* J. Chromatogr. A, 1996. ***766***: p. 245-254.

21. Altria, K.D., et al., *Application of chemometis experimental designs in capillary electrophoresis.* Electrophoresis, 1995. **16**: p. 2143-2148.

CHAPTER 5

SEPARATION OF NITROFURANS AND THEIR METABOLITES USING MICELLAR ELECTROKINETIC CAPILLARY ELECTROPHORESIS

5.1 Introduction

Evaluation of bound residues of veterinary drugs such as furazolidone, furaltadone, nitrofurazone, and nitrofurantion which belong to the class of nitrofurans (NFs), have been acknowledged as a vital aspect of food safety. Use of nitrofuran antibiotics (NFAs) in food-producing animals has been banned in the European Union and United States of America due to mutagenicity and carcinogenicity concerns. The analysis and measurement of nitrofuran metabolites (NFMs) in foods however is still required as an important issue in food safety. In the past NFAs were used as veterinary drugs and added to feedstock in order to prevent some protozoan and bacterial infections, including fowl choleran swine enteritis. NFAs were also commonly used as a feed additive to maintain adequate growth rate and feed conversion. Due to the suspected carcinogenic nature of NFMs, the European Union (EU) prohibited their use in food animal production by their listing in Annex 1V of the Council Regulation 2377/90 [1] . Due to the absence of a maximum residue limit (MRL) of NFs, the presence at any concentration in animal feed can violate the law [2, 3]. However with the improvement of analytical methods the EU Commission Decision of 13 March 2003 has set up a minimum required performance limit (MRPL) set at 1µg/ kg for each NFM for any method combine with the analysis of NFs in poultry meat and aquaculture products [4].

The molecular structures of NFAs and NFMs are presented in Fig. 5.1. The presence of the 5-nitro group is a common feature of NFAs, which contributes to antimicrobial activity [5]. The NFAs consist of bi-polar molecules having an antibiotic moiety and a neutral chemical residue, which varies from one molecule to another. When the drug is administered to an animal, the antibiotic moiety reacts quickly and the inactive counter part is rapidly excreted in the urine. In the same time, the neutral chemical residue (metabolite) covalently binds to circulating tissue proteins, leaving traces within the animal after months of administration. When the NFM binds to the protein, it produces a very stable adduct due to the amide bond, which is most probably inactive. This adduct can serve as a probe for determination of nitrofuran residues in food.

In 2002, it was discovered that NFA residues (NFMs) occurred in fish products like shrimp and catfish originating from Southeastern and Asian countries. A continuing interest in analysis and information on the subject still persists today because the problems related to NFMs have not yet been eliminated. Imported products may still contain these residues due to questionable farming practices in other countries. In addition to public health implications, the presence of NFMs in food products can have significant economic consequences for worldwide food product importers and exporters.

Figure 5 .1: Structures of NFAs with their respective NFMs and numbering scheme used in electropherograms

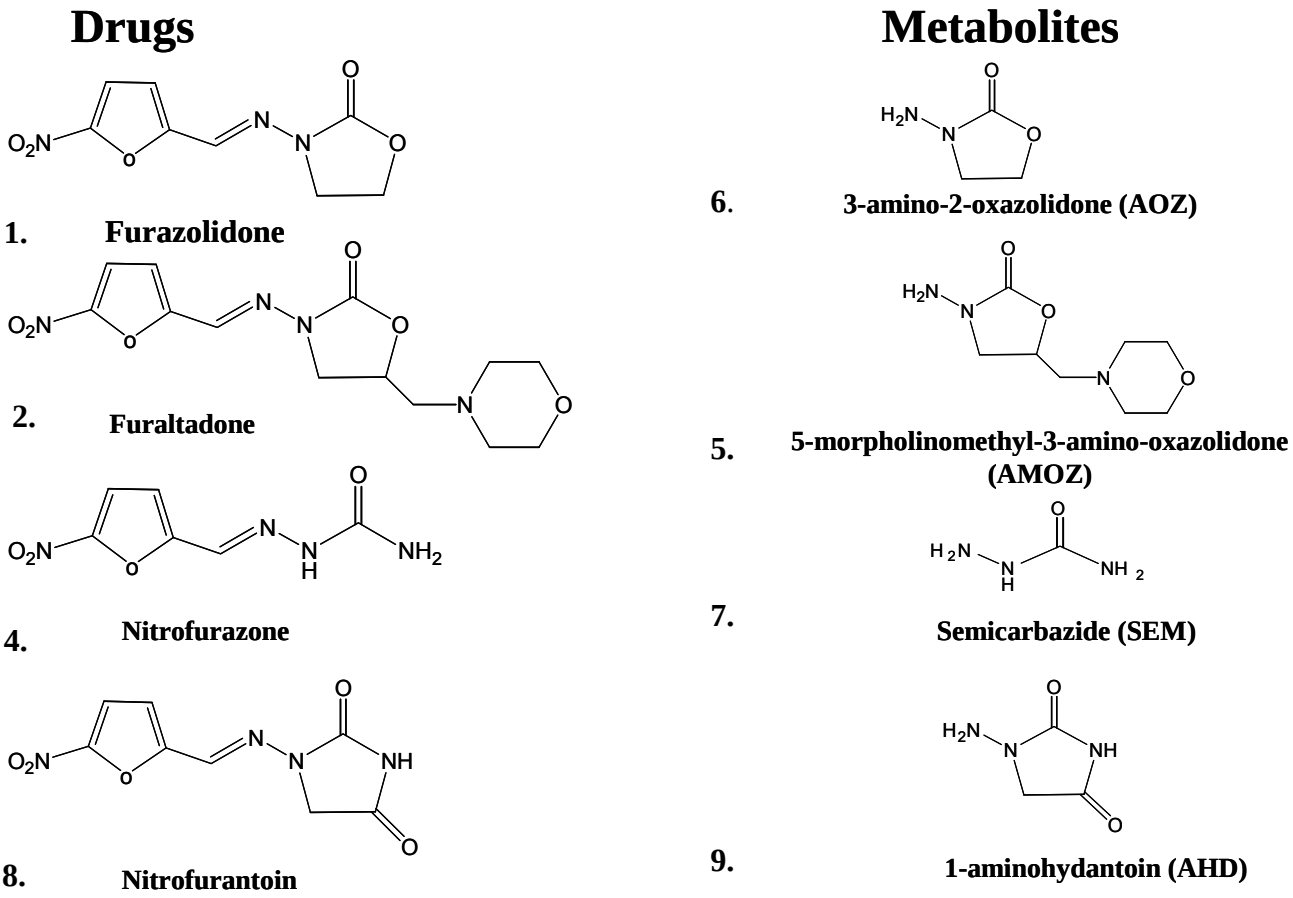

Note: 2-NBA (peak 3 in electropherograms) not shown

Recently a number of laboratories have been involved in analytical research to develop methods to detect NFMs. However there is no reference method for analysis of these NFAs or NFMs. It is impossible to detect NFMs by measuring their parent drugs because NFAs metabolise rapidly, with *in vivo* half lives of less than a few hours [6, 7]. However, NFMs are very stable and are detectable for several months after administration. Fig. 5.2 represents the metabolism of NFAs in animal tissue.

Figure 5.2: Proposed nitrofuran metabolism (example for Furazolidone)

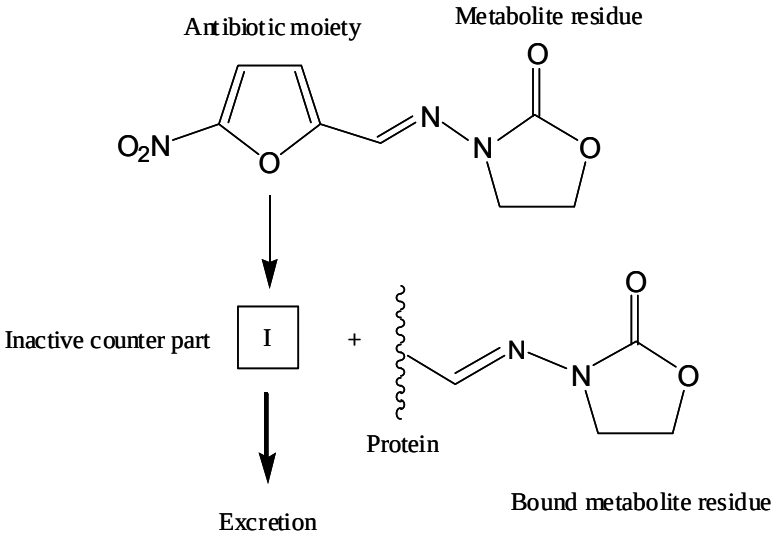

The NFMs are very small molecules and do not contain a UV chromophore. Hence for UV detection metabolites are derivatised using 2-nitrobenzaldehyde (2-NBA), under moderate acidic conditions, to introduce a UV absorbing chromophore, as shown in Fig.5.3 [5]. During the derivatising process, the carboxylic acids are converted to their corresponding acyl chlorides and these intermediates can react with a suitable amine to form a UV-vis absorbing derivative [8]. An increase in molecular mass and absorptivity accompanies derivatisation of NFMs with 2-NBA. The increase in molecular mass of NFMs hence enabled analysis by chromatography.

Figure 5.3: Derivatisation reaction of four nitrofuran metabolites with 2-NBA to yield 2- nitrophenyl derivatives.

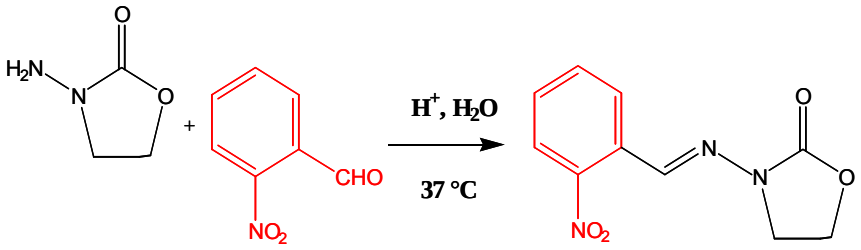

3-amino-oxazolidone

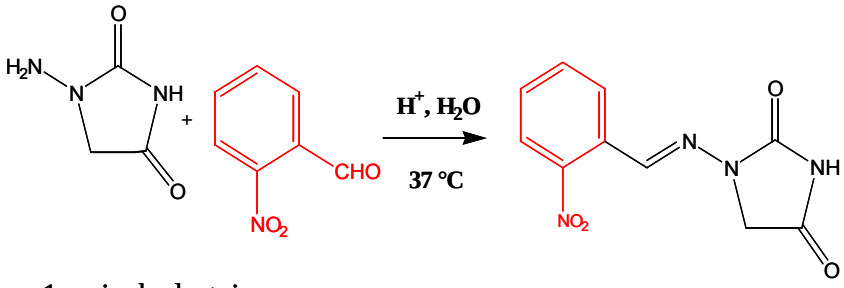

1-aminohydantoin

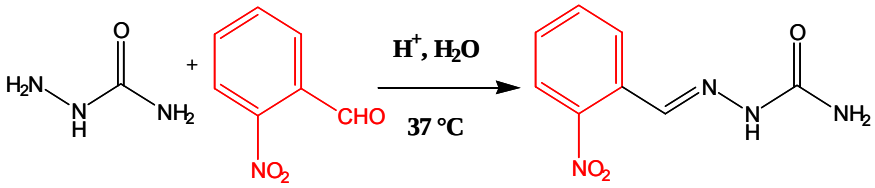

Semicarbazide

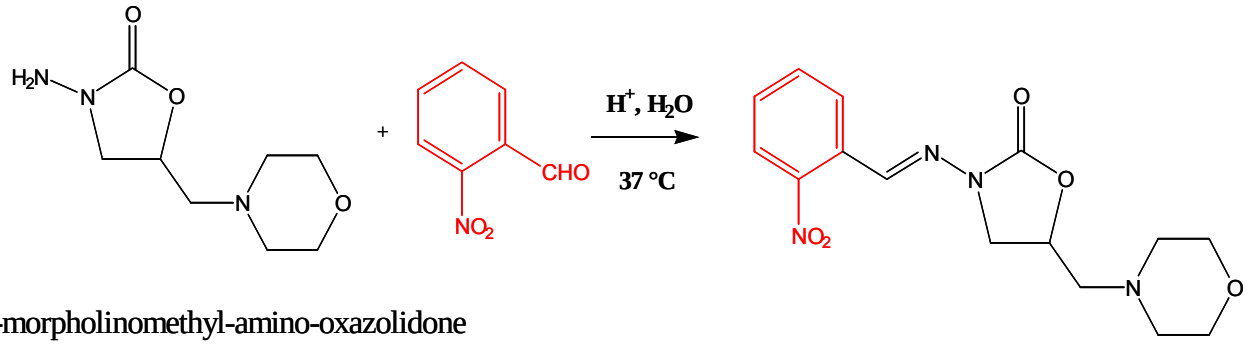

5-morpholinomethyl-amino-oxazolidone

During derivatisation process, HCl and 2-NBA were mixed with NFMs and the mixture was then heated. The details of derivatisation steps are described in 3.5.1.2 of Chapter 3. Derivatisation helps to prevent the rebinding of NFMs to protein and also to produce derivatives, which possess chromophores suitable for UV detection. Analyte enrichment and clean up was performed by Solid phase extraction (SPE). This is a good technique for the extraction of the nitrophenyl derivative. The details of SPE procedure is described in 3.5.1.3 of Chapter 3.

5.2 Results and Discussion

The separation of NFAs and NFMs was attempted using Capillary Zone Electrophoresis (CZE) mode and various buffers such as borate and phosphate with varying pH and voltage. No Nitrofuran peaks were observed using this CZE technique. The separation was then attempted using the MEKC technique with sodium dodecyl sulphate (SDS) as the micelle forming agent and borate and phosphate as the buffer electrolyte. However better reproducibility and ease of dissolution was observed when using sodium deoxycholate (SDC) as the micelle forming agent. The chromatogram of the NFAs and NFMs mixture prior to optimisation of the separation conditions is shown in Fig 5.4.

Figure 5.4: Electropherogram showing the separation of NFA and NFM prior to optimisation

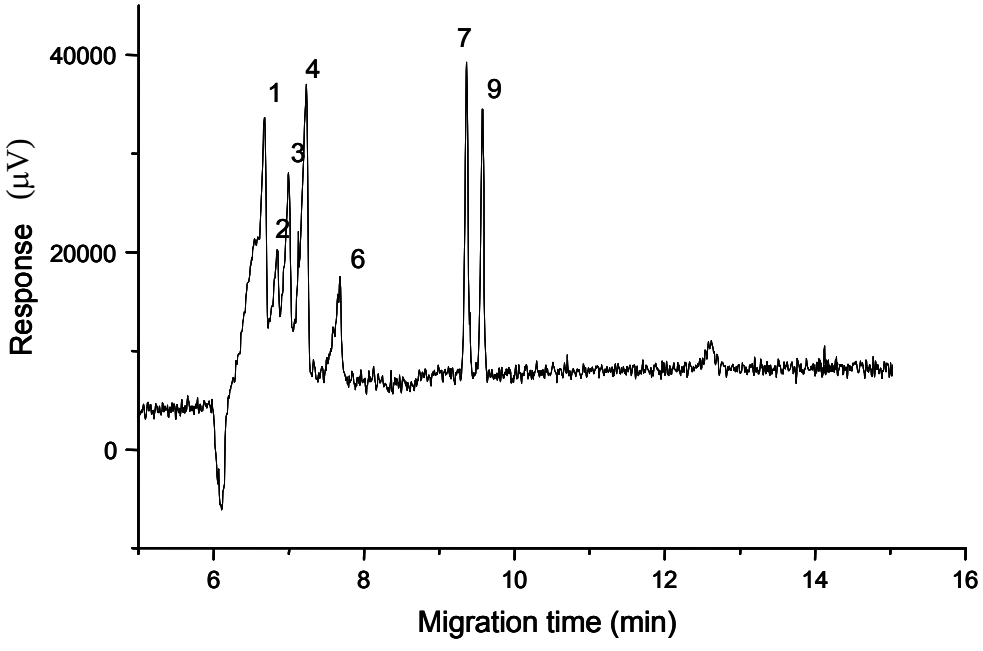

Different methods of sample injections were trialled. When using hydrodynamic injection (5 mbar 6 s), it resulted in broad peaks as shown in Figure 5.5.

Figure 5.5: Electropherogram showing the separation of NFAs and NFMs using hydrodynamic injection

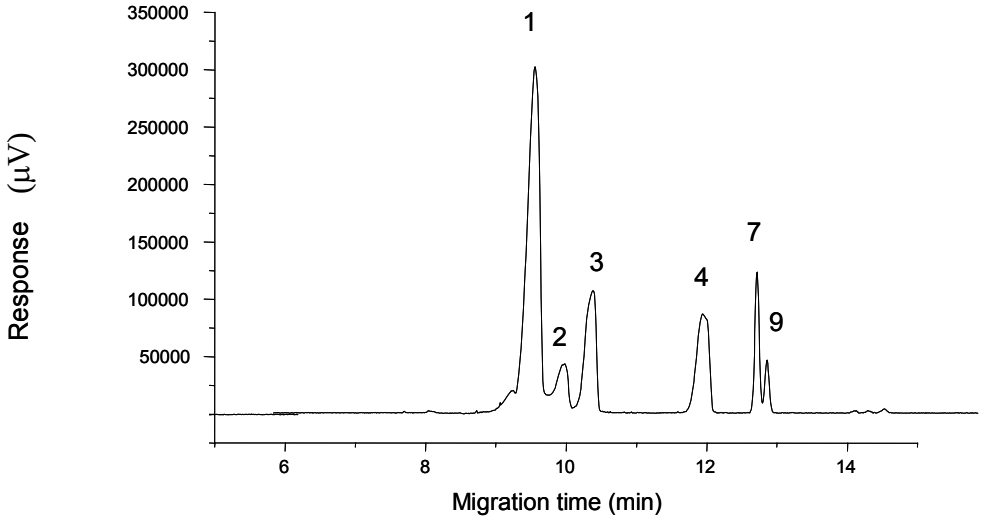

Sample injection was then tried using the electrokinetic mode. Electrokinetic injection of 5 kV for 12 s and 5 kV for 6 s were performed; the respective electropherograms are shown in Fig 5.6 a and b.

Figure 5.6 a: Electropherogram showing the separation of NFAs using electrokinetic injection of 5kV for 12 s

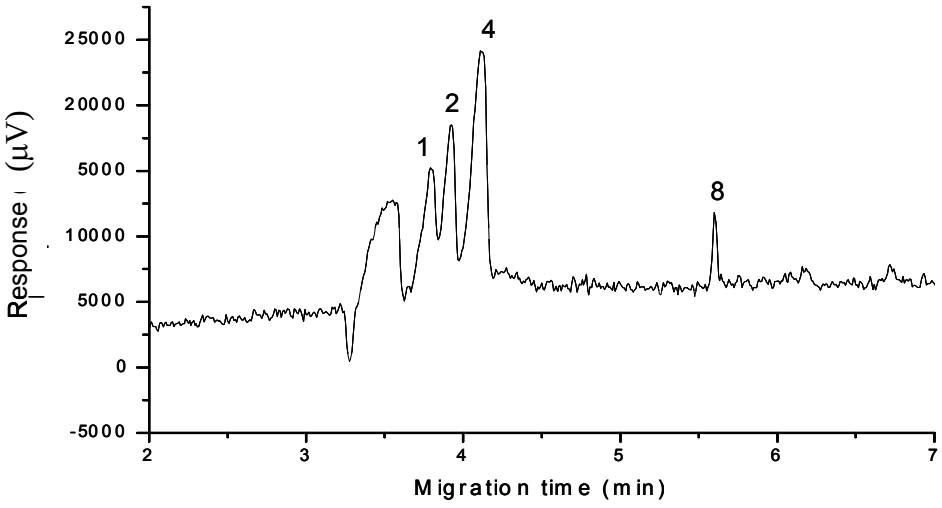

Figure 5.6 b: Electropherogram showing the separation of NFAs using electrokinetic injection of 5kV for 6 s

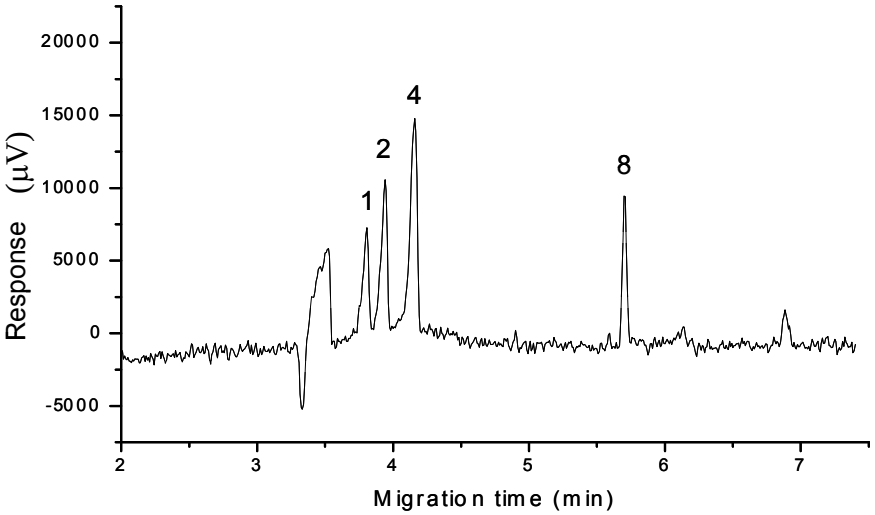

All subsequent analyses were performed using electrokinetic injection of 5 kV for 6 s injection due to observations of sharp narrow peaks.

The optimum wavelength for detection of NFAs was about 362 nm, whereas for derivatised NFMs 275 nm was preferred. Although NFAs exhibited a 40% reduction in signal response at 275 nm (the optimum wavelength for NFMs), 275 nm was chosen to analyse both NFAs and NFMs in a single run due to the interest in maximising response for the analytically more important metabolites. Fig 5.7a and 5.7c show the responses of NFAs at 362 nm and 275 nm respectively and the responses of the mixture of NFAs and NFMs at 362 nm and 275 nm are shown in Fig 5.7b and 5.7d respectively.

Figure 5.7 a: Electropherogram showing the separation of NFAs at 362 nm

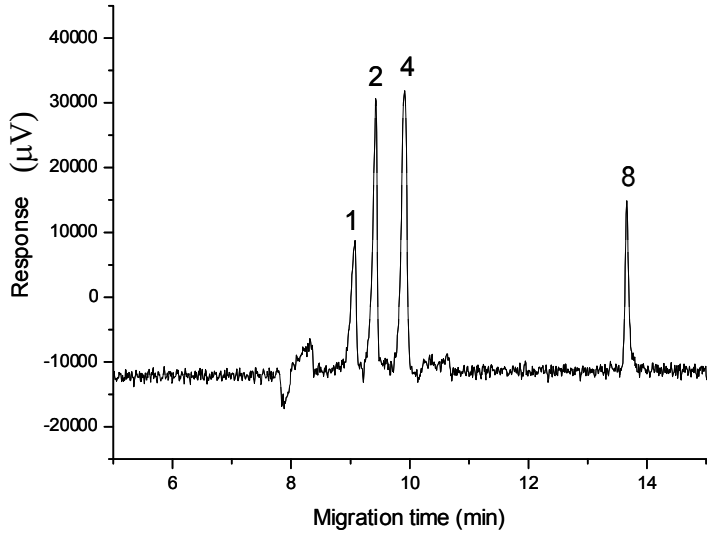

Figure 5.7 b: Electropherogram showing the separation of NFAs at 275 nm

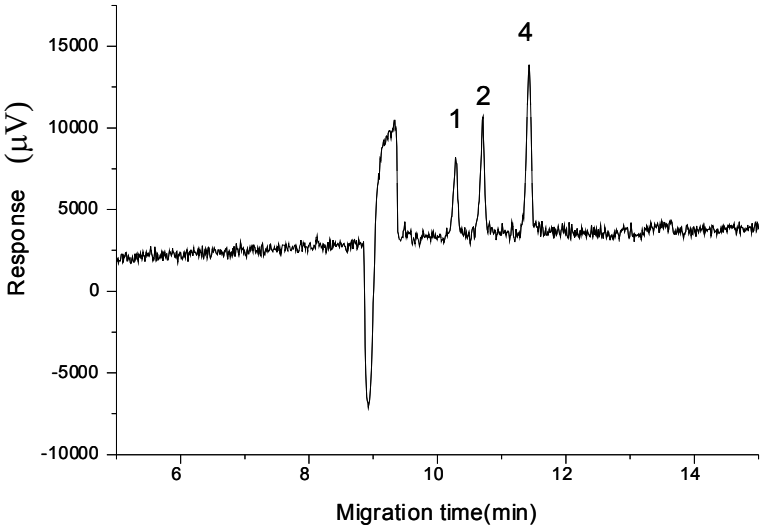

Figure 5.7 c: Electropherogram showing the separation of NFAs and NFMs at 362 nm

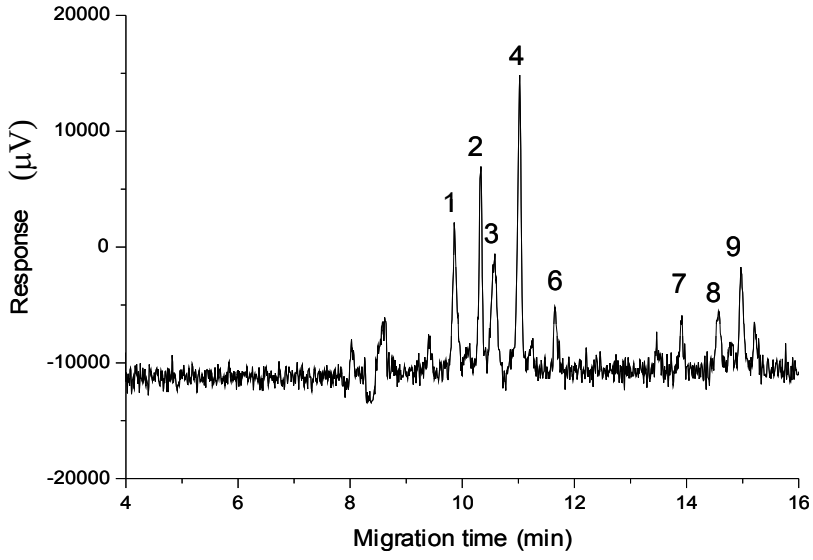

Figure 5.7 d: Electropherogram showing the separation of NFAs and NFMs at 275 nm

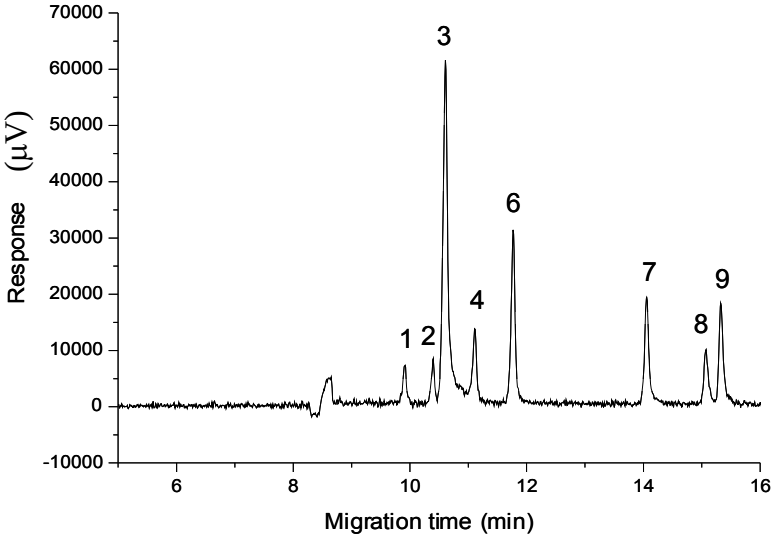

Capillary columns with internal diameter of 75 μm ID uncoated fused silica capillary of varying total lengths 53 cm, 73 cm and 93 cm were attempted to find the best possible separation of NFAs and NFMs within the shortest run time. Fig 5.8 a, 5.8 b and 5.8 c show the separation of NFs using capillary column lengths of 50 cm, 93 cm and 73 cm respectively. A Capillary column of total length 73 cm and effective length of 56 cm was chosen to conduct the subsequent sample analysis.

Figure 5.8 a: Electropherogram showing the separation of NFAs and NFMs using 53 cm capillary column

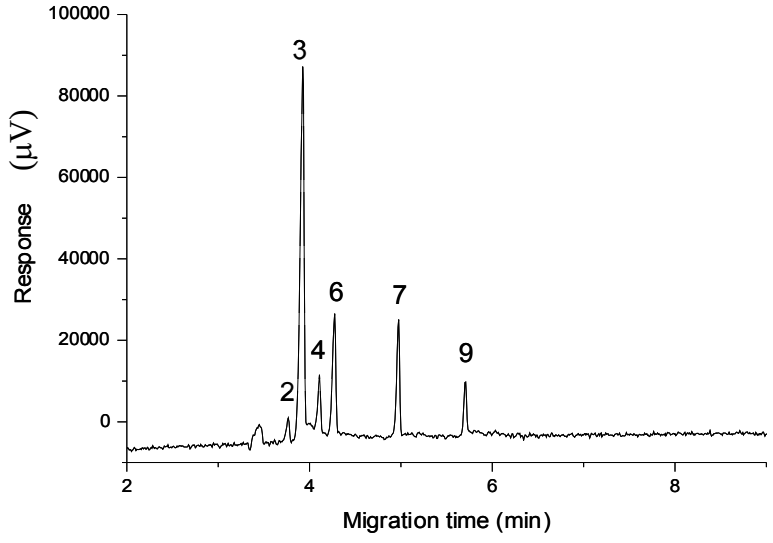

Figure 5.8 b: Electropherogram showing the separation of NFAs and NFMs using 93 cm capillary column

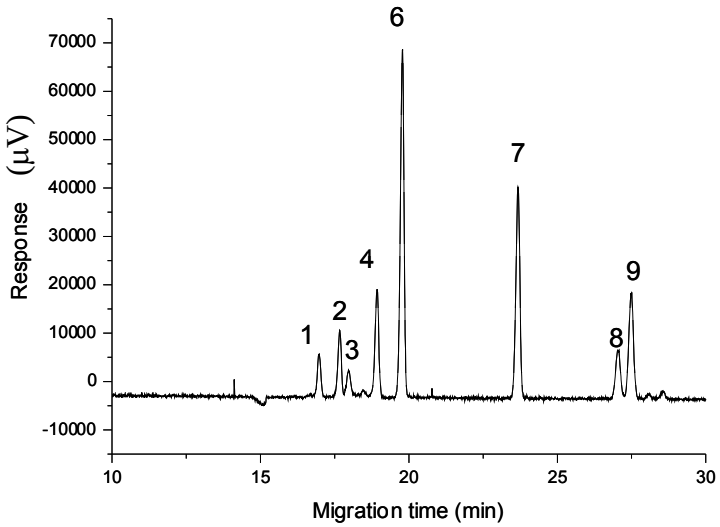

Figure 5.8 c: Electropherogram showing the separation of NFAs and NFMs using 73 cm capillary column

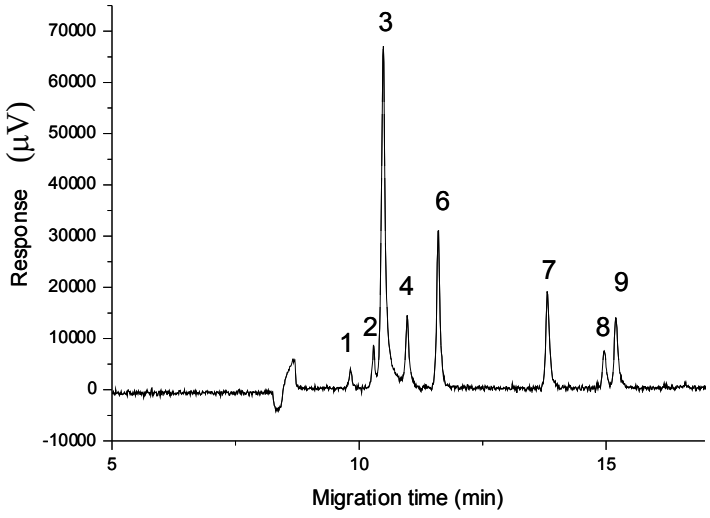

After deciding on the capillary column length and the injection type, the next step was to optimise the running buffer to obtain maximum resolution within minimal run time. The first step was to define the experimental domain by finding the extremes for parameters such as borate and phosphate concentrations in the buffer, SDC concentration, applied voltage and the pH of the running buffer as shown in Table 5.1.

Table 5.1: Experimental boundary ranges of parameters

Parameters	SDC concentration	Voltage	Borate concentration	Phosphate concentration	pH
Range	0-100 mM	8-20 kV	0-40 mM	0-40 mM	7.0-10.0

After finding the workable ranges for each CE parameter, a Fractional Factorial Design (FFD) was then employed to screen for the significant factors. In this design, a five-factor system was used at two experiment ('high' and 'low') levels. This system required 24 runs for the experimental design as shown in Tables 4.3 and 4.4 of Chapter 4.The five variables screened in the initial FFD were: concentration of SDC (20 mM- 100 mM), pH of running electrolyte (7.5-9.5), voltage (10 kV-20 kV), concentration of potassium dihydrogen orthophosphate (0-40 mM) and concentration of sodium borate (0-40 mM) in the buffer. The centre point was at pH 8.5, 60 mM of SDC, 15 kV, 20 mM borate and 20 mM phosphate.

The quality of chromatograms were measured using chromatographic exponential function (CEF) [9] as shown in Table 4.4 of Chapter 4.The highest CEF values were detected when borate was absent in the buffer and the lowest CEF values of FFD were from centre points. The centre point of FFD study is shown in Fig 5.9 b and a selected CE trace from FFD is shown in Fig 5.9a.

Figure 5.9a: Electropherogram of a selected condition of FFD used in optimisation process (condition used: 40 mM borate, 40 mM phosphate, pH=7.5, 20 mM surfactant concentration, voltage 20 kV).

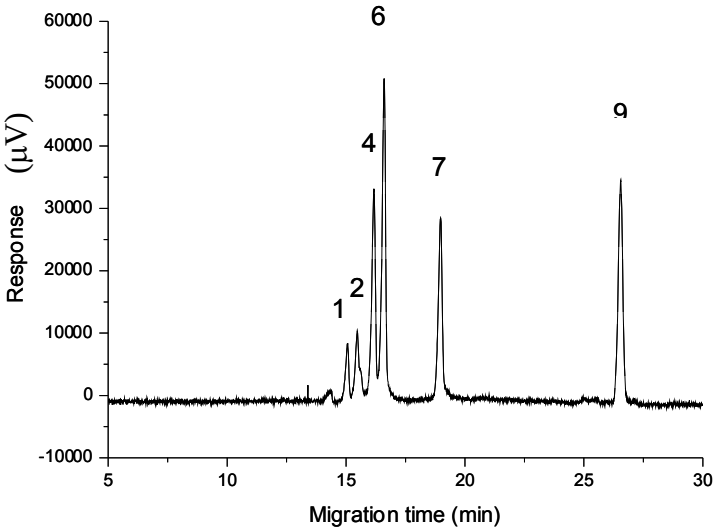

Figure 5.9b: Electropherogram showing the centre point of FFD used in optimisation process (conditions used: 20 mM borate, 20 mM phosphate, pH=8.5, 60 mM surfactant concentration, voltage 15 kV).

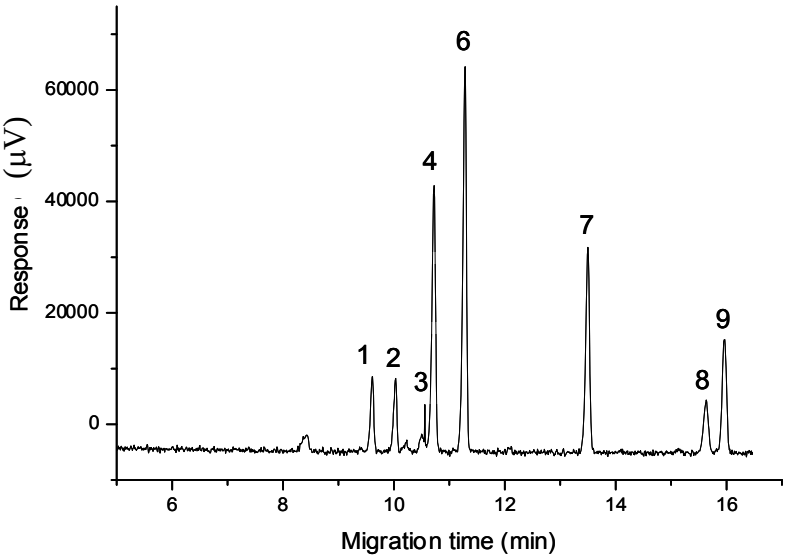

From the initial optimisation results, it was observed that three factors: pH, surfactant concentration and voltage have a significant influence on the responses. It was observed that SDC did not readily dissolve in phosphate buffer in the absence of borate in the electrolyte, and pH adjustments were aided when phosphate was present in the electrolyte with borate. This could be due to “salting out effect”.

A CCD was employed to optimise the significant factors. In the next step of optimisation, 3 variables were retained (pH, voltage and SDC). Borate to phosphate buffer ratio in the electrolyte was fixed to 20 mM borate: 20 mM phosphate, pH and SDC concentration was narrowed down in CCD design. The pH was varied between 8.5-9.5, SDC concentration between 60 mM to 100 mM and voltage was varied between 10 kV to 20 kV as shown in Table 4.5 and 4.6 of Chapter 4. The centre point was pH 9.0, 80 mM of SDC concentration and voltage 16 kV. A selected CE trace from CCD is shown in Fig 5.10.

Figure 5.10: Electropherogram of a selected condition of CCD used in optimisation process (conditions used: 20 mM borate, 20 mM phosphate, pH=9.0, 60 mM SDC, voltage 16 kV).

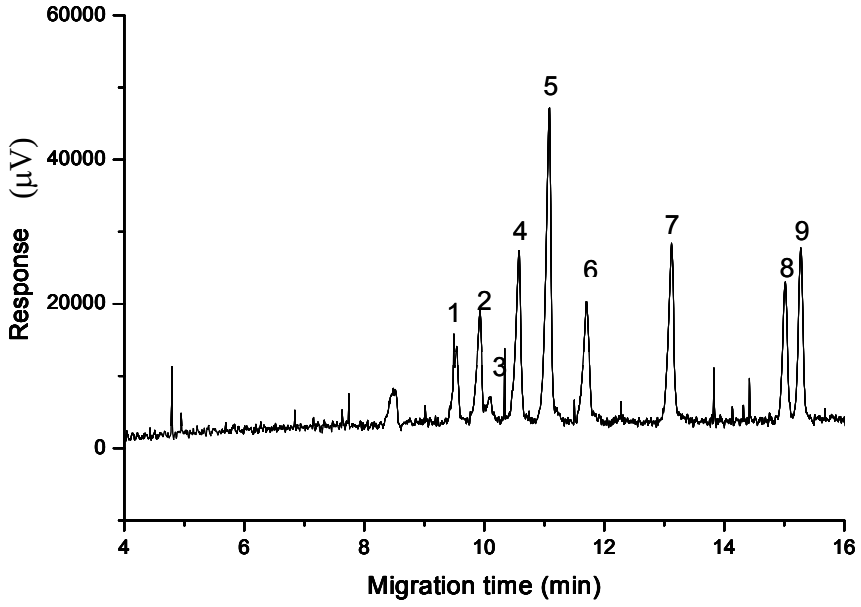

From the final optimisation results, it was observed that at a pH below 8.8, surfactant concentration below 70 mM, and voltage below 12 kV resulted in higher CEF values indicating either or combination of poor resolution and longer run time. The lowest CEF values were obtained with centre point (conditions: 20 mM borate, 20 mM phosphate, pH=9.0, 80 mM SDC, voltage 16 kV) and also with pH higher than 9.2 and voltage higher than 18 kV. However running electrolyte with pH above 9.2 and voltage above 18 kV, caused the CE traces to exhibit high baseline noise. A selected CE trace with high baseline noise and the centre point of CCD are shown in Fig 5.11 and 5.12 respectively.

Figure 5.11: Electropherogram of a selected condition of CCD used in optimisation process (condition used: 20 mM borate, 20 mM phosphate, pH=9.2, 90 mM SDC concentration, voltage 18 kV).

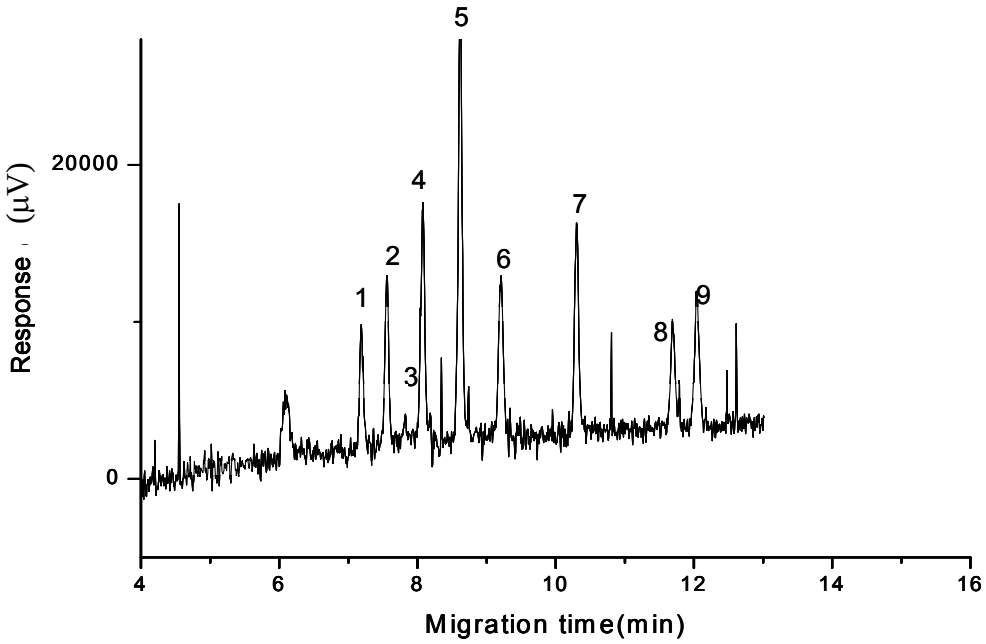

Figure 5.12: Electropherogram showing the centre point of CCD used in optimisation process (conditions used: 20 mM borate, 20 mM phosphate, pH=9.0, 80 mM SDC, voltage 16 kV).

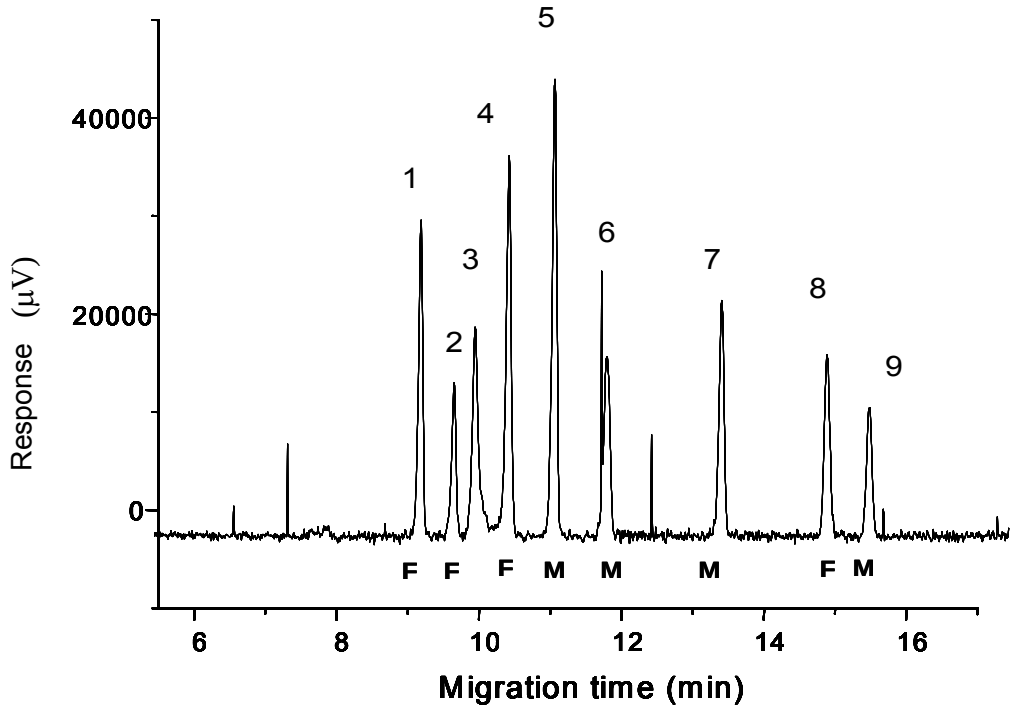

NFAs are indicated using **F** and NFMs are indicated using **M**.

5.2.1 The Effect of Voltage

The running voltage has an impact on separation as it affects the resolution between peaks, and the total completion time of analysis, hence affecting the CEF value. The electropherograms using voltages 14 kV and 20 kV are shown in Fig 5.13 a, b respectively. The lower the voltage used, the longer the analysis time as shown in Fig 5.13 a. The effect of voltage on resolution was investigated over the range of 10 kV to 20 kV. Although application of a higher voltage generally results in more efficient separation in respect of time and peak narrowness, here the optimum voltage (16 kV) was the highest possible, whilst limiting joule heating effects which would lead to band broadening, baseline disturbances, and a resultant loss of efficiency. Comparison of Fig. 5.13 a and b shows that at the higher voltage peak 8 migrates closer to peak 9, however qualitatively the relative electrophoretic peak positions are similar for most components.

Therefore an optimum voltage of 16 kV was used for future work in order to obtain the best resolution in the shortest time. The conditions used in Fig 5.13 were 20 mM phosphate, 20 mM borate, 80 mM SDC and pH 9.0 with varying voltage as specified below.

Figure 5.13 a: Electropherogram showing the separation of NFAs and NFMs using low voltage (14 kV)

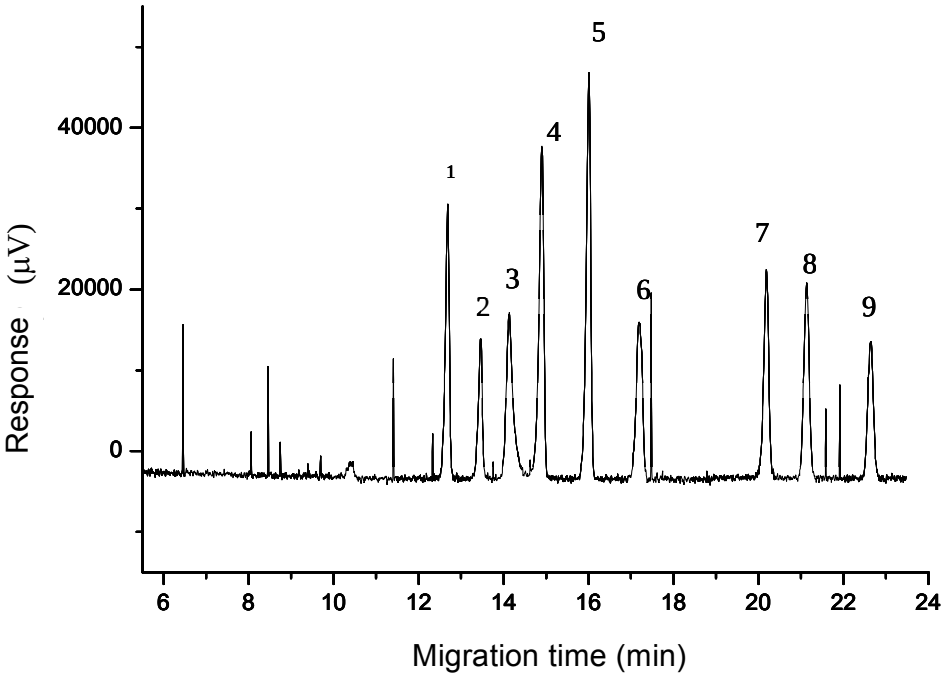

Figure 5.13 b: Electropherogram showing the separation of NFAs and NFMs using high voltage (20 kV)

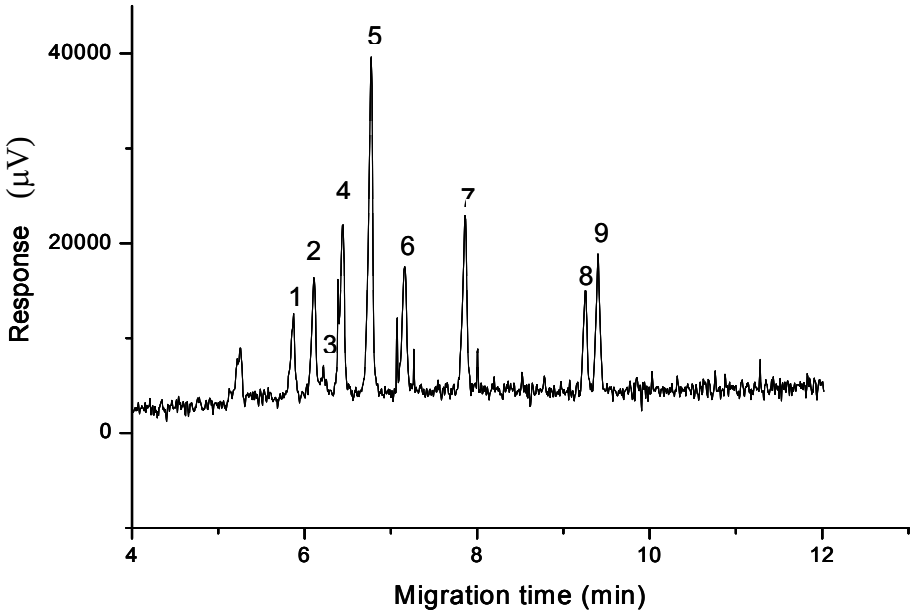

5.2.2 Effect of pH

The pH of the running electrolyte is one of the critical factors in resolution due to its impact on Electro-Osmotic Flow (EOF) in a fused-silica capillary, and the possible effect on solute charge altering relative migrations. Resolution can be improved by reducing EOF or by increasing the difference in the electrophoretic mobility of analytes. This can be achieved by changing pH and composition of the buffer. The effect of pH value on the resolution between peak pairs was investigated over the range of pH 7.5-9.5. Compared with the optimum separation between peak pairs obtained at pH 9.0 (Fig. 5.12), the impact of pH began to notice with a small lowering of pH (8.8) on resolution. The impact of lower and higher pH on the resolution and run time are shown in Fig 5.14 a and 5.14 b. The pH of the running electrolyte was adjusted by adding 2 M hydrochloric acid or 2 M sodium hydroxide as required. The residual derivatising reagent (peak 3) starts to interfere with peak 4. At lower pH (8.0) peaks 8 and 9 co-migrated and peaks 1-5 became a cluster of peaks with marginal resolution. Clearly, the separation shows pH sensitivity, and for a rugged separation, buffer pH needs to be well controlled, with ±0.2 pH unit suggested by data reported here. The conditions used in Fig 5.14 were 20 mM phosphate, 20 mM borate, 80 mM SDC and 16 kV with varying pH as specified below.

Figure 5.14 a: Electropherogram showing the separation of NFAs and NFMs using low pH (pH 8.5)

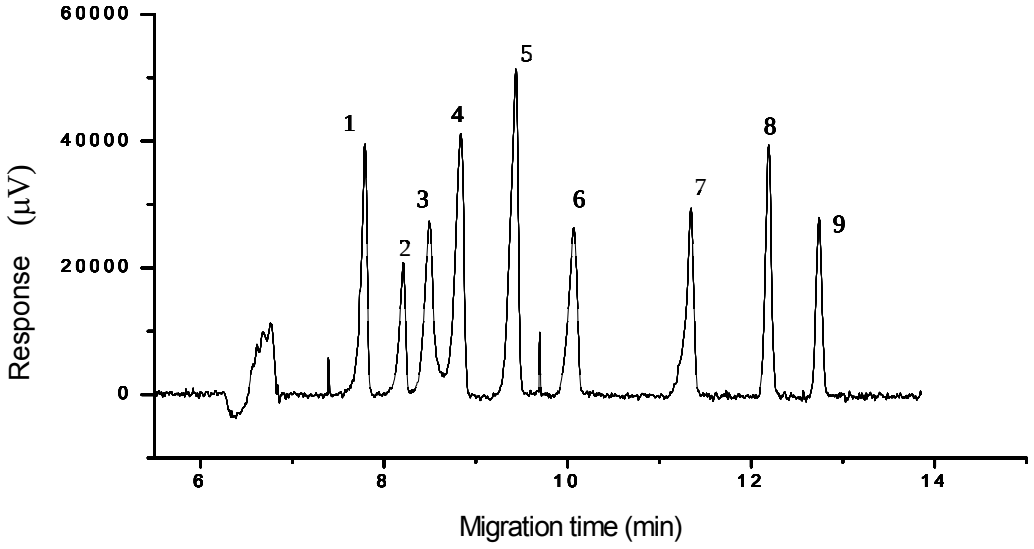

Figure 5.14 b: Electropherogram showing the separation of NFAs and NFMs using high pH (pH 9.2)

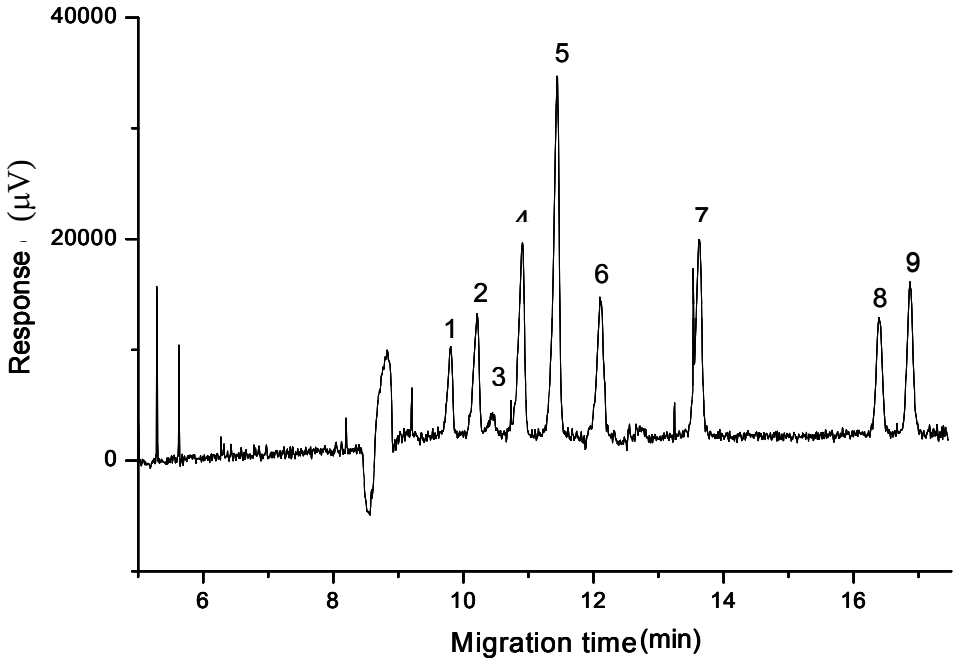

5.2.3 Effect of Surfactant

Both SDS and SDC were tested for this separation. It was found that surfactant chemistry played a significant role in NFAs and NFMs separation. The latter was chosen as the preferred anionic surfactant in the separation of NFAs and NFMs by using MECC due to its apparent qualitative improvement over SDS. The micelle controls the relative retention of the solutes by the ease of solute absorption (partitioning) into the micellar phase. The formation of micelles in the running electrolyte solution may be considered as a hydrophobic pseudo stationary phase [6]. Addition of SDC micelles to the running electrolyte increases the resolution between peaks significantly; in the CZE case, no peaks were found in the absence of SDC micelles. A few peaks were observed when SDC concentration was at the level of 5 mM in the running electrolyte, as shown in Fig 5.15 a.

The effect of SDC concentration on resolution was investigated over the range of 20 mM to 100 mM. Optimum separation was at an SDC concentration of 80 mM as shown in Fig. 5.12. The effect of increase in surfactant concentration from 5 mM to 100 mM on the resolution and total run time are shown in Fig 5.15 a-d. The elution order of the nine peaks is dependent on the hydrophobic nature of the analytes. The partition coefficient of analytes plays a major role in partitioning between the aqueous phase and the pseudo stationary phase. The stronger the interaction between analyte and micelle, the slower the elution, since the micelles are a slowly migrating species. Components 8 and 9 appear to migrate more closely together as SDC concentration decreases. Indeed, component 8 can be seen to migrate with peaks 7 or 9 simply by altering SDC concentration. At low SDC concentration (e.g. 20-40 mM), total migration time is short, and peaks 1-6 are presented as a poorly resolved cluster. Thus a higher SDC concentration is preferred. Peak 3 partially overlaps component 2 at 70 mM SDC. The conditions used in Fig 5.15 were 20 mM phosphate, 20 mM borate, 15 kV and pH 8.8 with varying SDC concentration as specified below.

Figure 5.15 a: Electropherogram showing the separation of NFAs and NFMs using low SDC concentration (5 mM SDC concentration)

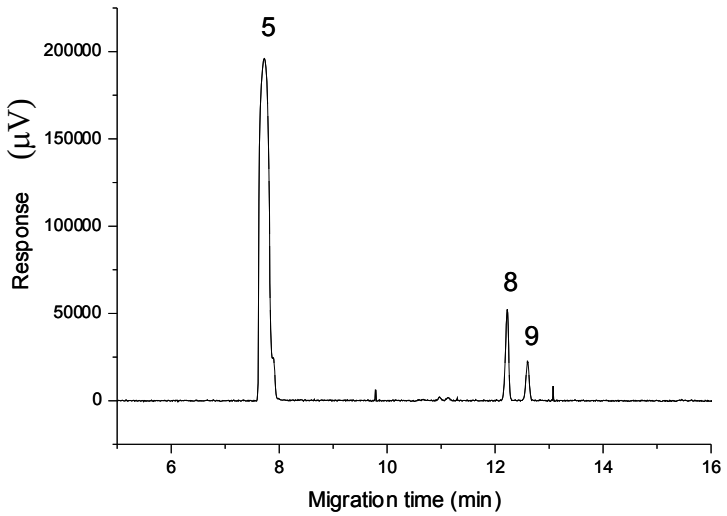

Figure 5.15 b: Electropherogram showing the separation of NFAs and NFMs using low SDC concentration (20 mM SDC concentration)

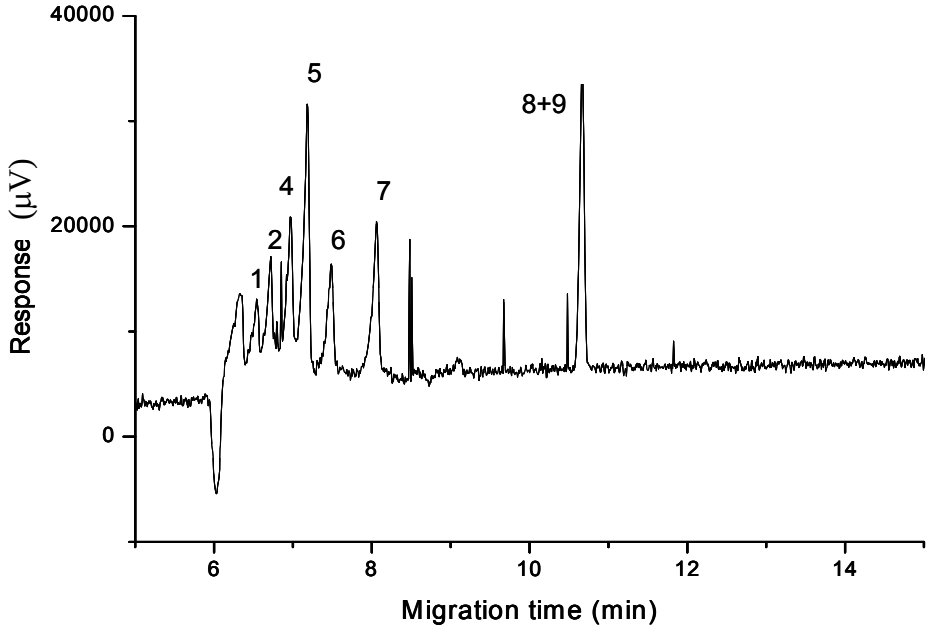

Figure 5.15 c: Electropherogram showing the separation of NFAs and NFMs using low SDC concentration (70 mM SDC concentration)

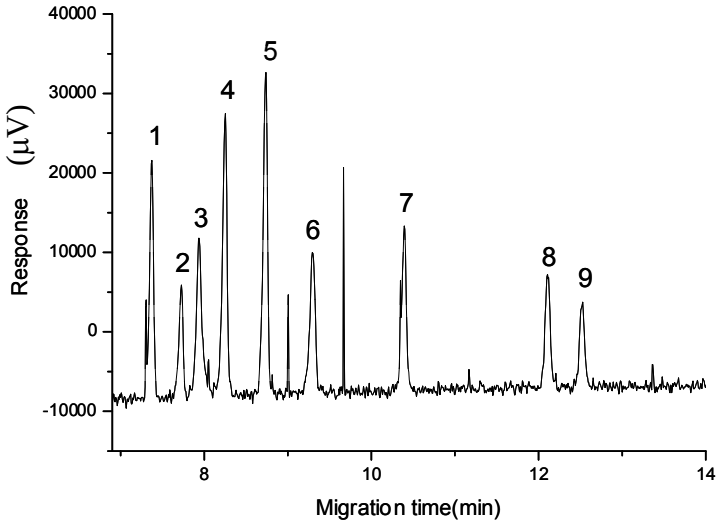

Figure 5.15 d: Electropherogram showing the separation of NFAs and NFMs using high SDC concentration (100 mM SDC concentration)

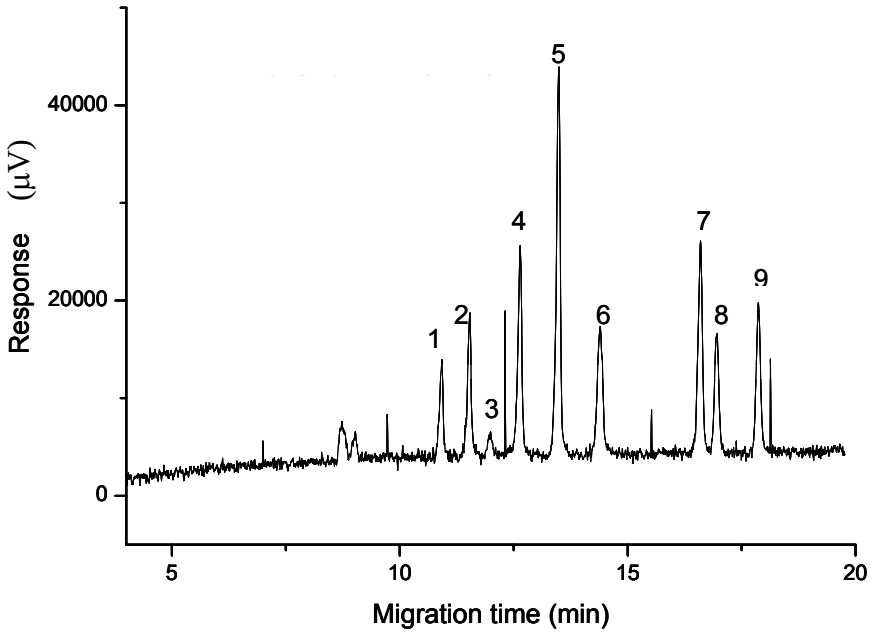

5.2.4 Validation of and Ruggedness of the Nitrofuran Separation Method

After completing the runs of CCD optimisation study, ruggedness of the method was performed. The ruggedness check is carried out to evaluate the ruggedness of the chosen settings. The ruggedness of an analytical method is a measure of its capacity to remain unaffected by small deliberate variations in the method parameters and provide an indication of its reliability during normal usage (i.e. where small changes with experimental settings may arise from uncertainties or small errors in the procedure).

The validation and the ruggedness test were conducted using a full factorial design with 12 runs (4 centre points were included), after obtaining the optimum conditions. Three significant factors were varied (pH, voltage and surfactant concentration) at three different levels as shown in Table 5.2. Borate to phosphate

buffer ratio in the electrolyte was fixed to 20 mM borate: 20 mM phosphate. Refer to Tables 4.7 and 4.8 of Chapter 4 regarding details of the design used in ruggedness study.

Table 5.2: Ranges of parameters used in ruggedness study

Parameters	SDC concentration	Voltage	pH
Range	70-90 mM	14-18 kV	8.8-9.2

The centre point was pH 9.0, 80 mM of SDC concentration and voltage 16 kV. The CEF values between 16-17 were obtained after repeating the centre point 4 times. The centre point of ruggedness test is shown in Fig 5.17 a. A selected sample CE trace of the ruggedness test is shown in Fig 5.17 b (variation of voltage and SDC concentration). CEF values of electropherograms of the ruggedness test varied between 16-34 indicating that the chosen conditions are robust for NFAs and NFMs separation. The lowest CEF values were obtained from the centre point and the highest CEF value was obtained when using voltage of 14 kV, resulting in the longest run time.

The CEF values from the validation and ruggedness test were used to produce main effect plots of significant factors using Minitab software as shown in Fig 5.16. The main effect plots indicate that the lowest CEF can be obtained with pH 9.0, 16 kV and 80 mM of SDC concentration. Higher or lower values than pH 9.0, voltage 16 kV and SDC concentration of 80 mM would result in an elevated CEF value (ie: worse separation).

Figure 5.16: Main Effect plots of significant factors

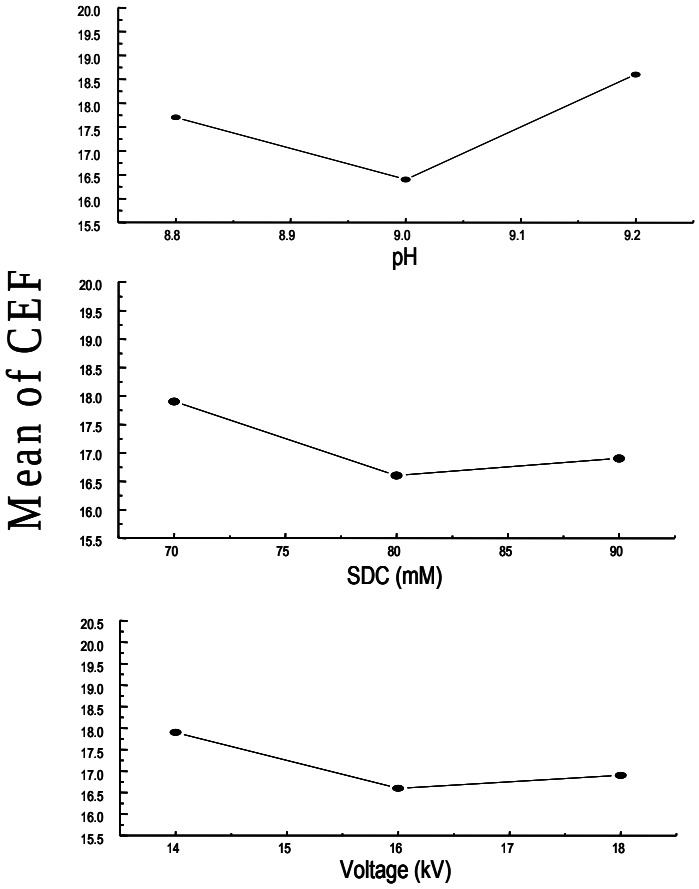

Figure 5.17 a: Electropherogram showing the centre point of ruggedness test of separation of NFAs and NFMs (Separation conditions: pH=9.0, voltage 16 kV, SDC of 80 mM)

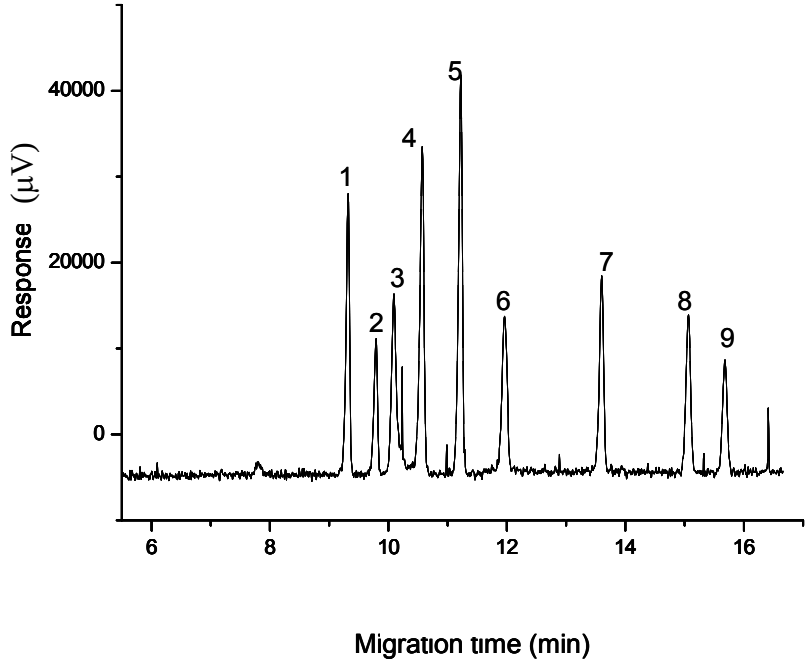

Figure 5.17 b: Electropherogram of a selected condition during the ruggedness test of NFAs and NFMs (Separation conditions: pH=9.2, voltage 18 kV, SDC of 90 mM).

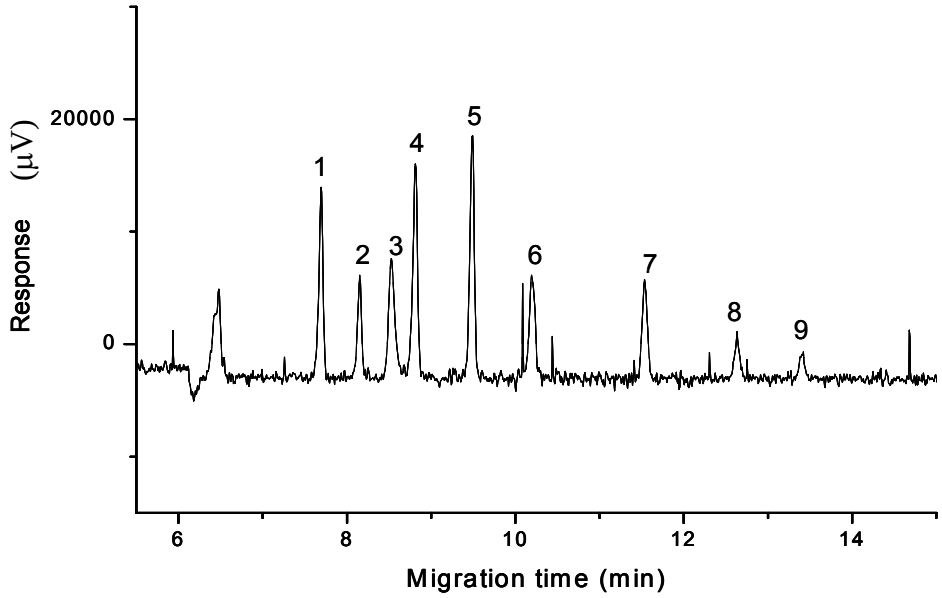

5.2.5 Reproducibility of the Nitrofuran Separation Method

The precision of an analytical method demonstrates the closeness of agreement between a series of measurements obtained from the homogeneous sample under the prescribed conditions. Reproducibility demonstrates the precision of the method. The reproducibility of the system was determined by performing five replicates under the optimum conditions. Good repeatability in migration times and areas was observed for NFAs and NFMs separation under the optimal conditions. The reproducibility data of migration times and areas are shown in Tables 5.3, 5.4 and 5.5, 5.6 respectively.

Table 5.3: Data showing reproducibility of migration times for selected NFAs and NFMs (concentration of peaks 5, 7, 9: 30 μg mL^{-1} and peak 2: 100 μg mL^{-1})

Run #	Absolute t_{mig} values (min)				
	Compound				
	2	NBA	5	7	9
1	9.68	10.42	11.06	13.40	15.48
2	9.81	10.59	11.24	13.61	15.70
3	9.68	10.45	11.09	13.43	15.49
4	9.79	10.57	11.22	13.60	15.68
5	9.80	10.59	11.26	13.66	15.72
Mean	9.75	10.52	11.17	13.54	15.61
rsd %	0.68	0.78	0.82	0.86	0.76

As shown in Table 5.3, the relative standard deviation of absolute migration times of Nitrofuran peaks were within 1% indicating good reproducibility of the chosen method.

Table 5.4: Data showing reproducibility of relative migration times vs 2-NBA for selected NFAs and NFMs (concentration of peaks 5, 7, 9: 30 μg mL^{-1} and peak 2: 100 μg mL^{-1})

RUN #	Relative t_{mig} vs 2- NBA				
	Compound				
	2	NBA	5	7	9
11	0.929	1	1.061	1.286	1.486
12	0.926	1	1.061	1.285	1.483
14	0.926	1	1.061	1.285	1.482
15	0.926	1	1.061	1.287	1.483
16	0.925	1	1.063	1.290	1.484
Mean	0.927	1.000	1.062	1.287	1.484
sd	0.001	0.000	0.001	0.002	0.001
%rsd	0.147	0.000	0.080	0.152	0.093

As shown in Table 5.4, the relative standard deviation of relative migration times of Nitrofuran peaks vs 2-NBA were within 0.2% indicating good reproducibility of the chosen method.

Table 5.5: Data showing reproducibility of areas for selected NFAs and NFMs (concentration of peaks 5, 7, 9: 30 μg mL^{-1} and peak 2: 100 μg mL^{-1})

Run #	Peak Areas (μV.s)				
	Compound				
	2	NBA	5	7	9
1	18282	46806	54024	30464	18978
2	14742	41507	50774	26634	16003
3	16931	46022	56861	29584	18659
4	16874	46685	54774	28806	19133
5	15173	42645	50304	26781	16312
Mean	16400	44733	53347	28454	17817
sd	1441	2477	2771	1699	1528
rsd %	8.8	5.5	5.2	6.0	8.6

As shown in Table 5.5, the relative standard deviation of areas of Nitrofuran peaks was within 9% indicating good reproducibility of the chosen method.

Table 5.6: Data showing reproducibility of areas for selected NFAs and NFMs (concentration of peaks 5, 7, 9: 30 mg L^{-1} and peak 2: 100 mg L^{-1})

RUN #	Relative peak areas vs 2- NBA				
	Compound				
RUN #	2	NBA	5	7	9
11	0.391	1	1.154	0.651	0.405
12	0.355	1	1.223	0.642	0.386
14	0.368	1	1.236	0.643	0.405
15	0.361	1	1.173	0.617	0.410
16	0.356	1	1.180	0.628	0.383
mean	0.366	1.000	1.193	0.636	0.398
sd	0.015	0.000	0.035	0.013	0.013
%rsd	3.982	0.000	2.902	2.114	3.194

As shown in Table 5.6, the relative standard deviation of relative areas of Nitrofuran peaks vs 2-NBA were within 3% for peaks 5 and 7 however peaks 2 and 9 were within 4% indicating good reproducibility of the chosen method.

5.2.6 Linearity of the NF Separation Method

The linearity of an analytical method is its ability (within a given range) to obtain test results, which are directly proportional to the concentration (amount) of analyte in the sample. Linearity was performed for all NFAs and NFMs except AMOZ due to lack of availability.

5.2.6a Linearity and Calibration of NFMs

The linearity data (area) of NFMs are shown in Table 5.7. NFMs (AOZ, SEM, and AHD) were linear over the range between 2 mgL^{-1} to 30 mgL^{-1}. The linearity of AMOZ was not performed due to lack of availability of the sample. Good linearities with coefficient of regression higher than 97% were obtained for NFMs as shown in Fig 5.18 a-c.

Table 5.7: Data showing linearity of area of NFMs

Concentration		NFM	
(mg L^{-1})	AOZ	SEM	AHD
2	8294	10634	6472
4	13819	17000	9606
8	28643	36730	18863
20	66557	90746	37869
30	107034	147149	49693

Figure 5.18 a: Linearity Plot for AOZ peak area

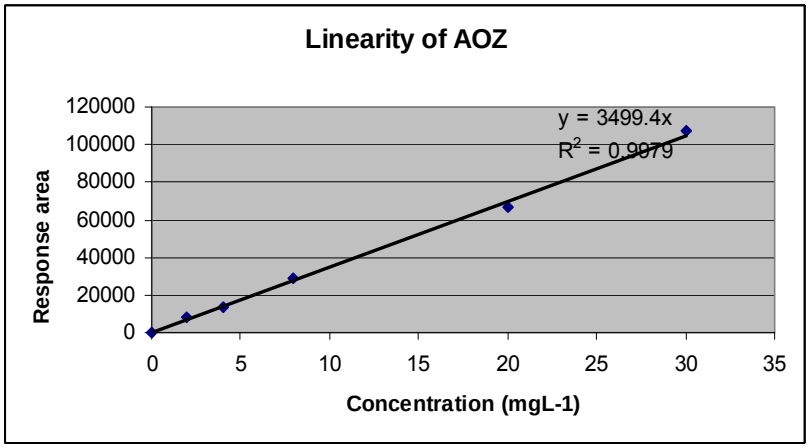

Figure 5.18 b: Linearity Plot for SEM peak area

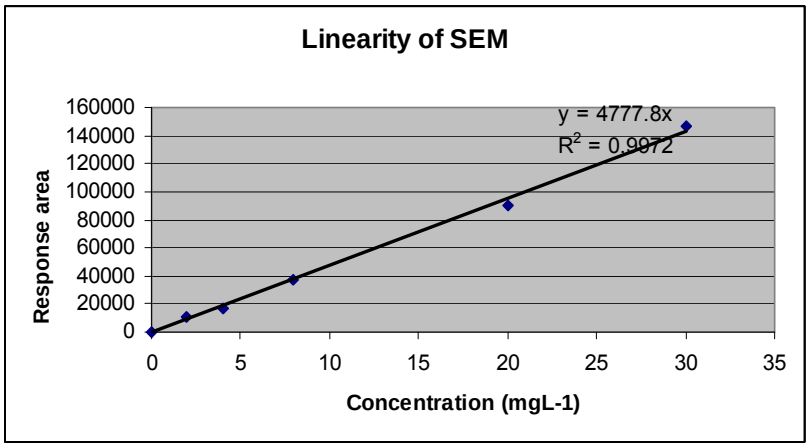

Figure 5.18 c: Linearity Plot for AHD peak area

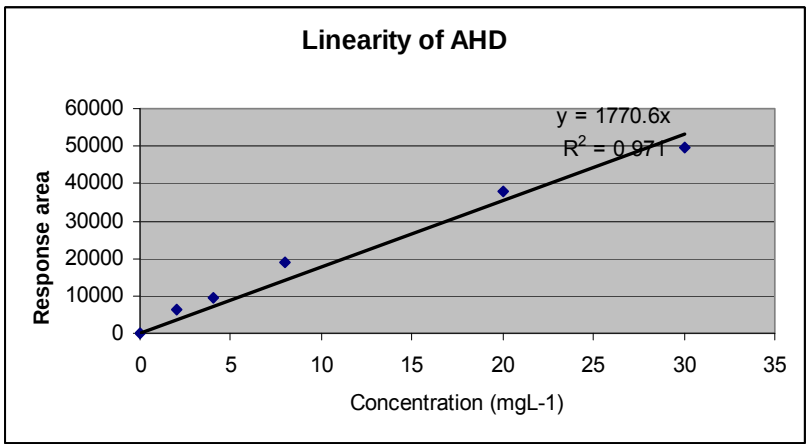

5.2.6b Linearity of NFA

The linearity data (area) of NFAs are shown in Table 5.8. NFAs (Furazolidone, Furaltadone, Nitrofurazone and Nitrofurantoin) were linear over the range between 20 mgL^{-1} to 100 mgL^{-1}. Good linearities with coefficient of regression higher than 98% were obtained for NFAs as shown in Fig 4.19 a-d.

Table 5.8: Data showing linearity of NFAs

Concentration mgL^{-1}	NFAs			
	Furazolidone	Furaltadone	Nitrofurazone	Nitrofurantoin
20	8941	7645	13645	4045
40	15165	13323	23731	9882
60	25992	21446	39245	14309
80	36246	30083	55453	20541
100	45734	38333	72530	25072

Figure 5.19 a: Linearity Plot of Furazolidone peak area

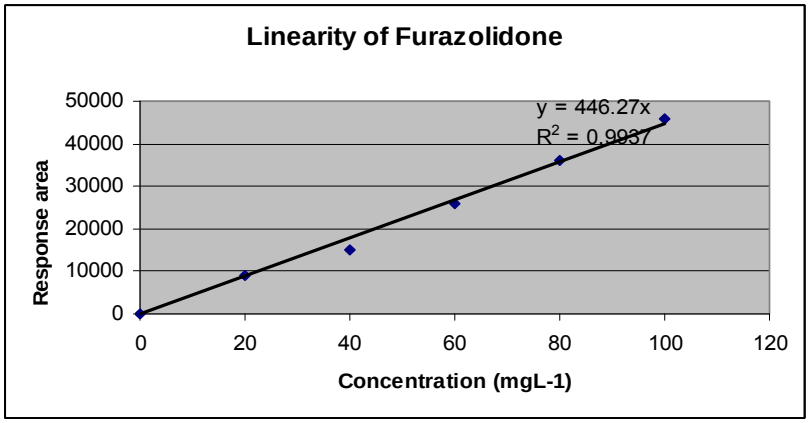

Figure 5.19 b: Linearity Plot of Furaltadone peak area

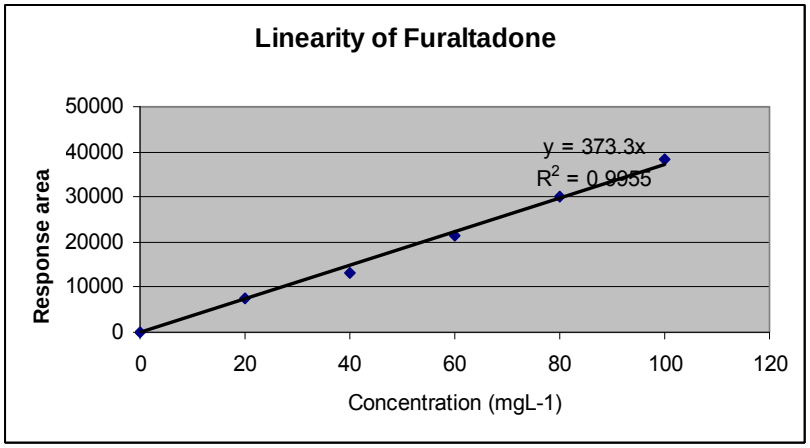

Figure 5.19 c: Linearity Plot of Nitrofurazone peak area

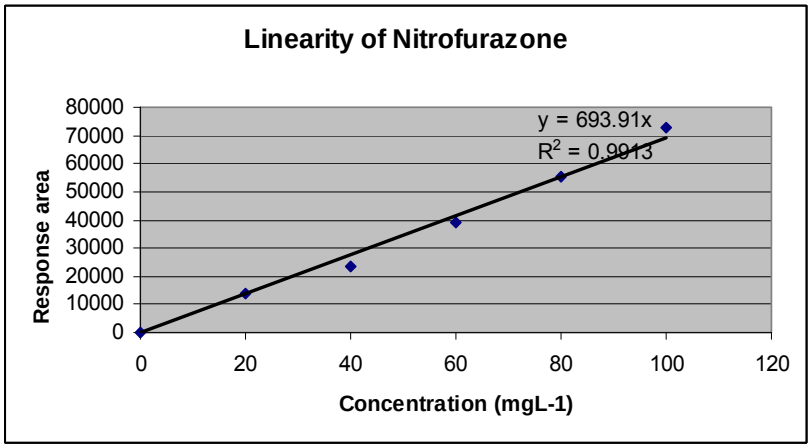

Figure 5.19 d: Linearity Plot of Nitrofurantoin peak area

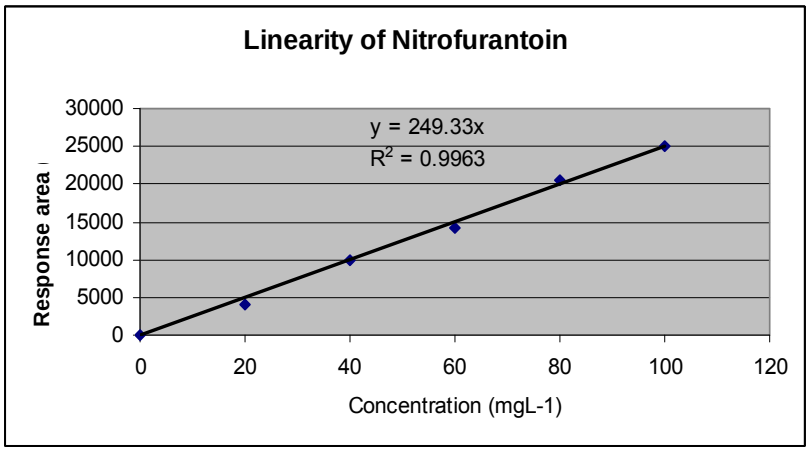

5.2.7 Limit of Detection

The detection limit is the lowest amount of analyte in a sample that can be detected but not necessarily quantitated as an exact value.

Two calibration curves were constructed separately for NFMs and for NFAs. Calibration curves for NFMs over the range 4 μg mL^{-1} - 20 μg mL^{-1}, and for NFA over the range 20 μg mL^{-1}- 100 μg mL^{-1} were prepared. The limit of detection (LOD) for NFAs and NFMs was estimated by extrapolating to a signal-to-noise ratio (S/N) of 3 for the concentration of NFAs, which gives a signal three times the response of the magnitude of noise for a blank solution at 275 nm. The detection limits for each analyte under optimum conditions are specified in Table 4.9. Generally, LOD of around < 1 μg mL^{-1} were found for the NFMs. Since this is obtained for direct injection, it can be assumed the LOD can be significantly improved for methods incorporating large-volume sampling/stacking/sweeping methods.

Table 5.9: Limit of detection for each component under reported optimum CE conditions

Peak	Limit of detection (μg mL^{-1})
1	0.9
2	2.0
4	1.6
5	0.6
6	0.2
7	0.4
8	1.8
9	1.7

5.2.8 Analysis of Spiked Prawn samples

Refer to section 3.5.1.4 of Chapter 3 regarding preparation of the prawn sample for analysis. All four NFM and 2-NBA peaks were observed in spiked frozen prawn sample as shown in Fig 5.21. The sample was spiked to a level of 3.6 μg mL^{-1} in each metabolite, and recovery was observed to be 30 % for AOZ, 50 % SEM and 20 % for AHD. Although AMOZ was detected in the prawn sample, the concentration was not determined for AMOZ due to an insufficient standard to prepare an external calibration graph. The recoveries of NFMs in spiked prawn sample were low, this could be due to loss of analytes occurred during grinding and centrifuging process. NFMs were not detected in the non-spiked frozen prawn sample. The purpose of running a spiked sample is to investigate whether the NFMs can be separated from, and be detected in, the sample matrix, and estimate recovery of metabolites by using SPE C_{18} cartridges.

Figure 5.21: Electropherogram of prawn sample spiked with NFMs.

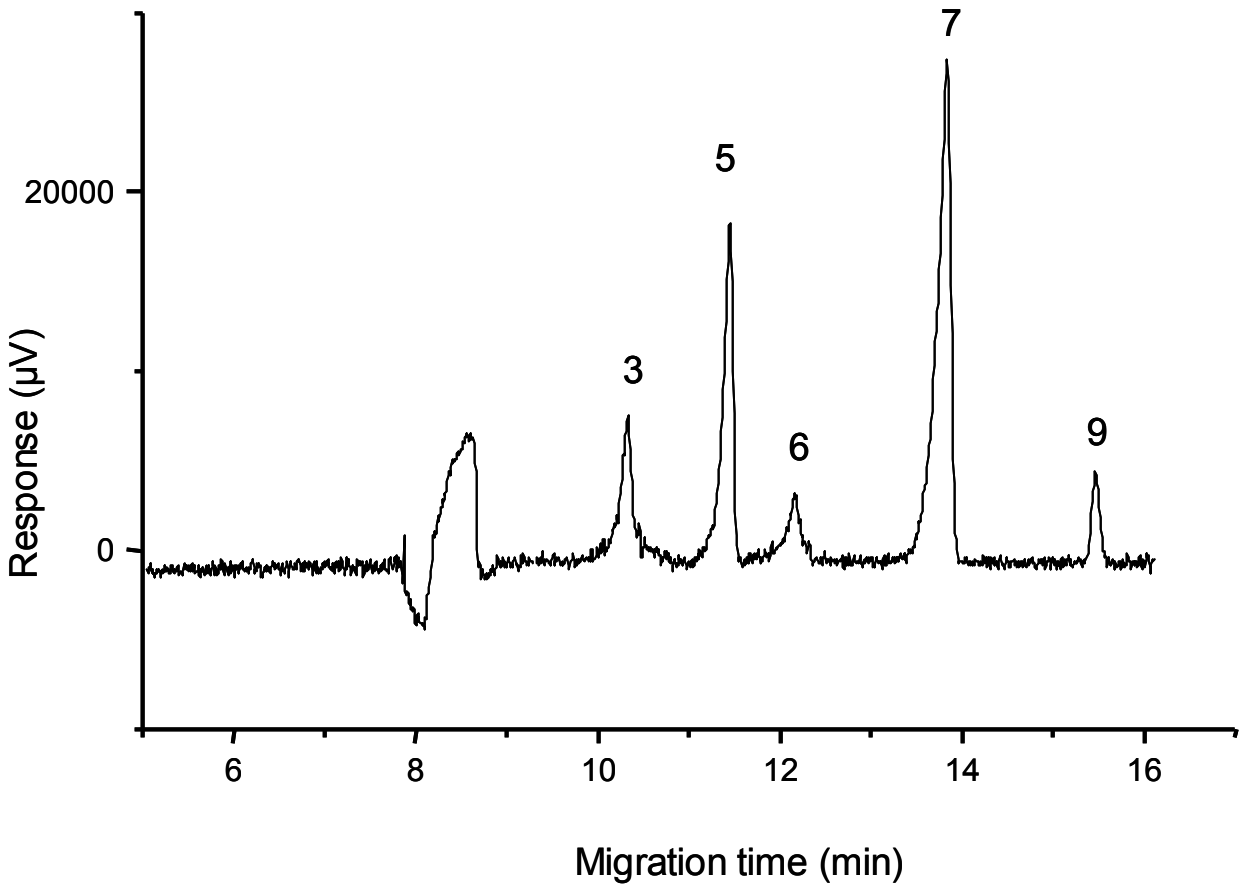

5.3 Conclusion

Statistically based experimental designs proved to be valuable tools in optimising separation of a mixture of NFAs and NFMs. FFD was an efficient approach for screening purposes, to determine which factors affect the resolution significantly. CCD was useful in determining the optimum levels in separation of NFAs and NFMs. The best conditions found to give optimum resolution from the optimization study was pH 9.0, 80 mM SDC concentration, 16 kV with running buffer consisting of 20 mM borate and 20 mM phosphate concentration using a 73 cm x 75 μm column, resulting in completely resolved NFAs and NFMs within 16 min. Whilst all antibiotics have shorter migration time than their respective derivatised metabolites, as a group apart from nitrofurantoin the antibiotics elute before the metabolites. The analytical figures of merit for CE analysis exhibited excellent reproducibility of absolute and relative migration times, and acceptable reproducibility of relative response areas. Successful separation of metabolite derivatives was achieved when the developed method was applied to a spiked prawn sample.

5.4 References

1. 1442/95, E.U.C.R., *ammending Annexes 1, 11, 111 and 1v of Regulation (ECC) No 2377/90 laying down a Community procedure for the establishement of maximum residue limits of veterinary medicinal products in fooodstuffs of animal origin.* Off.J.Eur.Communities., 1995. **L143**: p. 26-30.

2. Leitner, A., P. Zollner, and W. Linder, *Determination of the metabolites of nitrofuran antibiotics in animal tissue by high-performance liquid chromatography-tandem mass spectrometry. J. Chromatogr. A*, 2001. ***939***: p. 49-58.

3. Takino, M., *Determination of the Metabolites of Nitrofuran Antibacterial Drugs in Chicken Tissue by Liquid Chromatograph-Electrospray Ionization-Mass Spectrometry (LC-ESI-MS).* Agilent Technologies in house technical paper (www.getech.com): p. 1-9.

4. 2003/181/EC, E.U.C.R., *Amending decision 2002/657/EC as regards the setting of minimum performance limits (MRPLs) for certain residues in food animal origin.* Off.J.Eur.Communities., 2003. **L71**: p. 17-18.

5. Weston, A. and P.R. Brown, *HPLC and CE- principles and practice*. 1997, Califonia: Academic Press Limited.

6. Conneely, A., et al., *Isolation of bound residues of nitrofuran drugs from tissue by solid-phase extraction with determination by lidquid chromatography with UV and tandem mass spectrometric detection. Anal. Chim. Acta*, 2003. ***483***: p. 91-98.

7. Effkemann, S. and F. Feldhusen, *Triple-quadrupole LC-MS-MS for determination of nitrofuran metabolites in complex food matrixes.* Anal Bioanal Chem, 2004. **378**: p. 842-844.

8. Henk, L. and W.J.M. Underberg, *Detection- Orientated Derivatization Techniques in Liquid Chromatography*. 1990, New York: Marcel Dekker, Inc.

9. Morris, V.M., et al., *Optimization of the capillary electrophoresis separation of ranitidine and related compounds.* J. Chromatogr. A, 1997. ***766***: p. 245-254.

CHAPTER 6

CHIRAL SEPARATION of TRIADIMENOL FUNGICIDES by USING MICELLAR ELECTROKINETIC CAPILLARY ELECTROPHORESIS

6.1 Introduction

Chirality is a very important field of stereoisomerism. Stereoisomers are compounds made up of the same atoms, bonded to the same sequence of bonds, but possessing different three-dimensional structures which are not interchangeable [1]. In one form of chirality, the carbon is bonded to four different groups or atoms. This introduces asymmetry or chirality because two distinct spatial arrangements of such a molecule are possible, which are non-superimposable mirror images of each other. Non-identical stereoisomers exist in which the only distinction between them is that one is the mirror image of the other. However, these mirror images are nonsuperimposable. Stereoisomerism of this type can exist in two spatial configurations that correspond to reflections of each other. These stereoisomers are specifically called enantiomers. A 1:1 mixture of both enantiomers forms a racemate or racemic mixture [1]. Chirality of enantiomeric molecules is caused by the presence of one or more chirality elements in their structure [2].

Over the past decades considerable attention was given to chiral separation especially in agrochemical and pharmaceutical industries. Chiral molecules occur frequently in nature [1]. The increasing importance of chiral separation is linked with the discovery that a pair of enantiomers, even though exposed to an identical biological environment, may reveal different properties with respect to metabolism, excretion, receptor binding, uptake and distribution [3, 4] . As a result of these differences in properties, enantiomers commonly tend to have unequal biological activities and providence during their routes of function. Hence it is accepted, when enantiomers are exposed to a biological coordination, that a pair of enantiomers should be treated as two different compounds [5].

For most human, commercial or industrial purposes, the two forms of chiral molecules are equally effective, i.e. they have the same reactivity, the same chemical and physical properties. However, for some extremely important applications, one form is more effective than the other. For example, the effectiveness of pharmaceuticals is often based on the precise matching of the drug molecule with the structure of the receptors in the body. Therefore, one of the two mirror image forms is frequently more

effective in providing the desired therapeutical results. Thus the interaction between compounds and biological systems is often very specific according to the enantiomeric structure of the molecule.

Techniques of chiral separation stand for very rigorous worked on field. Chromatographic techniques used in chiral separation include gas chromatography (GC), liquid chromatography (LC), thin layer chromatography (TLC), and supercritical fluid chromatography (SFC). CE is increasingly used for enantioseparation of chiral compounds. The high theoretical plate counts make CE well suited for chiral separation [6]. After almost 20 years of since the initial publication of chiral separation using CE, there has been no decline in new chiral CE applications.

Very high peak efficiency leading high-resolution power during chiral resolution is a unique feature of CE. Chiral analysis by CZE usually involves an addition of a chiral selector to the running electrolyte. As the two enantiomers do not possess different charges, their separation cannot be achieved on the basis of “pure electrophoretic principles” [1]. In general, a chiral environment is required for enantioselective separations, and therefore, the most common approach in CE is the addition of a chiral selector to the buffer electrolyte in order to form a dynamic diasteroisomeric association complex.

About 25 % of agrochemicals are reported to be chiral molecules, although a few of the new commercial formulations contain only the active enantiomer [7]. The biological activity may be due to only one enantiomer, even though the two enantiomers of a chiral molecule possess the same physicochemical properties. Therefore, analytical methods for the separation of enantiomers of agrochemical compounds such as fungicides are needed to monitor the stereoselectivity processes of the agrochemicals in organisms and in the environment. Fig 6.1 represents an example of chirality of the herbicide dichlorprop [1].

Figure 6 .1: An example of chirality of the herbicide dichlorprop

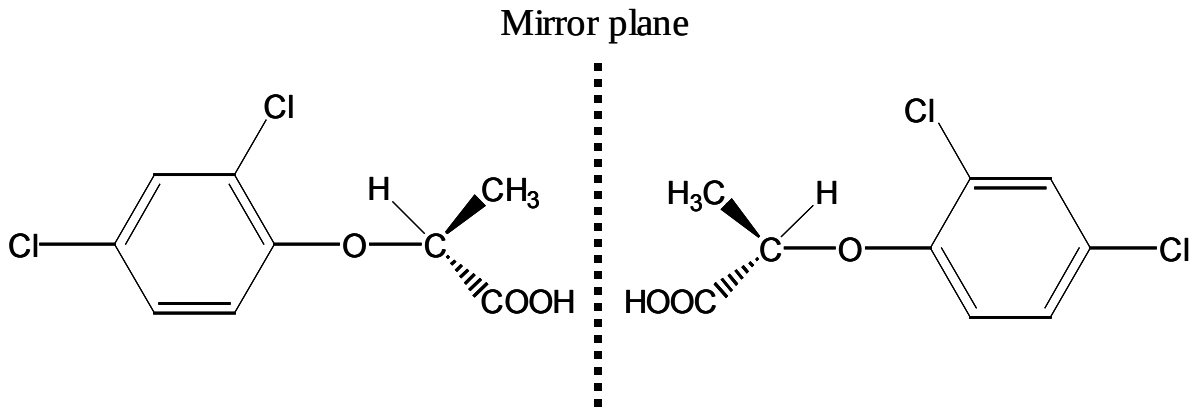

In CE, a combination of borate with CDs in the buffer has allowed the chiral resolution of compounds containing cis-diol functionality, such as phenyl-1, 2-etanediol and 3-benzyloxy-1, 2-propanediol [8]. Jira et al. [9] showed that various diol compounds, including some quinazoline derivatives of potential pharmaceutical interest and containing diol groups in the side chain, could be resolved as borate complexes with CD chiral selectors in the buffer. A dual chiral recognition mechanism is proposed based on inclusion of the aromatic substitute of the diol-borate complex into the cavity of the CD and interaction of the borate with the hydroxyl groups at C-2 and C-3 at the mouth of CD. These interactions can simply be due to the hydrogen bonds.

CDs are non-reducing oligosaccharides, which originate from amylose by the action of glycosyltransferease. The native nonionic CDs used containing six, seven and eight glucopyranose units are named α, β and γ-CD respectively. Shown in Fig 6.2 is the structure of typical CDs. They have the shape of truncated cones with hydrophilic outside surfaces, whereas their inner cavities are hydrophobic as shown in Fig 6.2 a and b. Derivatised neutral CDs include dimethyl (DM- β-CD), trimethyl (TM β-CD) and hydroxy propyl (HP-β-CD). At the present stage, several ionic derivatised ionic CDs i.e. sulfated and carboxymethylated CDs are available.

The cavity of the molecule is lined with hydrogen atoms and glycosidic oxygen bridges. Native-β -CD is the most popular electrophoretic chiral selector [10, 11]. Separation occurs via formation of a complex

between the solute and CD cavity. Dalgliesh proposed a three-point rule for successful enantiomeric separation, where three types of interaction must occur between the solute and CD [12].

When regular CDs are employed, the affinity of the analyte for the CD is due to hydrophobic interactions between the analyte and the CD-cavity and hydrogen bonding of analyte to hydroxyl groups or other introduced functionalities on the CD-ring. The other type of interaction can include electrostatic, dipole-dipole, attractive and repulsive interactions [12, 13]. They can thus form inclusion (host-guest) complexes with hydrophobic molecules, or with hydrophilic molecules, which possess hydrophobic moieties. The different interaction of target molecules with CDs will moderate their electrophoretic migration and thus this offers a means to alter relative separations of molecules. It is important to realise that for successful chiral resolution, the enantiomers will necessarily have different energies for association with the host chiral selector. The Dalgliesh model illustrates that should one stereoisomer have geometry will not produce the same net interactions with the selector. Hence chiral differentiation occurs. Almost all publications reported using CDs as well as some of their chemical derivatives in CE as chiral selectors.

Figure 6 .2a: Structures of underivatised (native) CDs

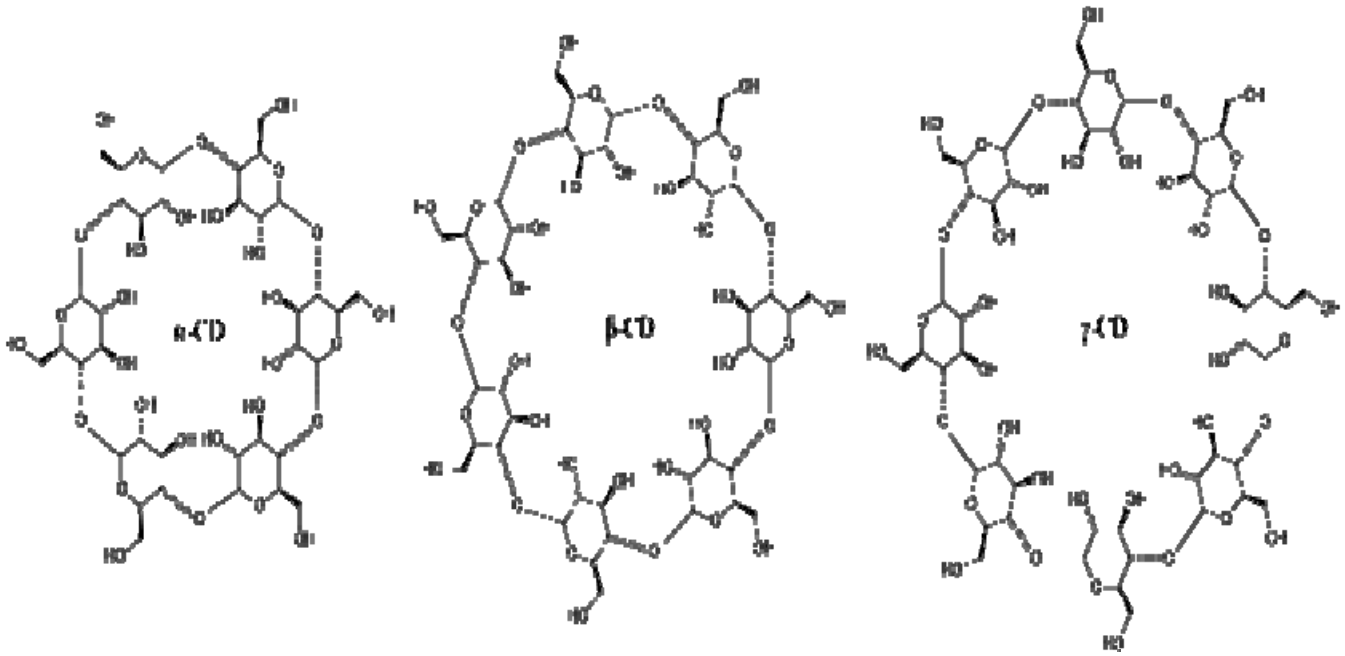

Figure 6 .2b: Model of β-CD as a truncated cone

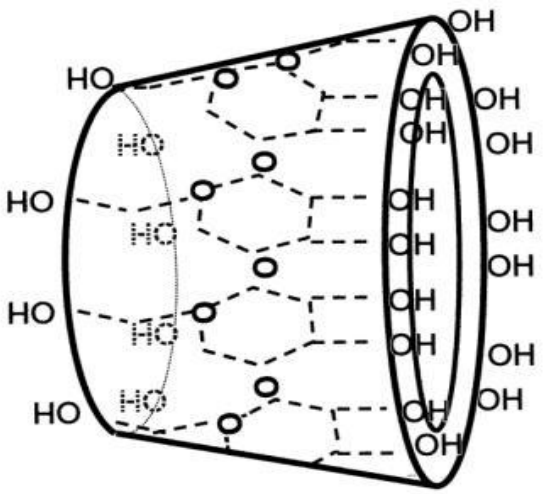

Triadimenol is a systemic fungicide, which belongs to the triazole family. It was first evaluated in early 1970, and it exhibits protective, curative and eradicant actions against wide range fungal strains, such as powdery mildews, rusts and other fungal pests on cereals, fruits, vegetables, turf, shrubs and trees [14].

Triadimefon is a semi-polar, non-volatile pesticide that has two optically active isomers and is a moderately toxic compound. According to [5], in which the authors referred to previous literature, in late 1970 it became clear that the antifungal activity of triadimefon is largely due to the transformation of triadimefon to triadimenol, in which the carbonyl group of triadimefon, the prochiral point, is reduced to form a secondary alcohol, thus creating an additional chiral center. Biotransformation of triadimefon to triadimenol, mediated by a microorganism, is stereospecific [5].

Structures of triazole fungicides have a common structural moiety the 1, 2, 4-triazole ring, which is connected to the hydrophobic backbone through position 1.Typically, the hydrocarbon backbone has a substituted phenyl group at one end, and an alkyl group or a different substituted phenyl at the other end. Asymmetrical carbons are generally present attached to the triazole ring, which makes chirality almost

ubiquitous for triazole-type fungicides [15]. Triadimenol has two pairs of diastereoisomers (See structure 6.3 below). It is used to improve winter survival and drought tolerance of cereals, and may eliminate the need for early season foliar sprays. It was demonstrated that the four diastereomers of triadimenol possess different biological responses, with the (-)-thereo- 1S, 2R isomer giving the highest antifungal activity against the rhizoctonia solani among the four enantiomers [5]. Triadimefon's soil half-life ranges from 6 to 18 days and triadimenol's soil half-life ranges from 110 to 375 days [16].

Triadimenol consist of two pairs of enantiomers, or four individual stereoisomers, i.e. (-)-thereo- 1S, 2R -, (+)-threo-1R, 2S-, (-)-ery-thro-1S, 2S-, and (+)-erythro-1R, 2R-, due to two chiral centres. Triadimenol consists of two diastereoisomers in the ratio of 8:2 for the threo and erythro forms respectively [17]. Whilst enantiomers have identical chemical and physical properties, diastereoisomers have different properties, which explains their different ratio in synthetic preparations.

Figure 6 .3: Structures of Triadimenol and Triadimefon fungicides (the starred carbons are chiral)

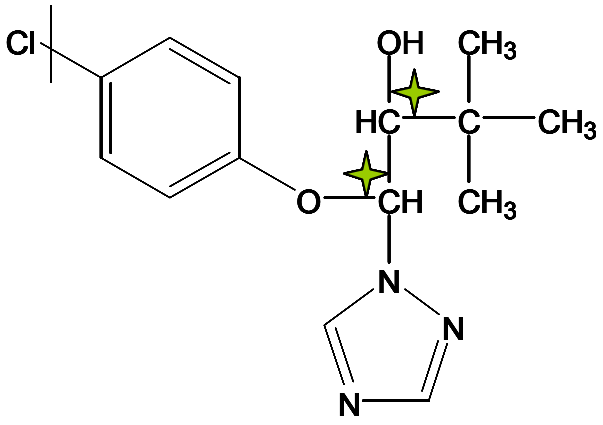

Triadimenol

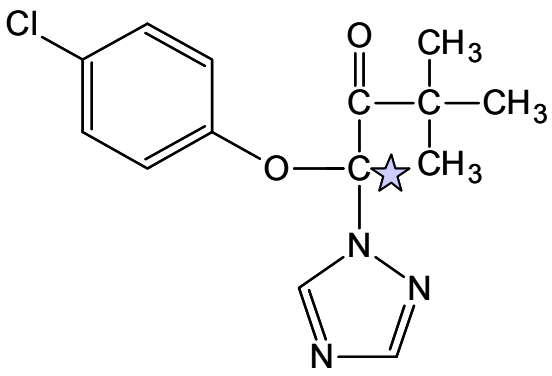

Triadimefon

Due to basicity of triazole fungicides, they are too weak to be analysed by CZE [5]. pKa values were not available for triadimenol fungicides. However, it is understood that the triazoles display both acidic and basic pKa [18]. Previous study [15] has shown that the migration times of stereoisomers of triadimenol fungicides are dependent on the pH of the buffer electrolyte and the concentration of cyclodextrin. Lee et al. reported simultaneous resolution of all chiral isomers of triadimenol as well as triadimefon, achieved by using a phosphate buffer with 2% sulfated β-CD at pH 2.5. The triadimenol isomers had low effective mobility in acidic media and they were detected as overlapping tailing peaks ahead of the EOF signal. The addition of chiral selectors, such as various CD derivatives, into the running buffer electrolyte, did not result in chiral separation [5].

The aim of this study was to investigate the possibility of chiral resolution of all Triadimenol isomers within the shortest possible time and to apply the optimised conditions to Triadimenol spiked grape extract to investigate whether the Triadimenol can be separated from, and be detected in, the sample matrix. Finally to investigate the ratios of the optical isomers of the fungicides in real samples after application.

6.2 Results and Discussion

The instrument, injection and column details used in this study have previously been desribed in the section 3.1.1 of Chapter 3. Initially, the analysis of triadimenol samples was attempted using sodium dihydrogen phosphate in CZE mode. No peaks were observed even after 100 min. Due to the weak basicity of these fungicides, it was then decided to switch to MEKC mode with SDS micelles. The initial step was to define the experimental domain by finding the extremes for parameters such as borate and phosphate concentrations in the buffer, surfactant concentration, applied voltage, % methanol and the pH of the buffer electrolyte. Previously used phosphate and borate concentrations in buffer electrolyte (20 mM phosphate and 20 mM borate) from Chapter 4, together with 50 mM SDS were tried. Table 6.1 shows the experimental parameters used in the initial attempts at separation of Triadimenol.

Table 6. 1: Parameter ranges tested during preoptimisation of separation of Triadimenol

Parameter	Chiral selector (β-CD)	pH	% Methanol	Voltage
Range	10- 30 mM	5.5- 9.5	10- 25%	14- 20 kV

Triadimenol A and B diastereoisomres were analysed separately with borate and phosphate buffer with SDS micelles. The electropherograms of Triadimenol B diastereoisomer and the mixture of Triadimenol A, B analysis using MEKC mode is shown in Fig 6.4a and b respectively.

Figure 6.4 a: Electropherogram showing elution of Triadimenol B diastereoisomer by using MEKC mode

Peaks 1- 6 in electropherograms represent Triadimenol isomer 1 of diastereoisomer A, isomer 2 of diastereoisomer A, isomer 1 of diastereoisomer B, isomer 2 of diastereoisomer B, Triadimenol diastereoisomer A, Triadimenol diastereoisomer B 2 respectively [i.e., peaks 5 and 6 represent the unresolved diastereoisomer pairs (5= 1+2, 6= 3+4)]

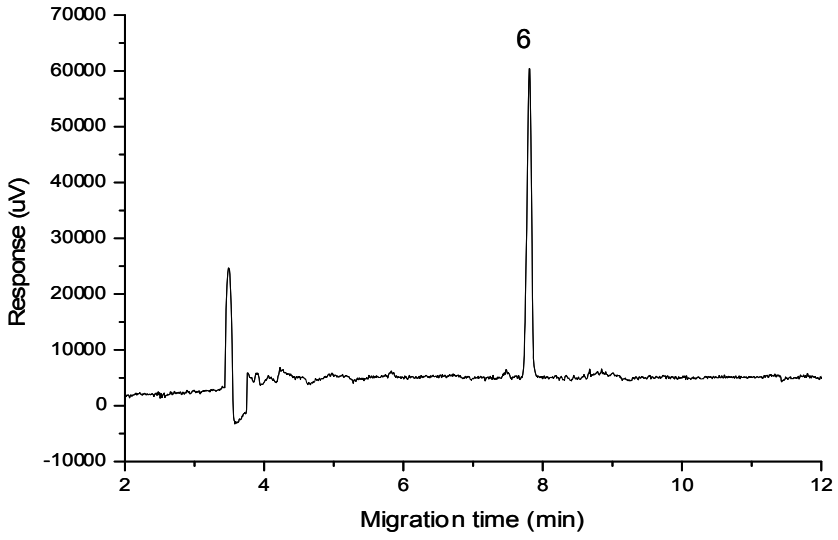

Figure 6.4 b: Electropherogram showing the resolution of Triadimenol diastereoisomers by using MEKC mode (peak numbering as in the text of Fig 6.4a)

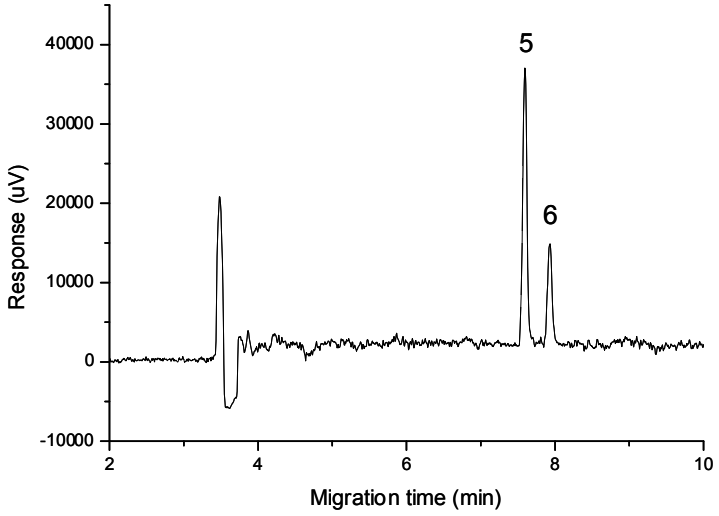

The pH of the buffer electrolyte consisting of borate and phosphate was varied between 5.5 and 9.5 to investigate the possibility of chiral resolution of individual enantiomers of diastereoisomer A and B. It was found that using MEKC mode with the presence of SDS micelles in the buffer without a chiral selector would result in two diastereoisomer peaks and not four individual isomer peaks. The next step was to add β-CD (chiral selector) to the borate-phosphate buffer electrolyte. After observing splitting of diastereoisomer A with 10 mM β-CD in the buffer electrolyte, the concentration of β-CD was increased up to 30 mM to investigate further resolution of isomers. Triadimenol A with 10 mM, 20 mM and 30 mM β-CD in buffer electrolyte are shown in Fig 6.5 a, b and c respectively. The same concentrations of β-CD in buffer electrolyte were conducted for Triadimenol B and the concentration of 10 mM of β-CD in buffer electrolyte is shown in Fig 6.6. By increasing the concentration of chiral selector, the selector-selectand interactions can be strengthened in CE.

Figure 6.5 a: Electropherogram showing Triadimenol A diastereoisomer with 10 mM β-CD (peak numbering as in the text of Fig 6.4a)

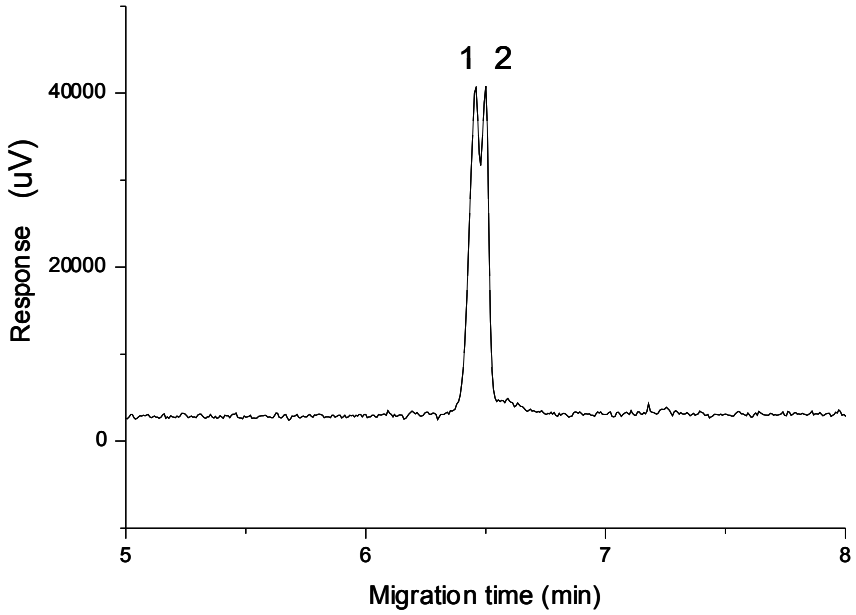

Figure 6.5 b: Electropherogram showing Triadimenol A diastereoisomer with 20 mM β-CD (peak numbering as in the text of Fig 6.4a)

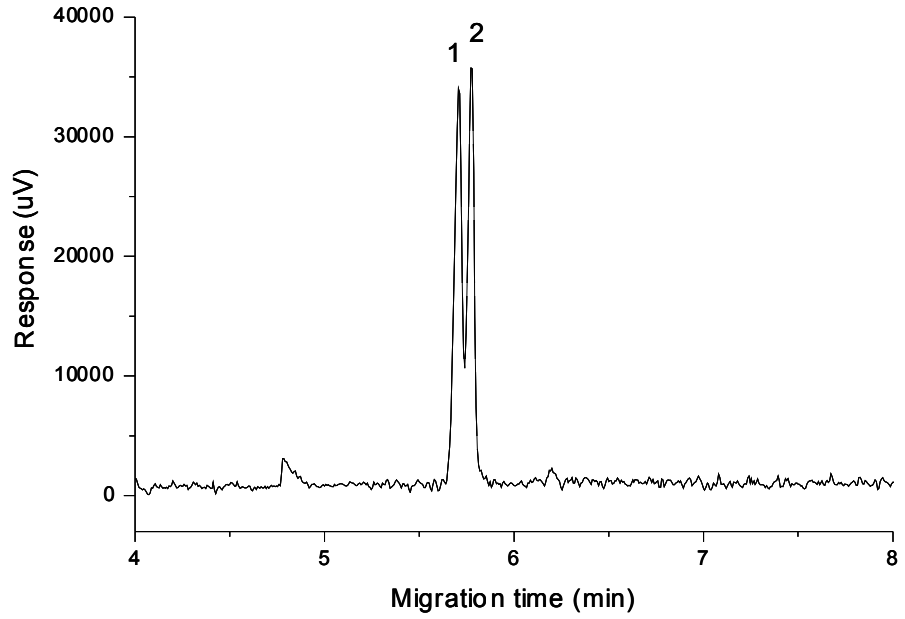

Figure 6.5 c: Electropherogram showing Triadimenol A diastereoisomer with 30 mM β-CD (peak numbering as in the text of Fig 6.4a)

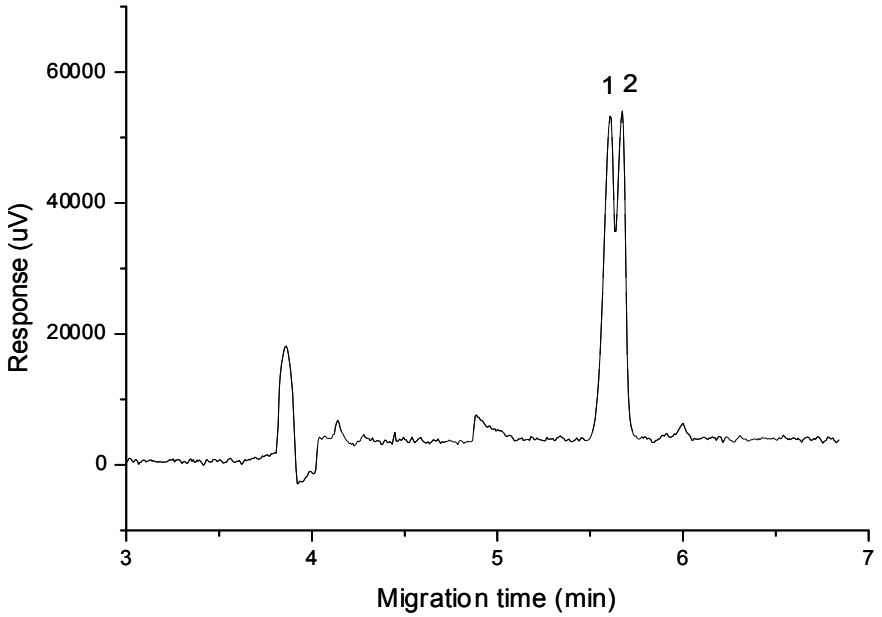

Figure 6.6: Electropherogram showing Triadimenol B diastereoisomer with 10 mM β-CD (peak numbering as in the text of Fig 6.4a)

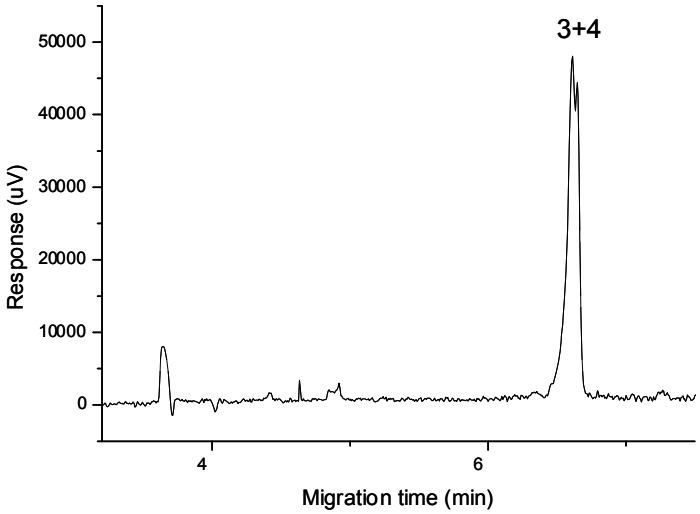

Increase in chiral resolution was observed (from 10-20 mM) with the increase in β-CD concentration in the buffer electrolyte. However decrease in migration time was observed with increase in β-CD concentration. Complete baseline resolution was not achieved with increasing β-CD. The next step in method development was to investigate the impact of changing the chiral selector from β-CD to neutral derivatised hydroxy propyl β-CD (HP- β-CD). Electropherograms of separation of Triadimenol A and B using 20 mM borate and phosphate buffer with 50 mM SDS and 20 mM HP- β-CD is shown in Fig 6.7 a and b respectively.

Figure 6.7 a: Electropherogram showing the separation of Triadimenol A with 20 mM HP-β-CD (peak numbering as in the text of Fig 6.4a)

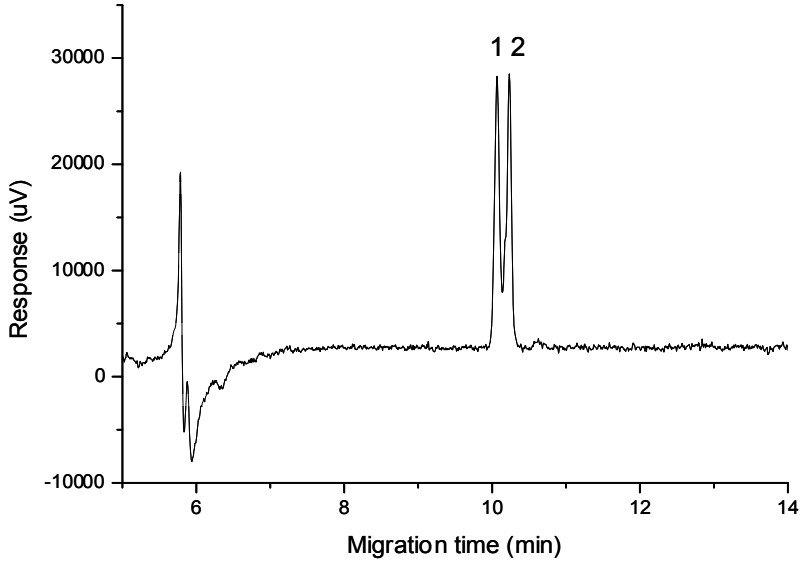

Figure 6.7 b: Electropherogram showing the separation of Triadimenol B with 20 mM HP-β-CD (peak numbering as in the text of Fig 6.4a)

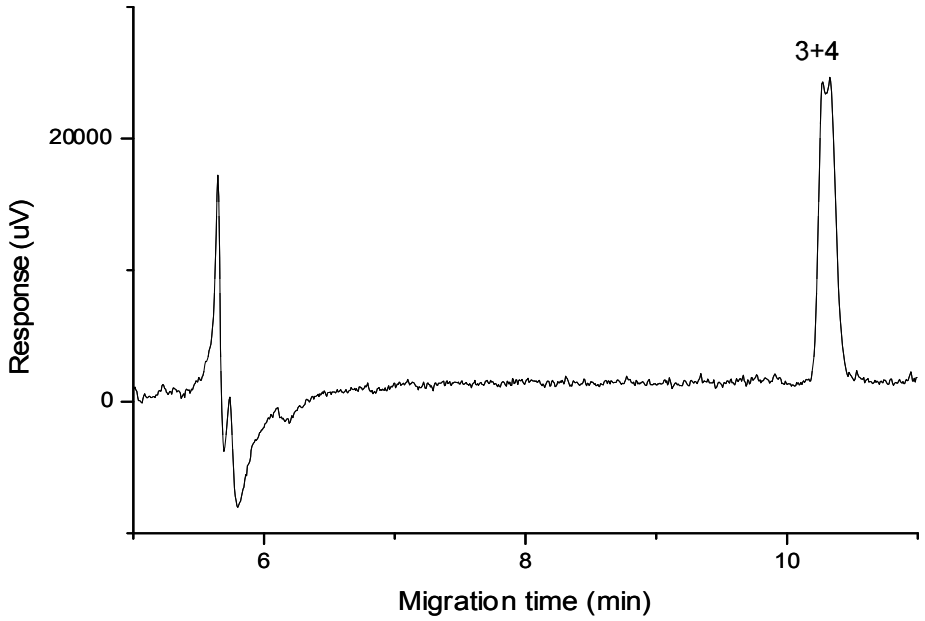

HP-β-CD as a chiral selector was a better choice since the separation of peaks 1+2 in Fig 6.7a is better than the best separation using β-CD (Fig 6.5b), but for isomer B, there is not much difference in chiral separation of peaks 3+4 with HP-β-CD and β-CD. The resolution occurs on the basis of differences in the stability of formation of the solute-CD inclusion complex for each enantiomer. Hence it is now important to investigate if other buffer additives can enhance the resolution offered by HP-β-CD, so the next step in method development was to investigate the impact of the presence of methanol in buffer electrolyte. Fig 6.8 shows an electropherogram of chiral resolution with the presence of 20% methanol in the buffer electrolyte.

Figure 6.8: Electropherogram showing the separation Triadimenol mixture with 20 mM HP-β-CD and 20% methanol (peak numbering as in the text of Fig 6.4a)

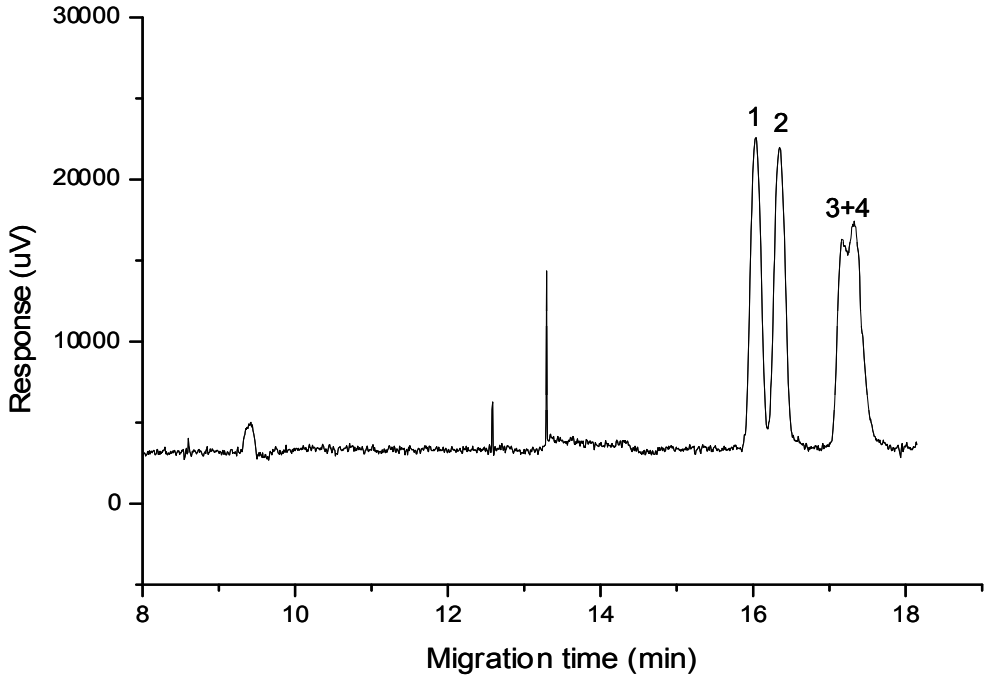

The presence of methanol in buffer electrolyte increased the chiral resolution. The next stage of method development was to examine primarily for diastereoisomer A (1+2) the impact of pH of buffer electrolyte on chiral resolution. The presence of 20 mM borate and phosphate with 50 mM SDS and 20 mM HP-β-CD in buffer electrolyte resulted in a pH of 8.6. It was decided to reduce the pH to find the impact of pH on the chiral resolution. The electropherograms showing the chiral separation of Triadimenol A and B with pH 8.0 buffer are shown in Fig 6.9a and b respectively. Fig 6.10 shows the chiral separation of the mixture of Triadimenol A and B with pH 7.8 buffer electrolyte.

Figure 6.9 a: Electropherogram showing the separation Triadimenol A with pH 8.0 buffer electrolyte (other conditions: 20 mM borate, 20 mM phosphate, 50 mM SDS, 20 mM HP-β-CD and 20% methanol,18 kV) (peak numbering as in the text of Fig 6.4a)

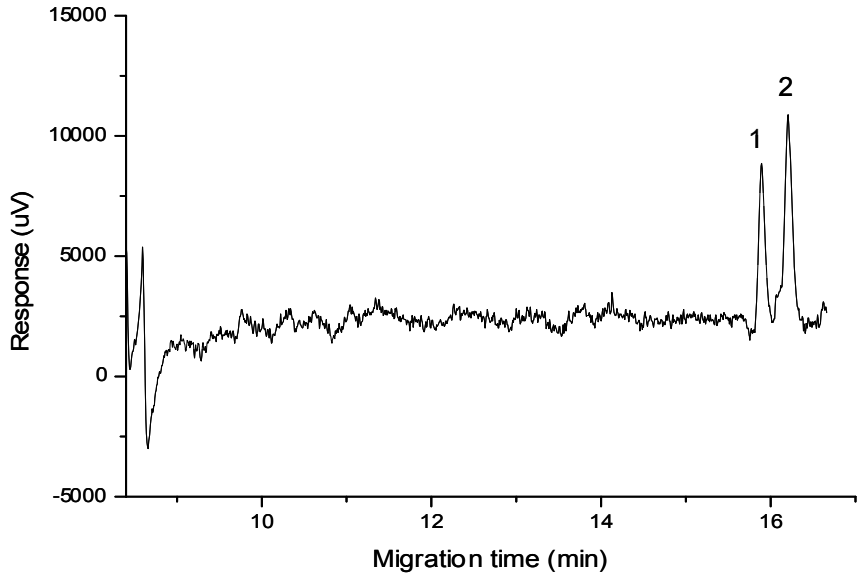

Figure 6.9 b: Electropherogram showing the separation Triadimenol B with pH 8.0 buffer electrolyte (peak numbering as in the text of Fig 6.4a and other conditions as in the text of Fig 6.9a)

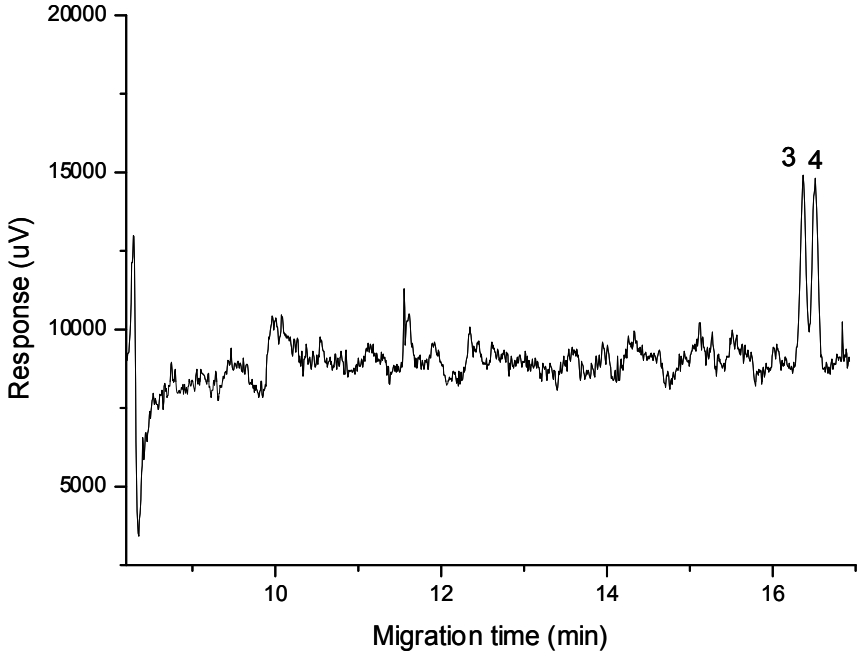

Figure 6.10: Electropherogram showing the chiral separation of Triadimenol A and B with pH 7.8 buffer electrolyte (peak numbering as in the text of Fig 6.4a and other conditions as in the text of Fig 6.9a)

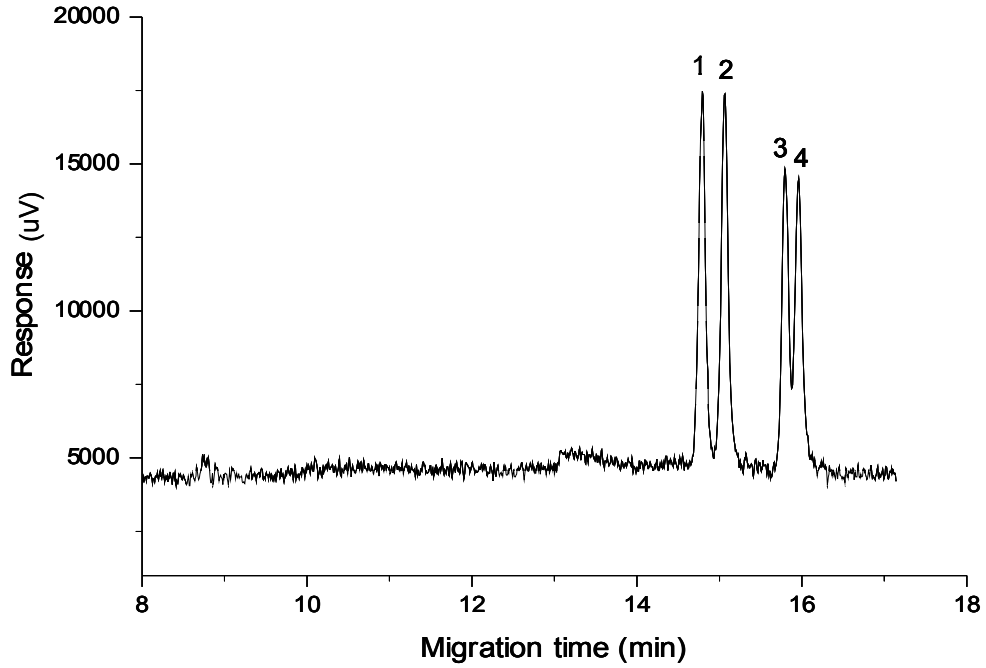

When using pH 6.0 buffer electrolyte, base line resolution of all four isomers of Triadimenol was obtained as shown in Fig 6.11 (optimum separation).

Figure 6.11: Electropherogram showing the chiral separation of Triadimenol A and B with pH 6.0 buffer electrolyte (peak numbering as in the text of Fig 6.4a and other conditions as in the text of Fig 6.9a)

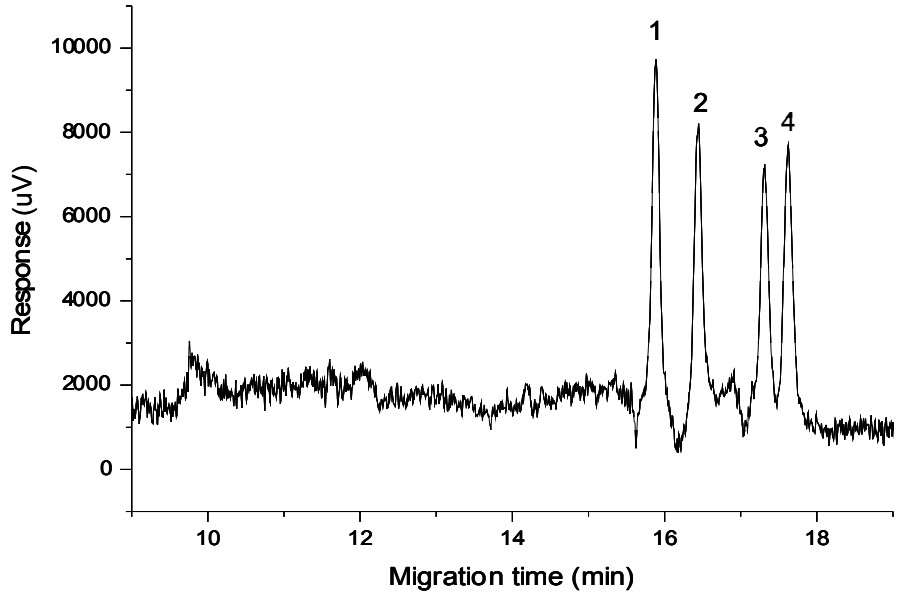

6.2.1 The Effect of Voltage

The running voltage has an impact on separation as it affects the resolution between peaks, and the total completion time of analysis, hence affecting the CEF value. The electropherograms using voltages 16 kV and 20 kV are shown in Figures 6.12 a, b respectively. The lower the voltage used, the longer the analysis time as shown in Figure 6.12 a. The optimum voltage (18 kV) was the highest possible whilst limiting joule heating effects which lead to band broadening, baseline disturbances, and a resultant loss of efficiency. Therefore an optimum voltage of 18 kV was indicated the best resolution within the shortest time as shown in Fig 6.11.

Figure 6.12 a: Electropherogram showing the resolution of Triadimenol A and B with voltage of 16 kV (Other conditions as in the text of Fig 6.9a except for voltage) (Traces were scanned due to original file corruption)

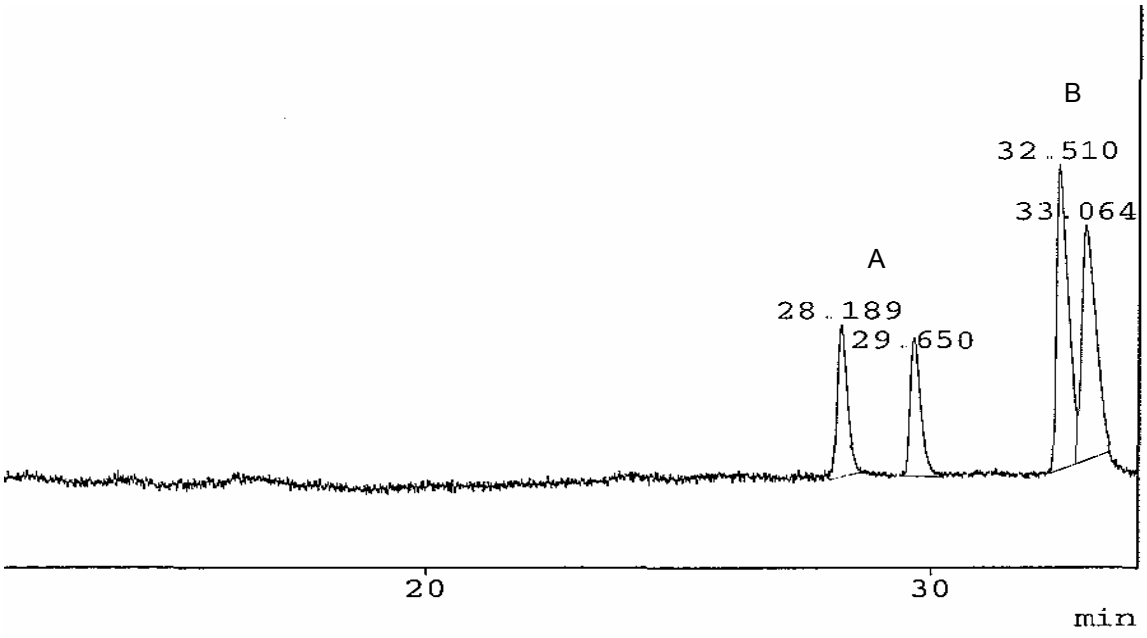

Figure 6.12 b: Electropherogram showing the resolution of Triadimenol A and B with voltage of 20 kV (Other conditions as in the text of Fig 6.9a except for voltage) (Traces were scanned due to original file corruption)

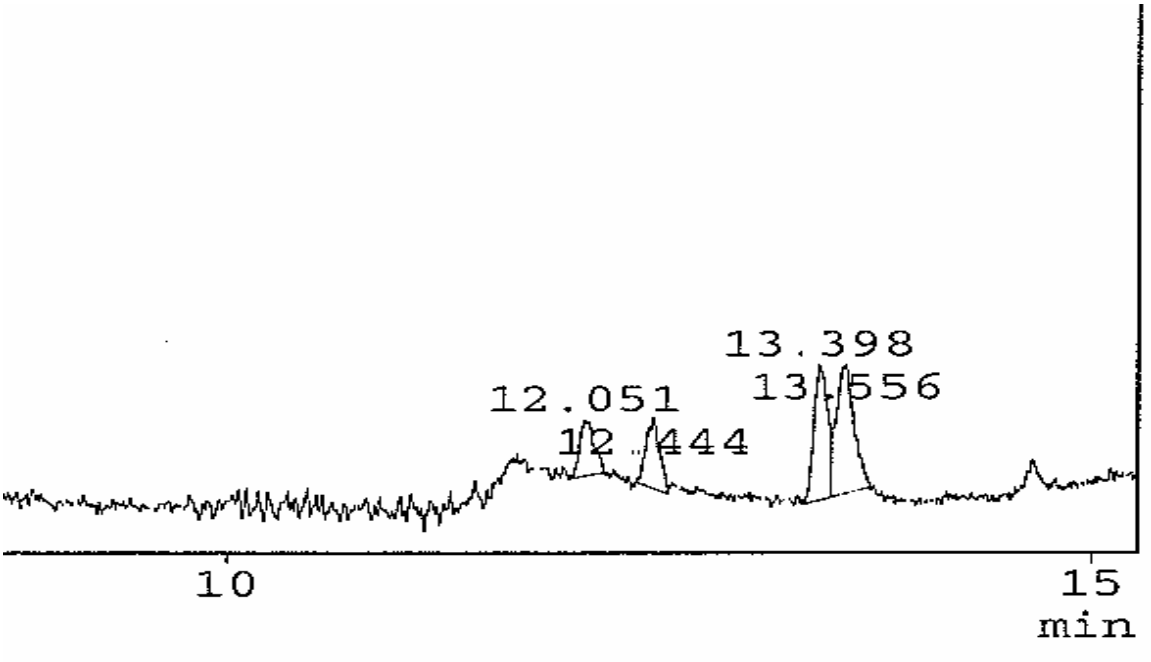

The pH of the running electrolyte is one of the critical factors in resolution due to its impact on EOF in a fused-silica capillary, and the possible effect on solute charge which has the effect of altering relative migrations. Resolution can be improved by reducing EOF or by increasing the difference in the electrophoretic mobility of analytes by judicious choice of conditions. This can be achieved by changing pH and composition of the buffer. The optimum separation of Triadimenol isomers was obtained at pH 6.0 (Fig. 6.11). The effect of a small change of pH (5.5 and 6.5) on resolution is shown in Fig 6.13. The impact of lower and higher pH on the resolution and run time is shown in Figs 6.13 a and 6.13 b. The pH of the running electrolyte was adjusted by adding 2 M hydrochloric acid or 2 M sodium hydroxide as required. The chiral resolution of Triadimenol B was the compound affected most by the pH change, and generally this diastereoisomer proved to be the more difficult to resolve.

Figure 6.13 a: Electropherogram showing the resolution of Triadimenol A and B of pH=5.5

(Other conditions as in the text of Fig 6.9a except for pH) (Traces were scanned due to original file corruption)

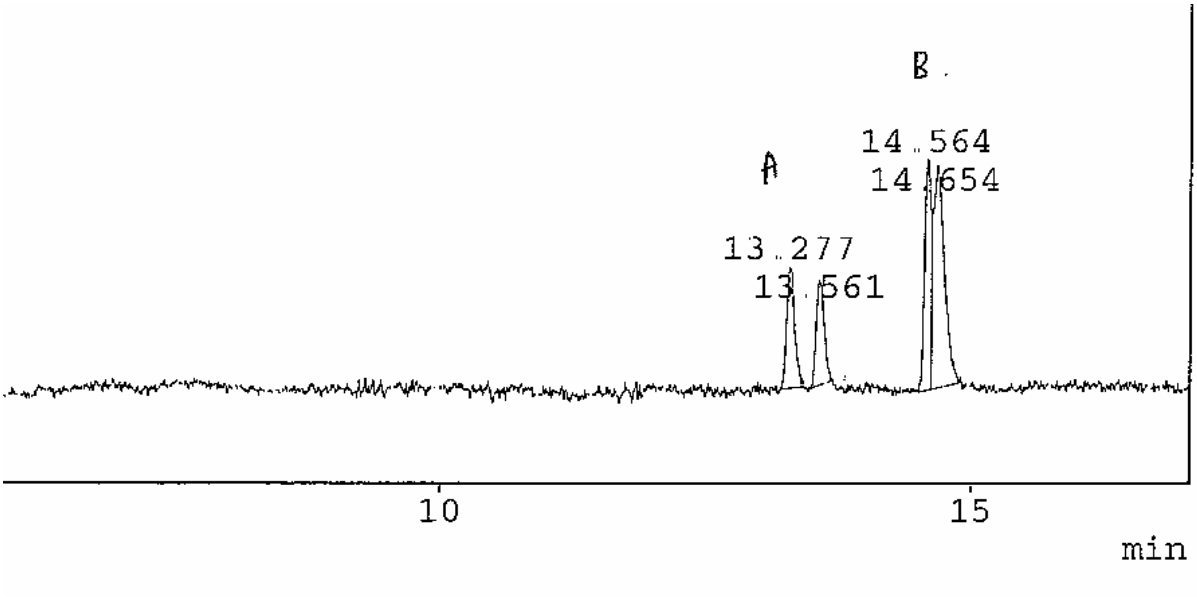

Figure 6.13 b: Electropherogram showing the resolution of Triadimenol A and B of pH=6.5

(Other conditions as in the text of Fig 6.9a except for pH) (Traces were scanned due to original file corruption)

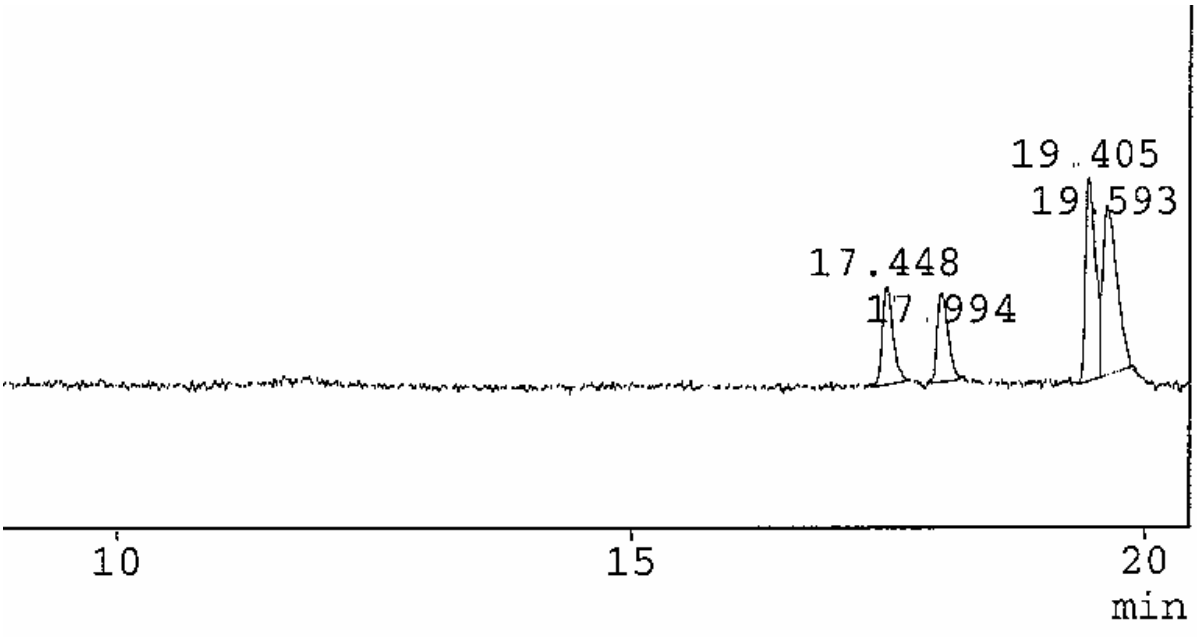

6.2.2 The Effect of Methanol

The organic solvents in buffer electrolyte alter the viscosity and polarity of the aqueous phase which improves the separation of enantiomers by altering the partitioning between the various components in the buffer [19, 20]. It is necessary to use organic solvents that do not absorb UV light, hence methanol was chosen in this study. The impact of lower and higher 20% methanol in buffer electrolyte on the resolution and run time are shown in Fig 6.14 a and 6.14 b respectively where the methanol percentage in buffer electrolyte ranged from 15% and 25%. The best separation of Triadimenol was achieved with 20% methanol (Fig 6.11) resulting in the lowest CEF value as shown in Table 5.10 of Chapter 5.

Figure 6.14 a: Electropherogram showing the resolution of Triadimenol A and B with Methanol 15% (Other conditions as in the text of Fig 6.9a except for % methanol) (Traces were scanned due to original file corruption)

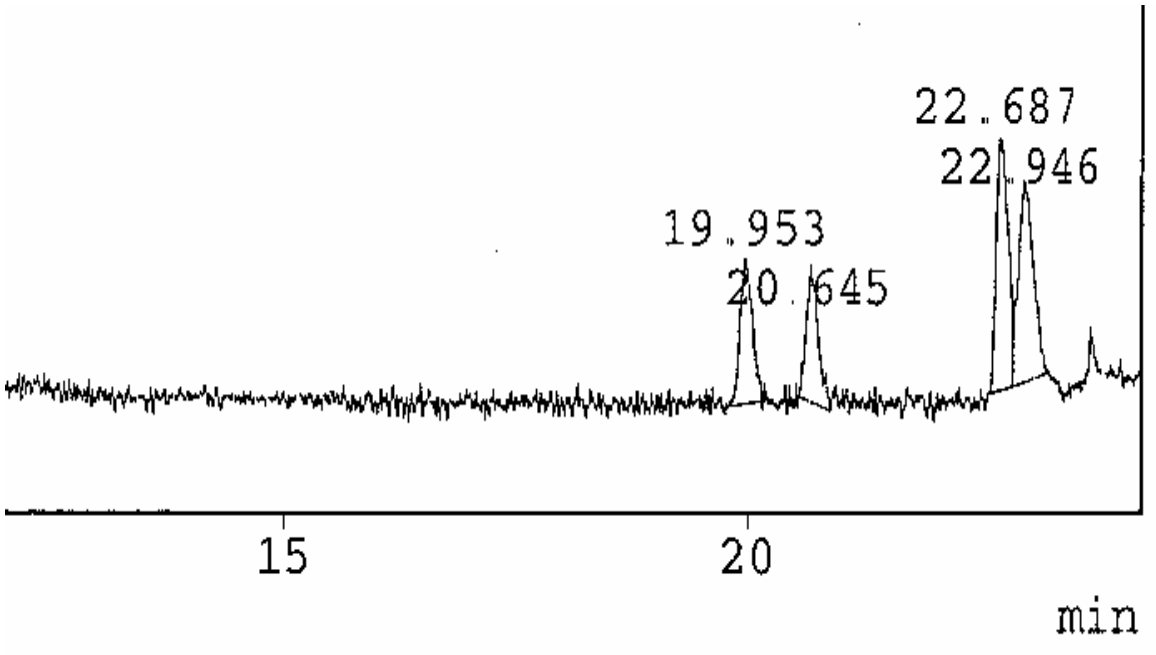

Figure 6.14 b: Electropherogram showing the resolution of Triadimenol A and B with Methanol 25% (Other conditions as in the text of Fig 6.9a except for % methanol) (Traces were scanned due to original file corruption)

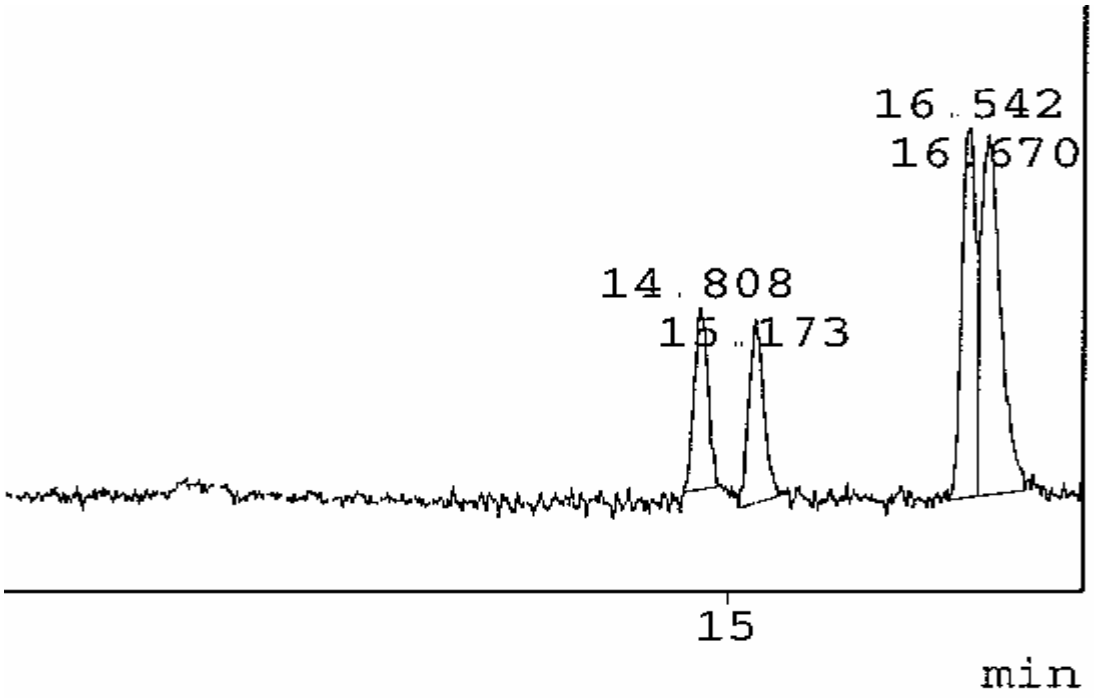

6.2.3 Analysis of spiked grape samples

The optimum separation of Triadimenol isomers was obtained with 20 mM phosphate, 20 mM borate, 50 mM SDS, pH 6.0, 20% methanol. The optimum separation conditions were then applied to spilked grape samples. The preparation of grape sample for analysis was described in section 3.5.2.2 of Chapter 3. The diastereoisomers of both Triadimenol A and B were observed in the spiked grape sample, after applying the optimised method. Triadimenol peaks were not detected in the non-spiked grape sample. The purpose of running a spiked sample is to investigate whether the Triadimenol can be separated from, and be detected in, the sample matrix, and to see what the ratio of the optical isomers is after application of Triadimenol to field samples. Electropherograms showing the blank grape sample and the spiked grape sample are shown in Fig 6.15 a and b respectively.

Figure 6.15 a: Electropherogram showing the blank grape sample (Other conditions as in the text of Fig 6.9a) (Traces were scanned due to original file corruption)

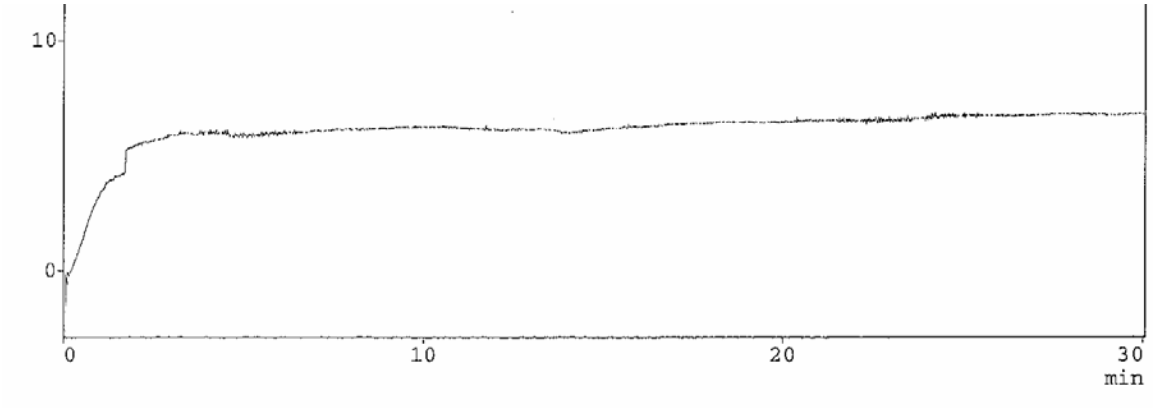

Figure 6.15 b: Electropherogram showing the resolution of Triadimenol A and B in the 20 mg L^{-1}spiked grape sample (Other conditions as in the text of Fig 6.9a) (Traces were scanned due to original file corruption)

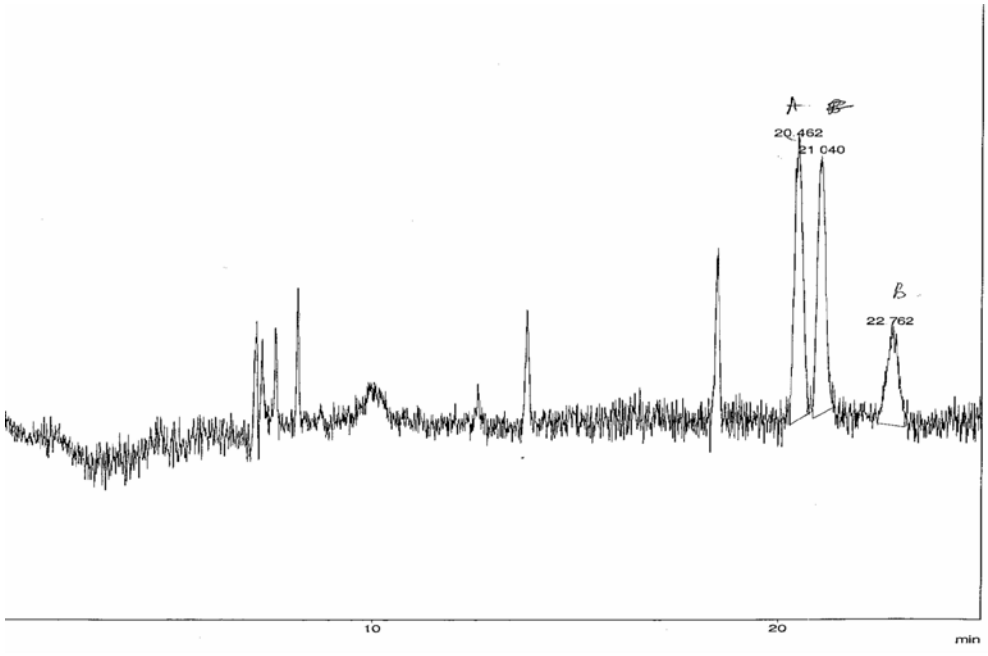

No peaks were observed in the blank grape sample whereas the spiked grape sample had two diastereoisomer peaks, though with poor detection sensitivity. The resulting signal-to-noise level (8.25) seemed insufficient for real sample analysis. Increase in detection sensitivity is necessary to determine the possibility of resolution of all the isomers of Triadimenol, in the spiked grape sample and the blank. Chapter 7 discusses the attempts to increase the detection sensitivity of Triadimenol.

6.2.4 Proposed mechanisms of chiral resolution of Triadimenol fungicides

It has been proposed that the enantioseparation mechanism in CE is chromatographic while the migration mechanism is electrophoretic [21]. Enantiomer resolution depends, among other things, on the extent to which each enantiomer partitions differentially between the pseudostationary phases produced between the cyclodextrin and the SDS micelles and free cyclodextrin in the aqueous phase. Once the Triadimenol mixture is in the separation capillary, diastereoisomers can be formed actively between the chiral selector and each enantiomer. The pair of enantiomers might gain unequal electrophoretic mobilities if the thermodynamic stabilities of these diastereoisomers are different as shown in Fig 6.16. The low thermodynamic selectivity together with high separation efficiency may allow the separations that are not possible to be observed by chromatographic techniques to be well observable in CE [22]. Hence the enantiomers are progressively separated through the separation capillary.

Fig 6.16: Triadimenol separation mechanism

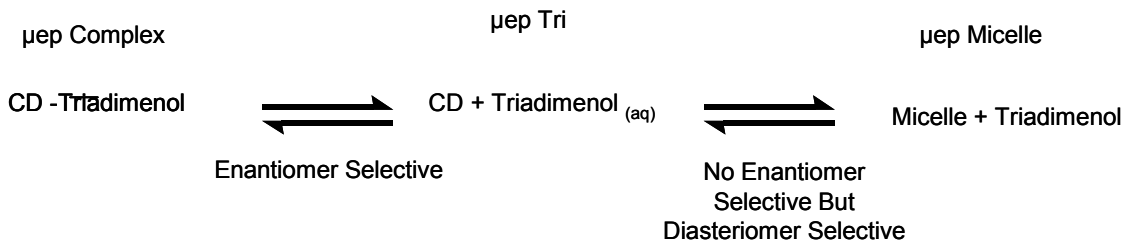

Wu et al. proposed [15] a chiral separation mechanism of fungicides as host-guest complexation. Chiral discrimination of fungicides is due to differences in host- guest complexation; the interaction between HP-β-CD and the triazole compounds which were found to be affected by a variety of factors (electrostatic forces, hydrogen bonding, hydrophobicity, steric effect, pH, voltage, surfactant concentration). These factors coupled with EOF were believed to be the major forces behind chiral selectivity.

6.3 Conclusions and Future work

The conditions found to give optimum resolution, arising from the optimisation study for Triadimenol were pH 6.0, 20% methanol, 50 mM SDS concentration, 20 mM HP-β-CD ,18 kV with running buffer consisting of 20 mM borate and 20 mM phosphate concentration using a 64.5 cm x 50 μm column. This resulted in baseline resolution of all Triadimenol isomers within 18 min. The optimised separation conditions were applied to a blank grape sample and to a spiked grape sample. No peaks were observed in the blank grape sample whereas the spiked grape sample had two diastereoismer peaks with poor detection sensitivity. Increase in detection sensitivity is necessary to determine the possibility of resolution of all the isomers of Triadimenol, in the spiked grape sample and the blank and to provide a method suitable for real sample analysis. Chapter 7 discusses the attempts to increase the detection sensitivity of Triadimenol.

6.4 References

1. Kallenborn, H. and H. Huhnerfuss, *Chiral environment pollutants- trace analysis and ecotoxicology*. 2001, New York: Springer-verlag Berlin Heidelberg.

2. IUPAC, *Pure Appl. Chem 69*. 1997. p. 1469.

3. Ariens, E.J., W. Soudijn, and P.B.M.W.M. Timmermans, *Stereochemistry and Biological Activity of Drugs*. 1982, Oxford: Blackwell Scientific Publications. 11-32.

4. Ariens, E.J., J.J.S. van Rensen, and W.E. Welling, *Stereoselectivity of Pesticides: Biological and Chemical Problems*. 1988, Amsterdam: Elsvier Science Publishers B. V.

5. Wu, Y.S., H.K. Lee, and S.F.Y. Li, *Simultaneous chiral separation of triadimefon and triadimenol by sulfated β-cyclodextrin-mediated capillary electrophoresis.* Electrophoresis. 2000. 21(8) 1611-1619.

6. Blaschke, G. and B. Chankvetadze, *Enantiomer separation of drugs by capillary electromigration techniques.* J. Chromatogr. A, 2000. **875**: p. 3-25.

7. Crosby, J., *Pestic Sci. 46*. 1996. p. 11.

8. Schmid, M.G., et al., *Capillary electrophoresis chiral resolution of vicinal diols by complexation with borate and cyclodextrin: Comparative studies on different cyclodextrin derivatives. Chirality.* 1997. **9**: p. 153-156.

9. Jira, T., et al., *Chiral resolution of diols by capillary electrophoresis using borate-cyclodextrin complexation.* J. Chromatogr. A, 1997. **761**: p. 269-275.

10. Fanali, S., *Use of cyclodextrin in capillary zone electrophoresis/ Resolution of terbutaline and propranolol enantiomers.* J. Chromatogr., 1991. **545**: p. 437-444.

11. Koppenhoefer, B., et al., *Separation of enantiomers of drugs by capillary electrophoresis III. â–cyclodextrin as chiral solvating agent.* J. Chromatogr. A, 1996. **735**: p. 333-343.

12. Ahuja, S., *Chiral separation by chromatography*. 2000, American Chemical Society: Wasington, D. C. p. 112.

13. Schmitt, T. and H. Engelhardt, *Charged and uncharged cyclodextrin as chiral selectors in capillary electrophoresis.* Chromatographia, 1993. **37**(9/10): p. 475-481.

14. Network, E.T., *http://www.pmep.cce.cornell.edu/profiles.extoxnet/pyrethrins-ziram/triadimefon-ext.html*. 1994.

15. Wu, Y.S., H.K. Lee, and S.F.Y. Li, *High-performance chiral separation of fourteen triazole fungicides by sulfated a-cyclodextrin-mediated capillary electrophoresis.* J. Chromatogr. A, 2001. **912**: p. 171-179.

16. Runes, H.B., J.J. Jenkins, and J.A. Field, *Method for the analysis of triadimefon and ethofumesate from dislodgeable foliar residues on turfgrass by solid-phase extraction and in-vial elution.* J. Agric. Food Chem., 1999. **47**: p. 3252-3256.

17. Williams, B.D. and V.C. Trenerry, *The direct separation of the diastereoisomers and enantiomers of the fungicide triadimenol by micellar electrokinetic capillary chromatography.* J. CAP. ELEC., 1996. **003**(4): p. 223- 228.

18. Albert, A., *Heterocyclic chemistry*. 2nd ed. 1968, Melbourne: Melbourne University Press.

19. Li, F., S. Cooper, and S. Mikkelsen, *Enantioselective determination of oxprenolol and its metabolites in human urine by cyclodextrin-modified capillary zone electrophoresis.* J. Chromatogr. B, 1995. **674**: p. 277-285.

20. Thunecke, F., et al., *Separations of enantiomers and diastereoisomers of 4-hydroxy-2H-1,4-benzoxazin-3(4H)-one by capillary electrophoresis.* Chromatographia, 1994. **38**: p. 470-474.

21. Chankvetadze, B., *Enantiomer separation of drugs by capillary electromigration techniques.* J. Chromatogr. A., 1997. **792**: p. 269.

22. Chankvetadze, B. and G. Blaschke, *Enantioseparations in capillary electromigration techniques: recent developments and future trends.* J. Chromatogr. A, 2001. **906**: p. 309-363.

CHAPTER 7

ONLINE CONCENTRATION TECHNIQUES:

SWEEPING of

TRIADIMENOL FUNGICIDES

7.1 Introduction

The high efficiency together with the small volumes injected enable HPCE to have very good mass sensitivity. However in many cases CE lacks sufficient sensitivity to detect trace levels of chromatographic analytes due to the short optical path length associated with on-column UV detection. Therefore to enhance the sensitivity in CE, various techniques have been developed to obtain on-column sample concentration. Online preconcentration based on electrophoresis represents one of the most versatile ways for analyte enrichment in CE since the preconcentration step is performed within the capillary. These techniques have been developed to compress analyte bands within the capillary, thus increasing the volume of sample that can be injected without loss of CE efficiency. The limit of detection and sensitivity is proportional to the amount of sample injected. The preconcentration techniques are based on either the manipulation of differences in the electrophoretic mobility of analytes at the boundary of two buffers with differing resistivities or the partitioning of analytes into a stationary or pseudostationary phase [1].These sample concentration techniques include on-line isotachophoresis (ITP) [2, 3] or sample stacking [4-9]. These techniques are based on electrophoretic principles however the separation is chromatographic.

7.1.1 Stacking

The implementation of preconcentration techniques for CE is relatively easier than the other preconcentration techniques, as most of the former do not require instrumental alterations. These electrophoretic preconcentration techniques are generally based on the principle of focusing of analytes due to their different velocities in two separate zones in the capillary.

The normal stacking mode (NSM) or field-amplified sample stacking (FASS) is one of the on-column sample concentration techniques, and was first used by Mikkers et al. [10] in HPCE. In this technique, a long plug of low concentration buffer (which functions as a much diluted buffer band) containing analytes to be resolved is introduced hydrodynamically into the capillary pre-filled with buffer of the same composition but of a higher concentration, creating a discontinuous electrolyte system.

Sample stacking is known as the movement of sample ions towards and across a boundary zone that separates the region of the injected sample buffer from the rest of the column containing the running buffer, such that sample ions are collected or concentrated at the boundary. Due to the matrix difference between sample region and running buffer region, the ions experience a lower electric field in the running buffer region than in the sample region. Hence the velocity of ions high in the sample plug, but decreases as they cross the boundary. The slower moving ions will “stack up” into a narrow zone, thus increasing the concentration in the sample zone. This focused zone of ions then electrophoretically migrates through the separation buffer and separates into individual zones by conventional CZE. The stacking technique occurs for both positively and negatively charged species. For conventional polarity operation (anode = injection end), the positive species stack up in front of the sample plug and the negative species stack up at the back of the sample plug. The neutral species are left uncharged in the sample plug and coelute without any stacking. If the analytes pass the boundaries to the separation compartment, their electrophoretic separation begins. Since the EOF velocity in the separation compartment is higher than the electrophoretic velocity of the analytes, the anions and the cations as well as the sampling compartment are pushed to the cathode. The fundamental principle of sample stacking of anions is summarised in Fig 7.1.

Fig 7.1 Schematic representation of the normal sample stacking; A) Hydrodynamic injection of sample (prepared in water), after conditioning the capillary with running buffer; B) Application of voltage at positive polarity with the running buffer in the inlet and outlet vials. The arrow indicates direction of stacking of analyte anions; C) Starting the separation of stacked zones (p, r, s = anions in sample)

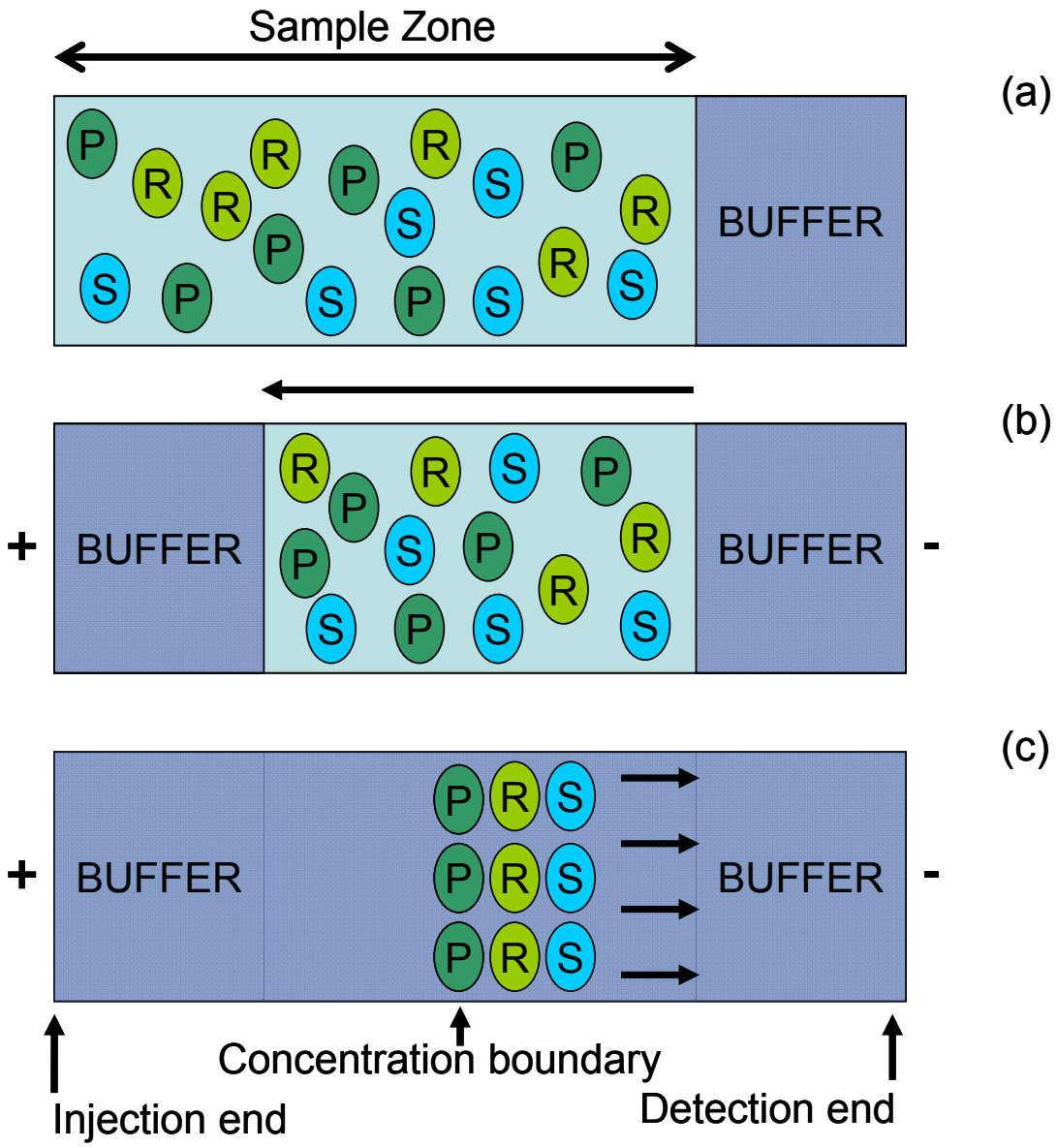

In theory, the amount of stacking for a given sample is proportional to the field enhancement ratio. The larger the difference in buffer concentrations (ionic strength), the narrower the peak (less dispersion in the stacked zone) and the greater the amount of stacking. An extrapolation can be made that a rather long sample plug prepared in water or very low concentration buffer should give stacked ions in a very thin zone at the interface with the higher concentration separation buffer. However, a laminar flow (back pressure effect) is created inside the column because of the mismatch between local electroosmotic velocities and bulk velocity. The laminar flow will broaden the sharp zone generated by the stacking process. The larger the difference in concentration will result in a larger laminar flow. Stacking and broadening work against each other, implying there is an optimal length of water plug that can be introduced into the column whilst still achieve high resolution [11].

Burgi and Chien [12] developed a technique known as large volume stacking, to stack anions. A large volume of low conductivity sample is introduced hydrodynamically into the capillary and a negative voltage is applied at the injection edge. The large solvent plug is then electroosmotically pushed out of the column while the negative ions stack up at the boundary between the sample zone and the background electrolyte. Hence stacking and removal of solvent occurs concurrently when the sample buffer is almost completely out of the column (monitored by observing the electric current). The polarity is then reversed back to the normal arrangement and separation of the negative species can proceed. Fig 7.2 shows the schematic representation of the volume sample stacking with polarity switching.

Fig 7.2 Schematic representation of the large volume stacking with polarity switching; A) Large volume of sample (prepared in water) introduced by hydrodynamic injection, no voltage used; B) high voltage (-20 kV) is applied to the capillary with polarity reversed (outlet positive); C) water is pushed out of the column while the capillary column retains the anions; D) Polarity is switched to normal (20 kV) when current reaches 90-95% of the original value (which monitors the reversal of the water plug where the longer water plug leads to reduced current). Further stacking occurs to improve sensitivity (p, r, s = anions in sample).

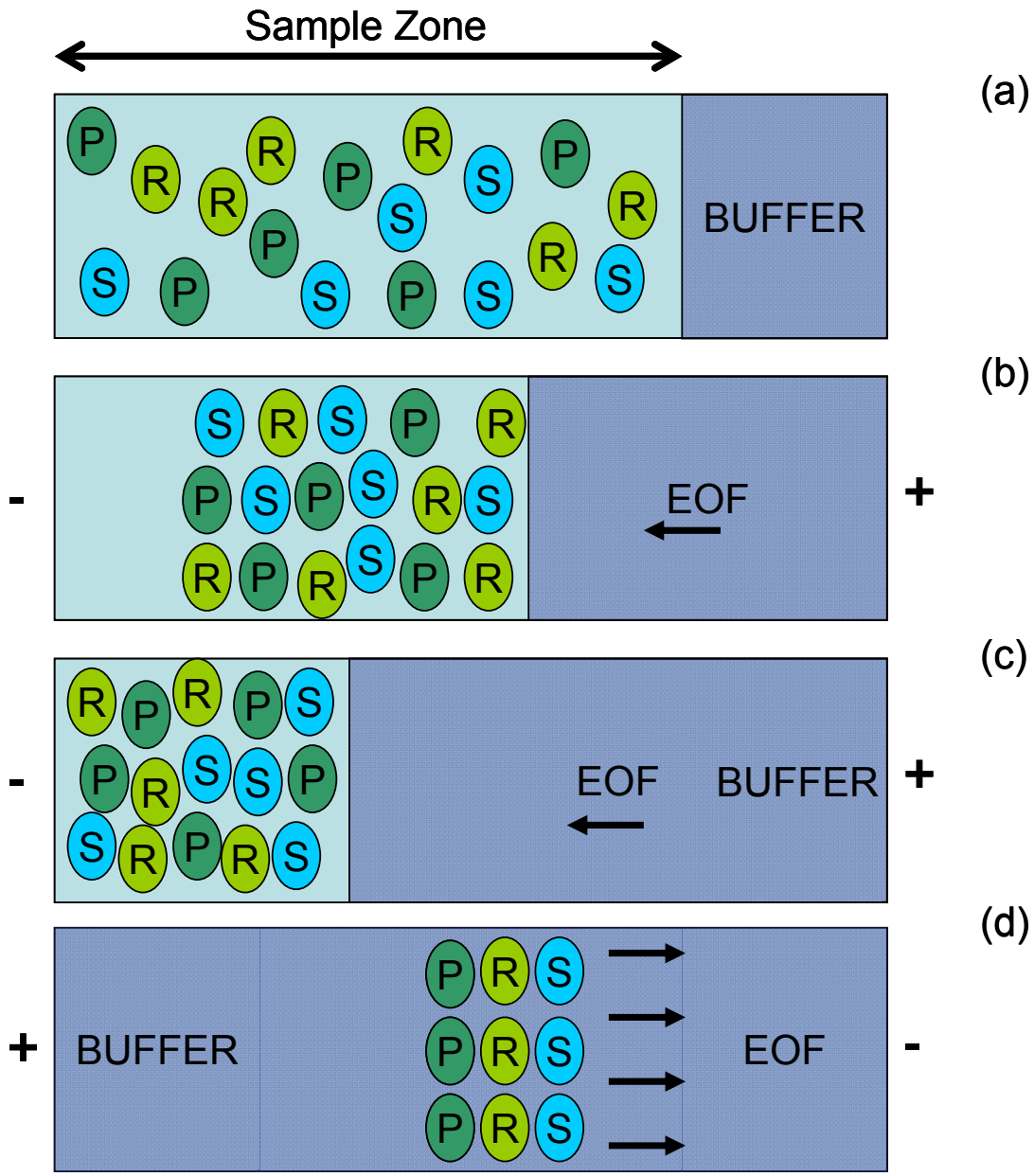

7.1.2 Sweeping

Sweeping, a new online sample concentration technique in electro kinetic chromatography (EKC), is defined as the sorption and accumulating of analyte molecules by a pseudostationary phase (PS) that enters and sweeps through to eventually fill the sample zone upon application of voltage [5]. However, this phenomenon, initially observed by Gilges [13], was not well studied until more recently. It occurs whenever the sample matrix is void of a charged carrier phase and it does not matter whether the sample matrix has a higher, similar, or lower conductivity compared to the background electrolyte. In sweeping, analyte zones are narrowed due to a chromatographic or partitioning mechanism as the sample molecules experience and are sorbed into the pseudostationary phase zone (PS). Figure 7.3 shows the schematic representation of micelles (PS) and negatively charged analyte molecules during sweeping in the presence of high EOF.

Several papers have been published on the use of this concentration technique in MEKC. Quirino et al. [5] developed the sample concentration technique by sample stacking and sweeping using microemulsion phase and a single isomer sulfated β-CD as a pseudostationary phase in MEKC. Monton et al. [14] employed sweeping technique as an online preconcentration of charged analytes in MEKC with nonionic micelles to acquire peak height enhancements up to 100-fold.

Nunez et al. [15] reported analysis of the herbicides paraquat, diquat and difenzoquat in drinking water by MEKC using sweeping and cation selective exhaustive injection (CSEI-sweeping –MEKC). More recently, the sweeping principle has been extended to CZE separations of neutral solutes involving complexation reaction of *cis*-diols with borate, demonstrating the versatility and wide applicability of the sweeping technique [16].

Recently, a combination of sample stacking and sweeping, referred to as CSEI-sweep, has acquired almost a million-fold enhancement in detector response for cationic hydrophobic analytes [17]. In particular, online concentration by sweeping was successfully applied to microchip MEKC by Sera et al [18].

Fig 7.3 Schematic representation of micelles (PS) and negatively charged analyte molecules during sweeping in the presence of high EOF; A) Starting situation, a longer than typical injection of sample solution (S) prepared in sample matrix having conductivity similar to the anionic micelle background solution (BGS); B) Application of a voltage at positive polarity, PS enters the sample zone and sweeps (concentrates) the analyte molecules; C) The injected analyte zone is assumed to be completely swept.

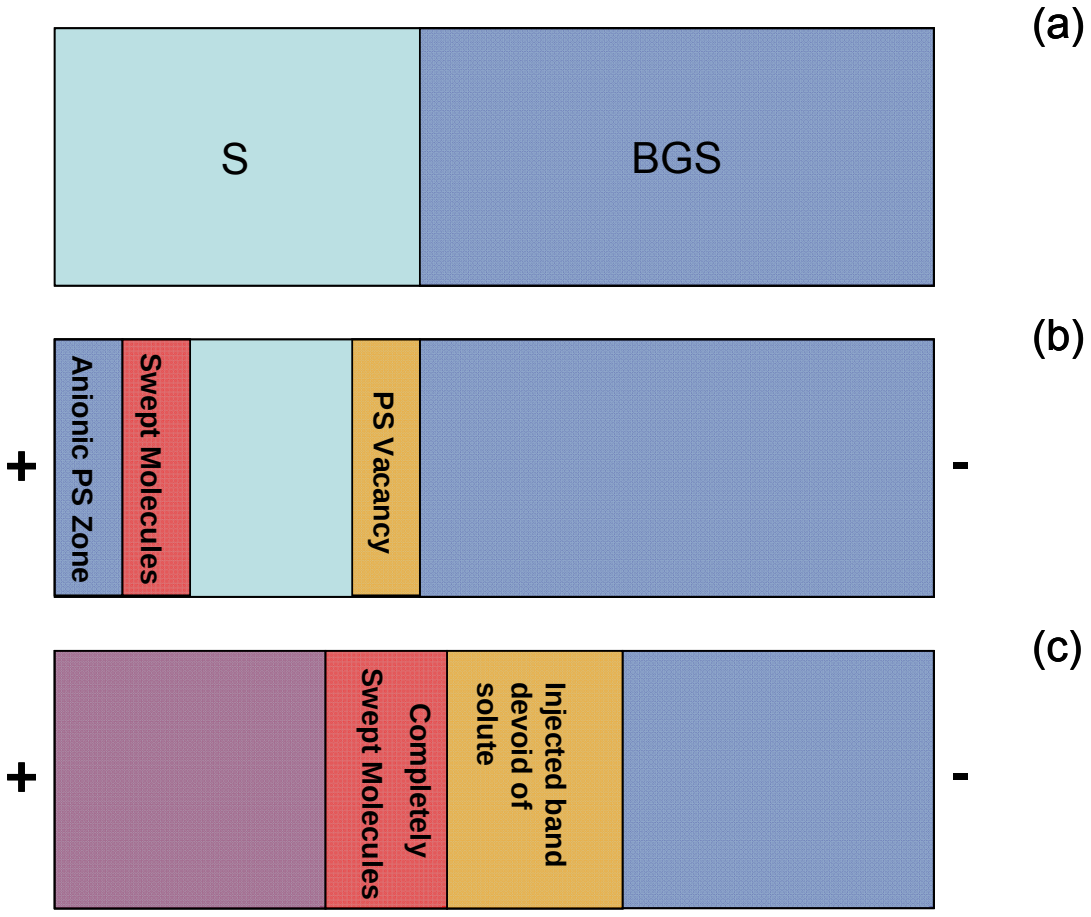

7.2 Results and Discussion

As discussed in Chapter 6, chiral separation of Triadimenol isomers was obtained using MEKC mode. However the detection sensitivity was too low to observe the separation in actual samples (at a level of interest to trace analysis in field samples estimated at µg/L) and to estimate the ratio of the optical isomers after the application. Hence the aim of this project was to increase the detection sensitivity of Triadimenol samples in order to estimate the ratio of optical isomers after application to field samples and to see the possibility of detecting Triadimenol in the spiked grape sample using preconcentration techniques.

The initial plan was to obtain high detection sensitivity for Triadimenol standards. To then ascertain if the adequate separation of diastereoisomers or enantiomers could be achieved, then to apply the developed method to Triadimenol spiked grape samples to estimate the ratio of optical isomers. NSM was the first preconcentration technique attempted. During NSM, buffer was prepared with 20 mM borate and phosphate with SDS micelles and HP-β-CD chiral selector. Samples were prepared either in water or low concentration buffer. Samples were injected hydrodynamically as a long plug and the plug length was varied to observe the impact of plug length on sensitivity and on separation. Acceptible separation was not achieved using NSM with varying sample plug length.

The next step was to attempt large volume stacking with polarity switching mode. The buffer was prepared with 20 mM borate and phosphate with SDS micelles and HP-βC-D chiral selector. In this technique, the sample was prepared in water and a large volume injected hydrodynamically. A negative voltage is applied at the injection end. The large solvent plug is then electroosmotically pushed out of the column while the negative species stack up at the boundary between the sample zone and the background electrolyte. The stacking and removal of solvent occurs concurrently when the sample buffer is almost completely out of the column (estimated by monitoring the electric current), the polarity is reversed back to the normal configuration and separation of the negative species can proceed. The initial attempted employed a sample plug length generated by 240 s injection at 50 mbar, and 20 kV of negative polarity allowed for 50 s. The duration of the negative polarity was then reduced sequentially to 40 s, 30 s and 20 s to observe any peaks. Fig 7.4 shows the large volume stacking with polarity switching mode with

injection conditions of 50 mbar for 240 s to generate the sample plug length, and 20 kV negative polarity for 30 s. However no clear peaks were observed. Peaks A, B represent Triadimenol diastereoisomer A and B respectively.

Figure 7.4: A selected electropherogram showing large volume stacking with polarity switching mode (injection conditions of 50 mbar for 240 s and 20 kV negative polarity for 30 s).

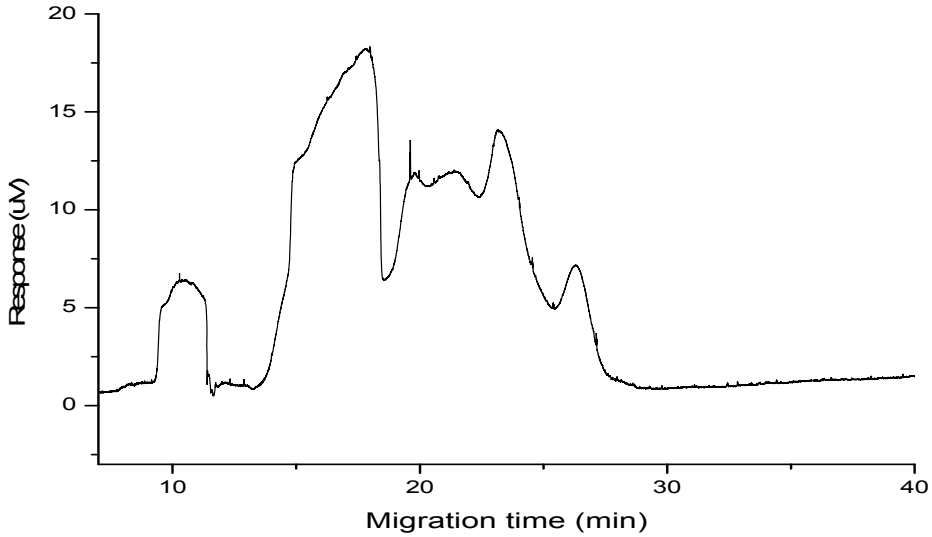

Due to the observation of no clear peaks with different durations of negative polarities with 240 s injection at 50 mbar, it was decided to change the sample plug length size. The sample plug length was changed by changing the injection to 60 s injection at 50 mbar, with 20 kV negative polarity for 60 s as shown in Fig 7.5.

Figure 7.5: A selected electropherogram showing large volume stacking with polarity switching mode (injection conditions of 50 mbar for 60 s and 20 kV negative polarity for 30 s).

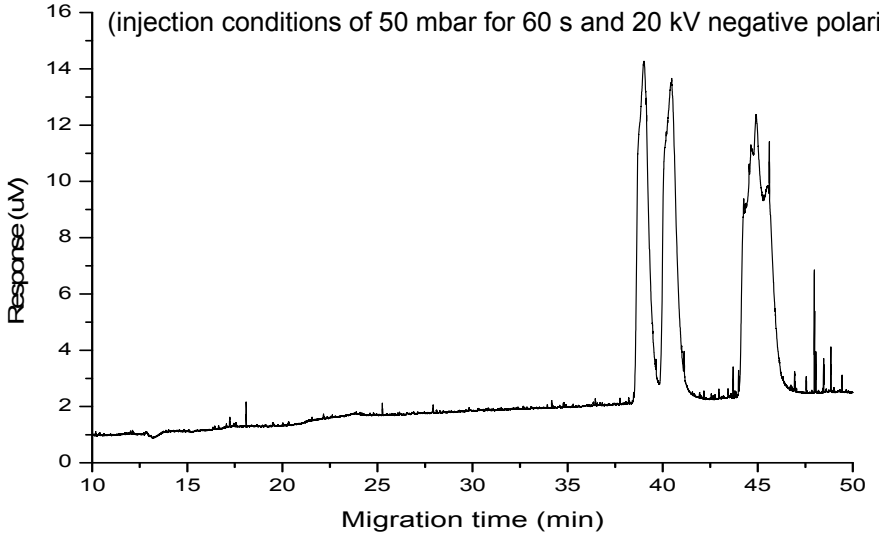

To examine the possibility of further separation of 3 peaks obtained from large volume stacking with polarity switching mode, it was decided to vary the duration of negative polarity. The duration of 20 kV negative polarity was reduced to 42 s and 36 s respectively. Fig 7.6 shows the electropherogram of 20 kV negative polarity for 36 s. No further peak splitting was obtained with varying the negative polarity; however all 3 peaks obtained were not symmetrical and they were not reproducible. The conductivities of the sample and the buffer electrolyte were measured to see whether it was necessary to introduce a water plug before the introduction of sample. The conductivity of the buffer electrolyte was 8.28 ms/cm whereas the conductivity of the sample was observed to be 0.20 ms/cm. Due to the large difference between the buffer electrolyte and the sample, it was not necessary to inject a water plug before the introduction of the sample.

Figure 7.6: A selected electropherogram showing large volume stacking with polarity switching mode (injection conditions of 50 mbar for 60 s and 20 kV negative polarity for 36 s).

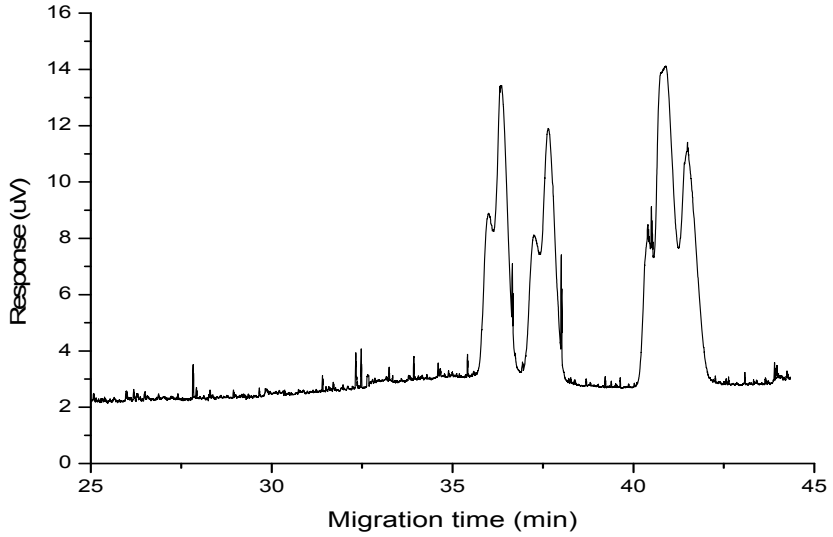

The next step was to change the preconcentration technique to sweeping after unsuccessful attempts at stacking techniques. Sweeping can be employed for the systems where any complexation or partitioning between the analyte and the PS is the major mechanism of focusing [19]. According to the literature, sweeping is usually performed under acidic conditions [20], hence the buffer electrolyte chosen was 20 mM phosphate, 50 mM SDS, 20% methanol and 20 mM HP-β-CD with varying pH. The sample was prepared in phosphate buffer without micelles. Two broad skewed peaks were observed when sweeping with HP-β-CD as shown in Fig 7.7.

Figure 7.7: A selected electropherogram from sweeping of triadimenol with HP-β-CD chiral selector

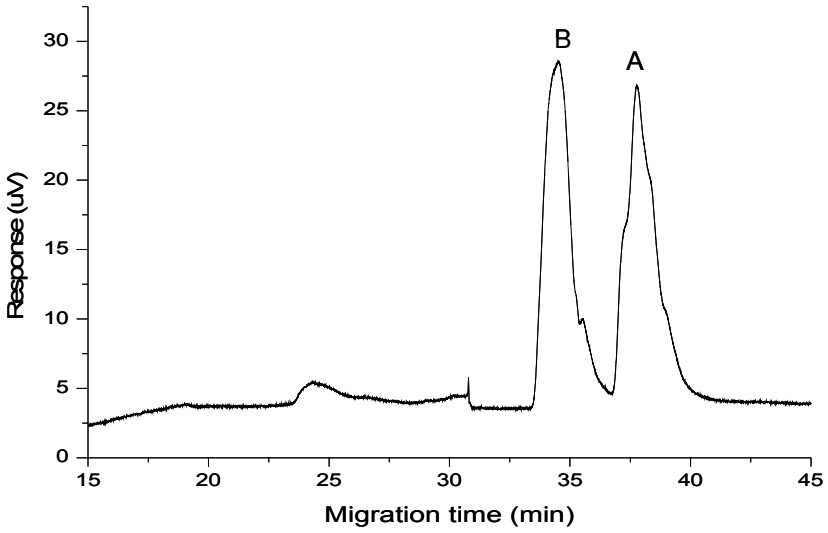

Sulfated-β-CD, a charged chiral selector, was then mixed with HP-β-CD in the buffer electrolyte to see whether the combination would increase chiral resolution of triadimenol in sweeping. The combination of charged and neutral CDs resulted in two skewed peaks. However no reproducible results were obtained. The chiral selector was then changed to sulfated-β-CD without changing other components in the buffer electrolyte. Two symmetrical peaks (triadimenol diastereoisomers) were observed when using a charged chiral selector Fig 7.8 shows the electropherogram from sweeping with sulfated-β-CD. The separation of Triadimenol diastereoisomers was obtained with the sweeping technique. However a change in migration order of the diastereoisomers was observed due to application of negative polarity. The conductivity adjustments were not necessary in sweeping.

Figure 7.8: A selected electropherogram from sweeping of triadimenol with sulfated-β-CD

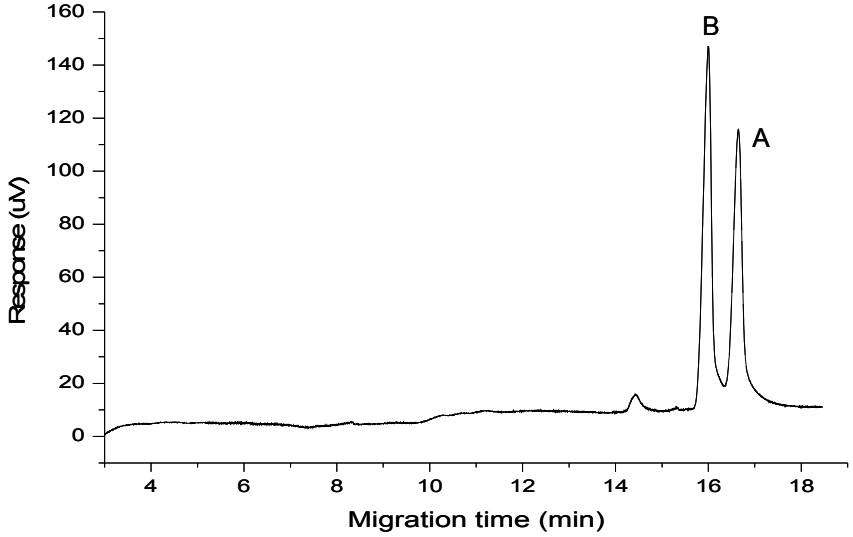

The concentration of sulfated-β-CD in the buffer electrolyte was increased gradually up to 3%. The detection of peaks started with increasing sulfated- β-CD > 1%. Increase in sulfated-β-CD in buffer electrolyte resulted in increase in migration time. This could be due to high ionic strength of sulfated-β-CD in the running electrolyte leading to rise in the temperature inside the capillary column thus affecting the thermodynamic equilibrium of the inclusion interaction. Usually inclusion interactions are exothermic, hence higher temperature leads to a decrease in the equilibrium constant and creates counteracting effects on the apparent mobilities of analytes [21]. Increase in sulfated-β-CD may lead to increase in EOF by adsorbing onto the inner surface of the capillary wall which causes the increase in migration time. Fig 7.9 and 7.10 show the electropherograms containing 1% sulfated-β-CD and 3% sulfated-β-CD respectively. 2% sulfated-β-CD was chosen for further analysis of Triadimenol sweeping. Base line resolved narrow sharp peaks were obtained with 3% sulfated-β-CD in the buffer compared to 1%.

Figure 7.9: Electropherogram obtained with 1% sulfated- β-CD

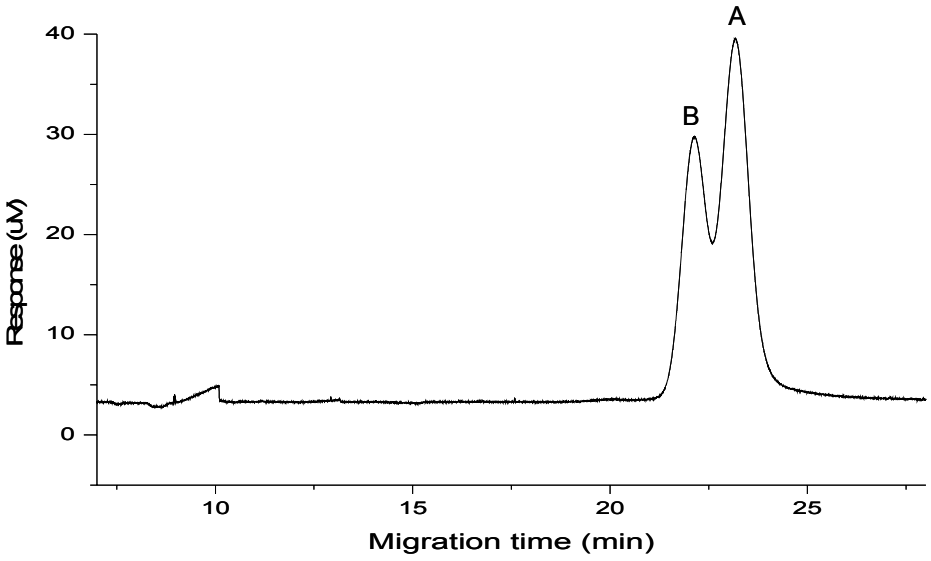

Figure 7.10: Electropherogram obtained with 3% sulfated- β-CD

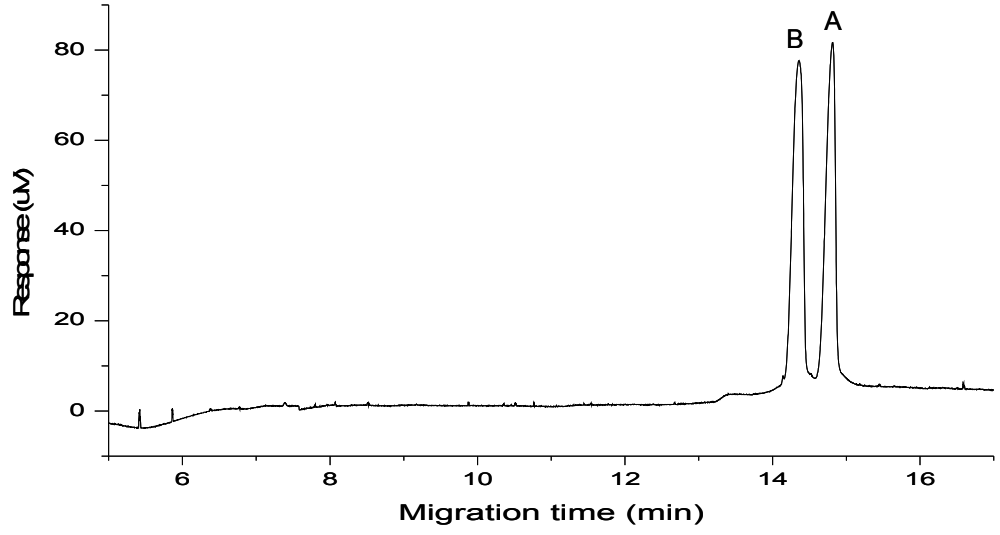

The impact of pH on Triadimenol sweeping was investigated by varying the buffer electrolyte pH between 2- 4. A decrease in pH from 4 to 2 resulted in reductions in migration time and decrease in sensitivity. The pH value of 2.5 was chosen for further analysis of Triadimenol sweeping. Fig 7.11 and 7.12 shows the electropherograms obtained with pH 2.5 and pH 3.0 respectively.

Figure 7.11: Electropheorogram with buffer pH 2.5

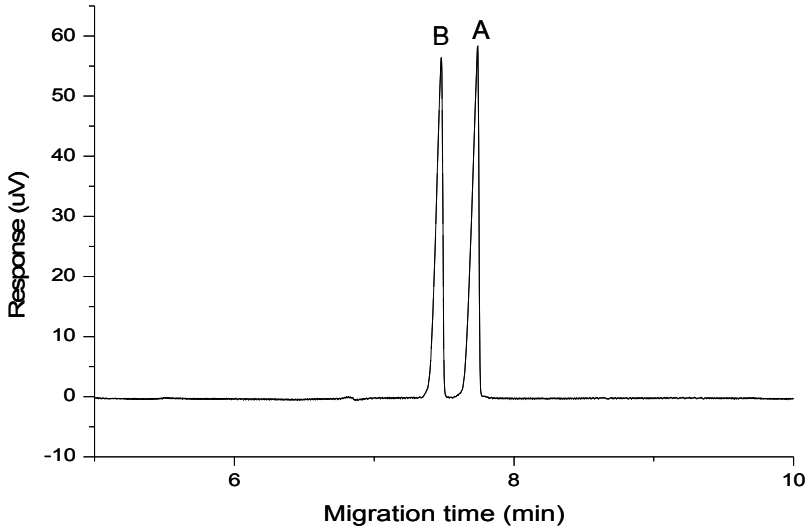

Figure 7.12: Electropherogram with buffer pH 3.0

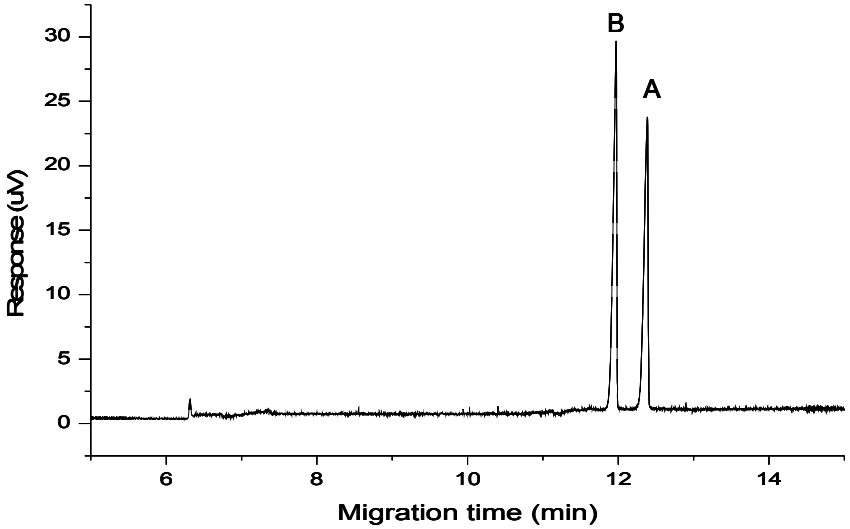

The impact of anionic surfactant sodium dodecyl sulfate (SDS) on resolution was investigated. It was observed that increasing concentration of SDS in the background electrolyte did not change overall

selectivity of separation but affected migration time. Fig 7.13 and 7.14 show the electropherograms, obtained with SDS in the buffer electrolyte at 50 mM and 60 mM respectively.

Figure 7.13: Electropherogram using 50 mM SDS

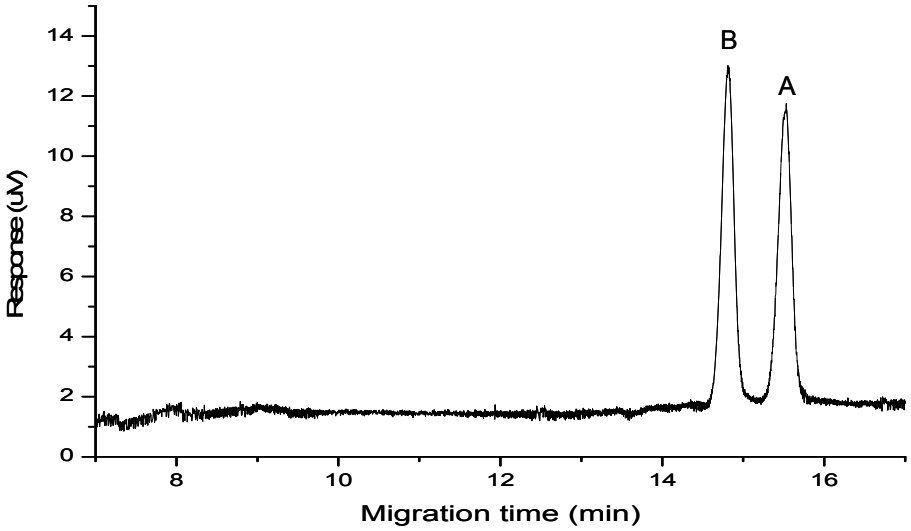

Figure 7.14: Electropherogram using 60 mM SDS

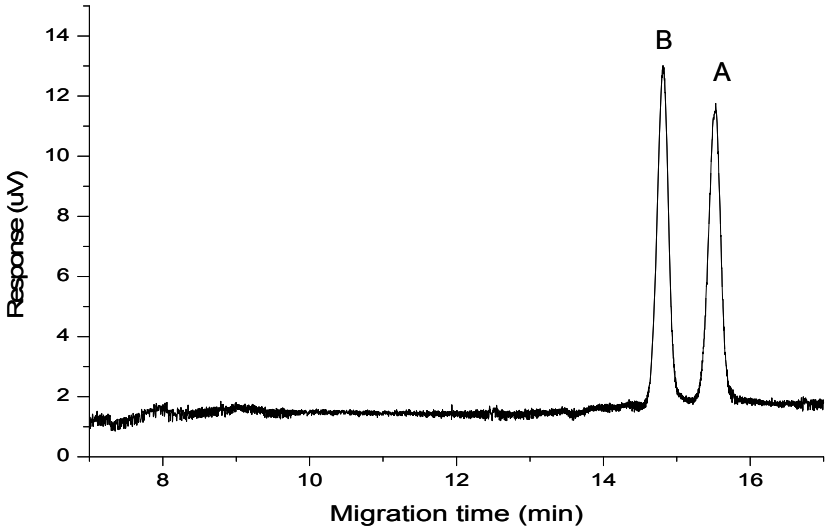

The effect of injection time was examined from 10 to 50 s using 50 mbar. The peak heights and areas increased in proportion with the injection time up to 25 s. However, when samples were injected for more than 25 s, the peaks were broadened and showed a degree of tailing. Hence 50 mbar 25 s injection was

chosen for Triadimenol sweeping. The best separation of Triadimenol diastereoisomers were obtained using 20 mM phosphate buffer, 2% sulfated-β-CD, 20% methanol, -20 kV at pH 2.5 as shown in Fig 7.15.

Figure 7.15: Electropherogram showing the separation of Triadimenol diastereoisomers (best separation)

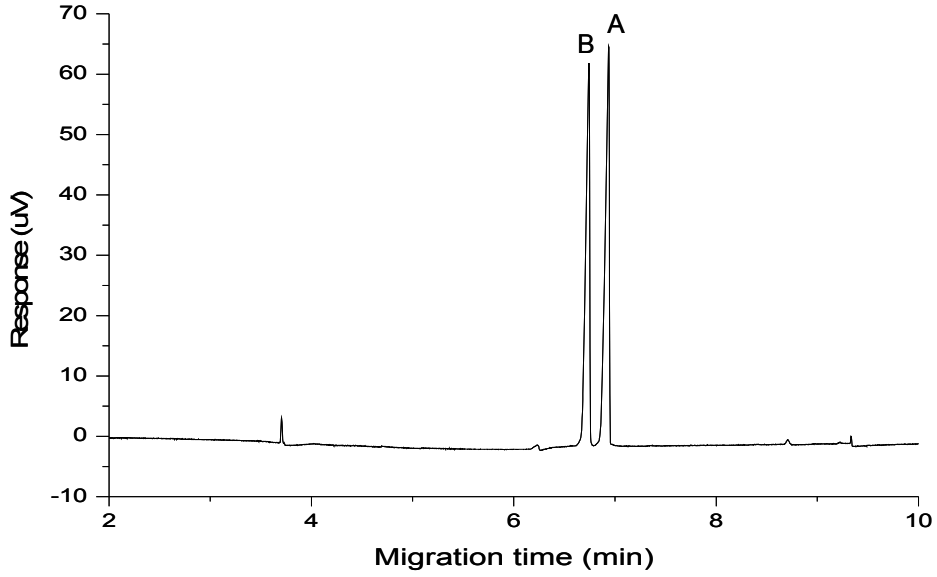

When using sweeping, a 30-fold increase in response was observed for triadimenol compared to MEKC mode of CE. However in sweeping, only diastereoisomer separation was possible with sulfated-β-CD and no enantiomeric (chiral) separation could be observed. This could be due to batch to batch variation in sulphonation of sulfated-β-CD.

7.2.1 Linearity of Triadimenol diastereoisomers

The linearity data for the Triadimenol diastereoisomers are shown in Tables 1. Triadimenol diastereoisomers analytical curves were linear over the range between 10 mg L^{-1} to 100 mg L^{-1}. Fig 7.16a and b show the linearity plots of Triadimenol A and B. The correlation coefficients of Triadimenol diastereoisomers ranged from 0.990 to 0.991, which is acceptable.

Table 7.1: Data (area) showing linearity of Triadimenol diastereoisomers A and B

	Triadimenol diastereoisomers	
Concentration (mg L^{-1})	A	B
2	26	21
4	42	38
8	74	60
20	170	138
30	235	195

Figure 7.16 a: Linearity Plot of Triadimenol diastereoisomer A

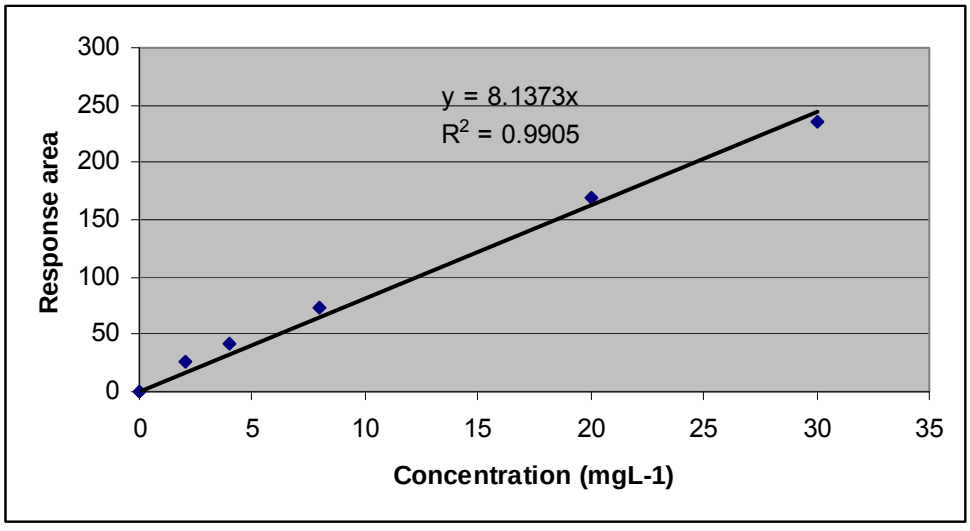

Figure 7.16 b: Linearity Plot of Triadimenol diastereoisomer B

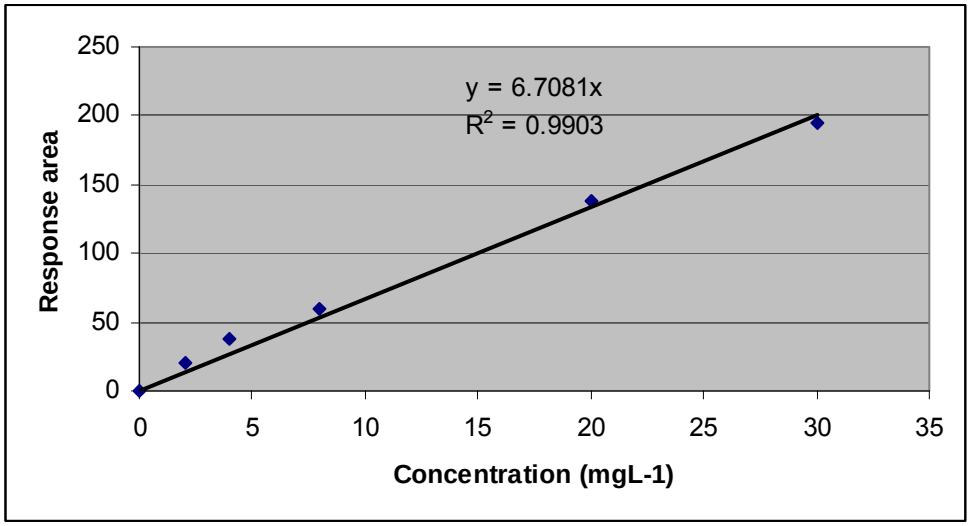

7.2.2 Analysis of spiked grape samples

Refer to section 3.5.2.2 and 3.5.2.3 regarding preparation of the grape sample for analysis. Two triadimenol peaks were observed when the optimised method was applied to the 20 mg L^{-1} spiked grape sample as shown in Fig 7.17. Due to interference of the sample matrix (CE analysis for sample matrix was performed separately), the base line separation of triadimenol diastereoisomers was not observed. However these peaks (7.8 and 8.0 min) were confirmed by diode array spectra. Triadimenol was not detected in the non-spiked grape sample.

Figure 7.17: Electropherogram of grape sample spiked with Triadimenol

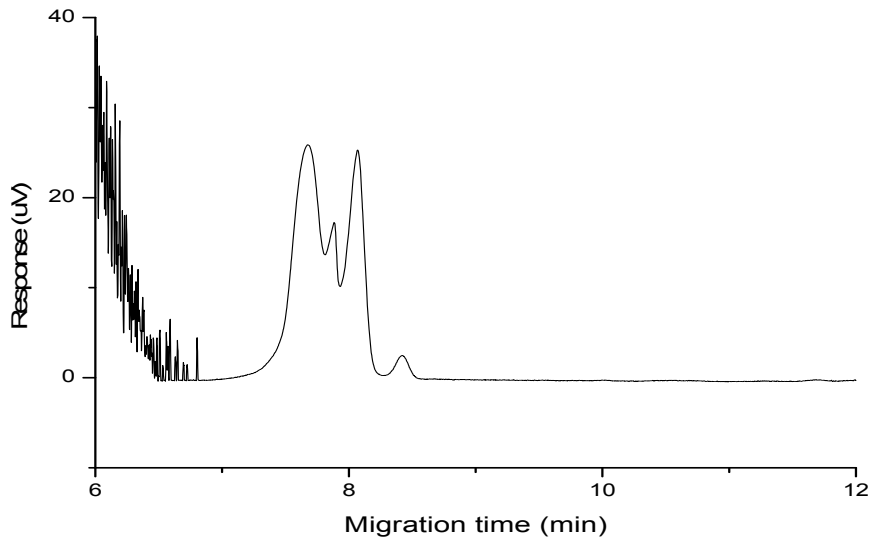

7.3 Conclusion

When using online preconcentration technique of sweeping, a 30-fold increase in detection sensitivity of Triadimenol was observed compared to MEKC mode. However enantiomer separation was not possible with sulfated-β-CD chiral selector. The best conditions were found to be pH 2.5, 50 mM SDS concentration, -20 kV with running buffer consisting of 20 mM phosphate concentration, using a 64.5 cm x 50 μm column, resulting in diastereoisomer separation within 8 min.

7.4 References

1. Osbourn, D.S., D.J. Weiss, and C.E. Lunte, *On-line preconcentration methods for capillary electrophoresis.* Electrophoresis, 2000. **21**: p. 2678-2779.

2. Kaniansky, D. and J. Marak, *On-line coupling of capillary isotachophoresis with capillary zone electrophoresis.* J. Chromatogr., 1990. **498**: p. 191- 204.

3. Stegehuis, D.S., et al., *Isotachophoresis as an on-line concentration pretreatment technique in capillary electrophoresis.* J. Chromatogr., 1991. **538**: p. 393- 402.

4. Quirino, J.P. and S. Terabe, *On-line Concentration of Neutral Analytes for Micellar Electrokinetic Chromatography. 3. Stacking with reverse Migrating Micelles. Anal. Chem.*, 1998. **70**(1): p. 149-157.

5. Quirino, J.P. and S. Terabe, *Exceeding 5000-fold concentration of dilute analytes in micellar electrokinetic chromatography.* Science, 1998. **282**: p. 465- 468.

6. Quirino, J.P. and S. Terabe, *On-line concentration of neutral analytes for micellar electrokinetic chromatography II. Reversed electrode polarity stacking mode.* Journal of Chromatography A, 1997. **791**: p. 255-267.

7. Quirino, J.P. and S. Terabe, *Sample stacking of fast-moving anions in capillary zone electrophoresis with pH-suppressed electroosmotic flow.* J. Chromatogr. A, 1999. **850**(1-2): p. 339- 344.

8. Palmarsdottir, S. and L.-E. Edholm, *Enhancement of selectivity and concentration sensitivity in capillary zone electrophoresis by on-line coupling with column liquid chromatography and utilizing a double stacking procedure allowing for microliter injections.* J. Chromatogr. A, 1995. **693**: p. 131- 143.

9. Burgi, D.S. and R.L. Chien, *Optimization in Sample stacking for high-performance capillary electrophoresis.* Anal. Chem, 1991. **63**(18): p. 2042- 2047.

10. Mikkers, F.E.P., F.M. Everaerts, and T.P.E.M. Verheggen, *High-performance zone electrophoresis.* J. Chromatogr., 1979. **169**: p. 11- 20.

11. Chien, R.L. and D.S. Burgi, *On-column sample concentration using field amplification in CZE.* Anal. Chem, 1992. **64**(8): p. 489A- 496A.

12. Burgi, D.S. and R.L. Chien, *Improvement in the method of sample stacking for gravity injection in capillary electrophoresis.* Anal. Chem, 1992. **202**: p. 306- 309.

13. Gilges, M., *Determination of impurities in an acidic drug substance by micellar electrokinetic chromatography.* Chromatographia, 1997. **44**: p. 191- 196.

14. Monton, M.R.N., et al., *Separation and on-line preconcentration by sweeping of charged analytes in electrokinetic chromatography with nonionic micelles.* J. Chromatogr. A, 2001. **939**(1-2): p. 99- 108.

15. Nunez, O., et al., *Analysis of the herbicides paraquat, diquat and difenzoquat in drinking water by micellar electrokinetic chromatography using sweeping and cation selective exhaustive injection.* J. Chromatogr. A., 2002. **961**(1): p. 65- 75.

16. Quirino, J.P., J.-B. Kim, and S. Terabe, *Sweeping: concentration mechanism and applications to high sensitivity analysis in capillary electrophoresis.* J. Chromatogr. A., 2002. **965**: p. 357- 373.

17. Quirino, J.P. and S. Terabe, *Approaching a million-fold sensitivity increase in capillary electrophoresis with direct ultraviolet detection: Cation- selective exhaustive injection and sweeping.* Anal. Chem, 2000. **72**(5): p. 1023- 1030.

18. Sera, Y., et al., *Sweeping on microchip: Concentration profiles of the focused zone in micellar electrokinetic chromatography.* Electrophoresis, 2001. **22**: p. 3509- 3513.

19. Markuszewski, M.J., et al., *Determination of pyridine and adenine nucleotide metabolites in Bacillus subtilis cell extract by sweeping borate complexation capillary electrophoresis.* J. Chromatogr. A., 2003. **989**(2): p. 293-301.

20. Otuska, K., et al., *On-line preconcentration and enantioselective separation of triadimenol by electrokinetic chromatography using cyclodextrins as chiral selectors.* Journal of Pharmaceutical and Biomedical Analysis, 2003. **30**: p. 1861-1867.

21. Wu, Y.S., H.K. Lee, and S.F.Y. Li, *High-performance chiral separation of fourteen triazole fungicides by sulfated a-cyclodextrin-mediated capillary electrophoresis.* Journal of Chromatography A, 2001. **912**: p. 171-179.

CHAPTER 8

REPLACEABLE STATIONARY PHASES
for
CAPILLARY ELECTRO CHROMATOGRAPHY

8.1 Introduction

CE is a powerful modern analytical separation technique [1-4] best known for its impact on research fields such as DNA fingerprinting, the Human Genome Project (separation of DNA fragments), and proteomics. CE separates species in an applied electric field based on the different velocities of the species in an electrolyte inside a separation capillary. Capillary Electro Chromatography (CEC) is similar to CE as it is also performed in a 'capillary format', but in this case the capillary also contains a chromatographic stationary phase, much as liquid chromatography (HPLC). The instrumentation and practice of CEC is in many ways similar to CE.

The stationary phase and the mobile phase are the two phases forming a chromatographic phase system. The stationary phase in a chromatographic system may be composed of a chromatographically active substance immobilised by chemical bonds attached to the chromatographically inert solid matrix or to the bulk phase of the porous matrix. The continuous bed-based products primarily developed as chromatographic media for biocompounds are regarded as the fourth generation of biochromatographic stationary phases after the polysaccharide- based, crosslinked, coated and monodispersed materials [5].

The non-particulate bed technique, which is also known as monolith or continuous bed, was first proposed by Hjerten et al. in 1989 and has revealed its outstanding compatibility with microchip format or capillary separations [5, 6]. A monolith phase can be regarded as an alternative technique for classical packed columns in chromatography. Due to the advantages of a monolith it has recently become the competitor of chip-based microanalysis.

Monoliths consist of a network structure rather than particle-packed columns as in HPLC. A monolithic column is a column consisting essentially of one piece of solid, which possesses interconnected skeletons and interconnected flow paths through the skeletons. Monolithic columns can be produced having a greater number of through-pore size/ skeleton size ratios compared to particle packed columns (monolith 3-5 ratio). The main features of monolithic silica columns include high porosities, large through-

pore size/ skeleton ratio leading to high permeability, and a higher number of theoretical plates per unit pressure drop. Faster separation can be achieved by large through-pores, small eddy diffusion path length, small sized skeletons, lower plate height and lower pressure drop compared to particle packed columns.

The pores of porous solids are classified according to the size of pores; as macropores, when bigger than 50 nm; mesopores- from 2 to 50 nm and micropores, when smaller than 2 nm [7]. The porosity of monolithic columns is higher compared to particle packed columns. Generally, monoliths contain micro or mesopores. Mesopores are formed in the network structure by treating with ammonia.

Monolithic columns can be prepared in a mold or directly in a fused silica capillary. Monoliths can be prepared in situ by filling the chromatographic column with an aqueous solution of monovinyl and bivinyl comonomers and initiator. Silanes such as tetramethoxy silane undergo hydrolytic polymerisation in aqueous acetic acid in polyethylene glycol to form monolithic silica having a network structure. Another way of preparing monolithics is to embed silica particles. High efficiency may be obtained for monoliths when prepared from a mold compared to fused silica. The network of silica structure should be attached to the wall in order to prepare a monolith in a fused-silica capillary. Monolith is networked by perfusive channels, which are permeable for the flow of the mobile phase.

The advantages of monoliths include small–sized skeletons and large through-pores. Smaller sizedd particles lead to high permeability and better column efficiency by small contribution of mobile phase mass transfer, eddy diffusion and shorter diffusion path length. When increasing column permeability (k), increase in theoretical plate count arises. Slow mobile phase mass transfer contributes to larger plate height. Eddy diffusion suggests irregularity of structure, presence of both small and large through-pores or inefficient exchange of stream paths. These effects can lead to increased band dispersion. High molar mass solutes can be separated efficiently even in the presence of slow mass transfer due to short diffusion path length.

Fig 8.1 shows a variety of approaches used for creation of CEC microcolumns. Upon application of voltage, the charged sites (could be positive or negative) provide electro-osmotic flow, and the stationary phase introduces distribution equilibria characteristic of conventional chromatography processes. The simplest approach is to prepare an open tubular column by coating the capillary walls with a stationary phase. However drawbacks of this approach include not retaining a lot of stationary phase in the separation capillary, low sample capacity and the small diffusion coefficients in the liquid phases can lead to low separation efficiency [1] .

Figure 8.1: Different types of stationary phases in miniaturised separation techniques

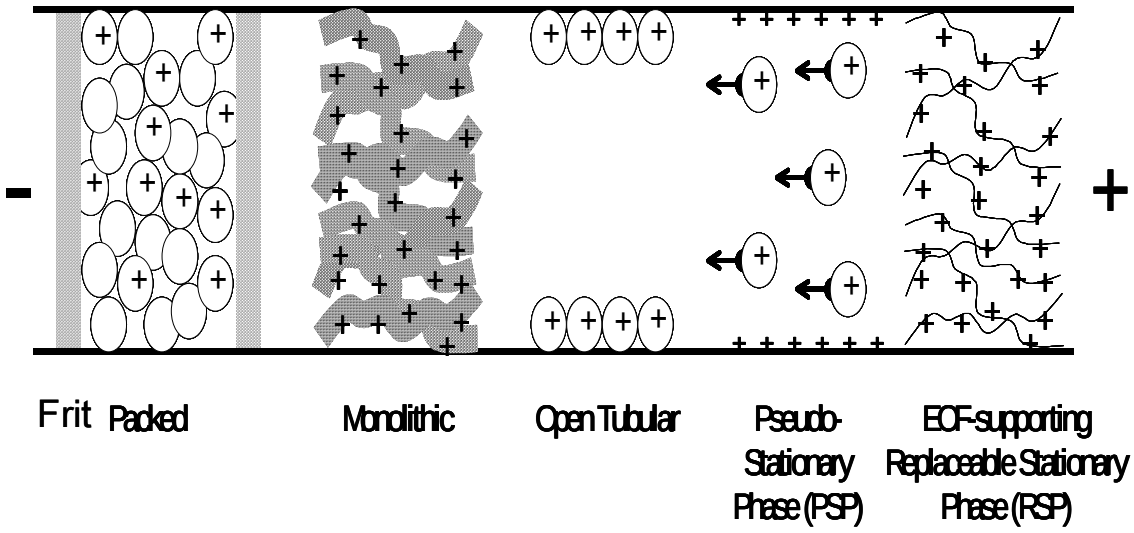

In the early development of CEC, capillaries were pressure slurry-packed with stationary phases held between miniature frits (Fig 9.1) created by sintering of the packing. These technologies are time demanding and unreliable. Packing CHIP microcolumns using electro-osmotic flow (EOF) to carry the chromatographic particles (packing) to a narrowed (tapered) retaining section of the channel [1] has proved to be slow and requires careful checking under the microscope. An alternative approach using photolithography (micromatching could be used as well) to create single chromatographic ‘particles’ on a

CHIP has been presented but is technologically demanding and expensive. Recently increasing emphasis has been placed on monolithic stationary phases formed *in-situ* in the CEC capillary or CHIP channel by organic polymer or sol-gel chemistries [1-4] . All the above result in stationary phases that can neither be re-created in, nor removed from, the separation capillary or channel, which limits their use. For instance, when the chromatographic stationary phase deteriorates because of void formation or by irreversible adsorption of matrix components in a sample, it would not be possible to remove this damaged stationary phase and create a new separation bed in the same capillary channel. The column will need to be discarded.

The presently available so-called replaceable phases for capillary gel electrophoresis (CGE) are pseudostationary phases, which are dissolved in the electrolyte (Figure 8.1) and do not form a solid column bed of chromatographic stationary phase. Their use is mainly for separations of biopolymers by CGE. Viscous solutions of entangled polymers such as polyacrylamide for CGE of DNA fragments are an example of such a replaceable phase. Examples of other pseudostationary phases include micellar solutions (MEKC) or solutions of charged polymers etc. [4, 8]. Pseudostationary phases have serious disadvantages: they compromise detection options (especially mass-spectroscopic, MS), and limit the sample preconcentration and matrix removal options that stationary phases normally offer.

Previously discussed chromatographic stationary phases incorporated in miniaturised separation systems lead to the conclusion that the technologies do not easily and quickly create stationary phase beds in capillaries and micro-channels that could be removed and re-created, thus providing a fresh stationary phase. Hence the aim of this study was to synthesize a polymer capable of forming homogeneous reversible gel phase compatible with aqueous-organic buffer electrolytes that provides sufficient zeta potentials for EOF. The replaceable stationary phase (RSP) can be used as an operating mode of CE/CEC. The practical aspect of such a material is that it must be readily introduced into the capillary (hence in a dissolved form), then set in the column as a semi-solid (which will not be removed by normal use) and then, if column performance deteriorates, alter conditions (i.e. alter temperature) to remove the

'spent' phase, ready for a fresh phase introduction. The process of 'setting' and removal can be termed 'switching'. We require a switch - chemical or physical condition that alters the phase property.

8.2 Results and Discussion

Delivering a liquid RSP to the column must be followed by its solidification to create a fixed RSP. The targeted RSP is required to include the following features: In their solidified state, these RSPs must (i) retain the analytes like a chromatographic stationary phase, based on hydrophobic, ion-exchange or other interactions with the analyte; (ii) be truly stationary, forming a solid microcolumn bed; and (iii) support EOF as a pump to deliver the mobile phase through the CEC or CEC-CHIP microcolumns (iv) possess UV transparency and exhibit capability of "in capillary" (in-gel) detection.

The procedure followed in novel RSP suggested in this project lies in the principle of creating, removing and re-creating a variety of stationary phases inside a capillary or CHIP separation channel. This was obtained as illustrated in Figure 8.2. First, the separation capillary was filled (by pressure) with a liquid RSP solution (a), and then the filled capillary is placed in electrolyte vials (b). The liquid RSP solution will be immobilised using a 'switch' (c). Remove RSP using a 'switch' (d). As a 'switch', any mechanism that can act upon the RSP precursor solution to result in formation of a porous solid and then reverse the process to remove the solid phase may be used.

Figure 8.2: Scheme of creation and removal of replaceable stationary phase

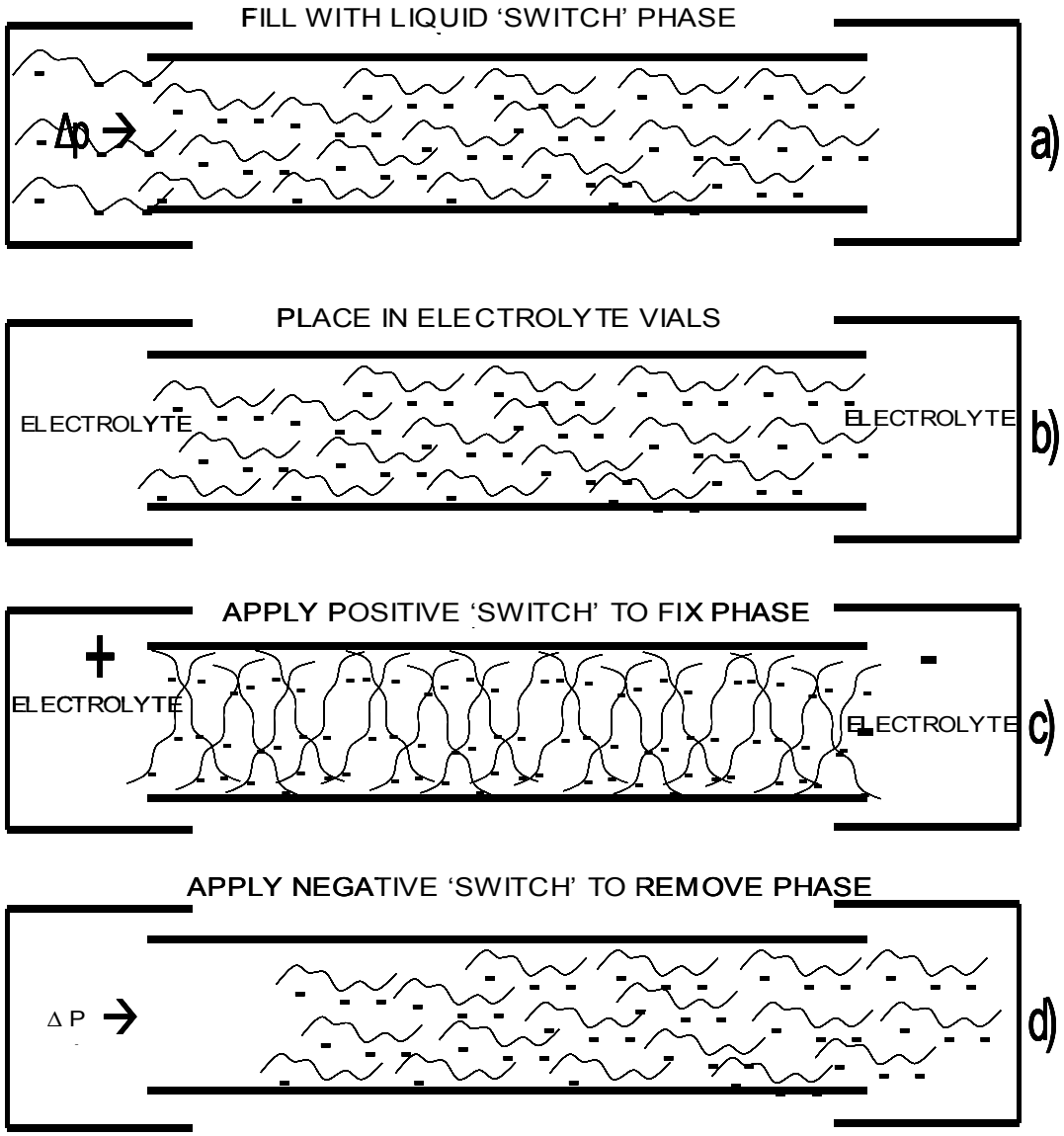

The initial step was to choose a suitable reagent to create a gel with the following characteristics. The reagent should allow prepareparation of solution of the thermoreversible gel, flow in to the capillary column, apply positive 'switch' (i.e. cool down) and form a gel inside the capillary. The gel should consist of pores (mesopores or macropores) to support significant EOF. The electrostatic double layer overlap in RSP is vital (EOF in relatively small pores can be substantially increased by increasing the ionic strength of the mobile phase electrolyte as it decreases the depth of the double layer).

Upon gelation inside the capillary, normal analysis can be performed until the stationary phase wears out. Temperature is the 'switch' described in Fig 8.2. Temperature can be applied to remove the stationary phase completely from the capillary and a new stationary phase can be filled for continued analysis.

It was decided to evaluate the suitability of pectin to form a gel inside the capillary column. The composition and characteristics of pectins differ with source, the processes used during preparation, and subsequent treatments. The term pectin indicates a family of compounds, and this family is part of a still bigger family known as pectic substances. The expression pectin is usually known in a generic sense to designate those water-soluble galacturonoglycan preparations of varying methyl ester contents and degrees of neutralisation, which are capable of forming gels. Some carboxyl groups in natural pectins are in the form of methyl ester. The remaining free carboxyl acid groups may be fully or partly neutralised and present as sodium, potassium or carboxylate groups depending on the isolation conditions. Preparations in which more than half of the carboxyl groups are in the methyl ester form ($-COOCH_3$) are categorised as high methoxy pectins (HMPs) as shown in Fig 8.3, with the remaining carboxyl groups present as a mixture of free acid (-COOH) and salt ($-COO-Na^+$) forms. Preparations in which less than half of the carboxyl groups are in the methyl ester form are known as low methoxy pectins (LMPs). The LMPs can be formed by the treatment of pectin preparation with ammonia dissolved in methanol, which converts some of the methyl ester groups into carboxamide groups [9].

8.2.1 Creating a RSP inside the capillary column

LMPs were chosen as the pore forming agent to create RSP. Refer to section 3.5.7.1 of Chapter 3 regarding the preparation of RSP. Low methoxy pectin met all the criteria of a thermoreversible gel capable of supporting EOF. LMP integrates the liquid and the solid polymer forming a uniform composition, it can be regarded as homogenous phase at a molecular level. A mixture of caffeine, aspartame, benzoic acid and saccharin (CABS mixture) was chosen for initial analysis by RSP. Refer to section 3.5.7.5 of Chapter 3 regarding buffer and sample preparation details for analysis of CABS mixture. The capillary column filled with RSP was treated the same as the unfilled column. The column was flushed with water for 2 min followed by the background electrolyte for 3 min. The sample was then injected into the column hydrodynamically as discussed in section 3.1.1.f. of Chapter 3. Upon application of voltage, the current was observed indicating successful EOF through the capillary column and pores inside are sufficient to support EOF. The temperature of the cassette was adjusted to 15° C for sample analysis to maintain low temperature inside the capillary column to ensure durability of RSP by minimising dissolution of gel. The capillary column was flushed with water between the runs. The electropherograms of CABS mixture with unfilled and filled columns are shown in Fig 8.6 and 8.7 respectively.

Figure 8.3: Structure of high methoxy pectin

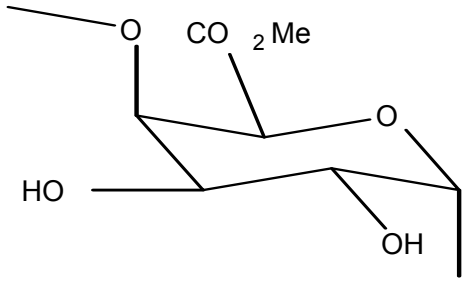

The separation of CABS mixture by RSP (Fig 8.6) was compared with the separation without RSP (Fig 8.6). It was observed that the migration time of caffeine is longer with the presence of RSP. The migration

time of caffeine by a column containing RSP was at 4.2 min compared to migration time of caffeine by an unfilled column at 3.2 min. However better separation was obtained for CABS mixture by RSP. This could be due to slow EOF through the pores of RSP compared to fast EOF through an unfilled column. The electropherogram of CABS mixture through an unfilled column is shown in Fig 8.7. The following analyses for CABS mixture were performed using 18 kV which resulted in current ~110 μA. The presence of good current in the LMP filled column confirmed good electrophoretic mobility of analytes.

The capillary should remain transparent even after filling with RSP to enable oncolumn detection with UV. The column with RSP was photographed under the microscope and compared with an unfilled column to observe any differences. The photographs of the column with RSP and an unfilled column are shown in Fig 8.4 and 8.5 respectively.

Photographs were taken under the 40 magnification. A clear inner surface was observed from the unfilled capillary column, whereas the inner surface of the column with RSP was observed to contain colourless network gel. The particles inside the filled column could be from RSP, however it cannot be clearly photographed without a greater colour contrast present. To enable UV detection, the gel cannot be coloured, however a stain can be added for visualisation.

Figure 8.4: Photograph showing the capillary column filled with RSP under 40 x magnifications.

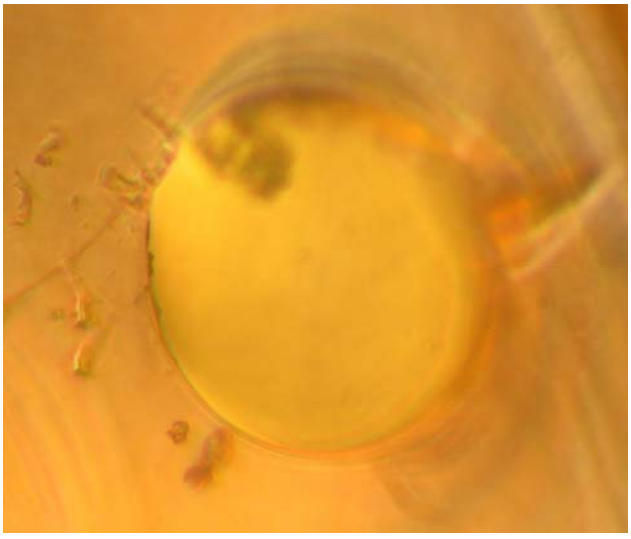

Figure 8.5: Photograph showing an unfilled capillary column under 40 x magnifications.

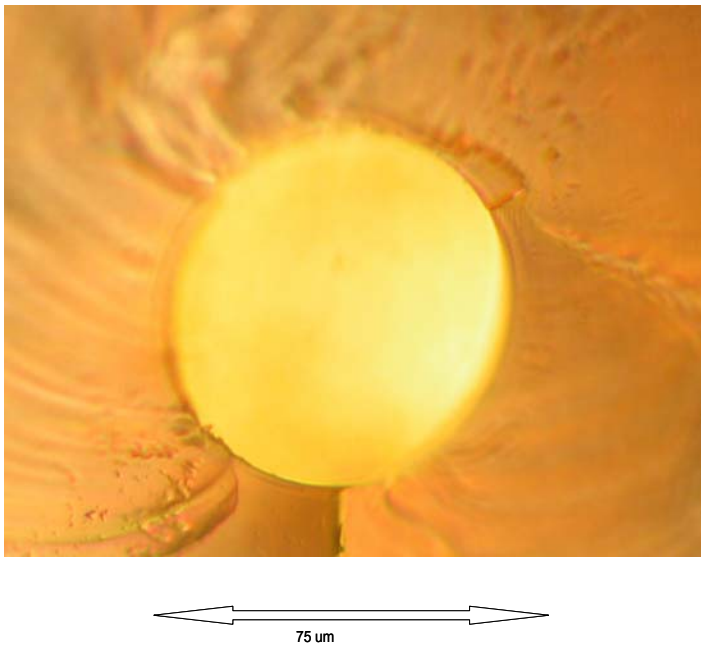

Figure 8.6: Electropherogram showing the separation of CABS mixture in the unfilled column

(Peaks 1, 2, 3, 4 in CABS mixture represent caffeine, aspartame, benzoic acid and saccharine. The concentration of all the components of the CABS mixture was 250 μg mL^{-1}).

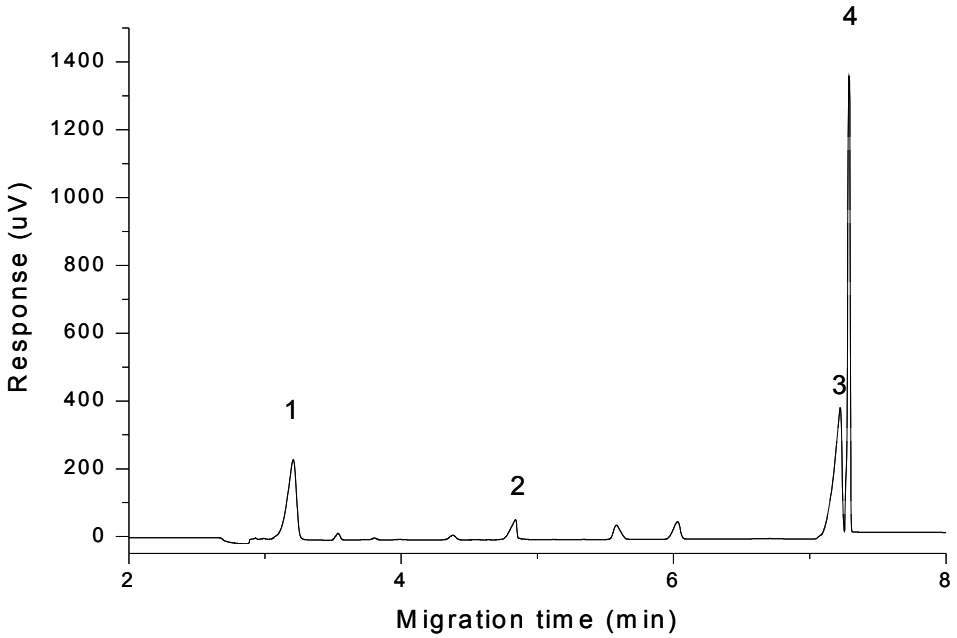

Figure 8.7: Electropherogram showing the separation of CABS mixture in the LMP filled column

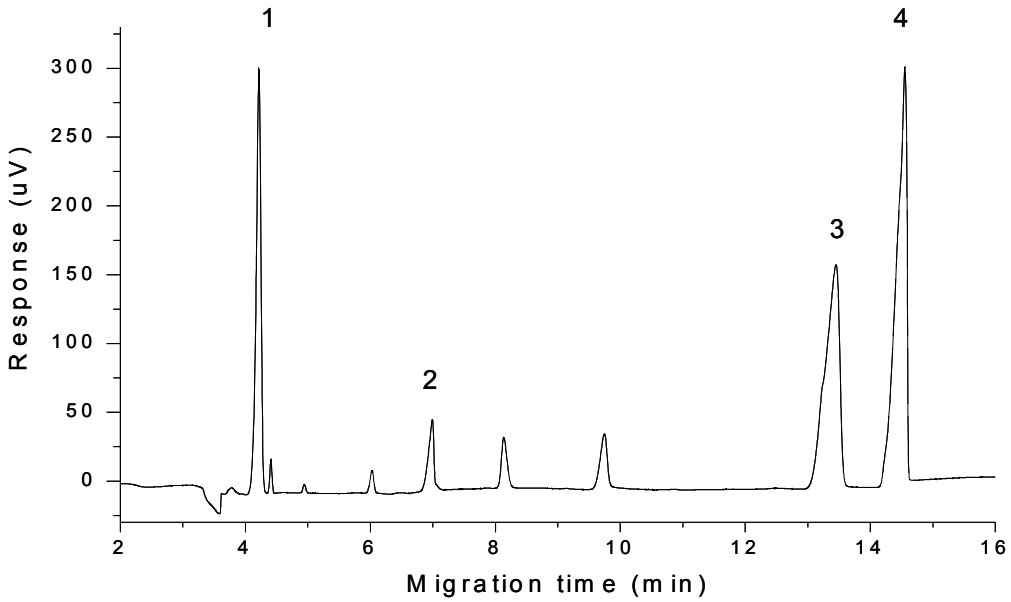

Separations of all four peaks in the normal capillary column were completed within 8 min whereas the column with RSP took 15 min for completion. Better separation and shaper peaks were observed from the column with RSP, although it took longer time to separate. It is evident, that the LMP has formed a gel phase inside the capillary column due to longer completion time and peak shape of CABS mixture.

8.2.2 Reproducibility of caffeine mixture in RSP

The reproducibility of the system was determined by performing five replicates. Good repeatability in migration times and areas was observed. The data showing reproducibility of migration times and areas are shown in Tables 8.1, 8.2 and 8.3 respectively.

Table 8.1: Data showing reproducibility of migration times (concentration of peaks 250 μg mL^{-1}), with the LMP filled capillary

Run #	Absolute t_{mig} values (min)	
	Compound	
	Caffeine	Aspartame
1	4.78	7.43
2	4.86	7.72
3	4.68	7.26
4	4.92	7.83
5	4.80	7.50
Mean	4.81	7.54
rsd %	1.90	3.02

The relative standard deviation (rsd) of absolute migration times was within 3% indicating good reproducibility from RSP. The peak shape of benzoic acid and saccaharine show some over loading. Hence these peaks were not included into reproducibility tables.

Table 8.2: Data showing reproducibility of relative migration times vs Caffeine (concentration of 250 μg mL^{-1}) with the LMP filled capillary

Run #	Relative t_{mig} vs Caffeine	
	Compound	
	Caffeine	Aspartame
1	1.00	1.55
2	1.00	1.58
3	1.00	1.55
4	1.00	1.59
5	1.00	1.56
Mean	1.00	1.57
rsd %	0.00	1.04

The rsd of relative migration time of Aspartame vs Caffeine was within 1.0% indicating good reproducibility when the RSP format capillary is employed.

Table 8.3: Data showing reproducibility of areas (concentration of peaks 250 μg mL^{-1}) with the LMP filled capillary

Run #	A: Peak Areas (μV.s)	
	Compound	
	Caffeine	Aspartame
1	1710	2368
2	1766	2446
3	1779	2505
4	1787	2532
5	1754	2410
Mean	1759	2452
rsd %	1.72	2.74

The rsd of areas of Caffeine and Aspartame were within 3% indicating good reproducibility from RSP.

The CABS mixture was continuously run in the RSP column with hydrodynamic flushing from water between the runs and filling with background electrolyte at the beginning of the run. Good reproducibility of migration times was observed up to 20 runs. The gradual increase in migration time for all the peaks and peak splitting was observed as more runs progressed. This observation could be due to aging of the RSP inside the capillary column. Fig 8.8 shows the peak splitting from aged RSP.

RSP was removed from the capillary column as described in 3.5.7.5 of Chapter 3 after observation of peak splitting. To ensure aged RSP is removing from the capillary, the runs were performed time to time, as shown in Fig 8.9 and the migration time of caffeine continuously reduced until the RSP was completely removed from the capillary column. Fig 8.9 shows an electropherogram in the process of removing aged

RSP. Hence the migration times of CABS mixture was in between the Fig 8.6 (fresh RSP) and 8.8 (aged RSP).

Figure 8.8: Electropherogram showing the separation of CABS mixture in aged LMP filled column

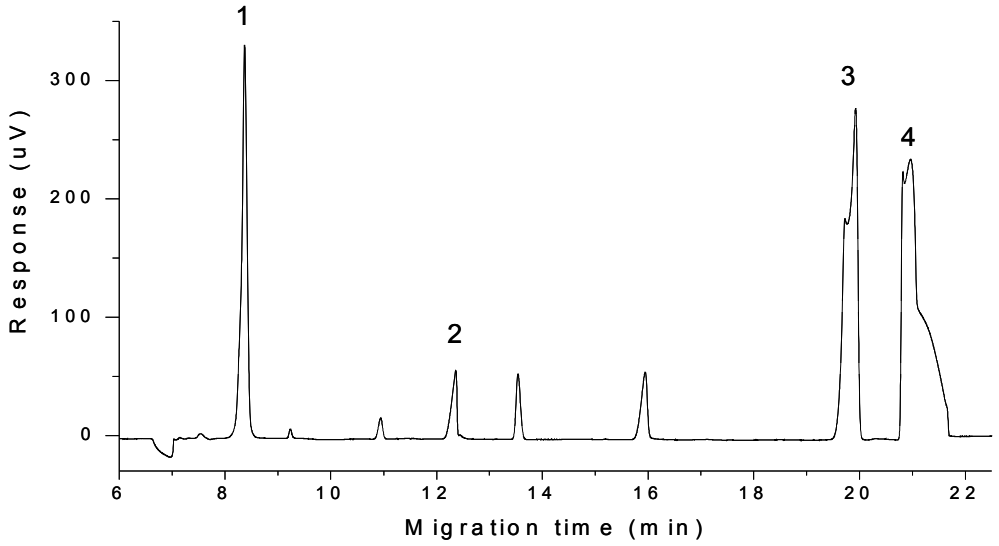

Figure 8.9: Electropherogram showing the separation of CABS mixture in the process of removing RSP

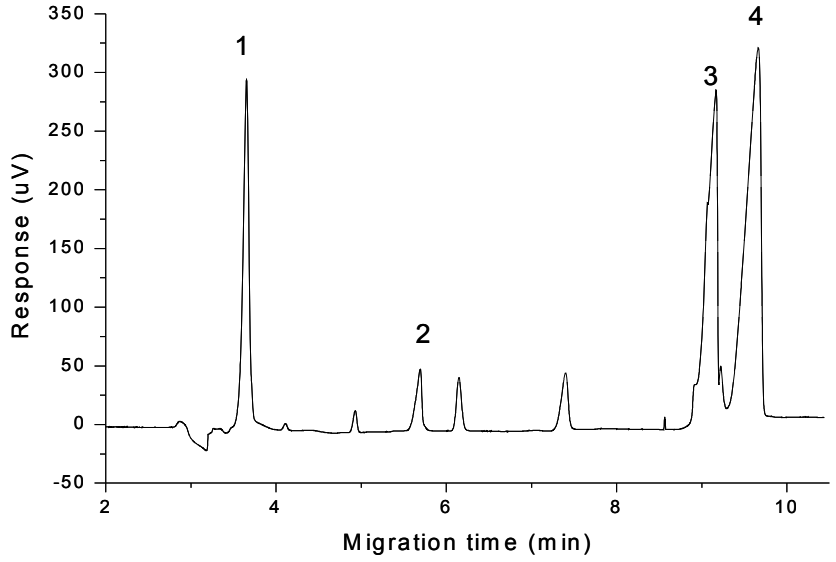

After ensuring complete removal of RSP from the capillary column, RSP was recreated inside the capillary column. Fig 8.10 shows an electropherogram after recreating RSP inside the capillary column. It was observed that the migration times for all the components in the CABS mixture of recreated RSP was similar to original migration times by RSP (Fig 8.7).

Figure 8.10: Electropherogram showing the separation of CABS mixture after recreating RSP

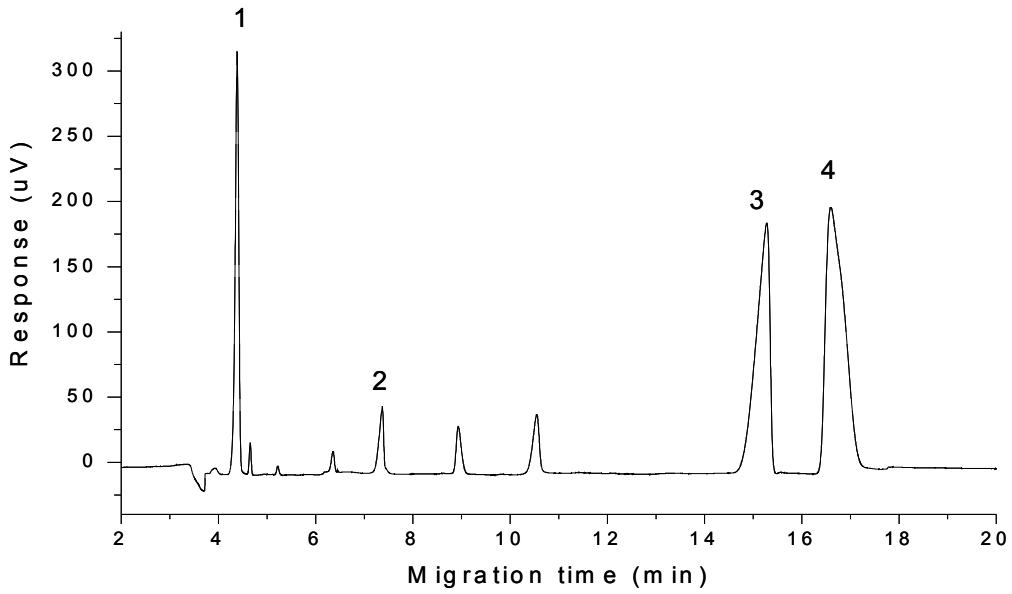

After successful separation of CABS mixture from the RSP, the next step was to investigate the capability of running organic solvents through RSP in the capillary column.

8.2.3 Analysis of Nitrofuran antibiotics (NFAs) by RSP

The column was flushed with water for 2 min followed by the background electrolyte for 3 min. The sample was then injected into the column hydrodynamically as discussed in section 3.1.1.g of Chapter 3. The temperature of the cassette was adjusted to 15° C for NFA analysis to maintain low temperature inside the capillary column to ensure durability of RSP by minimising dissolution of gel. The capillary

column was flushed with water between the runs. The electropherogram of NFAs mixture is shown in Fig 8.12. Refer to section 3.5.7.6 of Chapter 3 regarding buffer and sample preparation details for analysis of NFAs. Peaks 1, 2, 3, 4 in NFAs mixture represent Furazolidone, Furaltadone, Nitrofurazone and Nitrofurantoin respectively. The concentration of NFAs in all analyses was 500 μg mL^{-1} and voltage used was 16 kV.

Figure 8.11: Electropherogram showing the separation of NFAs in an unfilled column

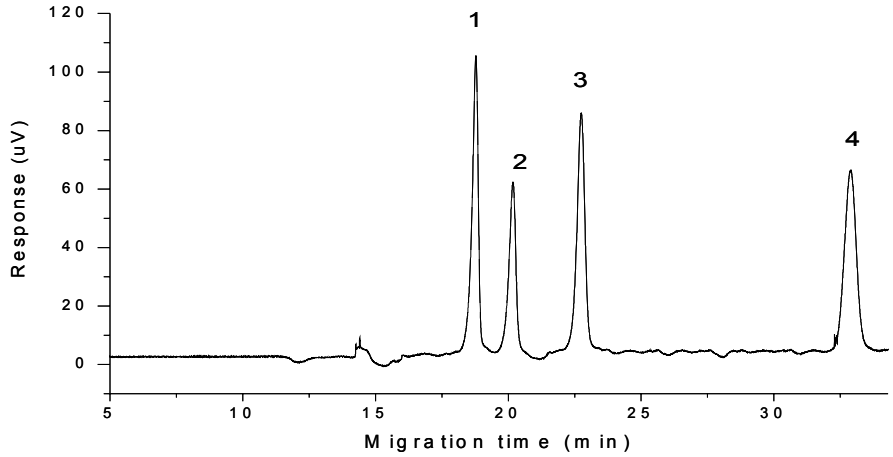

Figure 8.12: Electropherogram showing the separation of NFAs in the LMP filled column

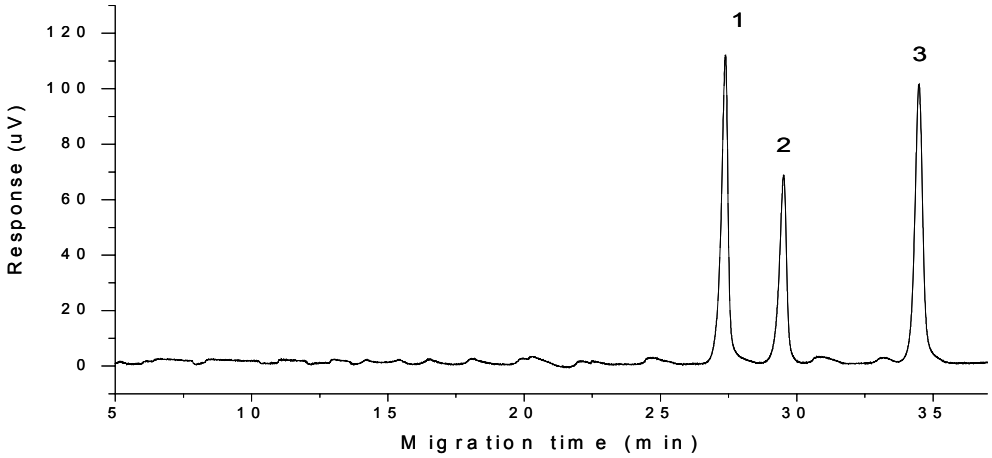

The separation of NFAs (Fig 8.12) by RSP was compared with the separation without RSP (Fig 8.11). It was observed that the migration time of NFAs is longer with the presence of RSP and confirmed the observations for CABS mixture. The migration time of NFAs by a column containing RSP was at 28 min compared to migration time of NFAs by unfilled column at 18 min (comparison of peak 1). Due to longer migration time of NFAs in the LMP filled column, only three peaks were observed. However better separation was obtained for NFAs by RSP. This could be due to slow EOF through the pores of RSP, hence taking longer time to reach the detector compared to fast EOF through the unfilled column.

The gradual increase in migration time and low responses for all the NFAs peaks and observation of baseline disturbances confirmed the aging of RSP. Fig 8.13 shows the electropherogram of NFAs separation in aged RSP.

Figure 8.13: Electropherogram showing the separation of NFAs in aged RSP

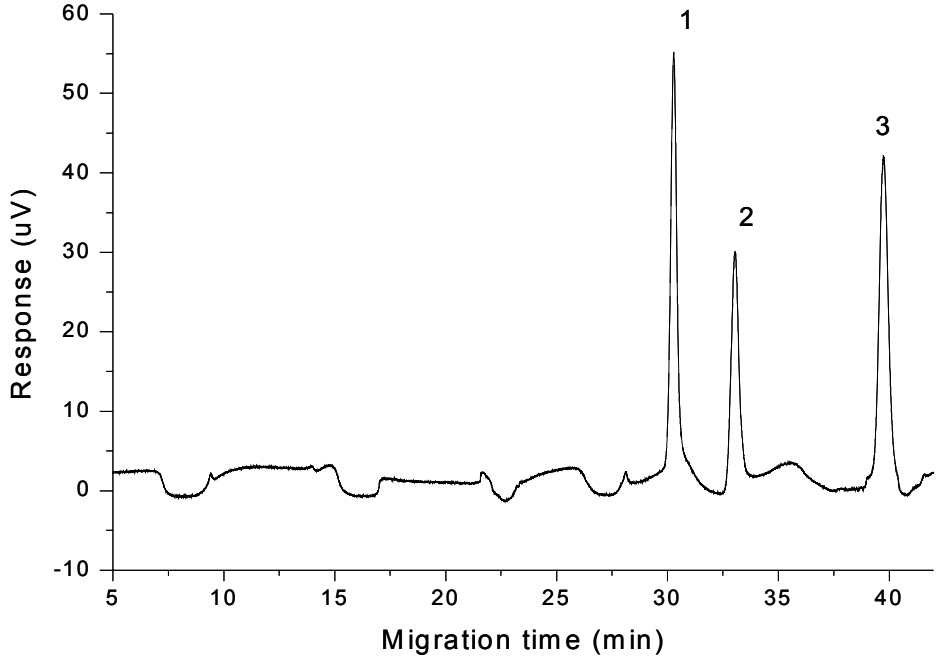

8.3 Conclusion

Preparation of RSP inside the capillary column was successfully performed using LMP. LMP renders a capability of reversible thermogelation. EOF and sufficient hydrophobicity of LMP gel allow separation of analyates. The porosity of LMP RSP was adequate to support EOF. Successful separation with good reproducibility of areas and migration times was obtained for CABS mixture and NFAs. After performing continuous analyses, the aging of RSP was observed. Temperature was the 'switch', which applied to remove aged RSP. RSP was recreated for further analysis of analytes. RSP was UV transparent, capable of handling various analytes and different buffer electrolytes including aqueous-organic solvents.

8.4 References

1. Landers, J.P., *Handbook of Capillary Electrophoresis*. 2nd ed. 1997, Boca Raton: CRC Press.

2. Shintani, H. and J. Polonysk´y, *Handbook of Capillary Electrophoresis Applications*. 1997, London: Chapman & Hall.

3. Khaledi, M.G., *High-Performance Capillary Electrophoresis. Theory, Techniques, and Applications*. 1998, New York: John Wiley & Sons, Inc.,

4. Camilieri, P., *Capillary Electrophoresis. Theory and Practice*. 1998, Boca Raton: CRC Press.

5. Iberer, G., et al., *Column watch: monoliths as stationary phases for separating biopolymers-fourth generation chromatography sorbents.* LC-GC Europe, 1999. **17**(11): p. 998-1005.

6. Svec, F. and J.M.J. Fréchet, *Continuous rods of macroporous polymer as high-performance liquid chromatography separation media.* Anal. Chem, 1992. **64**: p. 820- 822.

7. Unger, K.K., *Packing and stationary phases in chromatographic techniques.,* 1990, New York: Marcel Dekker.

8. Manz, A., *Ultimate speed and sample volumes in electrophoresis.* Biochemical Society Transactions, 1997. **25**(1): p. 278- 281.

9. Owen, R.F., *Food Chemistry*. 3rd ed. 1996, New York: Marcell Dekker.

CHAPTER 9

CONCLUSIONS

AND

RECOMMENDATIONS

9.1Conclusion

The first aim of the research was to establish a simple, fast CE method for simultaneous detection of NFAs and NFMs. The analysis and measurement of NFMs in foods however is still required as an important issue in food safety. The separation of NFAs and NFMs was not performed in a single run previously. Apparently no literature has been published for analysis of NFA or NFM by using CE. Hence the goal of this study was to develop a simple, fast analysis that enables simultaneous detection NFA and their metabolites. No NF peaks were observed using this CZE technique. The separation was then attempted using the MEKC technique with SDS as the micelle forming agent and borate and phosphate as the buffer electrolyte. However good reproducibility and ease of dissolution was observed when using SDC as the micelle forming agent. The wavelength of 275 nm was chosen to analyse both NFAs and NFMs in a single run due to the interest in maximising response for the analytically more important metabolites. A capillary column of total length 73 cm and effective length of 56 cm was chosen to enable detection of all NF peaks. The quality of the chromatograms was evaluated using the chromatographic exponential function (CEF), which gives a single number reflecting the quality of the separation; it incorporates both overall resolution quality and analysis time. The lower CEF value indicates higher quality of electropherogram.

After deciding the experimental domain, it was then screened for significant factors using a FFD. The significant factors observed were pH, buffer concentrations, voltage, and surfactant concentration. After identifying significant factors, next stage was to locate the conditions for an optimum separation. The five variables screened in the initial FFD were: concentration of SDC (20 mM- 100 mM), pH of running electrolyte (7.5-9.5), voltage (10 kV-20 kV), concentration of potassium dihydrogen orthophosphate (0-40 mM) and concentration of sodium borate (0-40 mM) in the buffer.

A CCD was employed to evaluate the optimum conditions for separation. In CCD, 3 variables were retained (pH, voltage and SDC). Borate to phosphate buffer ratio in the electrolyte was fixed to 20 mM borate: 20 mM phosphate, pH and SDC concentration was narrowed down. The pH was varied between 8.0-9.5, SDC concentration between 60 mM to 100 mM and voltage was varied between 10 kV to 20 kV

as shown in Table 5.5 and 5.6 of Chapter 5. The centre point was pH 9.0, 80 mM of SDC concentration and voltage 16 kV. In CCD, the lowest CEF value was obtained from the centre point indicated that the centre point is the true optimal.

The ruggedness check is carried out to evaluate the ruggedness of the chosen settings. The ruggedness of an analytical method is a measure of its capacity to remain unaffected by small deliberate variations in the method parameters and provide an indication of its reliability during normal usage Response surface plots and main effect plots were used to examine the criteria of validation and ruggedness study. The validation and the ruggedness test were conducted using a FFD. In the validation and ruggedness study, borate to phosphate buffer ratio in the electrolyte was fixed to 20 mM borate: 20 mM phosphate. The centre point was at a pH 9.0, 80 mM of SDC concentration and voltage of 16 kV. The main effect plots indicate that the lowest CEF value was obtained from the centre point. Higher or lower values than pH 9.0, voltage 16 kV and SDC concentration of 80 mM would result in an elevated CEF value. CEF values in the ruggedness study varied between 16-34 indicated that the chosen method is a rugged one.

The reproducibility of the system was determined by performing five replicates under the optimum conditions. Good repeatability in migration times and areas was observed for NFAs and NFMs separation under the optimal conditions. The calibration curves for NFMs were linear over the range between 2 mgL^{-1} to 30 mgL^{-1}. Good linearities with coefficient of regression higher than 97% were obtained for NFMs. The calibration curves for NFAs were linear over the range between 20 mgL^{-1} to 100 mgL^{-1}. Good linearities with coefficient of regression higher than 98% were obtained for NFAs.

The limit of detection (LOD) for NFAs and NFMs was estimated by extrapolating to a signal-to-noise ratio (S/N) of 3 for the concentration of NFAs, which gives a signal three times the response of the magnitude of noise for a blank solution at 275 nm. Generally, LOD of around < 1 $\mu g\ mL^{-1}$ were found for the NFMs.

A prawn sample was spiked with NFMs, derivatised and extracted using SPE. Successful separation of metabolite derivatives was achieved when the developed method was applied to a spiked prawn sample. No peaks were observed in blank (with NFMs spiking) sample.

The next stage of the research was involved with chiral separation of triadimenol fungicide. The aim of this study was to investigate the possibility of chiral resolution of all triadimenol isomers within the shortest possible time and to apply the optimised conditions to triadimenol spiked grape to investigate whether the triadimenol can be separated from, and be detected in, the sample matrix and to see what the ratios of the optical isomers are after application. Such a method will allow researchers to study the enantioselective attenuation of different isomers, to identify which is the active enantiomer in biological systems.

Initially, the analysis of triadimenol samples was attempted using sodium dihydrogen phosphate in CZE mode. No peaks were observed for 100 min. Due to the weak basicity of these fungicides, it was then decided to switch to MEKC mode with SDS micelles. After finding the experimental domain, a CCD was employed optimise the significant factors of triadimenol fungicides separation. The best conditions found to give optimum resolution from the optimisation study were pH 6.0, 20% methanol, 50 mM SDS concentration, 20 mM HP-β-CD, 18 kV with running buffer consisting of 20 mM borate and 20 mM phosphate concentration using a 64.5 cm x 50 μm column, and resulted in baseline resolution of all triadimenol isomers within 18 min.

The optimised separation conditions were applied to a blank grape sample and to a spiked grape sample, where grape was chosen due to the triadimenol fungicides being widely used for grape crop protection. No peaks were observed in the blank grape sample whereas the spiked grape sample had two diastereoismer peaks with poor detection sensitivity. Increase in detection sensitivity is necessary to determine the possibility of resolution of all the isomers of triadimenol, in the spiked grape sample and the blank.

The detection sensitivity of triadiemenol was too low to observe the separation in actual samples (at a level of interest to trace analysis in field samples estimated at~ μg/L) and to estimate the ratio of the optical isomers after the application. Hence it was necessary to increase the detection sensitivity of triadimenol samples in order to estimate the ratio of optical isomers after application to field samples, and improve the detection of triadimenol in the spiked grape sample using preconcentration techniques. Various preconcentration techniques such as normal stacking mode, large volume stacking with polarity

switching mode were attempted. Sharp, narrow diastereoisomer peaks with 30-fold increase in detection sensitivity were obtained from sweeping with sulfated-β-CD. The best conditions were found to be pH 2.5, 50 mM SDS concentration, -20 kV with running buffer consisting of 20 mM phosphate concentration, using a 64.5 cm x 50 μm column, resulting in diastereoisomer separation within 8 min. However enantiomer separation was not possible with sulfated-β-CD chiral selector, which remains a limitation of the procedure.

The research involved creating a replaceable stationary phase (RSP) inside the capillary that could be removed and re-created, thus providing a fresh stationary phase. The RSP can be used as an operating mode of CE/CEC. Preparation of RSP inside the capillary column was successfully performed using low methoxy pectin (LMP). The procedure involved in the principles of creating, removing and re-creating a variety of stationary phases inside a capillary or CHIP separation channel. LMP renders a capability of reversible thermogelation. EOF and sufficient hydrophobicity of LMP gel allow separation of analytes. The porosity of LMP RSP was adequate to support EOF. The RSP can operate as a remote system and can be used for routine analysis. RSP was UV transparent, capable of handling various analytes and different buffer electrolytes including aqueous-organic solvents.

Temperature was the ‘switch’ used in removing the phase from the column. The choice of LMP to create RSP inside the capillary column was successful. The developed phase was used to separate CABS mixture and NFAs. Separations of all four peaks in the CABS mixture with normal capillary column were completed within 8 min whereas the column with RSP took 15 min for completion. Better separation and shaper peaks were observed from the column with RSP, although it took longer time to separate. When analysing NFAs using RSP,

The migration time of NFAs using a column containing RSP was 28 min compared to migration time of NFAs in an unfilled column of 18 min (comparison of peak 1). However better separation was obtained for NFAs by RSP

9.2 Future Work

Further optimisation of the SPE cartridge sample preparation method is required to ensure maximum recovery of NFMs. Online concentration techniques can be attempted to further improve the detection sensitivity of NFMs. The developed method can be applied to non-spiked imported meat products to evaluate possible detection of NFMs.

Another chiral selector should be attempted inorder to increase detection sensitivity of Triadimenol using online preconcentration techniques. The developed technique can then be applied as a part of broader interest in chiral pesticides analysis in the environment. The developed method can then be applied to Triadimenol spiked grape sample to evaluate the ratio of isomers after application.

The RSP should be evaluated for routine analysis due it's capability of operating as a remote system. Different gels can be attempted to create RSP using the same technique of creating and removing the RSP. The developed gels can then be evaluated for protein separation.